3

ORNL/M--741

DE89 010600

U.S./JAPAN COLLABORATIVE PROGRAM
ON
FUSION REACTOR MATERIALS*

SUMMARY OF THE TENTH DOE/JAERI ANNEX I
TECHNICAL PROGRESS MEETING
ON
NEUTRON IRRADIATION EFFECTS IN
FIRST WALL AND BLANKET STRUCTURAL MATERIALS

*Research sponsored by the Office of Fusion Energy, U.S. Department of Energy under contract DE-AC05-84OR21400 with Martin Marietta Energy Systems, Inc., and with the Japan Atomic Energy Research Institute, Tokai-mura, Japan.

Prepared by the
Oak Ridge National Laboratory
Oak Ridge, Tennessee 37831
operated by
Martin Marietta Energy Systems, Inc.
for the
U.S. DEPARTMENT OF ENERGY
under Contract No. DE-AC05-84OR21400

SUMMARY OF THE TECHNICAL PRESENTATIONS

MADE AT THE TENTH DOE/JAERI ANNEX I

TECHNICAL PROGRESS MEETING

Compiled by A. F. Rowcliffe

This meeting was held at Oak Ridge National Laboratory on March 17, 1989, to review the technical progress on the collaborative DOE/JAERI program on fusion reactor materials. The purpose of the program is to determine the effects of neutron irradiation on the mechanical behavior and dimensional stability of U.S. and Japanese austenitic stainless steels. Phase I of the program focused on the effects of high concentrations of helium on the tensile, fatigue, and swelling properties of both U.S. and Japanese alloys. In Phase II of the program, spectral and isotopic tailoring techniques are fully utilized to reproduce the helium:dpa ratio typical of the fusion environment. The Phase II program hinges on a restart of the High Flux Isotope Reactor by mid-1989. Eight target position capsules and two RB* position capsules have been assembled. The target capsule experiments will address issues relating to the performance of austenitic steels at high damage levels including an assessment of the performance of a variety of weld materials. The RB* capsules will provide a unique and important set of data on the behavior of austenitic steels irradiated under conditions which reproduce the damage rate, dose, temperature, and helium generation rate expected in the first wall and blanket structure of the International Thermonuclear Experimental Reactor.

AGENDA FOR THE TENTH DOE/JAERI ANNEX I TECHNICAL PROGRESS MEETING

MARCH 17, 1989

DIRECTOR'S CONFERENCE ROOM (ROOM 284, 4500N)

OAK RIDGE NATIONAL LABORATORY

CO-CHAIRMEN: E. E. BLOOM (ORNL) T. KONDO (JAERI)

8:15–8:30 a.m.	Welcome and Introductory Remarks . . . . Discussion of Steering Committee Agenda .	E. E. Bloom/ T. Kondo
8:30–9:00	Summary of Phase I Swelling and Mechanical Property Data on JPCA J316	A. Hishinuma and P. J. Maziasz
9:00–9:20	Tensile and Fatigue Properties from the Phase I Experiments	M. L. Grossbeck
9:20–9:45	Microstructural Development in Austenitic and Ferritic Steels Irradiated in Phase I .	M. Suzuki
9:45–10:10	Correlation of TEM and Density Data . . .	T. Sawai
10:10–10:20	BREAK	
10:20–10:40	Status of Spectrally Tailored Experiments	A. W. Longest
10:40–11:00	Tensile Data from the ORR 6J/7J Experiment	M. L. Grossbeck
11:00–11:30	Microstructural Analysis of Austenitic Steels Irradiated in 6J/7J	T. Sawai
11:30–11:45	Status of Dosimetry Measurements	M. L. Grossbeck
11:45–1:15	LUNCH	
1:15–1:45	Low-Temperature Irradiation Creep Data from Spectrally Tailored Experiments . . .	M. L. Grossbeck
1:45–2:05	The Phase II HFIR Target Experiments . . .	R. L. Senn
2:05–2:25	Isotopically Tailored Alloys for the Phase II Target Experiments	P. J. Maziasz
2:25–2:55	Development of the ITER Design Data Base	M. L. Grossbeck
2:55–3:30	Stress Corrosion Cracking Sensitivity . . .	T. Inazumi
3:30	Discussion	

SUMMARY OF PHASE I SWELLING AND MECHANICAL PROPERTY DATA FOR JPCA AND J316

A. Hishinuma

ABSTRACT

Data of the swelling behavior and tensile properties were summarized on the candidate alloys of Japanese Primary Candidate Alloy (JPCA) and type 316 stainless steel (J316) irradiated in the High Flux Isotope Reactor (HFIR) at temperatures ranging from 573 to 873 K to the maximum dose of 56 dpa (4160 appm He). Little temperature dependence of small swelling less than about 1% was observed in both solution-annealed (SA) and cold-worked (CW) JPCA and J316 at irradiation temperatues ≤673 K up to nearly 56 dpa. At temperature 773 K, the swelling increased rapidly in SA although CW alloys still had good swelling resistance. Different tensile properties were also observed between temperatures below 703 K and above 773 K; in the low temperature region, no substantial change induced by irradiation on the work hardening character, while in the high temperature the apparent work hardening coefficient *n* became very large through the microstructural changes due possibly to precipitation. Decrease in ductility arose by decrease in fracture strength and/or fracture strain.

Table 2. Swelling of HFIR irradiated JPCA and J316 calculated from the cavity volume fraction.

Irrad. Temperature (K)	JPCA Damage (dpa/appm)	JPCA Swelling (%) SA	JPCA Swelling (%) CW	J316 Damage (dpa/appm)	J316 Swelling (%) SA	J316 Swelling (%) CW
573	33/2575	0.23	0.21	32/2232	0.13	0.15
	56/4011	0.18	-	56/3478	0.06	0.03
673	33/2575	0.25	0.40	32/2232	0.22	0.14
	56/3975	0.77*	0.62*	55/3445	0.53	0.08
773	34/2372	0.51	0.12	33/2057	1.1	0.16
	56/3975	3.7	0.42	55/3445	2.3	0.70

* the immersion density measurement

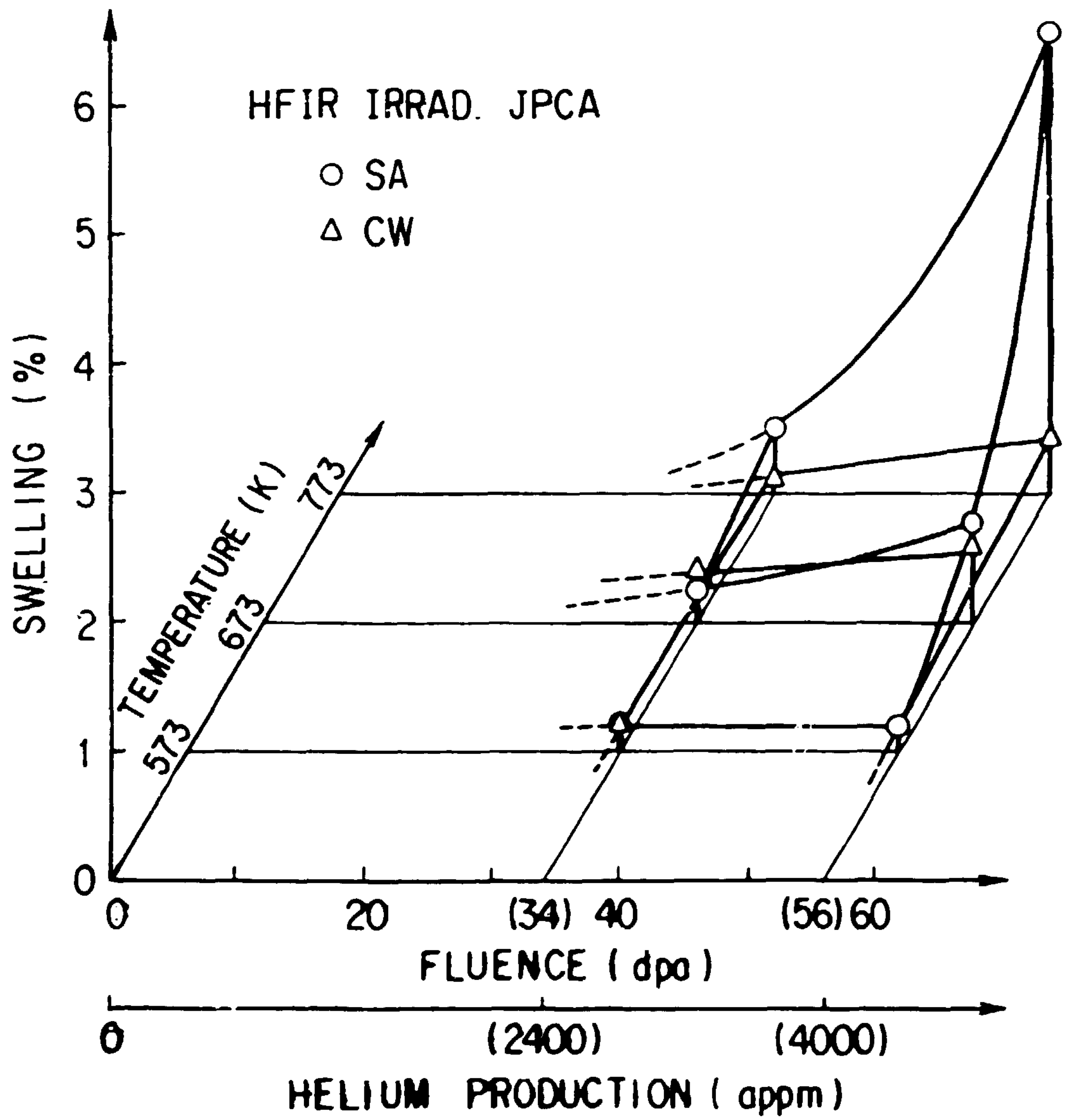
HFIR IRRAD. JPCA
○ SA
△ CW
SWELLING (%)
0
1
2
3
4
5
6
TEMPERATURE (K)
573
673
773
0
20
(34) 40
(56) 60
FLUENCE (dpa)
0
(2400)
(4000)
HELIUM PRODUCTION (appm)

Fig. 1

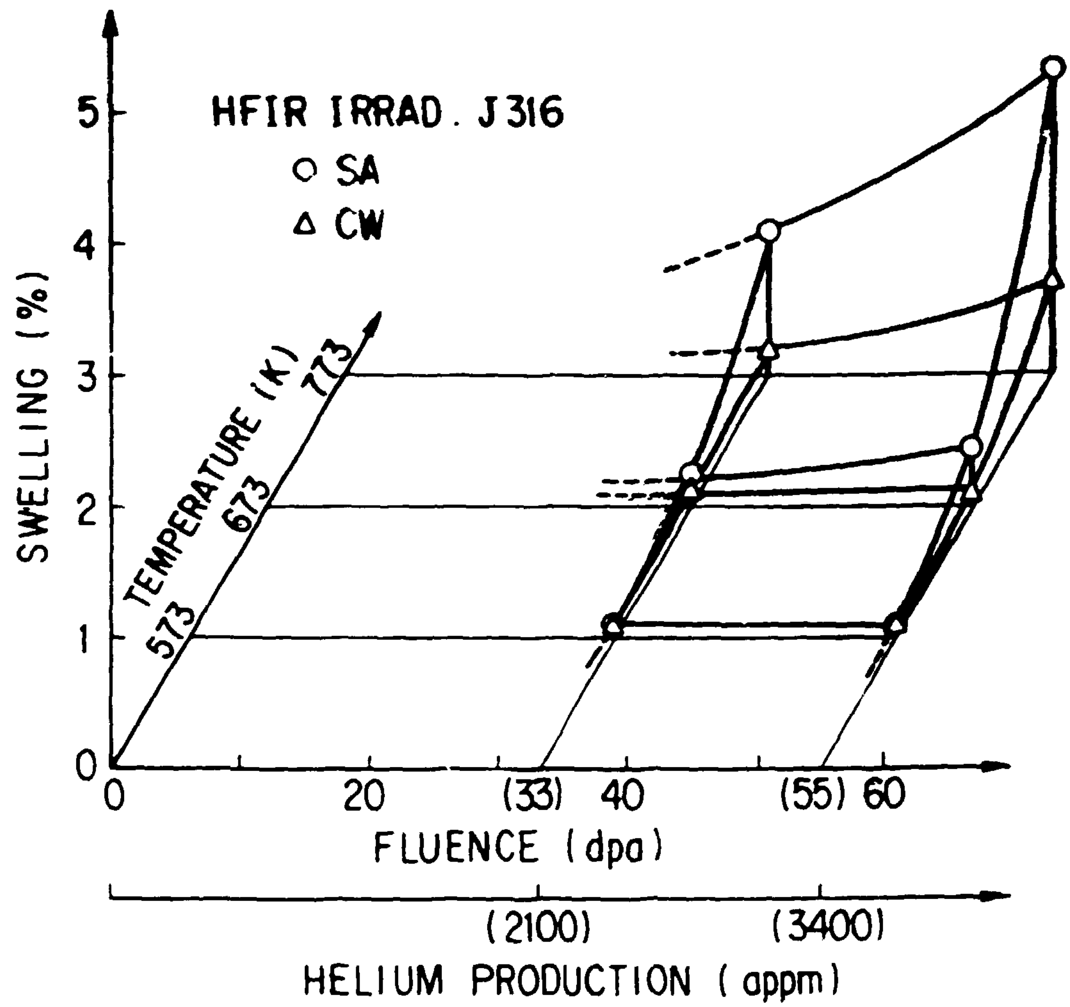
HFIR IRRAD. J316
○ SA
△ CW
SWELLING (%)
0
1
2
3
4
5
TEMPERATURE (K)
573
673
773
0
20
(33)
40
(55)
60
FLUENCE (dpa)
(2100)
(3400)
HELIUM PRODUCTION (appm)

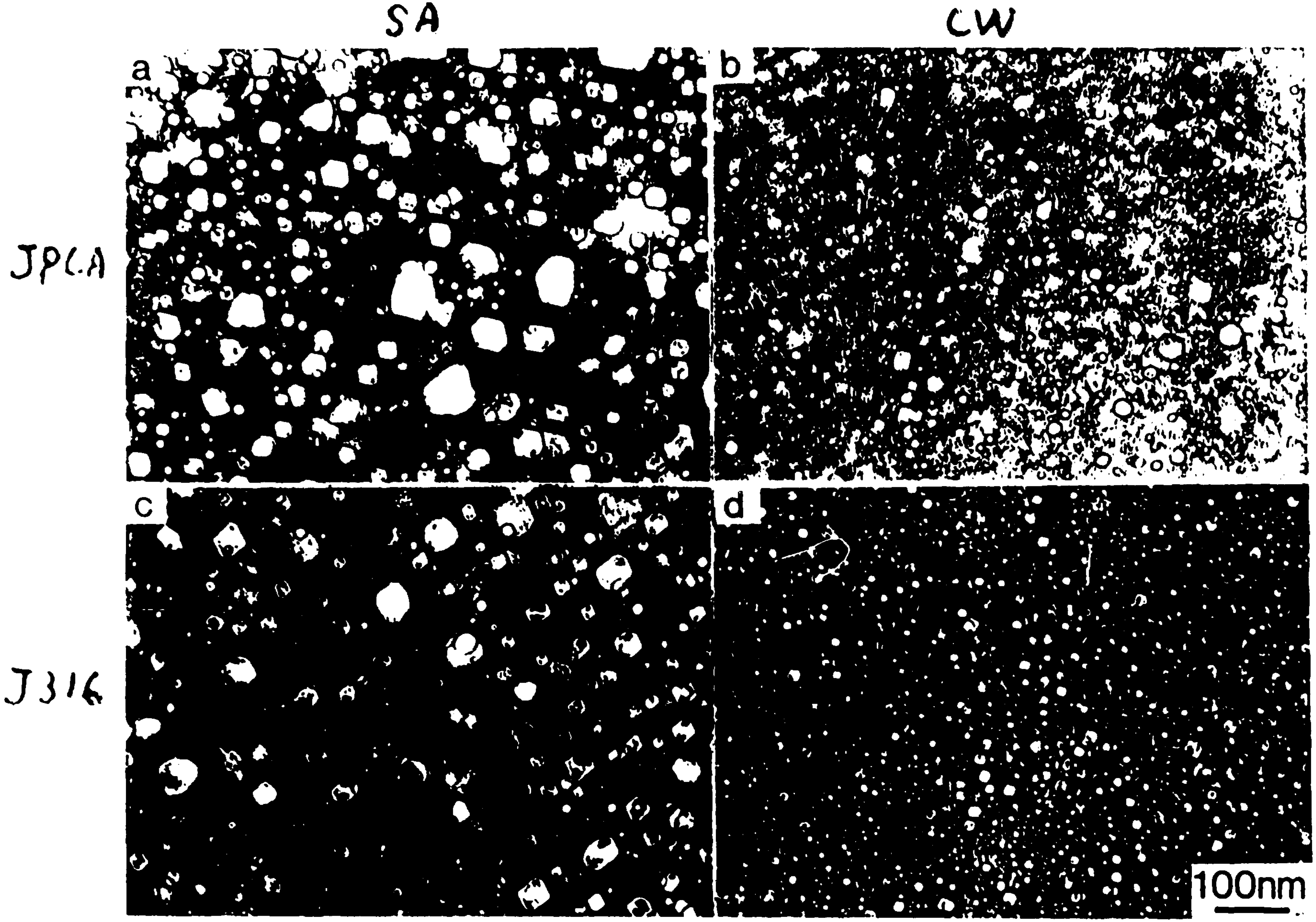
SA
CW
JPCA
J316
a
b
c
d
100nm

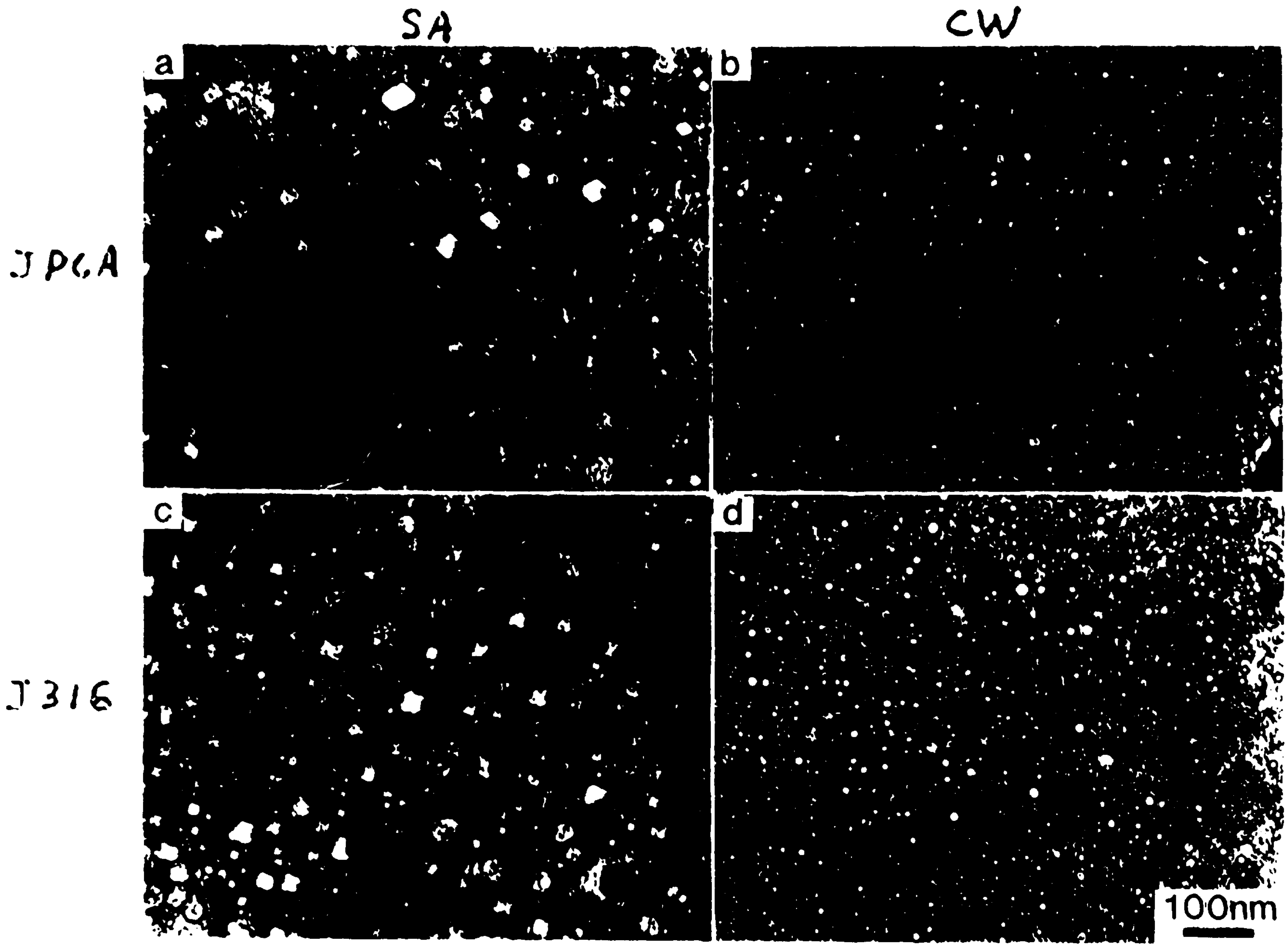
SA
CW
JPCA
J316
a
b
c
d
100nm

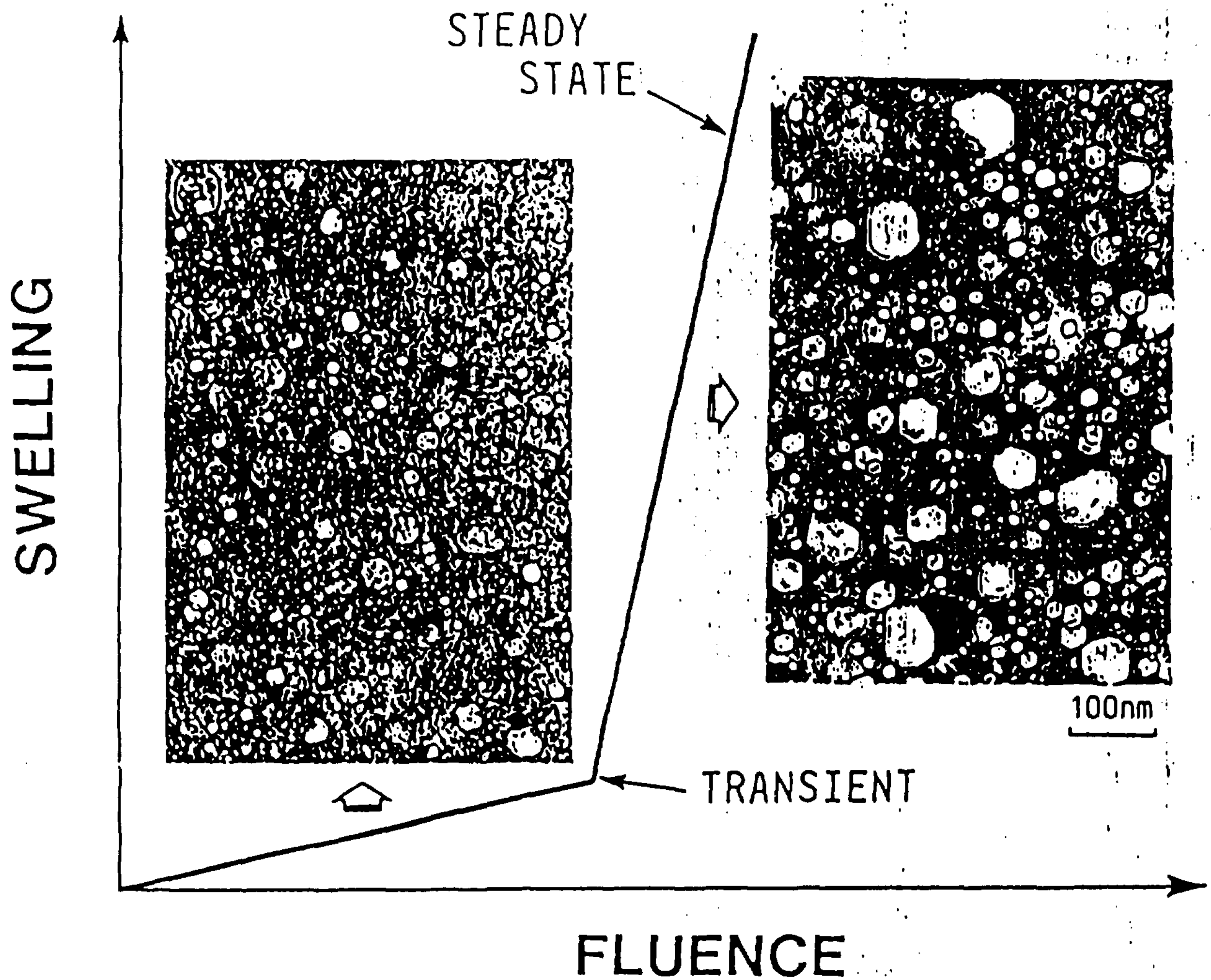

Schematic representation of the two regimes of irradiation-induced swelling-dose relationship and microstructures of PCA irradiated in HFIR at 500°C to 34 dpa(a) and 57 dpa(b).

Fig. 2

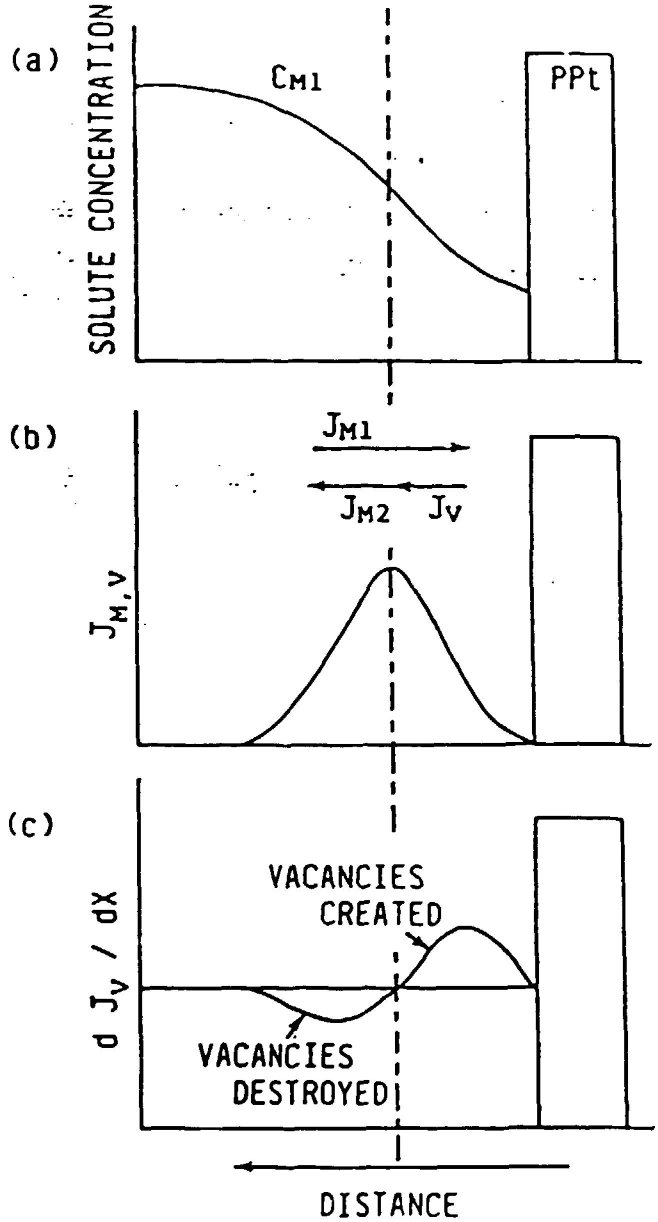

Distribution of solute concentration around the growing precipitate precipitate(ppt) and flows of both solute atom(J_M) and vacancy(J_V)

Fig. 1

Table 3 Tensile properties of irradiated JPCA

Irradiation and test temperature	Material and material condition	Damage (dpa/appmHe)	yield strength (MPa)	ultimate strength (MPa)	uniform elongation (%)	total elongation (%)
573K	JPCA-SA	16/1064	876	889	0.39	8.6
573K	JPCA-CW	16/1064	878	889	0.53	7.9
573K	JPCA-CW	16/1064	889	903	0.63	7.2
573K	JPCA-SA	27/1973	770	789	2.43	9.93
573K	JPCA-CW	27/1973	775	796	1.0	6.6
573K	JPCA-CW	27/1973	747	780	1.7	7.27
673K	JPCA-SA	22/1585	878	888	0.38	6.4
673K	JPCA-SA	22/1585	896	910	0.44	6.[illegible]
673K	JPCA-CW	22/1585	952	972	0.42	5.5
673K	JPCA-CW	22/1585	889	974	1.4	6.3
673K	JPCA-SA	38/1817	868	872	0.55	5.69
673K	JPCA-CW	38/1817	914	946	0.49	5.01
703K	JPCA-SA	47/3488	742	781	1.8	5.19
773K	JFCS-SA	27/2008	650	732	4.[illegible]	8.2
773K	JPCA-SA	27/2008	631	724	7.2	11.7
773K	JPCA-CW	27/2008	678	765	7.1	11.4
773K	JPCA-CW	27/2008	624	713	6.3	10.2
773K	JPCA-SA	46/3446	620	682	5.76	7.79
773K	JPCA-CW	46/3446	663	734	4.49	5.82
773K	JPCA-CW	53/3950	640	675	1.04	1.47
873K	JPCA-CW	33/2400	432	521	6.25	8.06
873K	JPCA-CW	33/2400	519	582	3.86	5.18
873K	JPCA-CW	56/4160	501	508	0.28	0.46

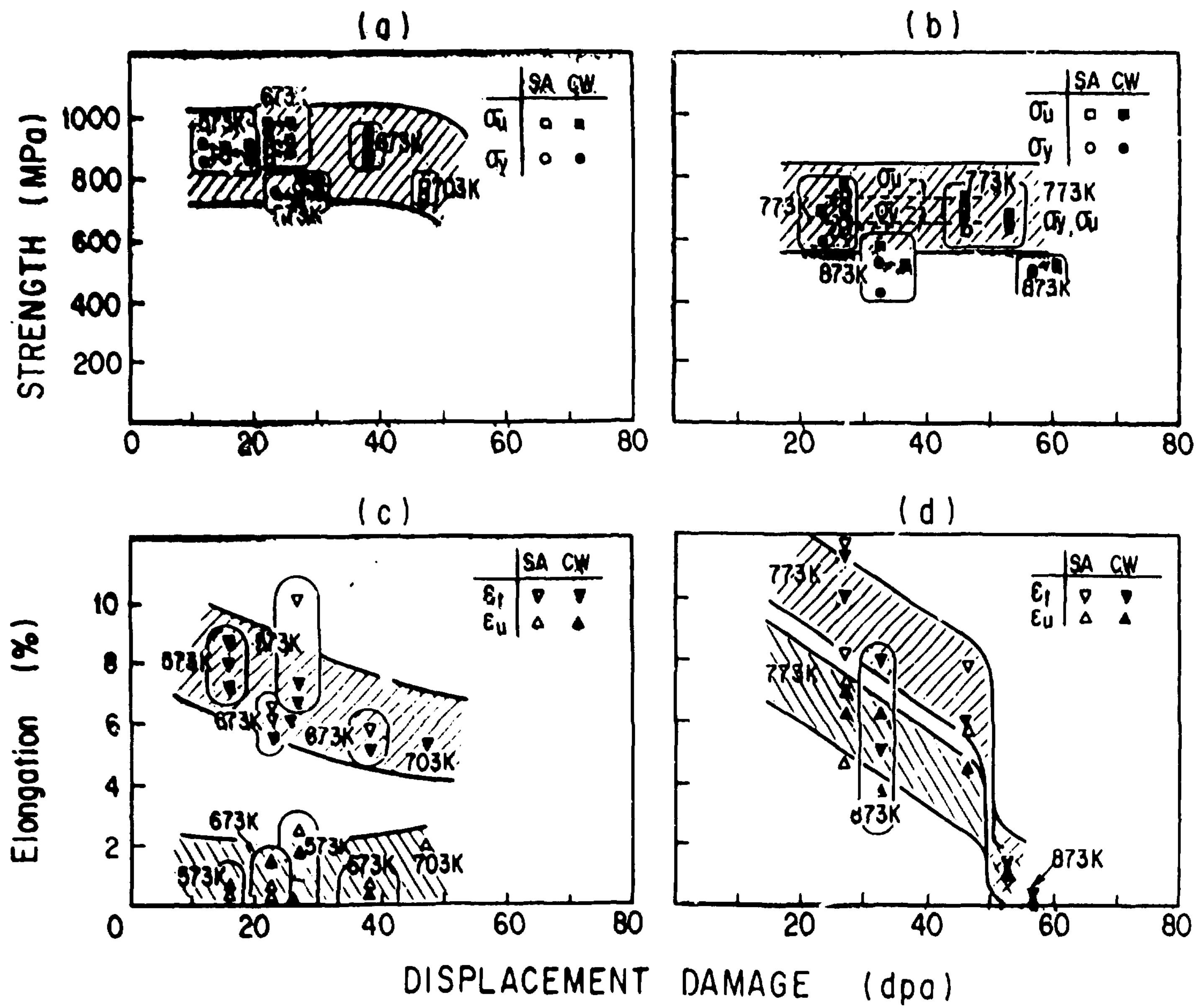
(a)
(b)
(c)
(d)
STRENGTH (MPa)
Elongation (%)
DISPLACEMENT DAMAGE (dpa)
SA CW
873K
773K
673K
703K

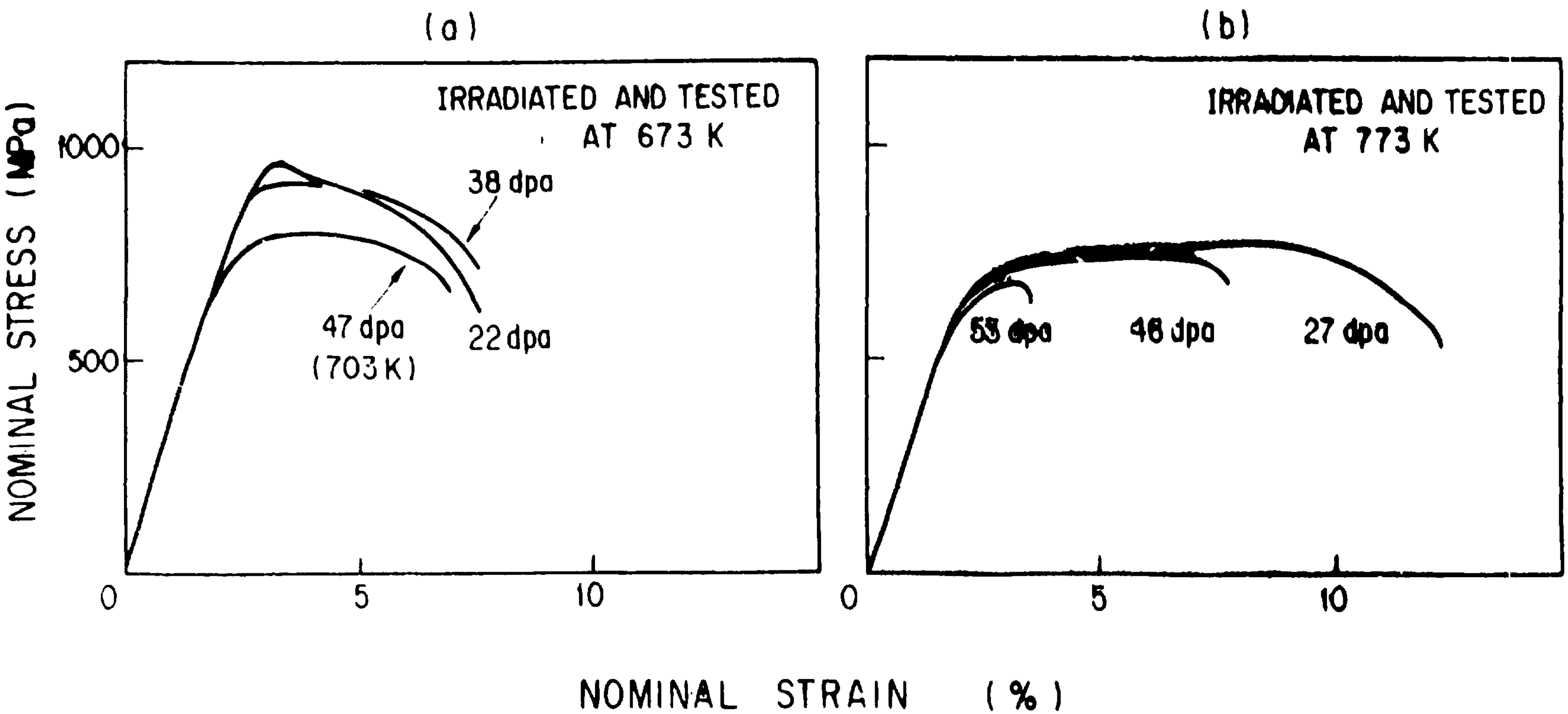

(a)
IRRADIATED AND TESTED
AT 673 K
38 dpa
47 dpa
(703 K)
22 dpa
1000
500
0
5
10
NOMINAL STRESS (MPa)
(b)
IRRADIATED AND TESTED
AT 773 K
53 dpa
46 dpa
27 dpa
0
5
10
NOMINAL STRAIN (%)

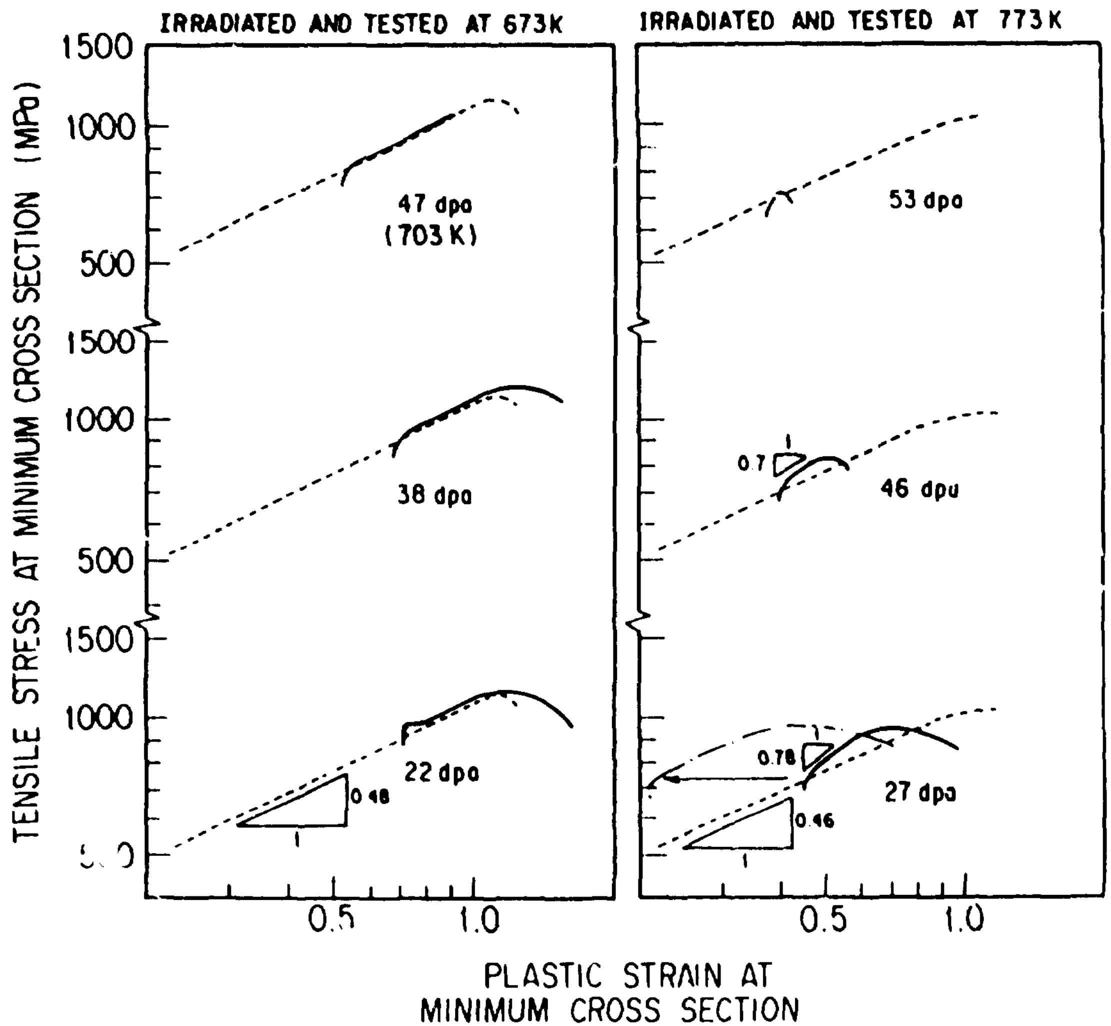

IRRADIATED AND TESTED AT 673K
IRRADIATED AND TESTED AT 773K
TENSILE STRESS AT MINIMUM CROSS SECTION (MPa)
1500
1000
500
47 dpa
(703 K)
38 dpa
22 dpa
0.48
1
53 dpa
46 dpu
0.7
27 dpa
0.78
0.46
0.5
1.0
PLASTIC STRAIN AT
MINIMUM CROSS SECTION

$$\sigma = A_0 (\varepsilon_0 + \varepsilon)^n$$

σ : true Tensile stress

A_0 : proportionality constant

ε_0 : equivalent plastic strain to irradiation hardening

n : work hardening coefficient

ε : Plastic strain by tensile deformation

Summary

Swelling in JPCA- and J316-CW is low and does not depend much on temperature. On the other hand, the swelling in SA specimens depends strongly on temperature; at 673K and below, they have a good swelling resistance, while at 773K and above, swelling increasesd steeply with tempreture. These data showed that the difference in swelling between SA and CW become significant at temperatures above 773K. The data also showed that better swelling resistance in JPCA lasted upto the dose of about 34 dpa. However, the swelling resistance appeared to decrease through the resolution of TiC particles which were considered to be an essential role for minimizing the swelling.

Tensile properties of irradiated specimens also changes between 703K and 773K, although the dose dependence of strength was very small with dose above 16 dpa. At temperatures of 703K and below, the temperature dependence of elongation was not so strong, especially the uniform elongation less than 2.5% were almost constant within the damage level of 50 dpa. While at temperatures of 773K and above, the total and uniform elongations decreased continuously with dose and moreover, those elongations were abruptly decreased to below 0.5% beyond 50 dpa. In the low temperature regiem, there were no substantial changes induced by irradiation on the work hardening character. At higher temperatures, apparent work hardening coefficiet became large possibly through the microstructual changes during the irradiation.

OVERVIEW OF IMMERSION-DENSITY SWELLING DATA FROM PHASE I HFIR EXPERIMENTS

P. J. Maziasz

ABSTRACT

A considerable data base of swelling values measured by immersion density has been accumulated from U.S. and Japanese TEM disks irradiated in the HFIR Phase I target experiments at 300 to 500°C to 34 and 57 dpa. After 34 dpa, swelling is very low at 300 and 400°C, but is much higher at 500°C. At 500°C, swelling is quite sensitive to alloy composition and thermomechanical pretreatment. Swelling in 20% CW JPCA is as low as 0.7%, but can be as high as 16% in SA JPCA-C.

After 57 dpa, swelling continues to increase in many alloys with dose at 500°C, as would be expected. However, in addition to positive swelling at various rates, alloys with nearly zero swelling rate and negative swelling rates are also observed in this dose range at 500°C. The phosphorus-modified D9 and PCA alloys from the U.S. side show constant low swelling (0.1 to 1.0%) over this same dose range, and 20% CW JPCA shows only a slight increase from 34 to 57 dpa. The swelling of the U.S. 25% CW PCA actually decreases somewhat with increasing dose, as do several other U.S. alloys which have varying amounts of swelling after 34 dpa. Swelling in the U.S. 25% CW D9 remains constant at about 3% with dose. The SA JPCA-C alloy shows 22% swelling after 57 dpa at 500°C.

Swelling at 400°C remains consistently low (0.3 to 0.8%) among all the U.S. and Japanese alloys from 34 to 57 dpa. At 300°C, however, some U.S. and Japanese alloys now show similar or slightly more swelling than at 400°C. The 25% CW PCA shows about 1.5 to 1.8% swelling at 300°C after 57 dpa.

While many of these swelling trends may seem strange relative to the behavior expected from FBR studies, data on these alloys irradiated to helium levels of about 4500 appm He are new, particularly high doses at temperatures of 300 and 400°C. Although unusual, most of the strange swelling behavior can be explained by helium effects on the mechanisms that cause microstructural evolution.

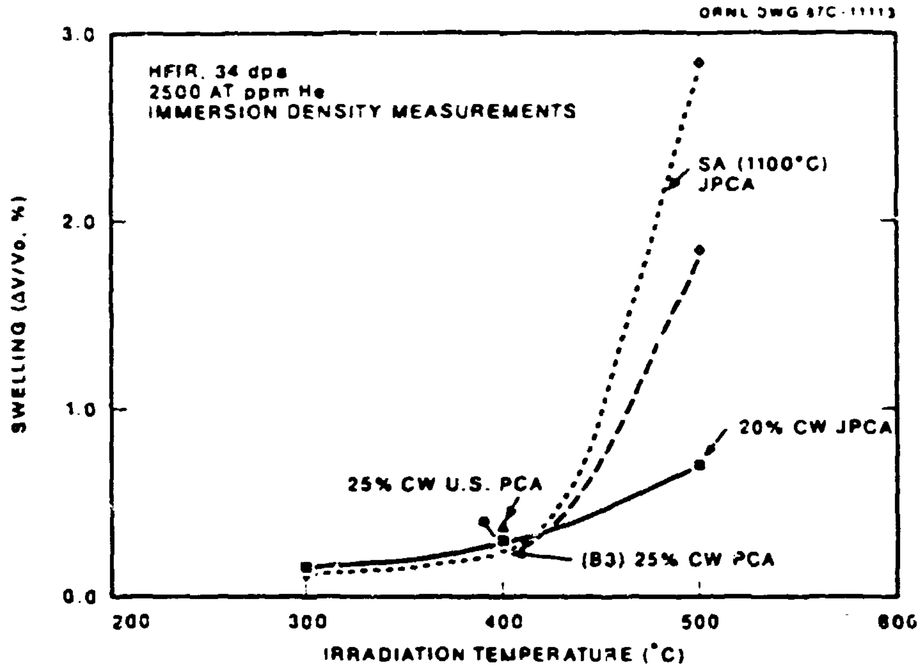
ORNL DWG 87C-11113
HFIR, 34 dpa
2500 AT ppm He
IMMERSION DENSITY MEASUREMENTS
SA (1100°C)
JPCA
20% CW JPCA
25% CW U.S. PCA
(B3) 25% CW PCA
SWELLING (ΔV/Vo, %)
IRRADIATION TEMPERATURE (°C)
3.0
2.0
1.0
0.0
200
300
400
500
600

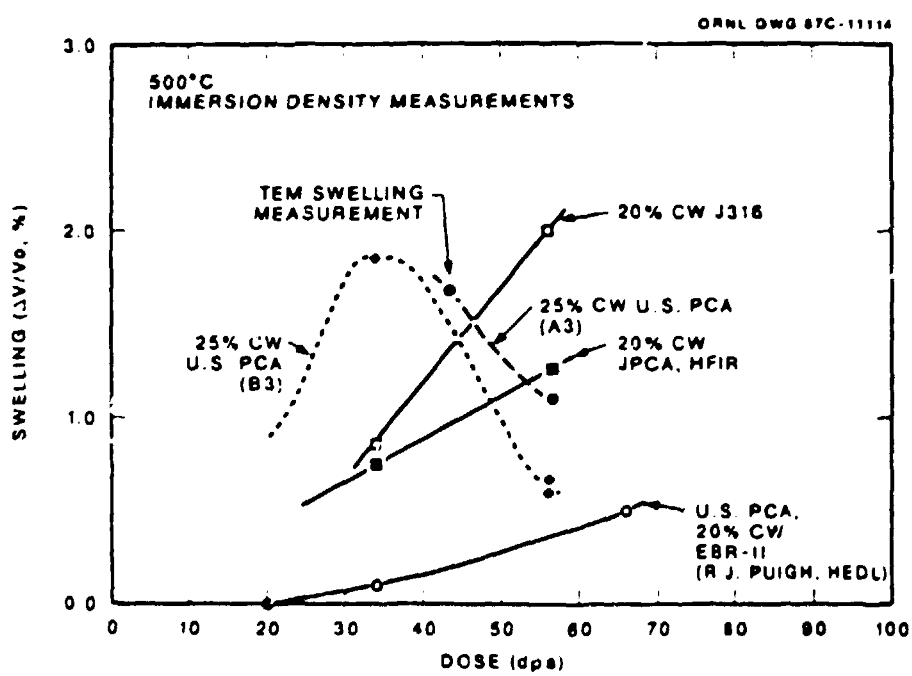
ORNL DWG 87C-11114
500°C
IMMERSION DENSITY MEASUREMENTS
TEM SWELLING
MEASUREMENT
20% CW J316
25% CW U.S. PCA
(A3)
25% CW
U.S. PCA
(B3)
20% CW
JPCA, HFIR
U.S. PCA,
20% CW
EBR-II
(R J. PUIGH, HEDL)
SWELLING (ΔV/Vo, %)
DOSE (dpa)
3.0
2.0
1.0
0.0
0
10
20
30
40
50
60
70
80
90
100

ORNL-DWG 88M-8183

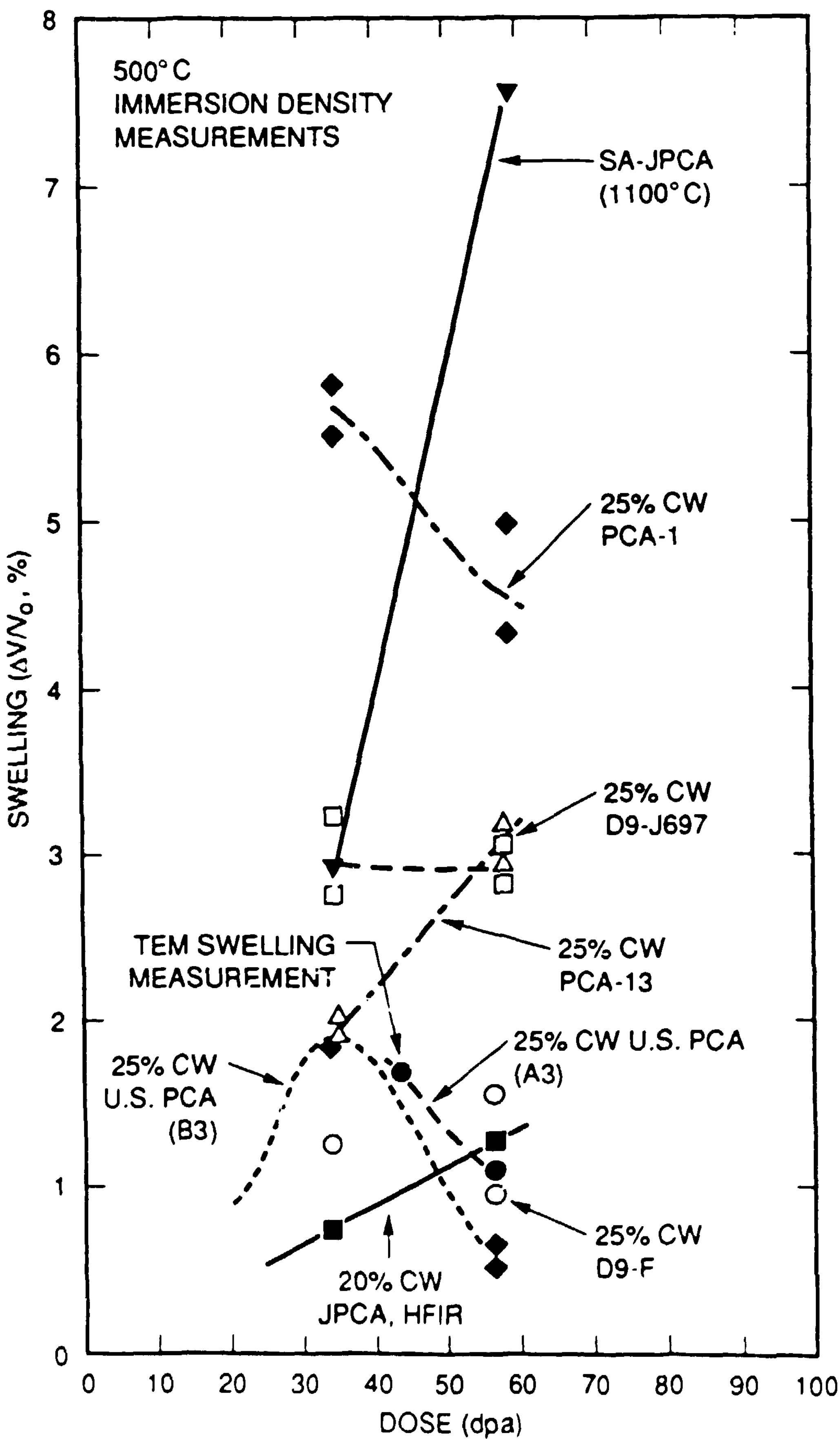

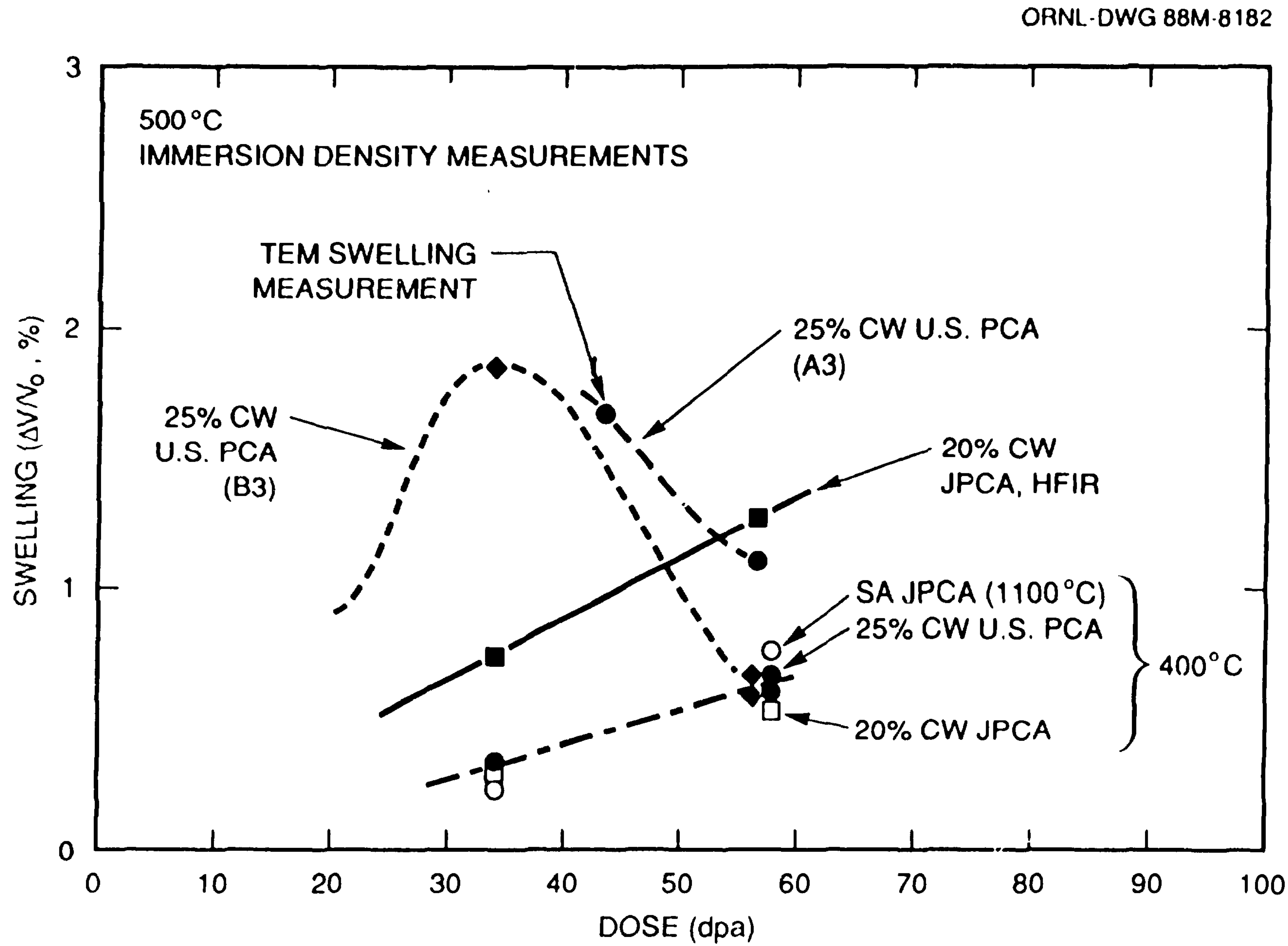
ORNL-DWG 88M-8182
500 °C
IMMERSION DENSITY MEASUREMENTS
TEM SWELLING
MEASUREMENT
25% CW U.S. PCA
(A3)
25% CW
U.S. PCA
(B3)
20% CW
JPCA, HFIR
SA JPCA (1100 °C)
25% CW U.S. PCA
20% CW JPCA
400 °C
SWELLING (ΔV/V₀ , %)
DOSE (dpa)
0
1
2
3
0
10
20
30
40
50
60
70
80
90
100

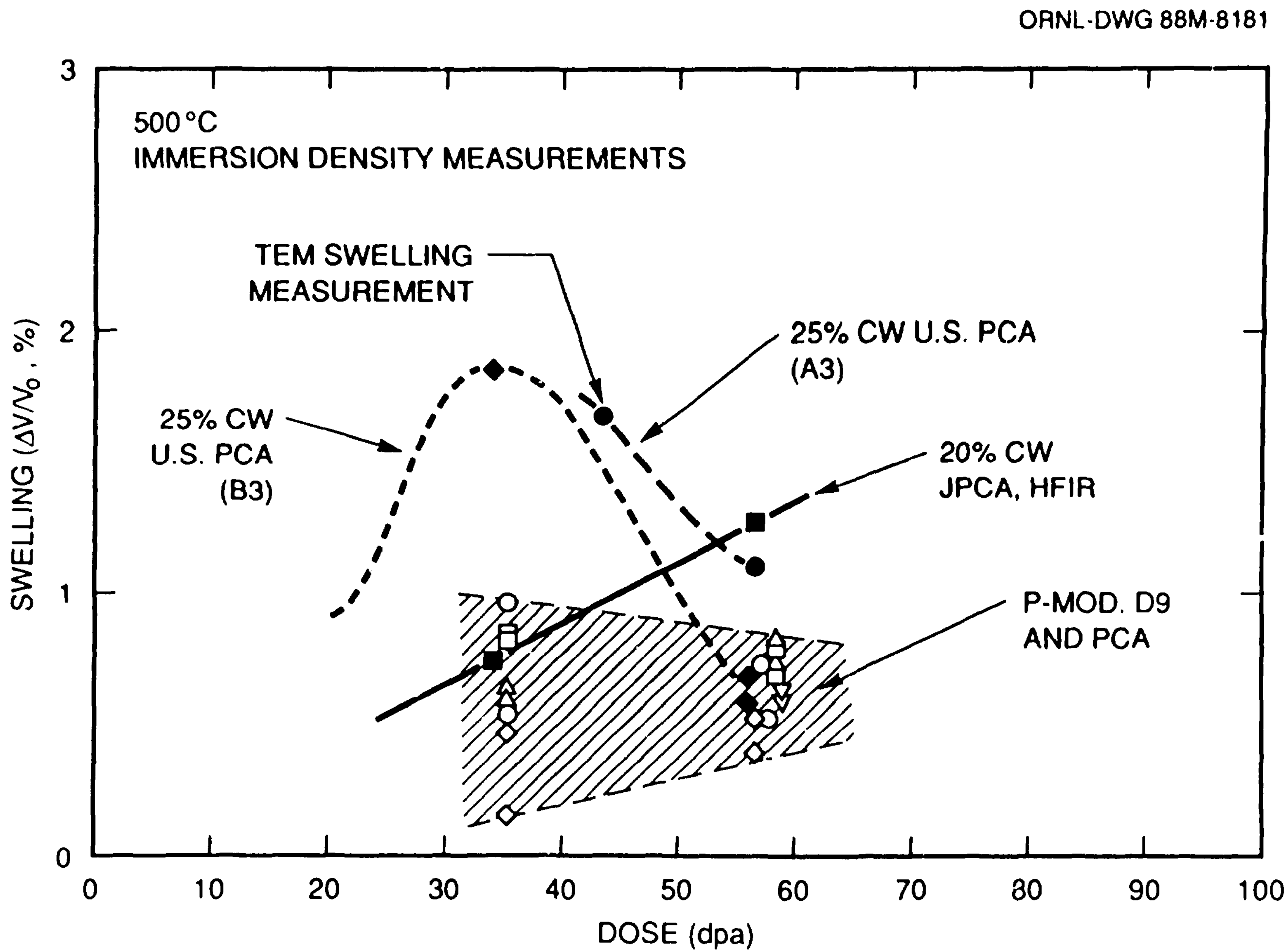

ORNL-DWG 88M-8181
500 °C
IMMERSION DENSITY MEASUREMENTS
TEM SWELLING
MEASUREMENT
25% CW U.S. PCA
(A3)
25% CW
U.S. PCA
(B3)
20% CW
JPCA, HFIR
P-MOD. D9
AND PCA
SWELLING (ΔV/V₀ , %)
DOSE (dpa)
0
1
2
3
0
10
20
30
40
50
60
70
80
90
100

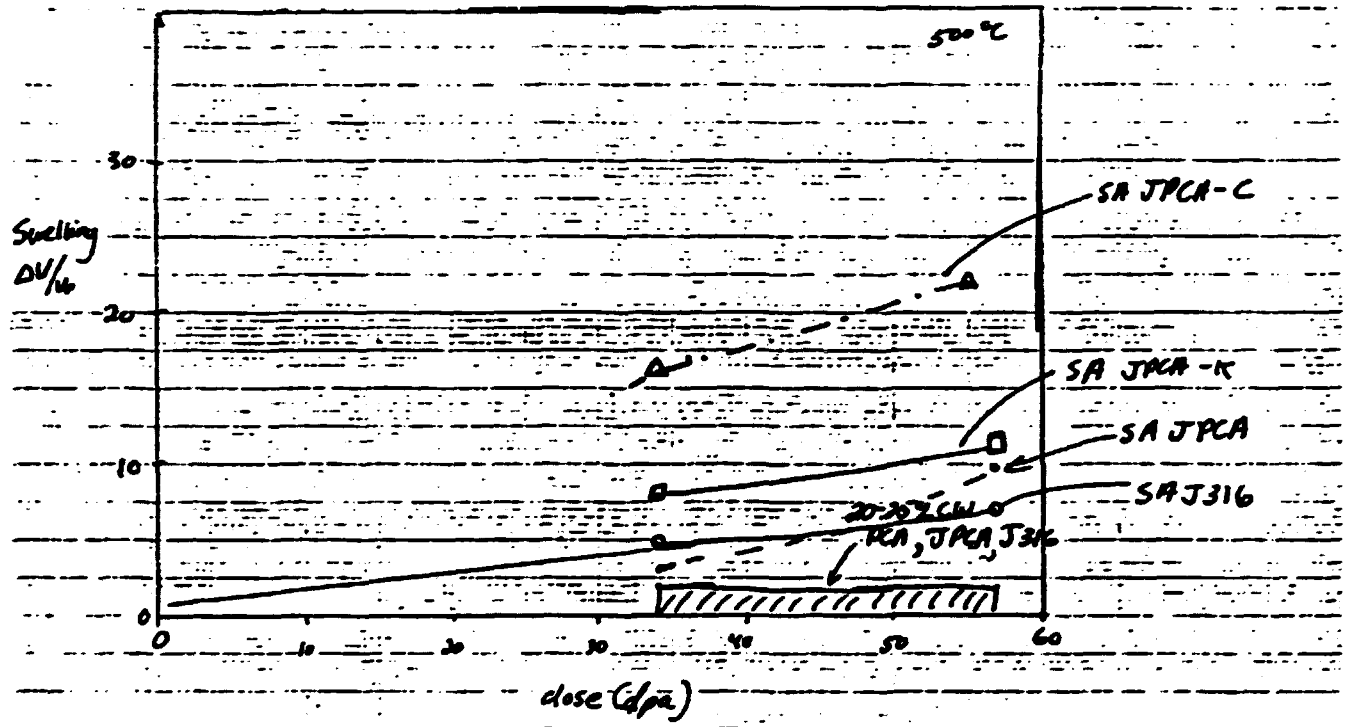
500°C
Swelling ΔV/V₀
30
20
10
0
SA JPCA-C
SA JPCA-K
SA JPCA
SA J316
20-30% CW
PCA, JPCA, J316
0
10
20
30
40
50
60
dose (dpa)

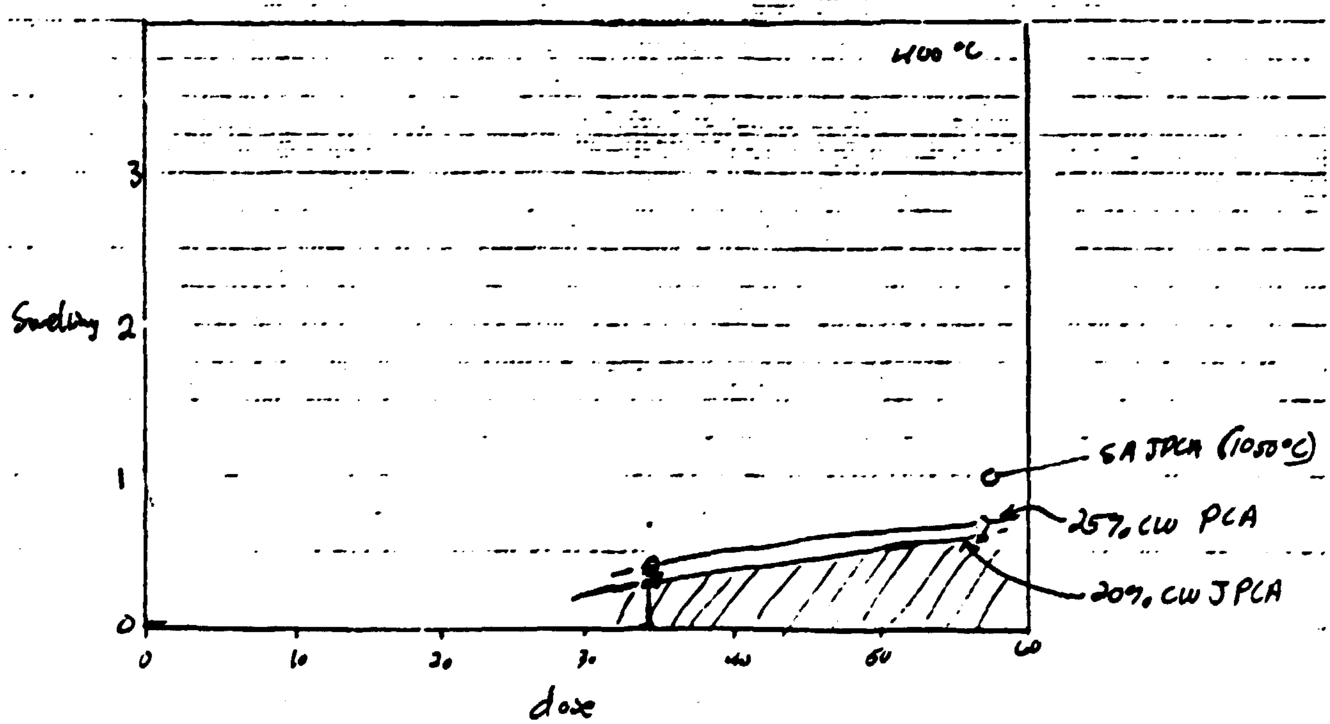
400°C
Swelling
3
2
1
0
SA JPCA (1050°C)
25% CW PCA
20% CW JPCA
0
10
20
30
40
50
60
dose

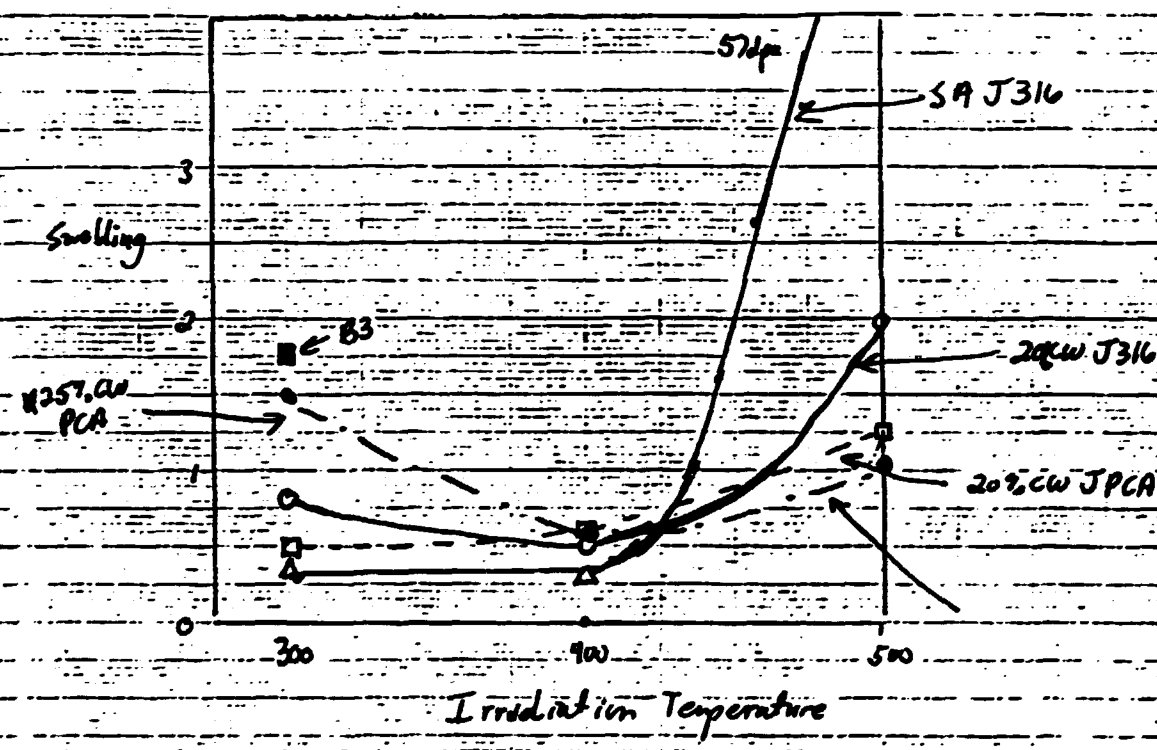

57dpa
SA J316
3
Swelling
2
B3
25% CW PCA
20% CW J316
1
20% CW JPCA
0
300
400
500
Irradiation Temperature

MAJOR SUMMARY POINTS

HFIR Phase I Data - 57 dpa, 300-500°C

* Dose dependence varies considerably at 500°C. Swelling rates vary from positive to nearly zero, to *negative* values.

* Swelling rates are uniformly low at 400°C.

* Swelling of several alloys increases with decreasing temperature from 300°C relative to 400°C.

MAJOR SUMMARY POINTS

HFIR Phase I Data - 34 dpa, 300-500°C

* Swelling is very low at 300 and 400°C. Swelling is much higher at 500°C, and very sensitive to alloy composition and pretreatment

Alloy	$\Delta V/V_o$ (%)
20%CW JPCA	0.7
SA JPCA	3.0
SA JPCA-K	8.0
SA JPCA-C	16

TENSILE AND FATIGUE PROPERTIES FROM THE PHASE I EXPERIMENTS

M. L. Grossbeck and T. Sawai

ABSTRACT

The U.S./Japan Phase I HFIR experiments are the first series of experiments where a single set of specimens of the same alloys was irradiated from 15 to 50 dpa over a temperature range of 60 to 600°C. This series of experiments has done more than any other single experiment to unveil the trends of tensile properties as functions of temperature and fluence at high helium levels. Two important conclusions are that strength is highly independent of alloy composition and that uniform elongation has very low values between 60 and 400°C even in annealed material. At higher temperatures, both uniform and total elongations decrease at 50 dpa more precipitously than for fast reactor irradiations. At this damage level, the helium concentration exceeds 3000 appm and is almost certain to be responsible for the onset of embrittlement at lower temperatures than previously observed.

Welds in both J316 and JPCA were irradiated at 60°C to 50 dpa. Tensile tests revealed large reductions in ductility as indicated by uniform elongation. In the case of 20% cold-worked material, JPCA exhibited lower ductility levels than J316. Welded annealed and cold-worked material had strength levels similar to annealed material following welding. Irradiation raised the strength of all materials, welded and unwelded, annealed and cold worked, to about the same level.

The fatigue program from JP 1 through -8 was particularly rewarding in that it was the first time that specimens irradiated to damage levels of 50 dpa and having 3000 appm He were tested. Unlike the previous, 15 dpa, 900 appm He, specimens where no effect of helium was observed, a reduction in fatigue life was observed. However, at 430°C, the reduction in fatigue life did not exceed the level of reduction observed at 15 dpa.

Future work will include primarily unirradiated tensile specimens. Fatigue testing will continue with the few remaining specimens to investigate the effect of irradiation on the endurance limit.

HFIR TARGET EXPERIMENTS

1. 15–55 dpa
1. 15 – 55 dpa
3. 300 – 600 C

   JPCA
   PCA
   US 316
   J 316

4. 900 – 4200 appm He
5. THE WIDEST RANGE OF FLUENCE FOR A CONSISTENT SET OF ALLOYS OF ANY HFIR EXPERIMENT

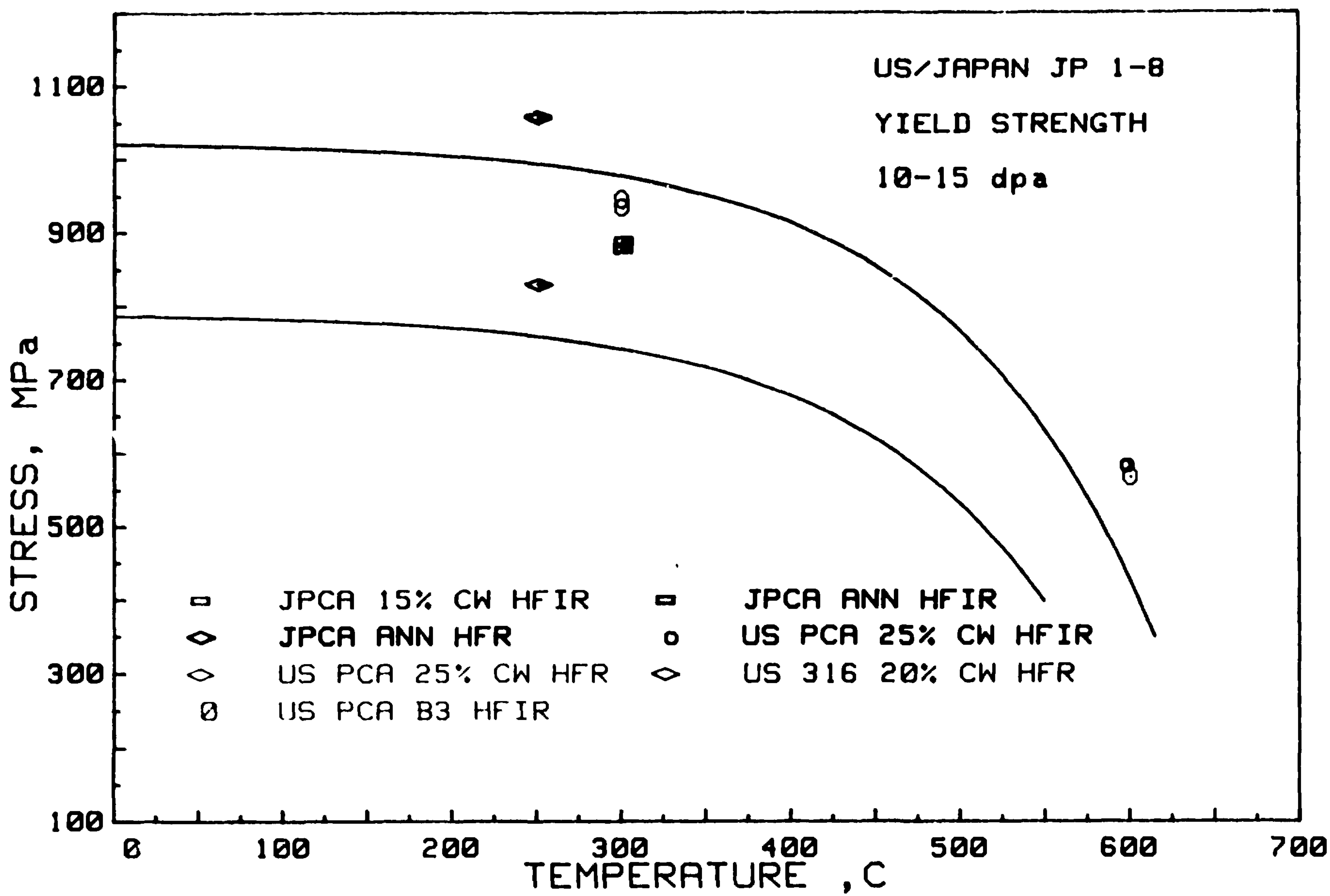

US/JAPAN JP 1-8
YIELD STRENGTH
10-15 dpa
JPCA 15% CW HFIR
JPCA ANN HFR
US PCA 25% CW HFR
US PCA B3 HFIR
JPCA ANN HFIR
US PCA 25% CW HFIR
US 316 20% CW HFR
STRESS, MPa
TEMPERATURE ,C

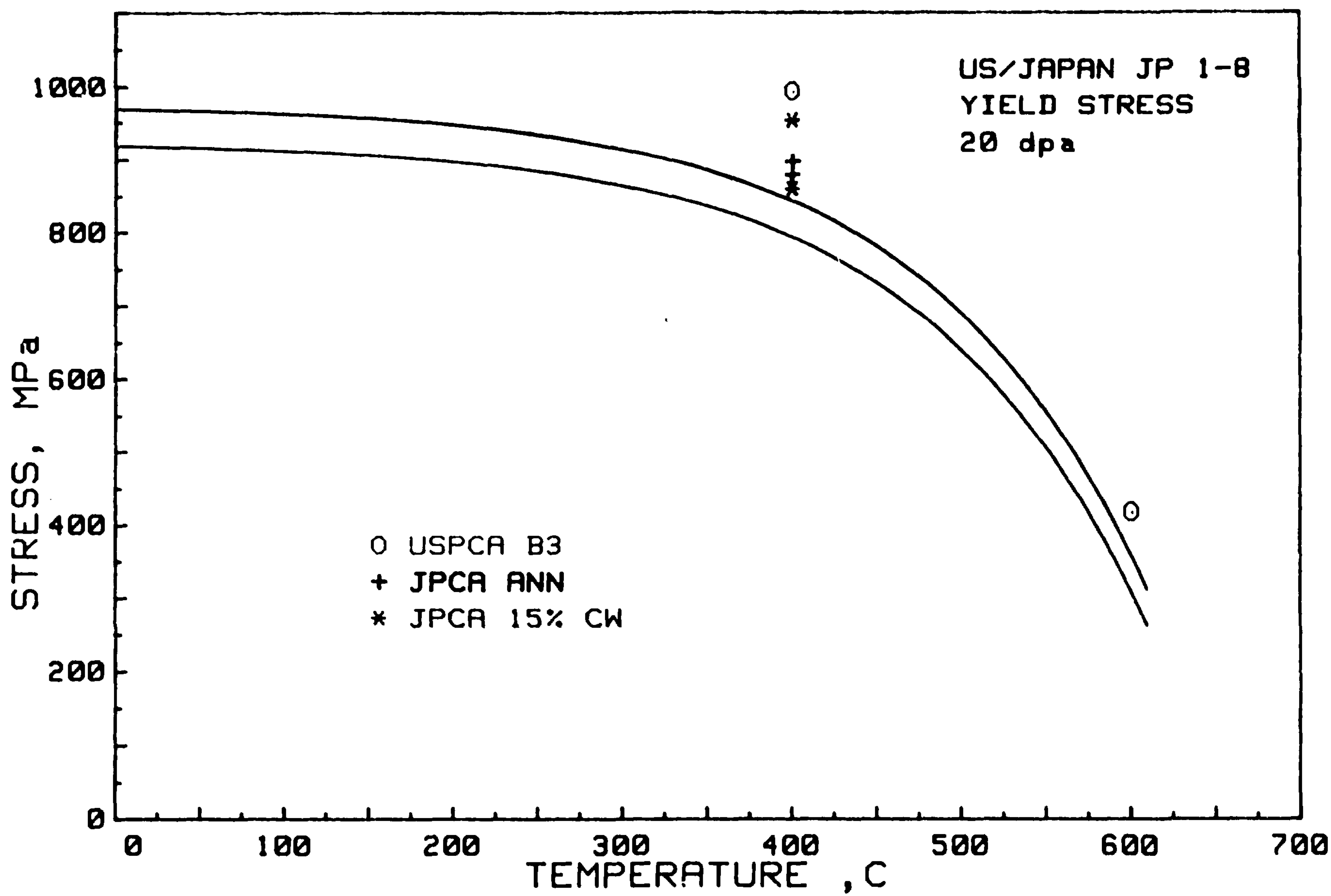
US/JAPAN JP 1-8
YIELD STRESS
20 dpa
O USPCA B3
+ JPCA ANN
* JPCA 15% CW
STRESS, MPa
1000
800
600
400
200
0
0
100
200
300
400
500
600
700
TEMPERATURE ,C

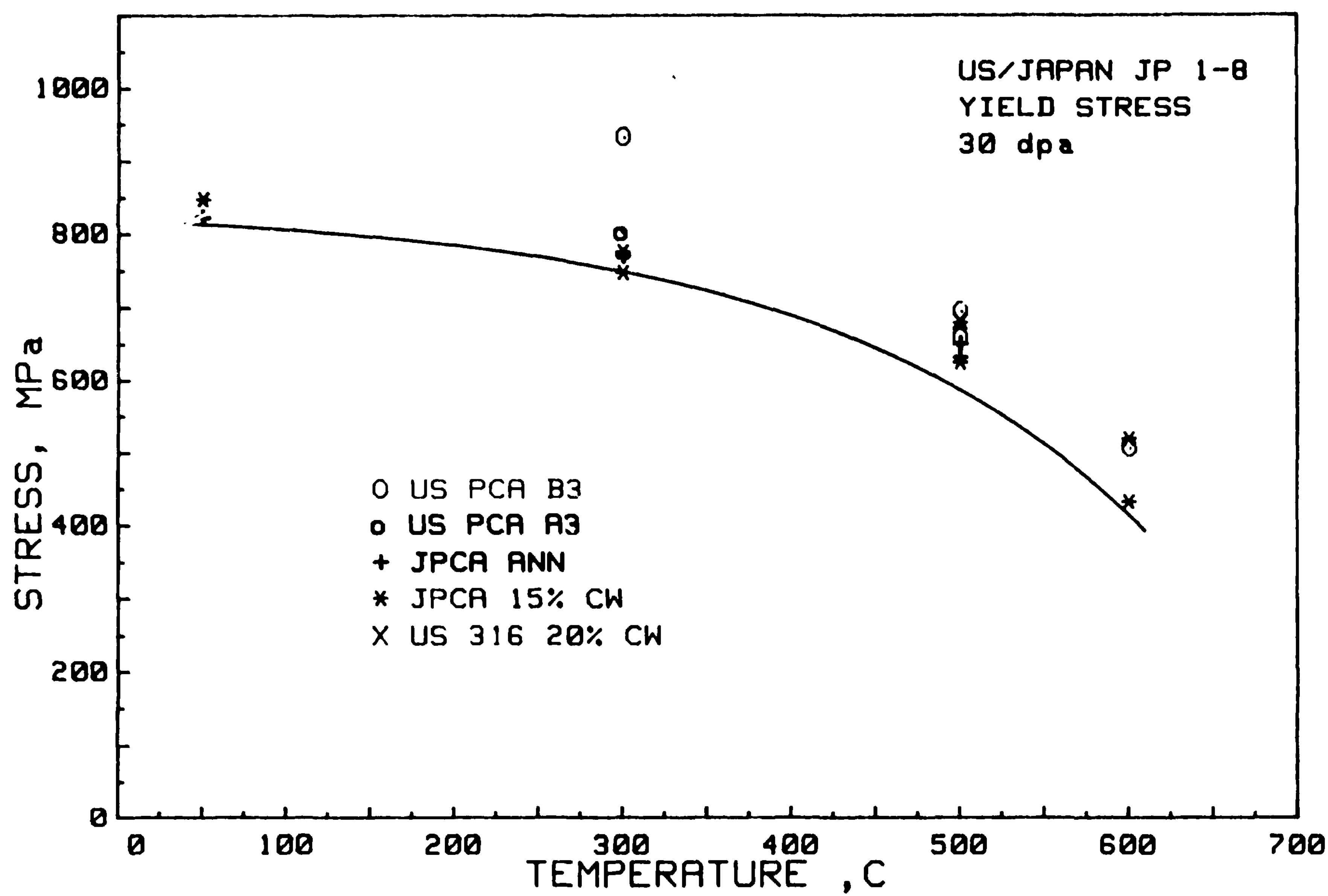
US/JAPAN JP 1-8
YIELD STRESS
30 dpa
O US PCA B3
o US PCA A3
+ JPCA ANN
* JPCA 15% CW
X US 316 20% CW
STRESS, MPa
TEMPERATURE ,C
0
200
400
600
800
1000
0
100
200
300
400
500
600
700

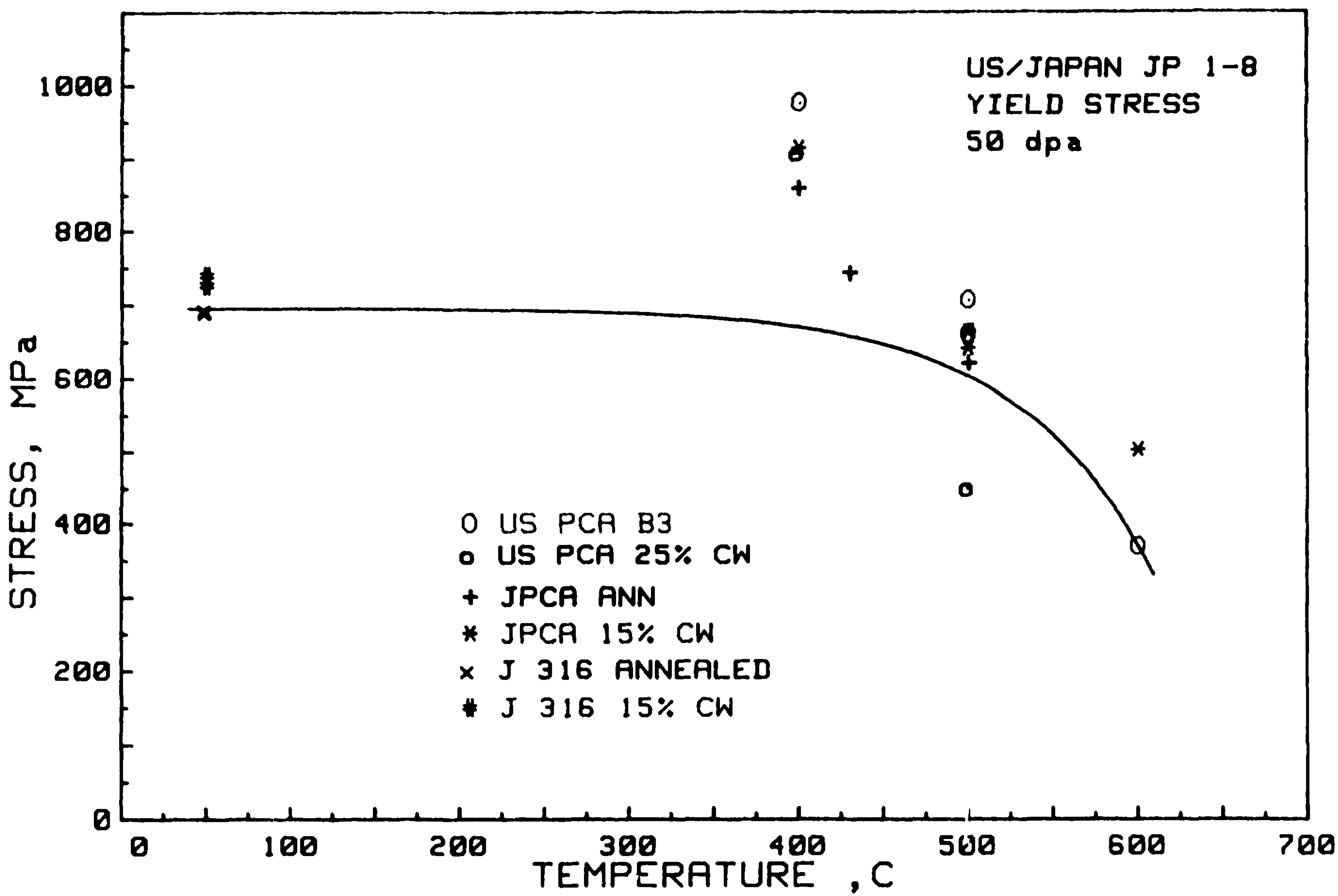
US/JAPAN JP 1-8
YIELD STRESS
50 dpa
O US PCA B3
o US PCA 25% CW
+ JPCA ANN
* JPCA 15% CW
x J 316 ANNEALED
J 316 15% CW
STRESS, MPa
TEMPERATURE ,C
0
200
400
600
800
1000
0
100
200
300
400
500
600
700

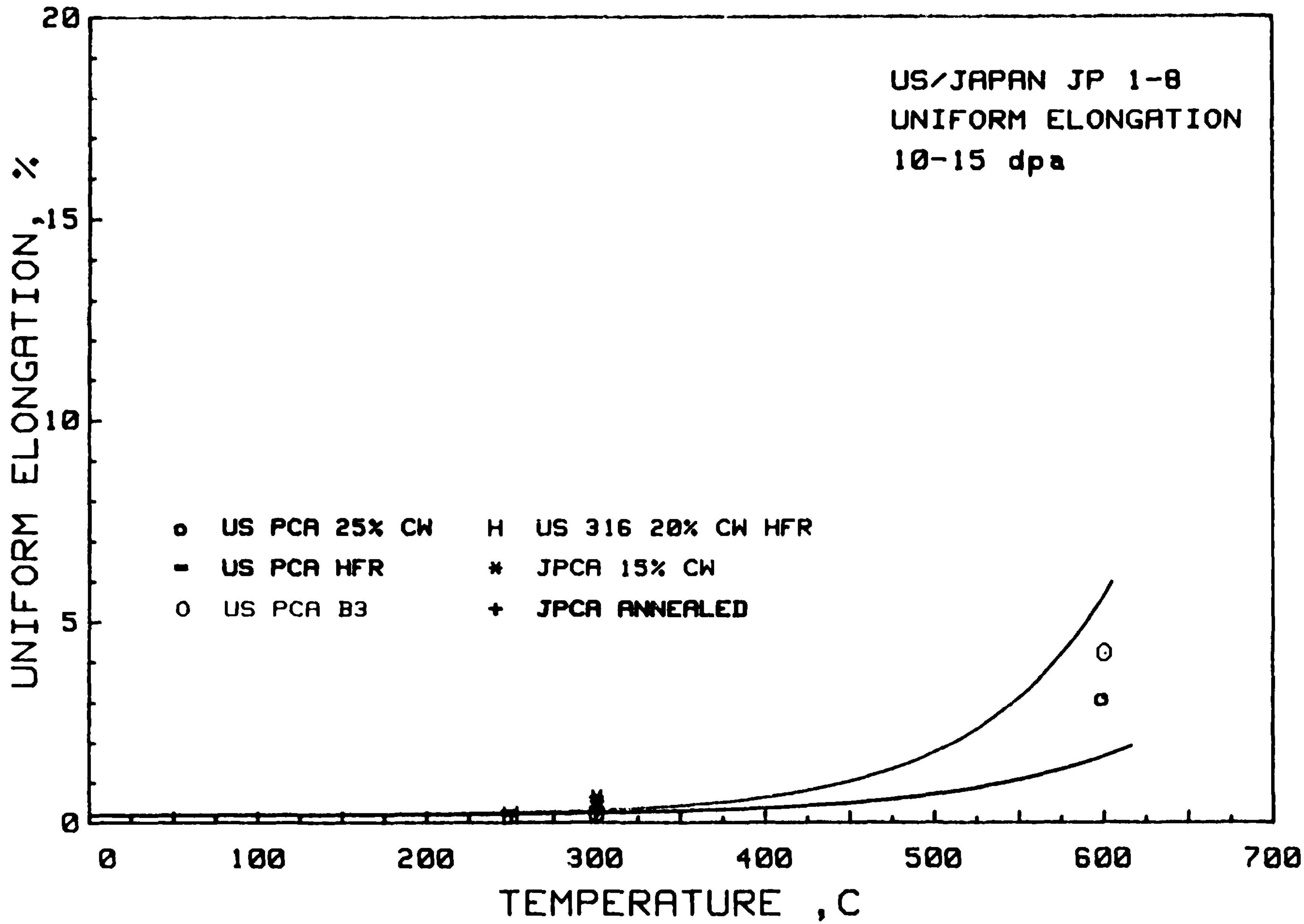

US/JAPAN JP 1-8
UNIFORM ELONGATION
10-15 dpa
US PCA 25% CW
US PCA HFR
US PCA B3
H US 316 20% CW HFR
JPCA 15% CW
JPCA ANNEALED
UNIFORM ELONGATION, %
TEMPERATURE ,C
0
5
10
15
20
0
100
200
300
400
500
600
700

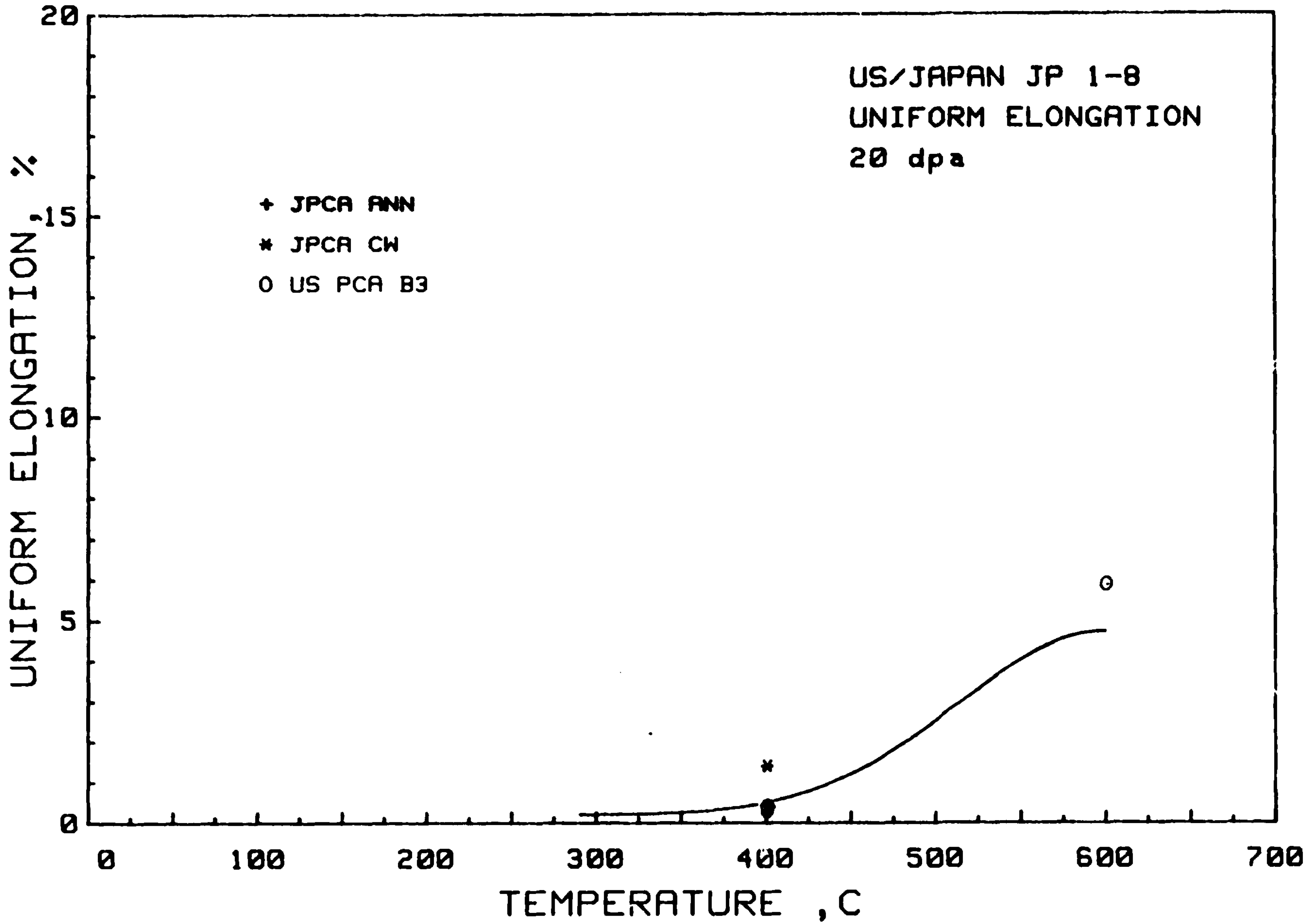
US/JAPAN JP 1-8
UNIFORM ELONGATION
20 dpa
+ JPCA ANN
* JPCA CW
O US PCA B3
UNIFORM ELONGATION, %
TEMPERATURE ,C
0
5
10
15
20
0
100
200
300
400
500
600
700

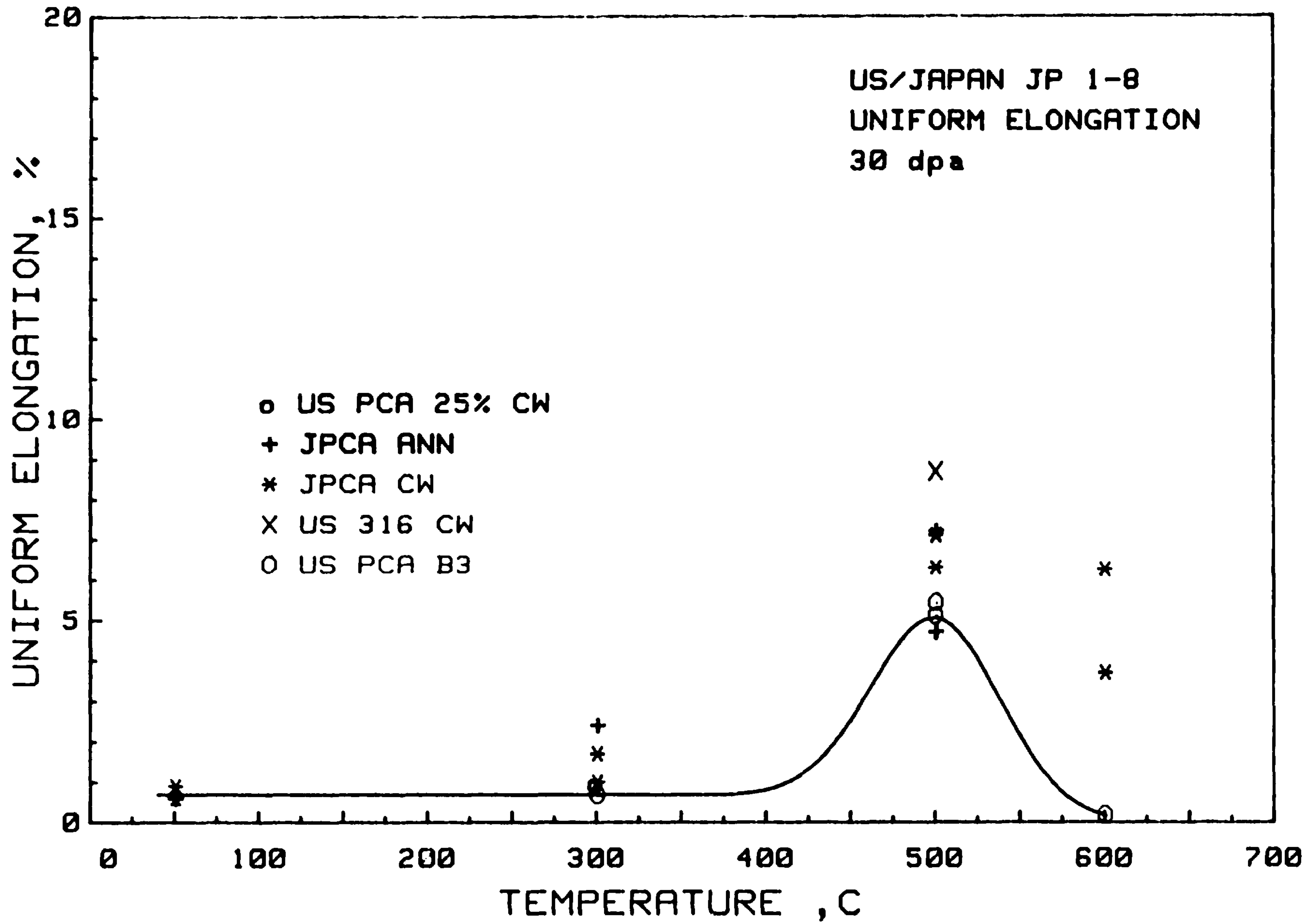

US/JAPAN JP 1-8
UNIFORM ELONGATION
30 dpa
o US PCA 25% CW
+ JPCA ANN
* JPCA CW
X US 316 CW
O US PCA B3
UNIFORM ELONGATION, %
TEMPERATURE ,C
0
5
10
15
20
0
100
200
300
400
500
600
700

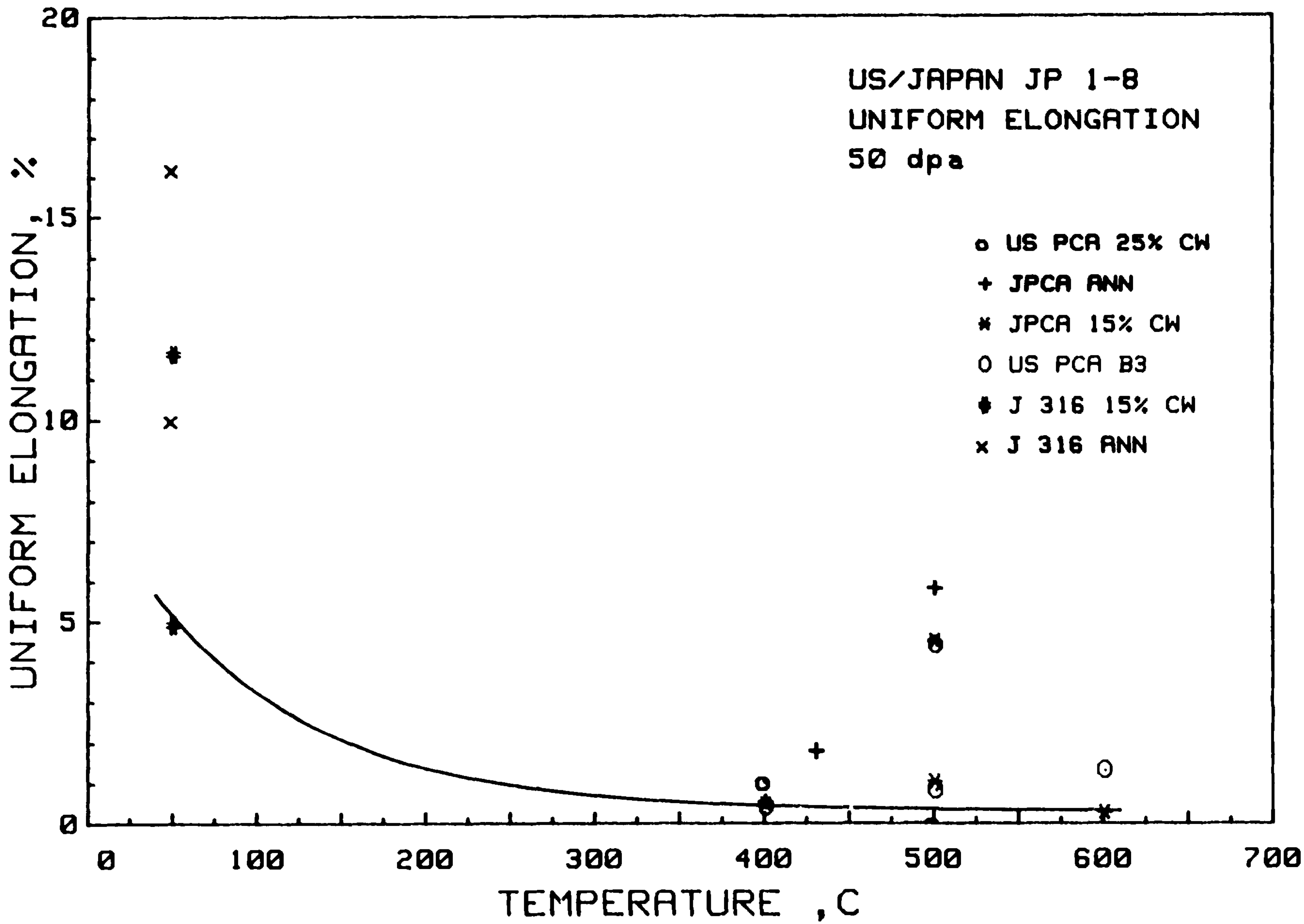
US/JAPAN JP 1-8
UNIFORM ELONGATION
50 dpa
US PCA 25% CW
JPCA ANN
JPCA 15% CW
US PCA B3
J 316 15% CW
J 316 ANN
UNIFORM ELONGATION, %
TEMPERATURE ,C
0
5
10
15
20
0
100
200
300
400
500
600
700

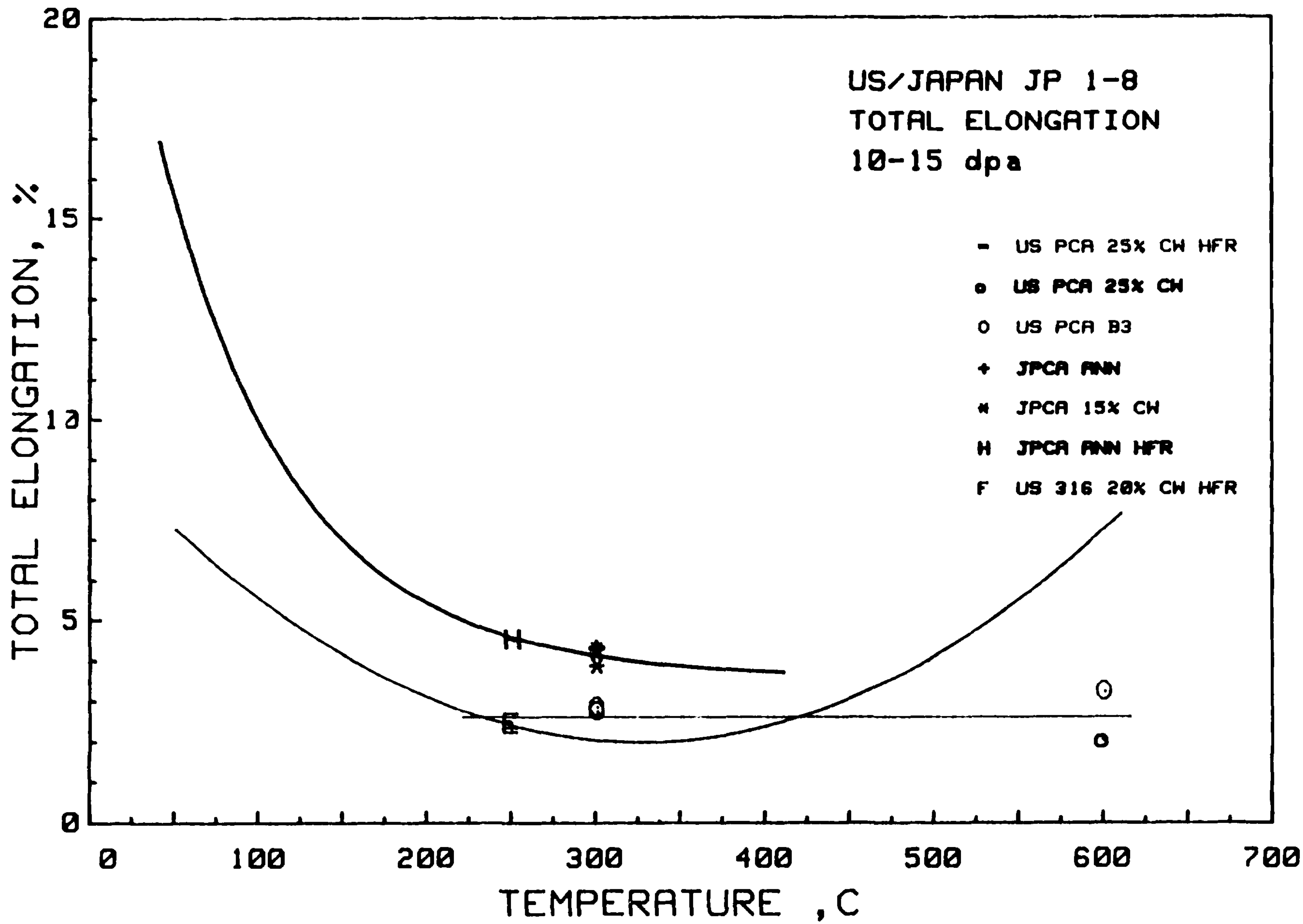
US/JAPAN JP 1-8
TOTAL ELONGATION
10-15 dpa
- US PCA 25% CW HFR
o US PCA 25% CW
O US PCA B3
+ JPCA ANN
* JPCA 15% CW
H JPCA ANN HFR
F US 316 20% CW HFR
TOTAL ELONGATION, %
TEMPERATURE ,C
0
5
10
15
20
0
100
200
300
400
500
600
700

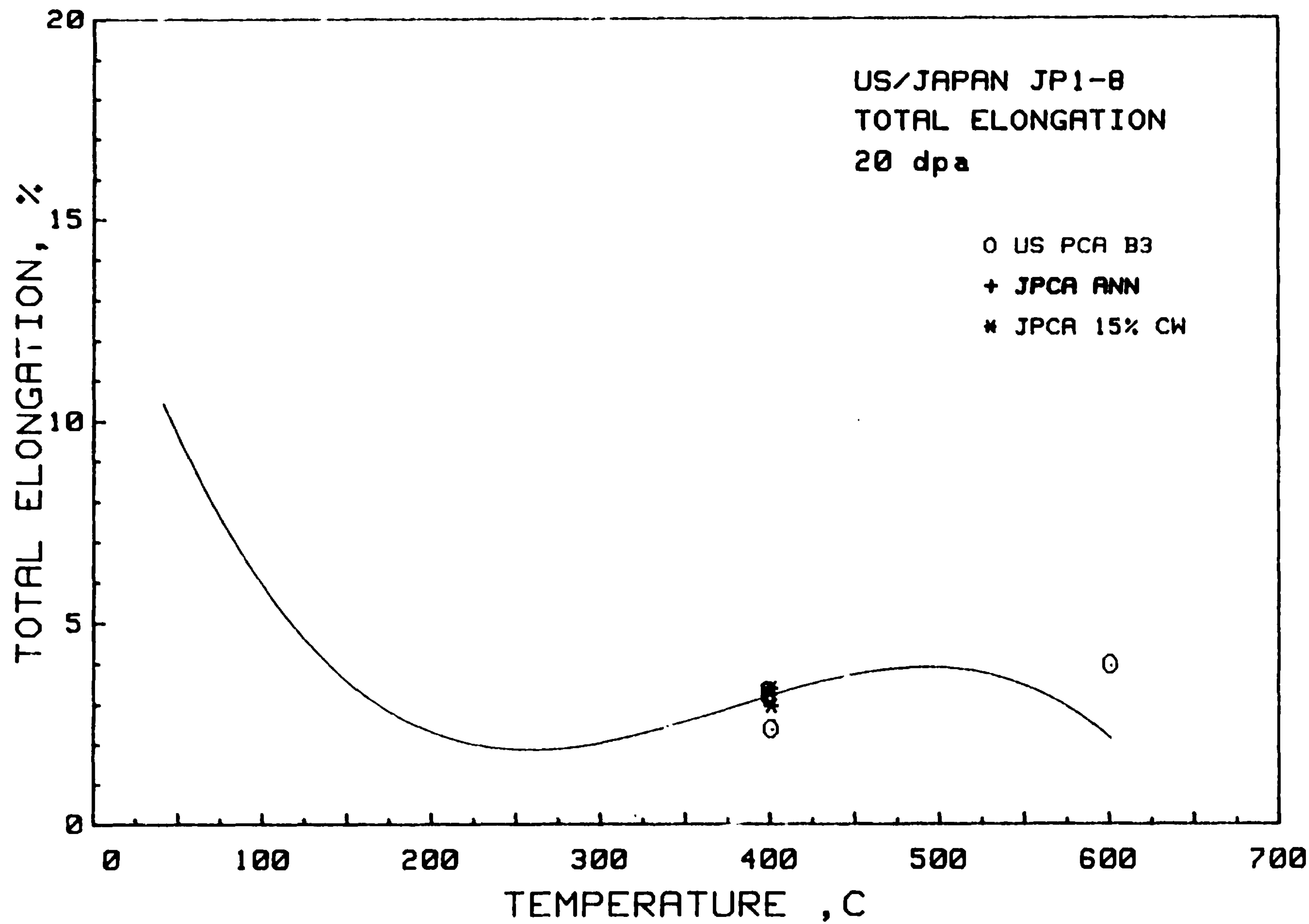
US/JAPAN JP1-8
TOTAL ELONGATION
20 dpa
O US PCA B3
+ JPCA ANN
* JPCA 15% CW
TOTAL ELONGATION, %
0
5
10
15
20
0
100
200
300
400
500
600
700
TEMPERATURE ,C

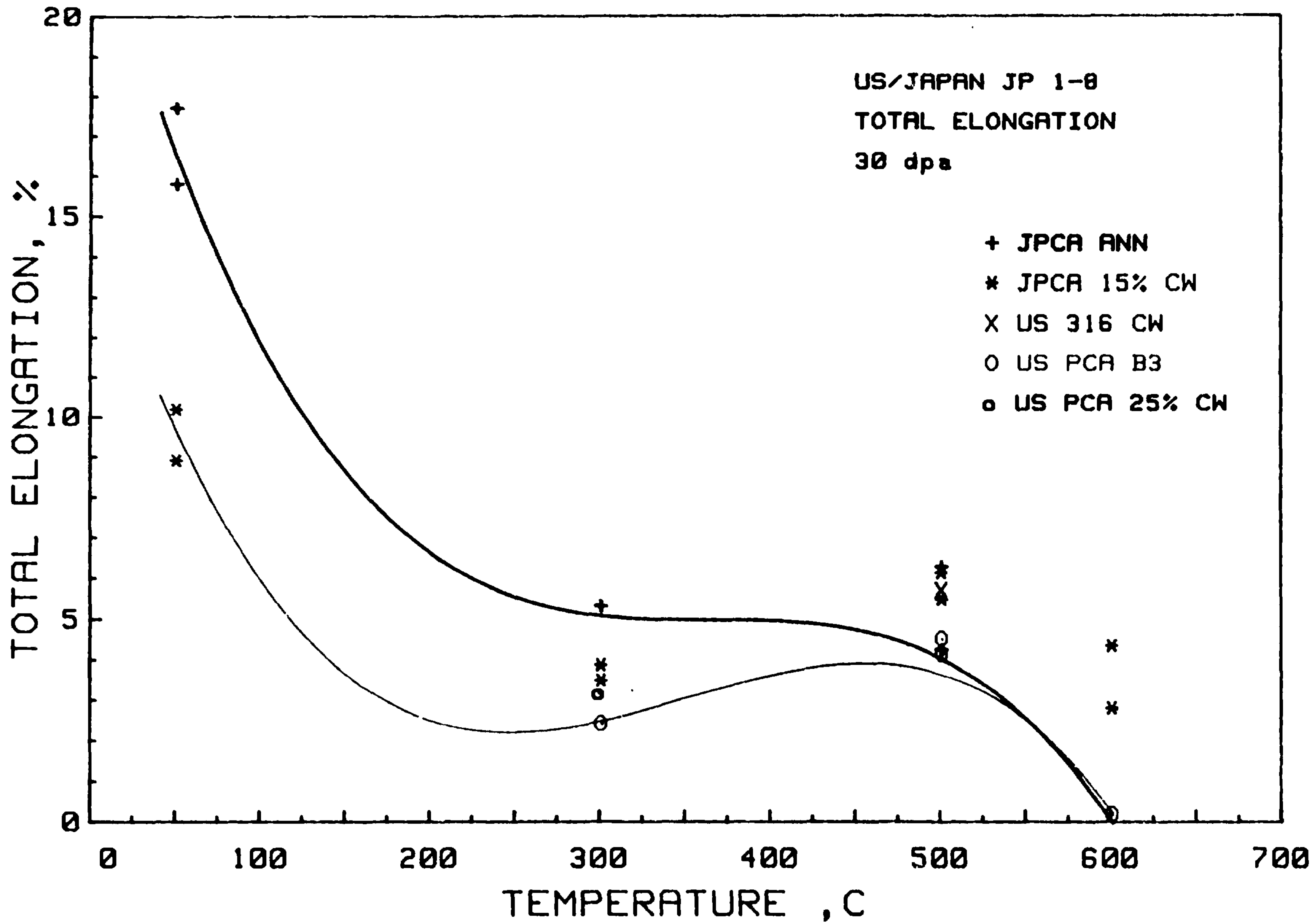
US/JAPAN JP 1-8
TOTAL ELONGATION
30 dpa
+ JPCA ANN
* JPCA 15% CW
X US 316 CW
O US PCA B3
o US PCA 25% CW
TOTAL ELONGATION, %
TEMPERATURE ,C
0
5
10
15
20
0
100
200
300
400
500
600
700

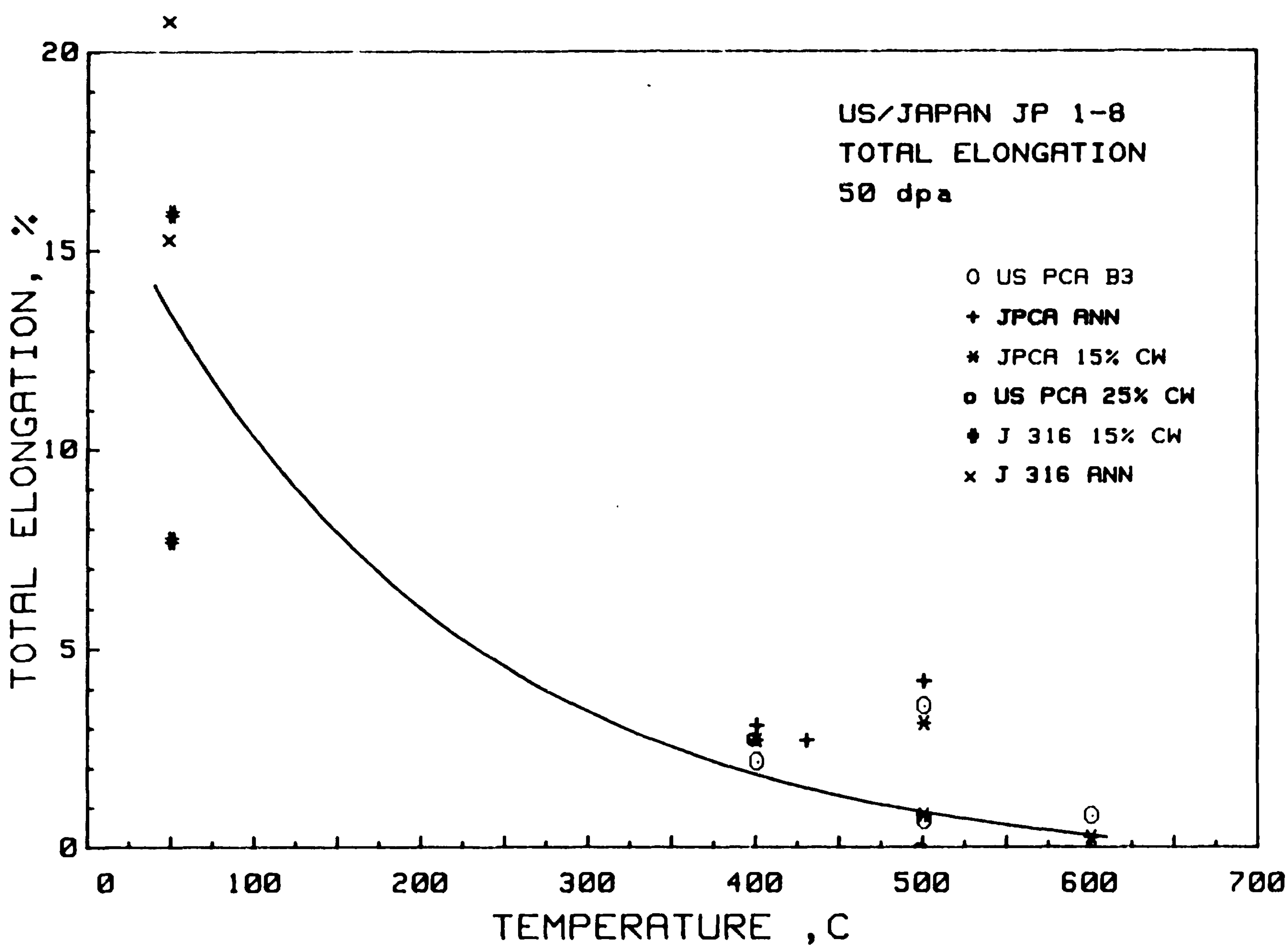
US/JAPAN JP 1-8
TOTAL ELONGATION
50 dpa
O US PCA B3
+ JPCA ANN
* JPCA 15% CW
o US PCA 25% CW
J 316 15% CW
x J 316 ANN
TOTAL ELONGATION, %
TEMPERATURE ,C
0
5
10
15
20
0
100
200
300
400
500
600
700

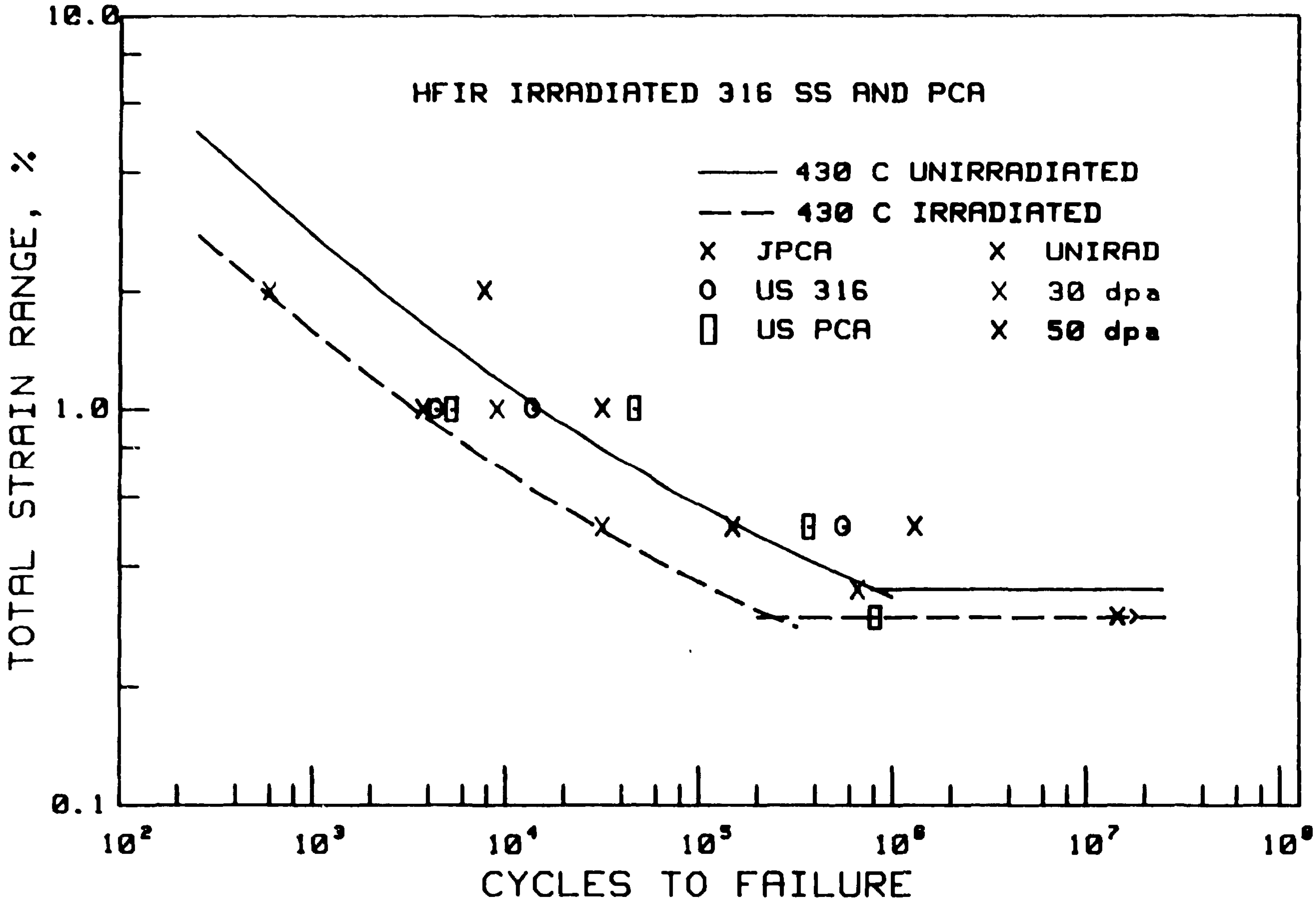
HFIR IRRADIATED 316 SS AND PCA
430 C UNIRRADIATED
430 C IRRADIATED
X JPCA
O US 316
[] US PCA
X UNIRAD
X 30 dpa
X 50 dpa
TOTAL STRAIN RANGE, %
10.0
1.0
0.1
10^2
10^3
10^4
10^5
10^6
10^7
10^8
CYCLES TO FAILURE

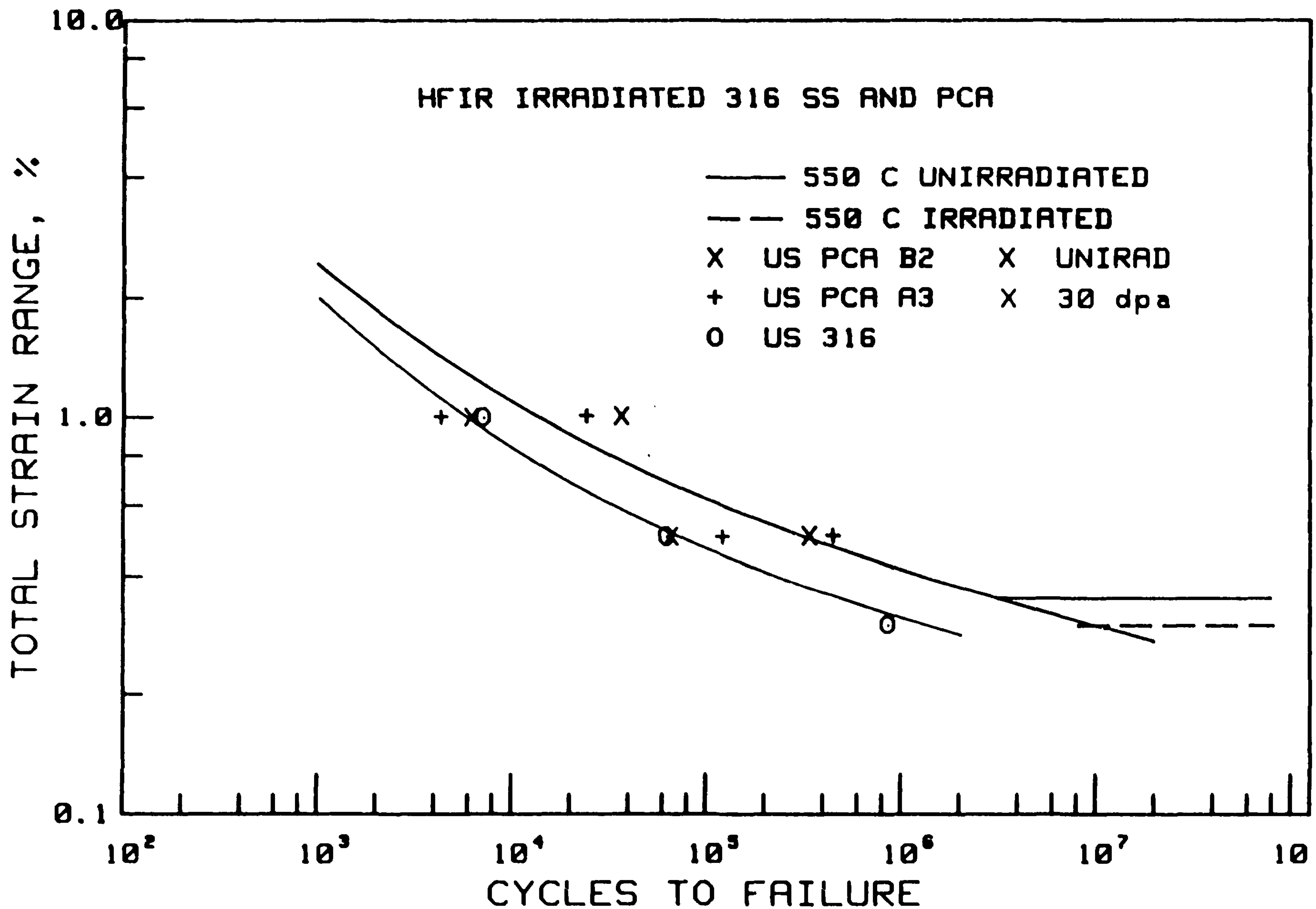
HFIR IRRADIATED 316 SS AND PCA
550 C UNIRRADIATED
550 C IRRADIATED
X US PCA B2 X UNIRAD
+ US PCA A3 X 30 dpa
O US 316
TOTAL STRAIN RANGE, %
10.0
1.0
0.1
10^2
10^3
10^4
10^5
10^6
10^7
10
CYCLES TO FAILURE

SUMMARY

1. LITTLE DIFFERENCE IN STRENGTH BETWEEN ALLOYS
2. DIFFERENCES BETWEEN COLD–WORKED AND ANNEALED ALLOYS VANISHES BY 30 dpa
3. UNIFORM ELONGATION IS VERY LOW BELOW 400 C
4. FATIGUE LIFE IS NOT DEGRADED FURTHER BETWEEN 15 AND 50 dpa AT 430 C
5. AN EFFECT OF He ON FATIGUE LIFE HAS BEEN OBSERVED AT 550 C.

MICROSTRUCTURAL DEVELOPMENT IN AUSTENITIC STEELS AND FERRITIC STEELS IRRADIATED IN PHASE I

M. Suzuki

ABSTRACT

This paper describes the microstructural evolution process in titanium-modified austenitic stainless steel and ferritic steel irradiated in HFIR, Phase I experiment, focusing on the precipitation behavior.

Swelling resistance of the Japanese prime candidate alloy (JPCA) appears to be strongly dependent on the behavior of fine titanium-rich MC precipitates. However, the onset of rapid void swelling began with coincident MC precipitate dissolution after 57 dpa at 500°C. Instability of the MC was interpreted in terms of solute segregation around the MC.

By contrast, swelling of ferritic steel was very low as compared with austenitic stainless steel even with helium generating condition, although the level of swelling was enhanced by the helium generation. For ferritic steel, understanding of the precipitate evolution is very important for considering its application to the fusion system, because it should affect the mechanical properties greatly. Some evidence of helium bubble-RIS-void interaction was observed, which have not been known well in the ferritic steel.

TOPICS

JAPANESE PRIME CANDIDATE ALLOY (JPCA)

(1) RADIATION INDUCED PHASE FORMATION
AND STABILITY

(2) PRECIPITATE EVOLUTION IN MATRIX AND C.. GRAIN
BOUNDARY

JAPANESE FERRITIC STEEL (JFMS)

(1) HELIUM EFFECT ON CAVITY FORMATION

(2) DISCUSSION ON HELIUM-RIS-VOID CORRELATION

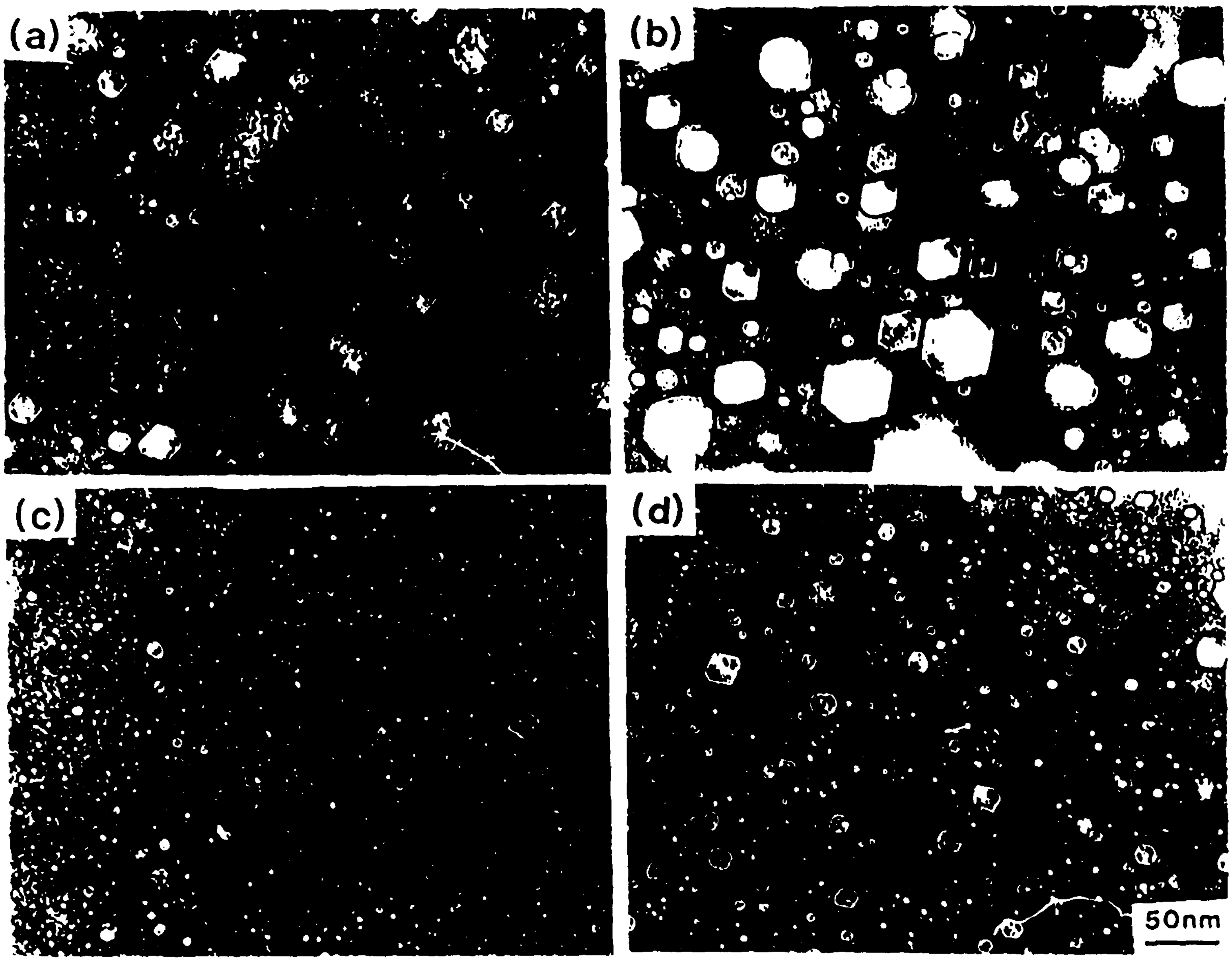
(a)
(b)
(c)
(d)
50nm

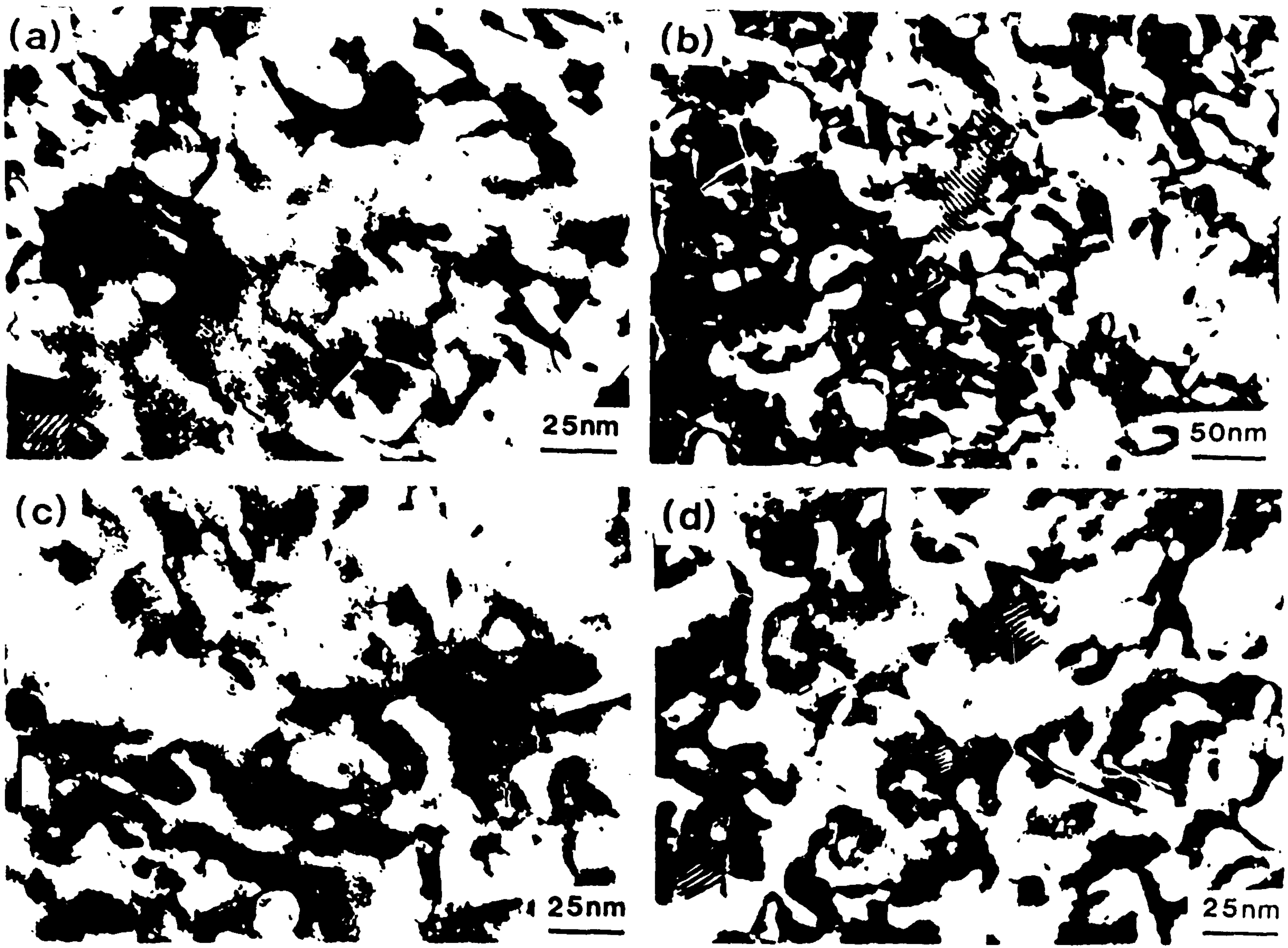
(a)
25nm
(b)
50nm
(c)
25nm
(d)
25nm

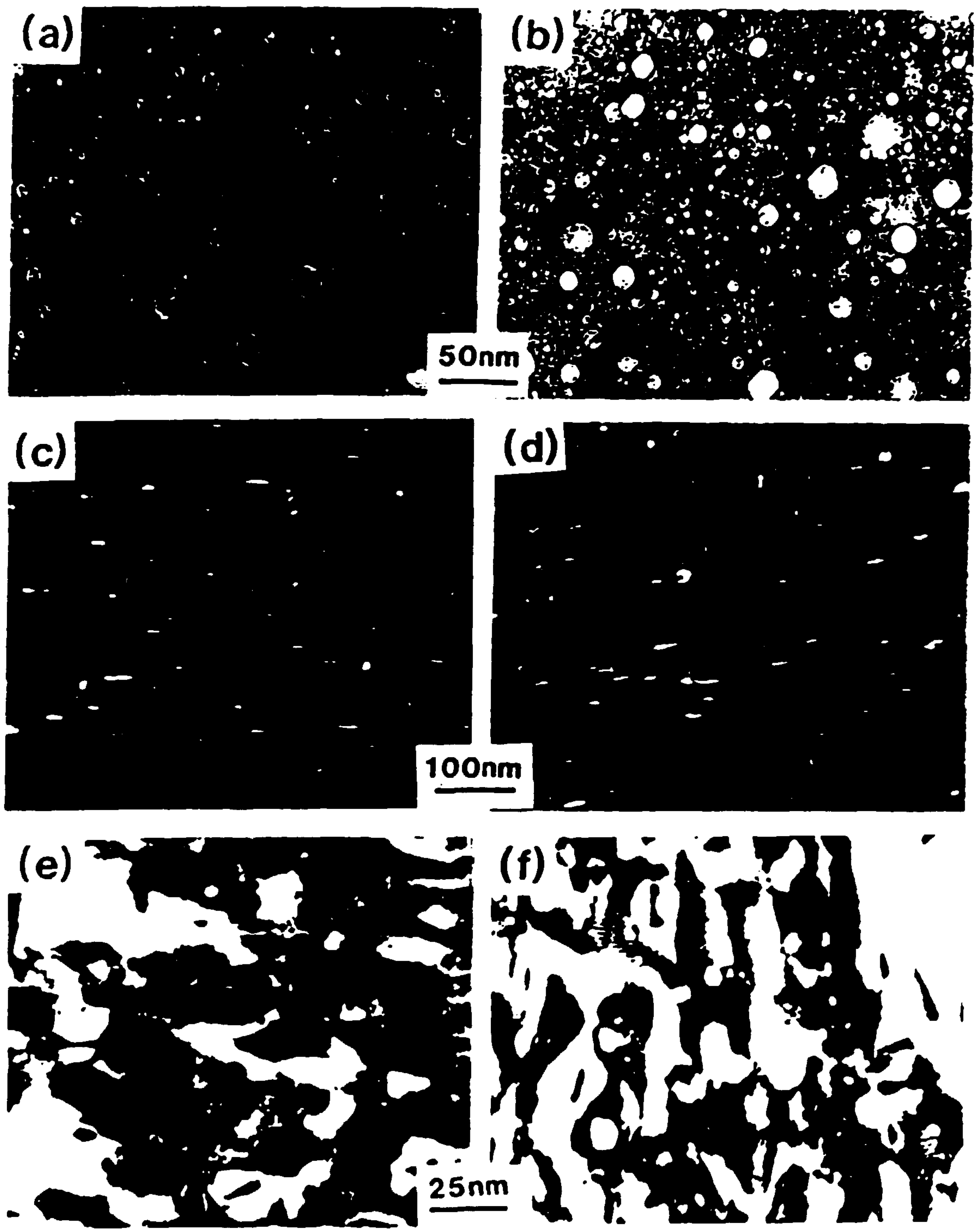
(a)
(b)
50nm
(c)
(d)
100nm
(e)
(f)
25nm

87-11321

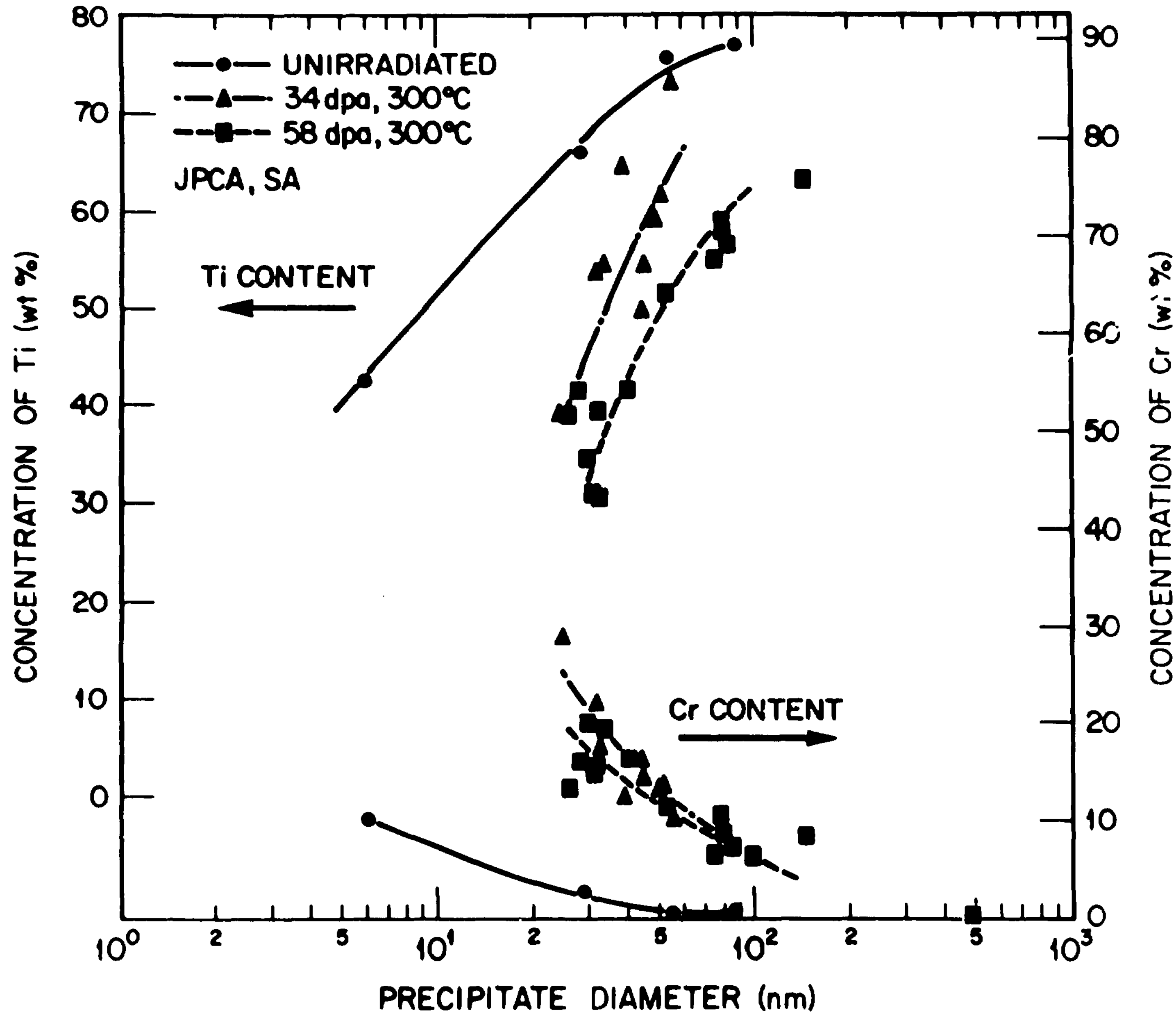

UNIRRADIATED
34 dpa, 300°C
58 dpa, 300°C
JPCA, SA
Ti CONTENT
Cr CONTENT
CONCENTRATION OF Ti (wt %)
CONCENTRATION OF Cr (wt %)
PRECIPITATE DIAMETER (nm)

98-8647

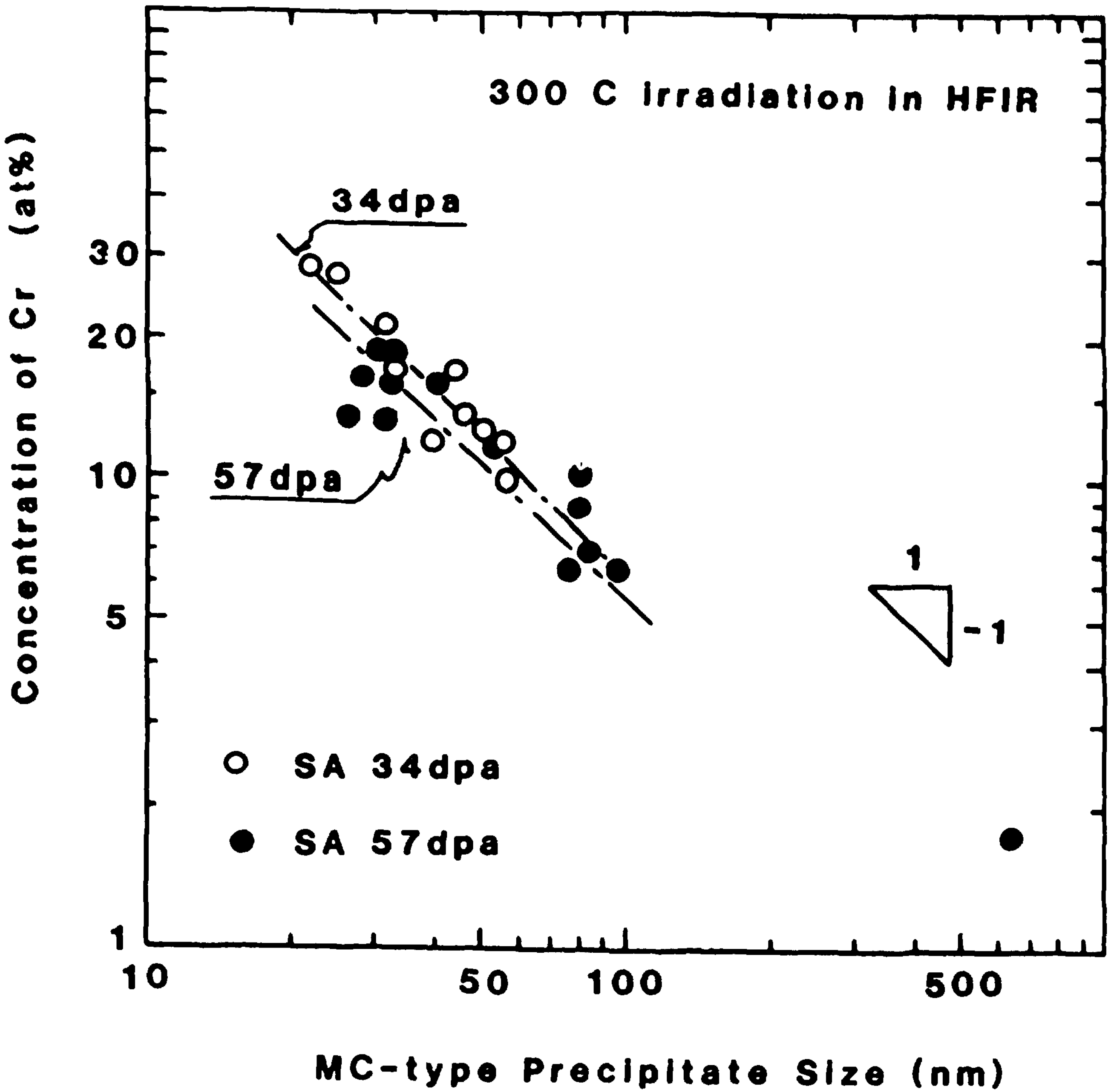

300 C Irradiation in HFIR
34dpa
57dpa
1
-1
SA 34dpa
SA 57dpa
Concentration of Cr (at%)
30
20
10
5
1
10
50
100
500
MC-type Precipitate Size (nm)

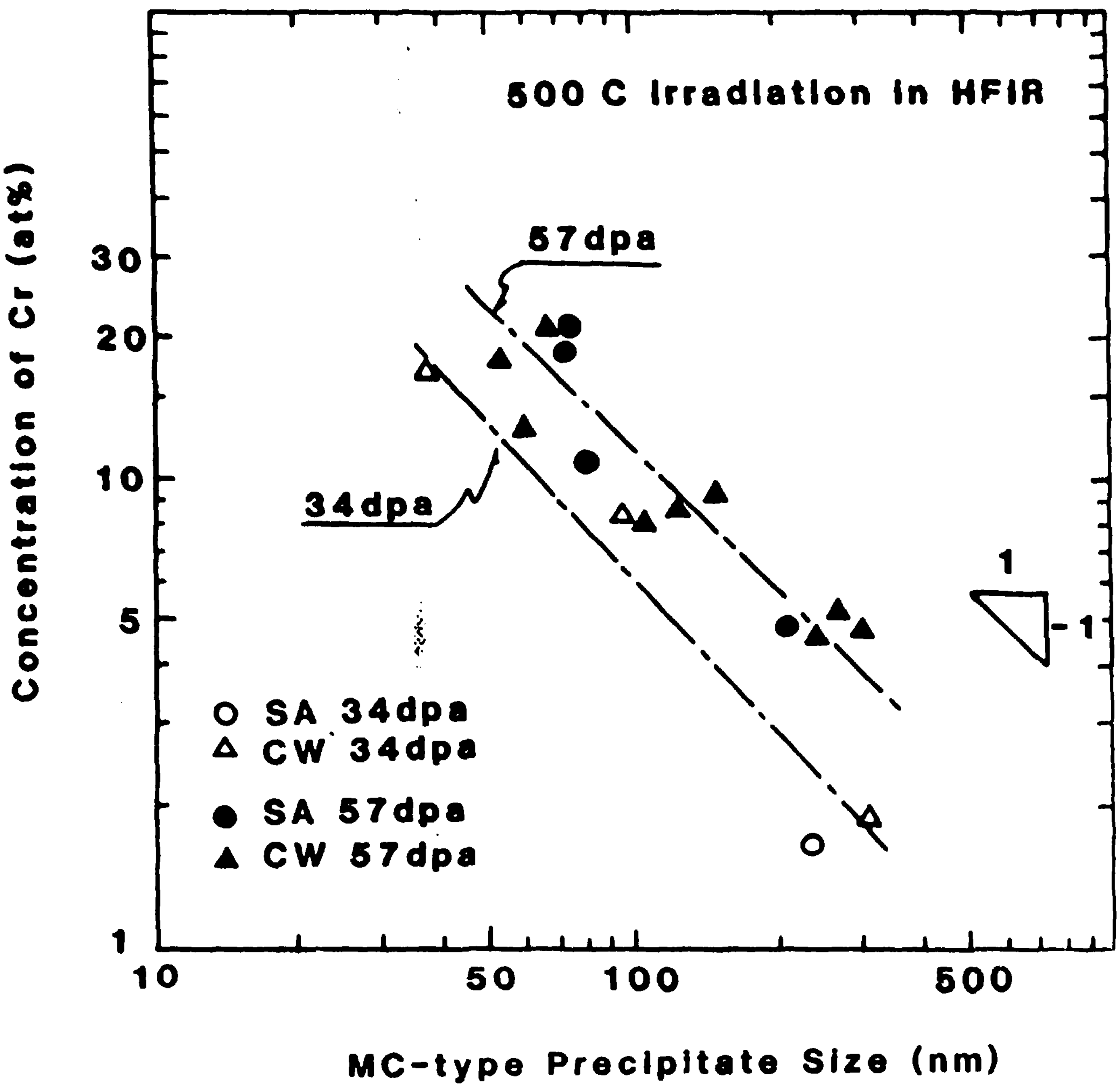
500 C Irradiation in HFIR
57dpa
34dpa
Concentration of Cr (at%)
30
20
10
5
1
10
50
100
500
MC-type Precipitate Size (nm)
1
-1
SA 34dpa
CW 34dpa
SA 57dpa
CW 57dpa

WS-6106

"MC Collapse through the development of Solute Segregation Zone"

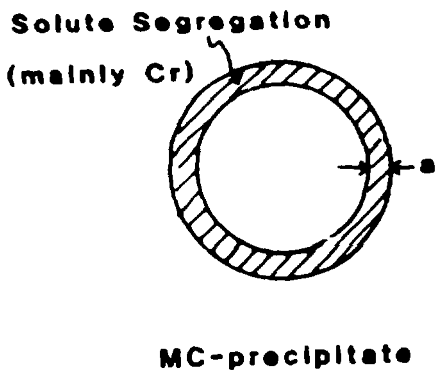

$[Cr] \propto A \times (d)^n$

d: particle size

n: ~1

A: constant related to a

a: independent of d

300 °C Irradiation: no development of solute segregation zone width, a with irradiaiton

500 °C Irradiation: development of the width "a"

→ As a result, M_6C formation through a certain mechanism

ORNL-Photo 4169-88

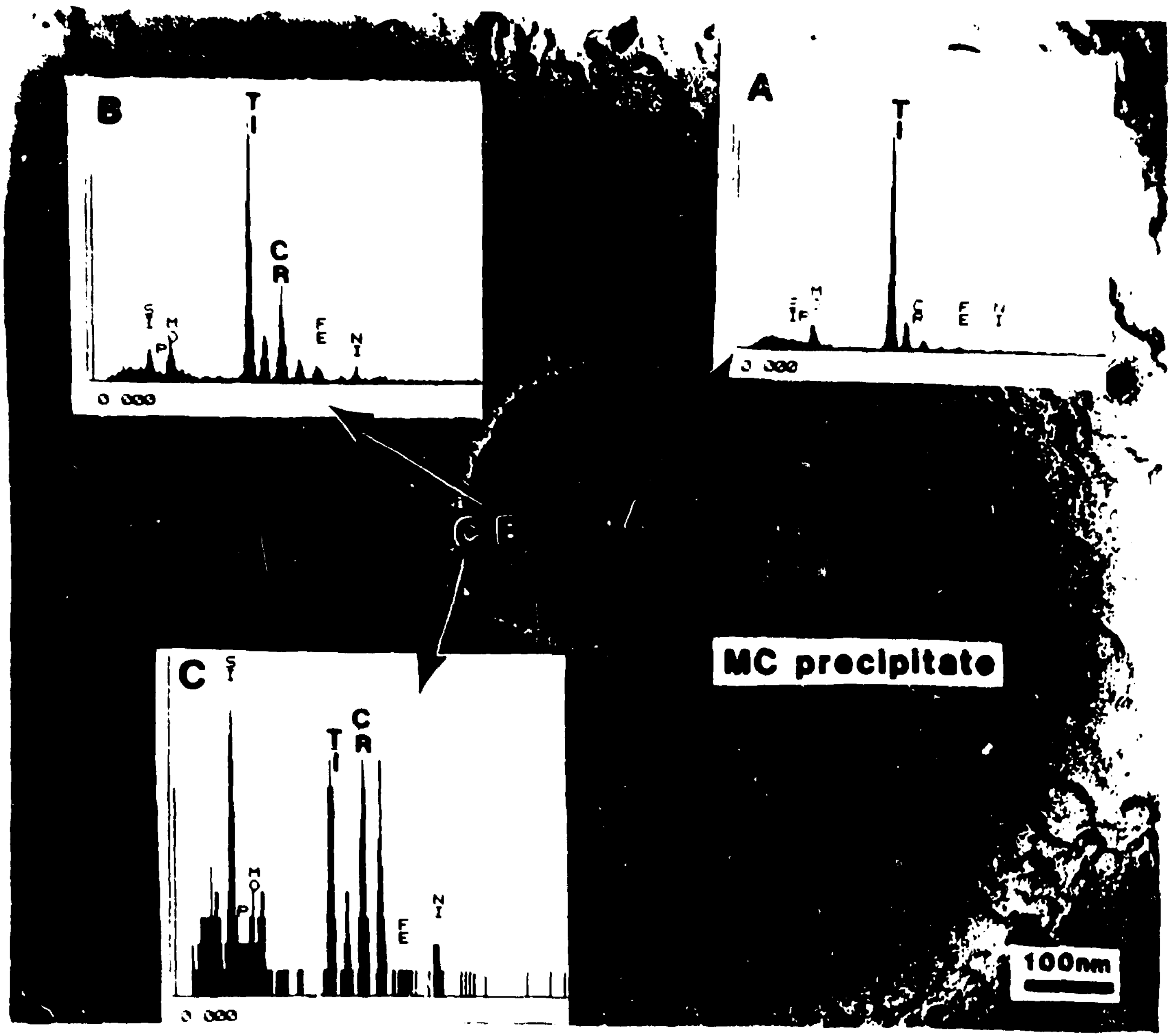

EXTRACTED REPLICA FILM AND BROAD BEAM XEDS SPECTRA

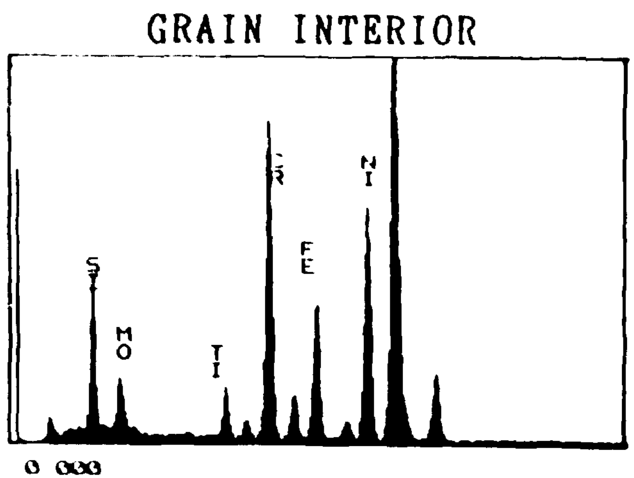

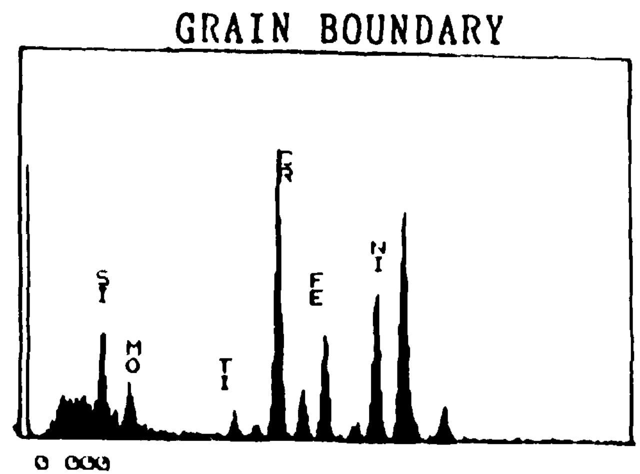

SA JPCA AFTER 500℃ 57 DPA, HFIR

EXTRACTED REPLICA FILM AND

BROAD BEAM XEDS SPECTRA

GRAIN INTERIOR

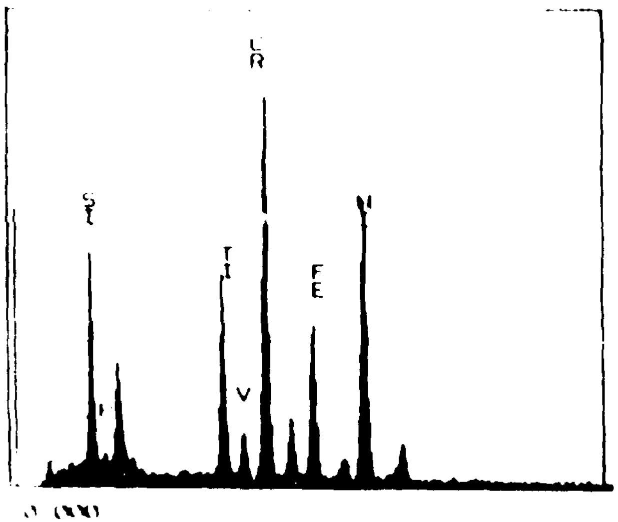

GRAIN BOUNDARY

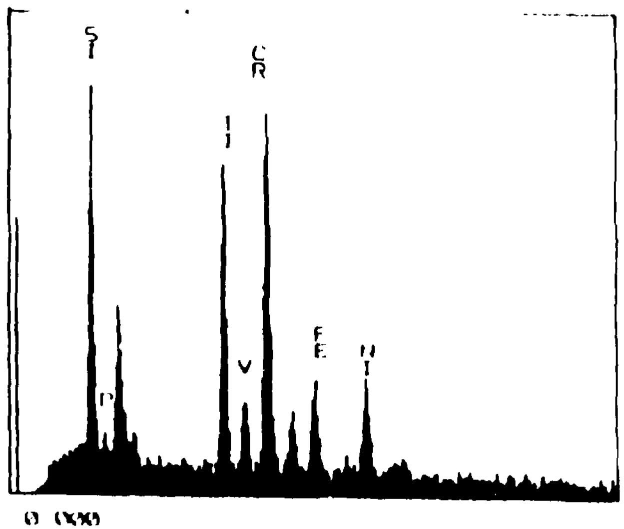

CW JPCA AFTER 500℃ 57 DPA, HFIR

WS 61

Table 3 Radiation Produced Precipitates Observed in SA and CW JPCA after irradiation in HFIR at 500 C

	500 C, 34 dpa	500 C, 57 dpa
SA	mostly MC small amount of M_6C	mostly M_6C small amount of MC very small amount of G-phase
CW	mostly MC small amount of M_6C	M_6C, MC roughly equall amount Cr-rich phase

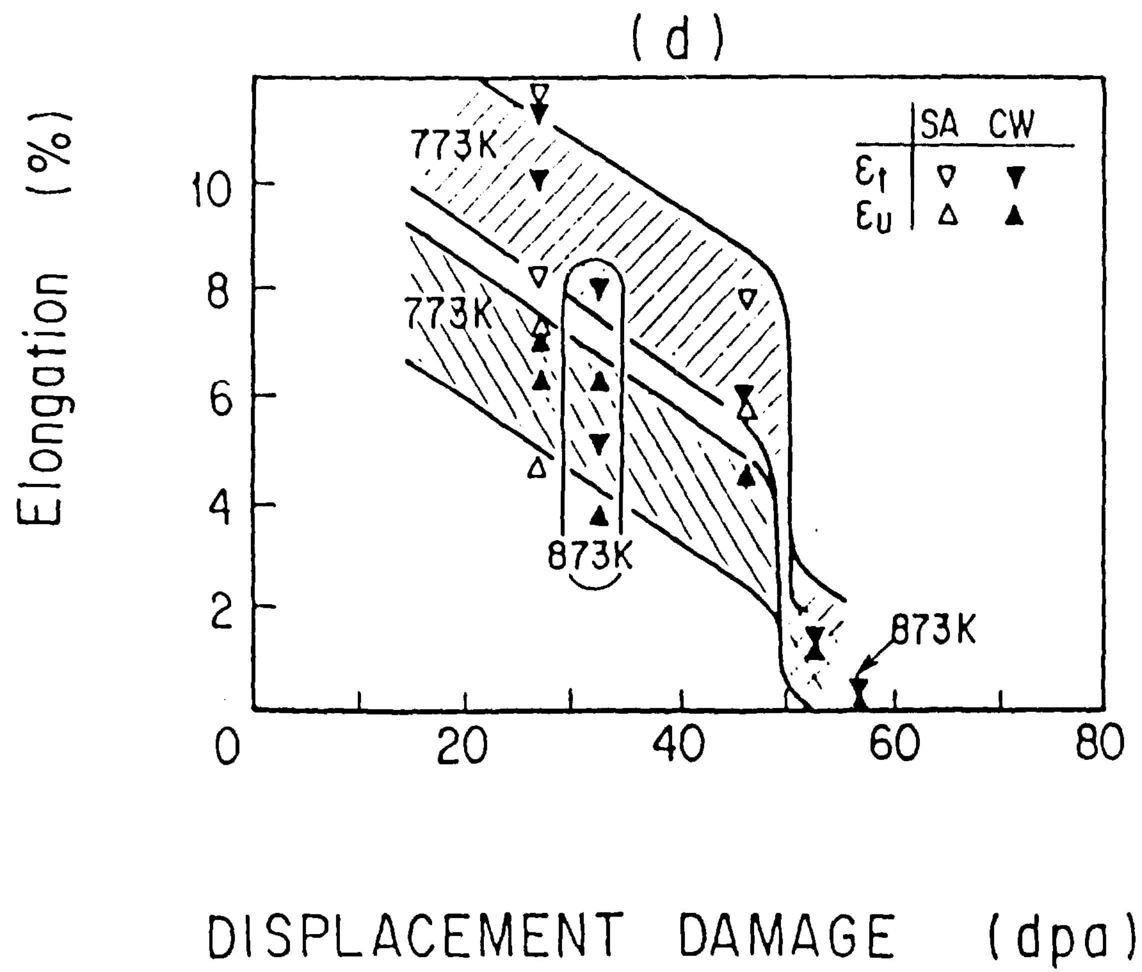

(d)
Elongation (%)
DISPLACEMENT DAMAGE (dpa)
0
20
40
60
80
2
4
6
8
10
773K
773K
873K
873K
SA CW
ε_t
ε_u

88-10888

CONCLUSION

1) JPCA in the solution annealed condition (SA) showed considerable evolution of void swelling after irradiation to 57 dpa at 500 C.
2) The onset of the regime of swelling at a high rate appeared to be associated with the dissolution of the titanium-rich MC type precipitate.
3) General trend for the precipitate evolution in the JPCA was determined. After MC precipitate developed initially during irradiation , they began to dissolve and/or coarsen, giving way to coincident formation of M_6C.
4) A key process leading to instability of fine MC particles appear to be the formation of a segregation zone at surface of the MC precipitate particles.

Swelling behavior of 9 -12 Cr ferritic-martensitic steels

Alloy	Reactor	Maximum Dose	Temperature Range (℃)	Results	Referenc
9Cr-1MoVNb	HFIR	36 dpa	300 - 600	max. ~0.2% at 400℃	(1)
9Cr-1MoVNb 9Cr-1MoVNb2Ni	HFIR	39 dpa	300 - 600	max. ~0.5% at 400℃	(2)
9Cr-2MoVNb	Rapsodie	50 dpa	400 - 580	negligible	(3)
9Cr-2MoVNb		~125 dpa	400 - 650	max.0.6% at 400-425℃	(4)
9Cr-2MoVNb		~118 dpa	400 - 460	< 1% at 400-430℃	(5)
12Cr-MoVW (HT9)		~75 dpa	400 - 650	max.0.2% at 400℃	(6)
12Cr-MoVW	HFIR	36dpa	300 - 600	max.0.07% at 400℃	(7)
13Cr-0.25Mo (AISI416)		~125 dpa	400 - 650	max.0.35% at 400℃	(8)
12Cr-MoV 12Cr-MoVNb (1.4923, 1.4914)		50 dpa	400 - 580	negligible	(9)
12Cr(FI) 12Cr-MoV(CRM-12) 12Cr-MoVNb(FV448)		~25 dpa	380 - 615	negligible	(10)
12Cr 12Cr-Mo		~14 dpa	450	negligible (<0.1%)	(11)
12Cr-MoVW 12Cr-MoVW(1Ni) 12Cr-MoVW(2Ni)		39 dpa	300 - 600	low swelling	(12)

Mechanisms which have been proposed to explain the swelling resistance
of ferritic/martensitic steels

1) Low intrinsic bias ; smaller relaxation volume of interstitials in b.c.c structure, giving an lower bias.

2) Dislocation loop evolution ; formation of a<100> dislocation within a network of a/2<111> dislocation , which is more neutral , enhancing the mutual point defect recombination.

3) Point defect-solute interaction ; enhancing mutual recombination, and lowering the vacancy supersaturation

4) Dislocation-solute interaction ; reducing the dislocation bias, and/or inhibiting the dislocation climb.

5) Subgrain structure as a primary sinks ;
and/or higher sinks

6) Higher self diffusion rates ;

Helium Effect on Swelling Behavior of Ferritic Steels
(Neutron Irradiation)

(1)	Gelles D.S. et al;	Voids observed in HT-9 irradiated in HFIR, but not in other reactors like EBR-II, 400℃, 39 dpa, 115 appm He
(2)	Vitek J.M., Klueh R.L. ; Maziasz P.J., et al	More voids in Ni doped 9Cr-1MoVNb, 12Cr-1MoVW ~39 dpa, 410 appm He (HFIR/FFTF)
(3)	Smidt F.A. et al ;	Ni addition enhanced swelling in iron ~3.6 dpa , 596℃

ORNL-Photo 2334-88

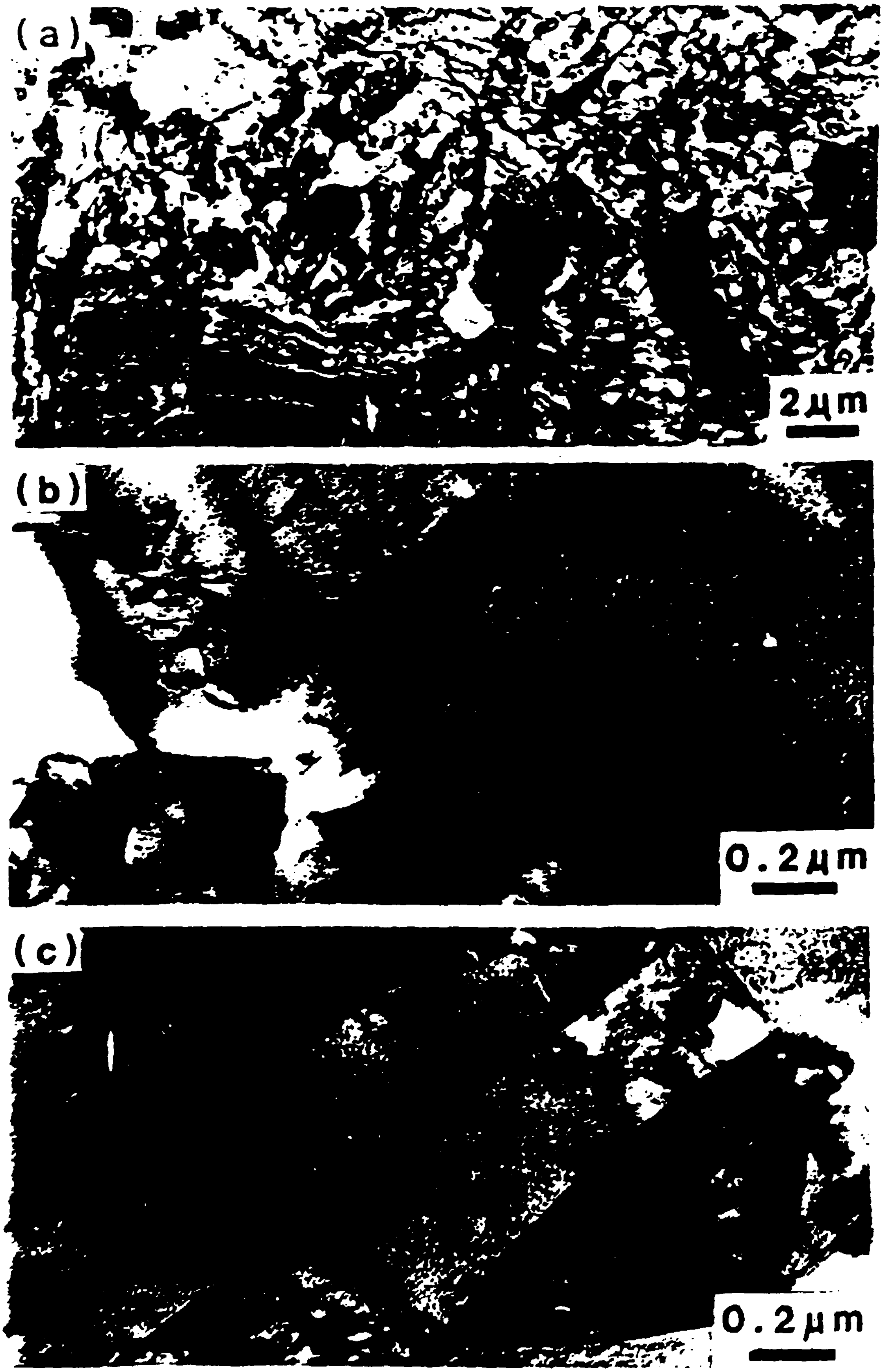

10Cr-2Mo δ-ferrite

500°C, 34dpa in HFIR

10Cr-2Mo δ-ferrite

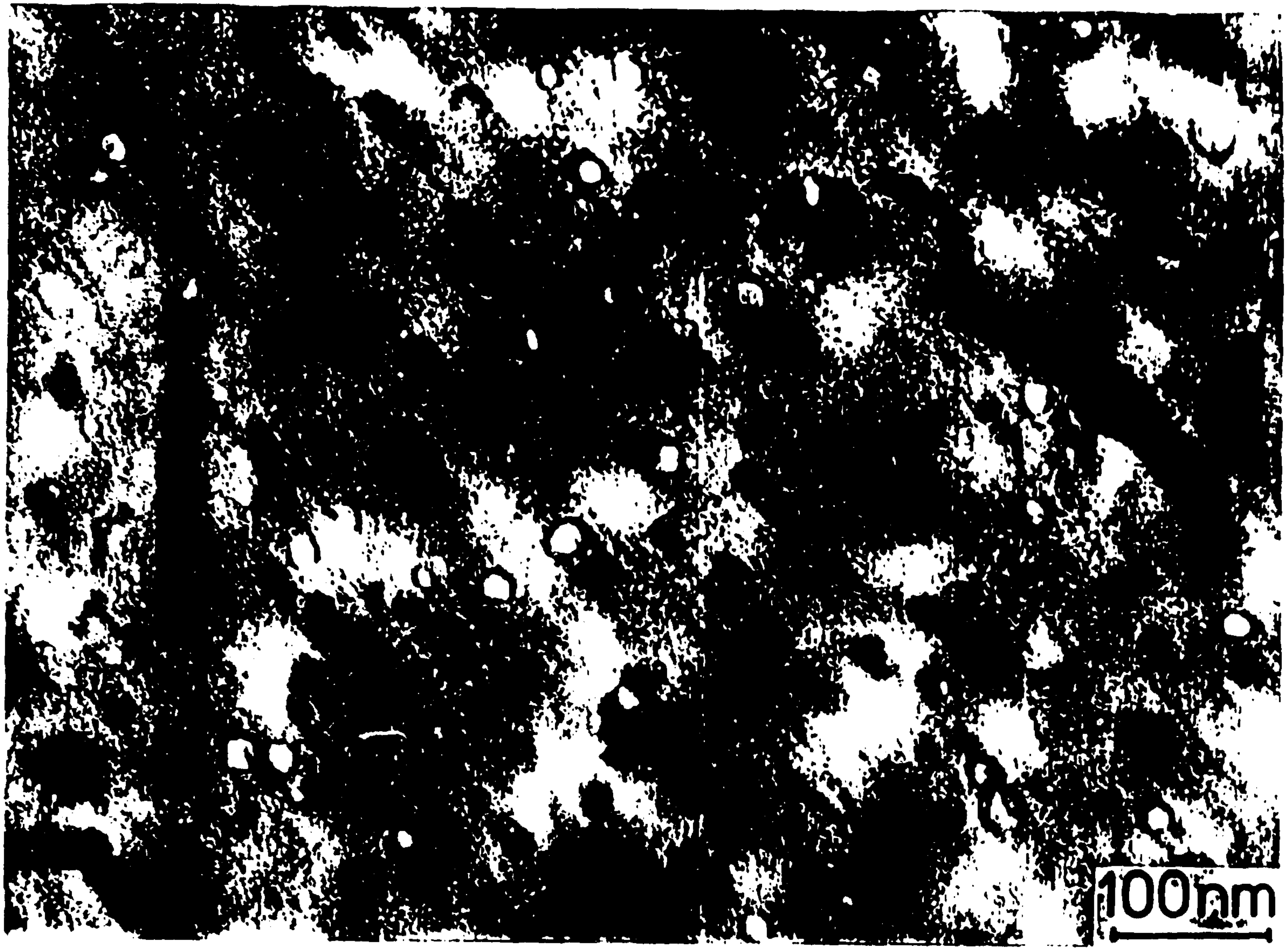

500°C, 57dpa in HFIR

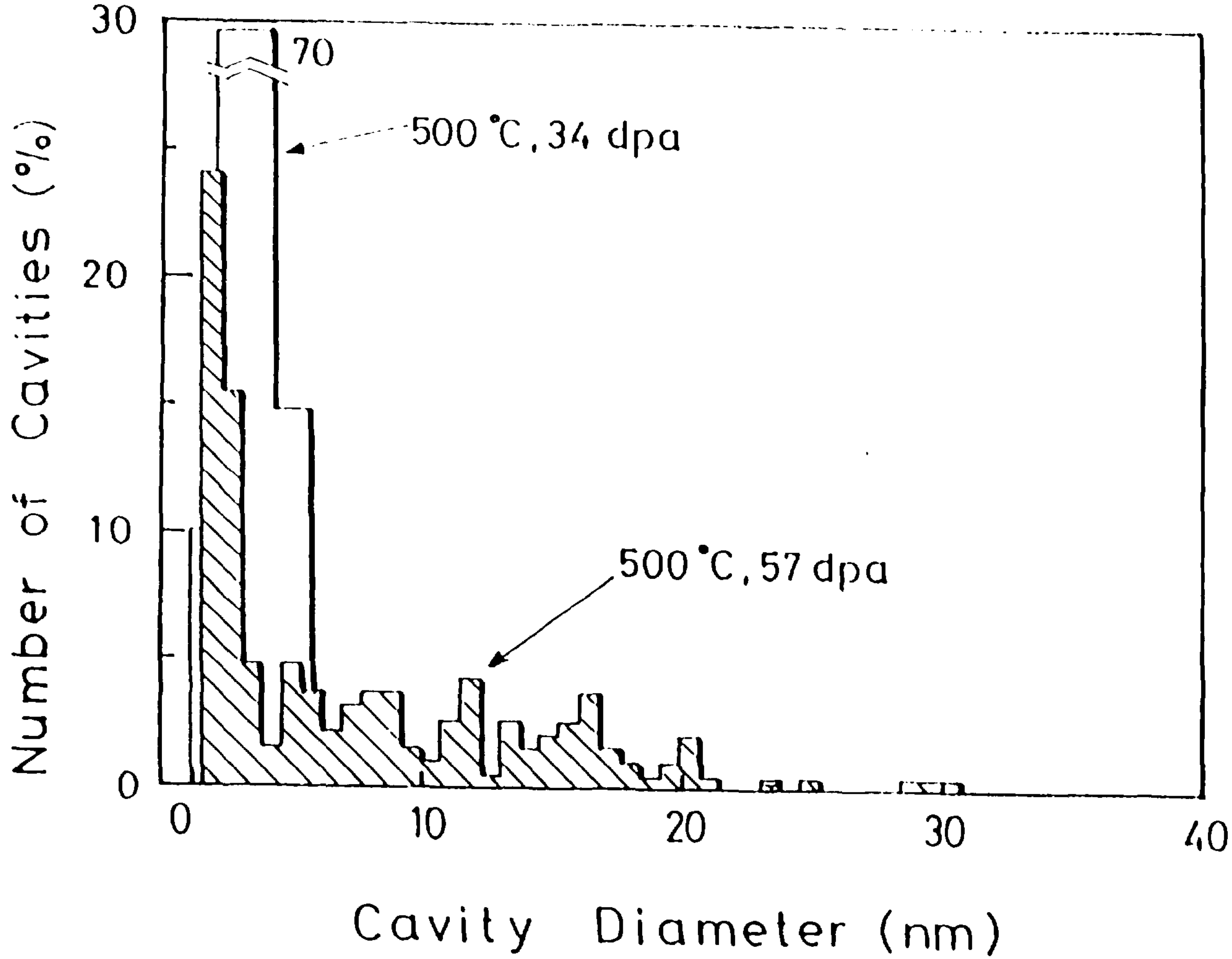
Number of Cavities (%)
30
20
10
0
70
500 °C, 34 dpa
500 °C, 57 dpa
0
10
20
30
40
Cavity Diameter (nm)

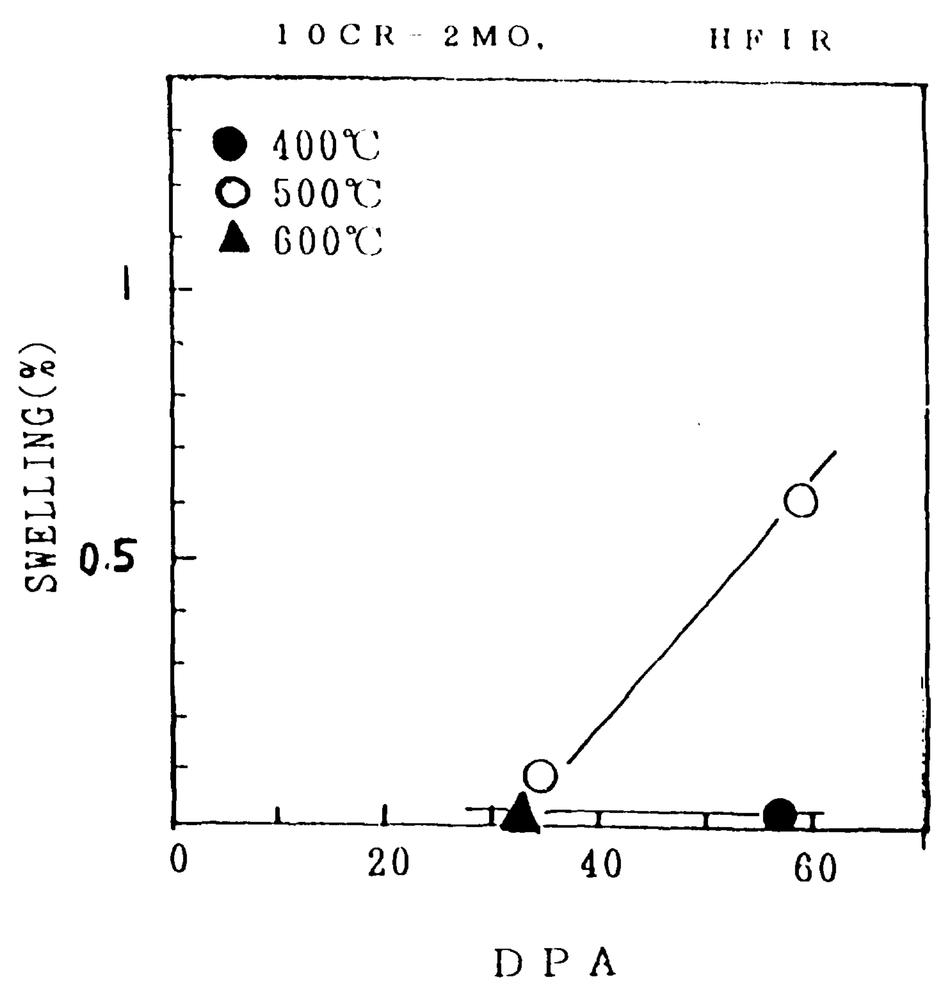

10CR - 2MO, HFIR
400℃
500℃
600℃
SWELLING(%)
0.5
1
0
20
40
60
DPA

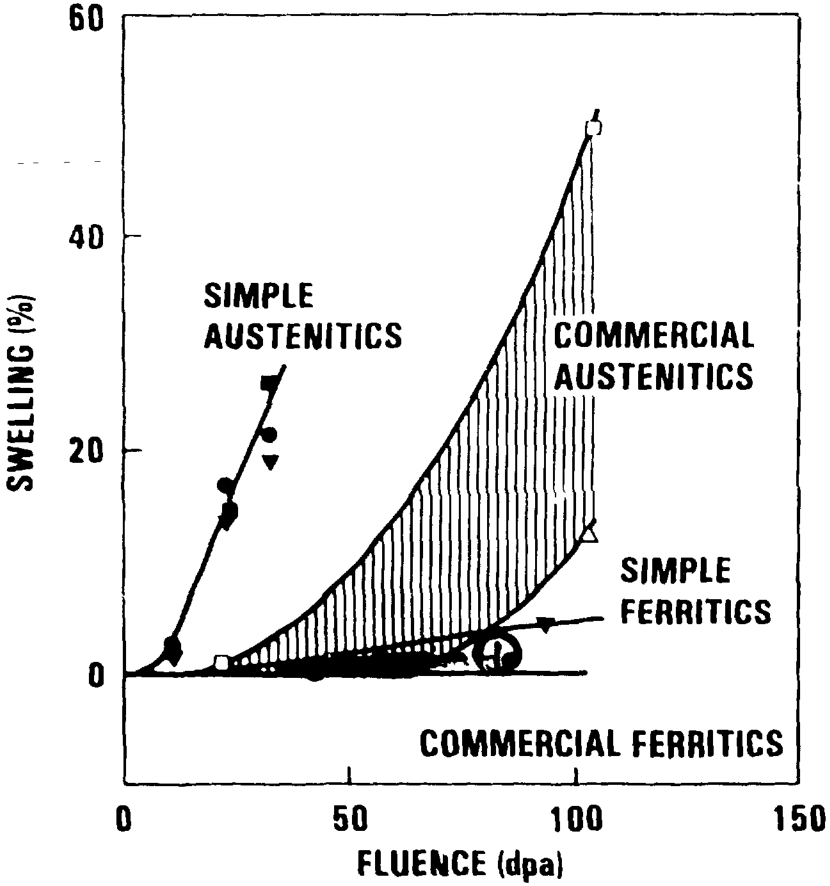

HOW HIGH IS THE STEADY STATE SWELLING RATE OF FERRITIC STEELS?

1) Most of the data including simple ferritics show less than 0.1%/dpa

2) Theoretical calculation showed 0.04%/dpa [1]

3) Present work for 10Cr-2Mo alloy indicated ~0.03%/dpa

[1] J. Sniegowski and W. Wolfer; Topical Conference on Ferrtic Alloys for Use in Nuclear Energy Technology, Snowbird, 18 June 1983

10Cr-2Mo   martensite/lath

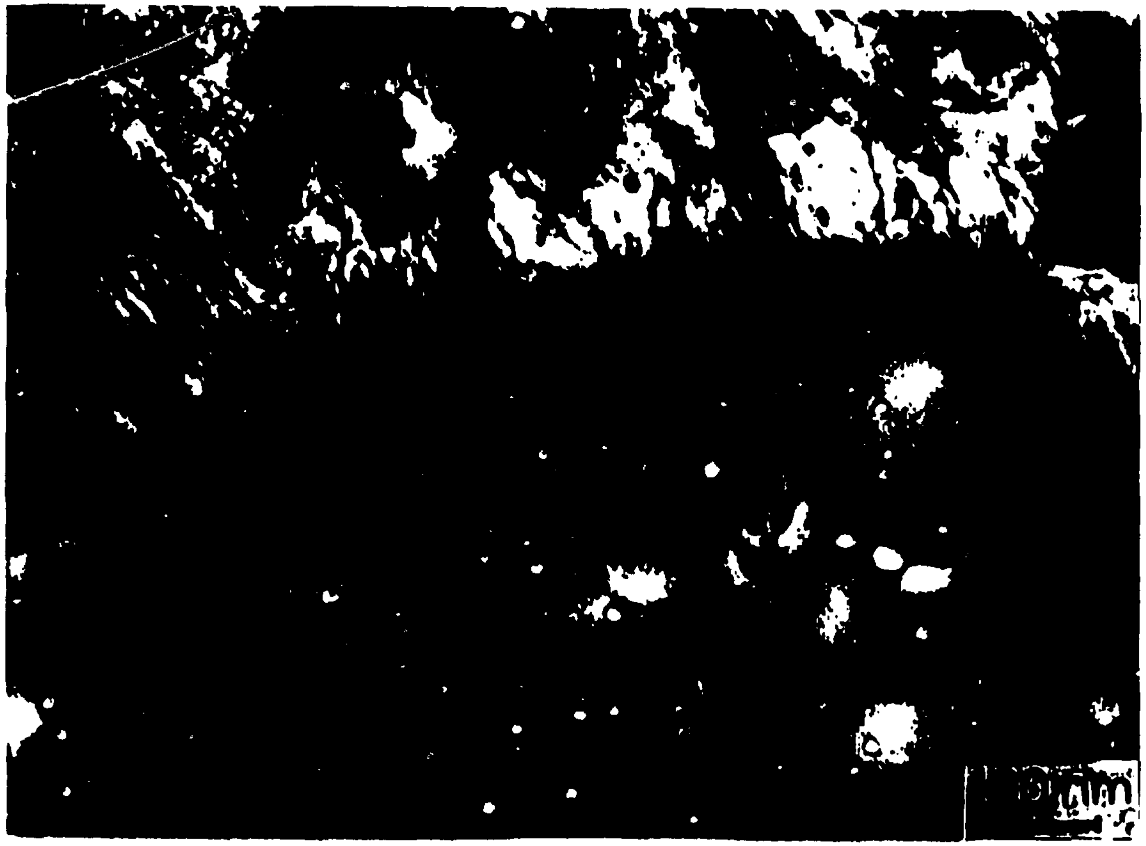

500°C, 57dpa in HFIR

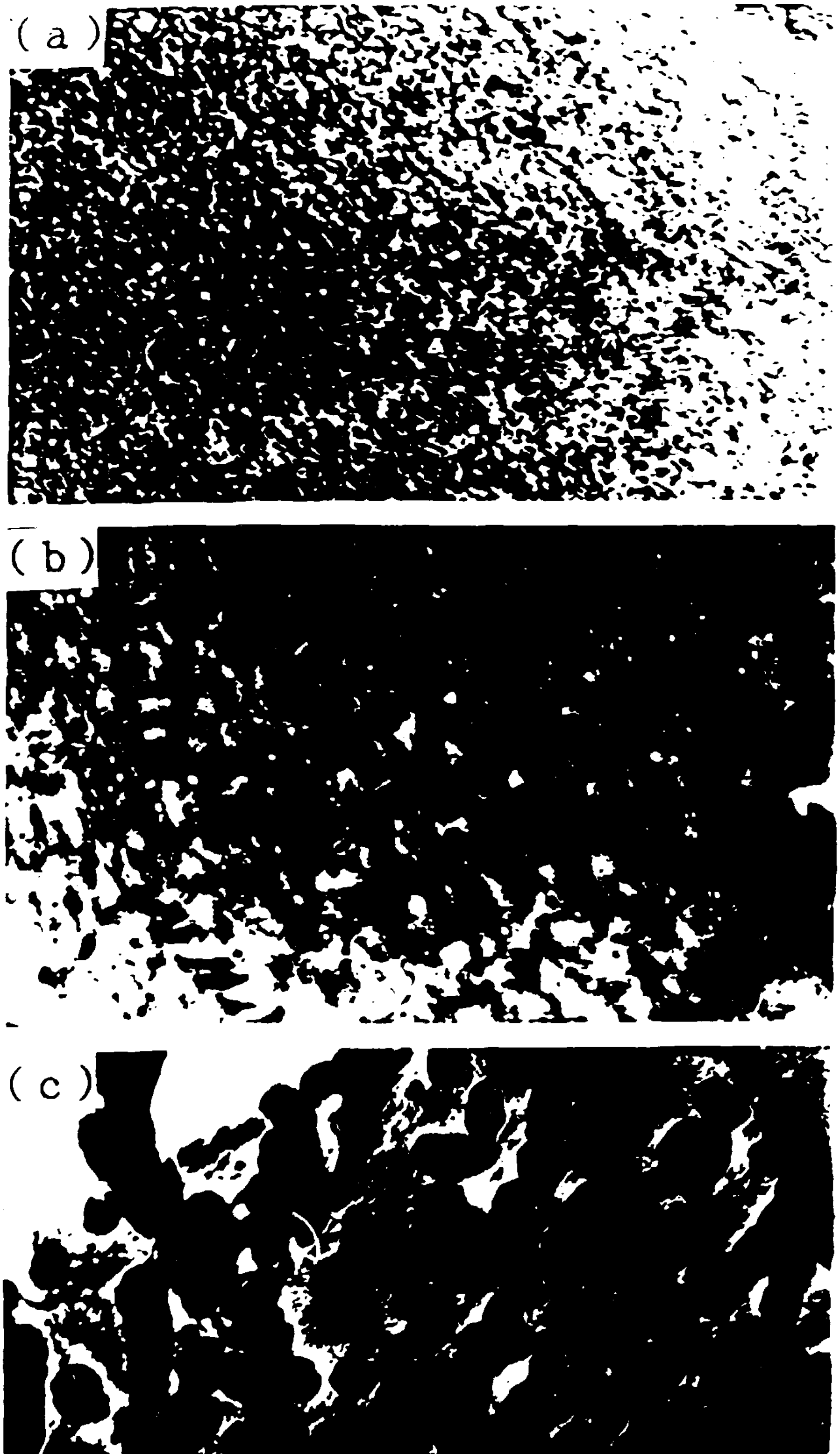

400℃, 57DPA

500℃, 57DPA

600℃, 34DPA

EFFECT OF HELIUM GENERATION ON SWELLING BEHAVIOR OF FERRITIC STEEL -FROM THE OBSEVATION OF 10CR-2MO STEEL IRRADIATED IN HFIR-

(1) Observation of fluence dependency of cavity development suggests that the swelling was enhanced by the conversion of helium bubbles into voids.

(2) Peak swelling temperature was observed at ~500℃, while most of the data without helium generation show ~400℃ as a peak swellinng temperature.

(3) The swelling rate was, however, still low compared with austenitic stainless steel; ~0.03%/dpa

(4) Further experiments are needed for the correct He/dpa ratio to higher dose.

HELIUM-RIS-VOID CORRELATION

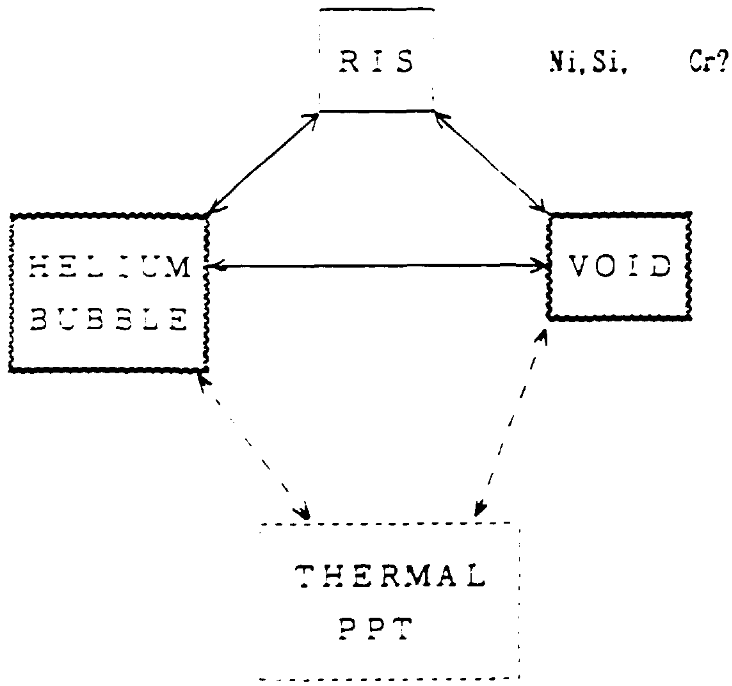

INFLUENTIAL FACTORS

1) BUBBLE DENSITY

2) THERMAL CHARACTERISTICS

3) DISLOCATION DENSITY

ETC.

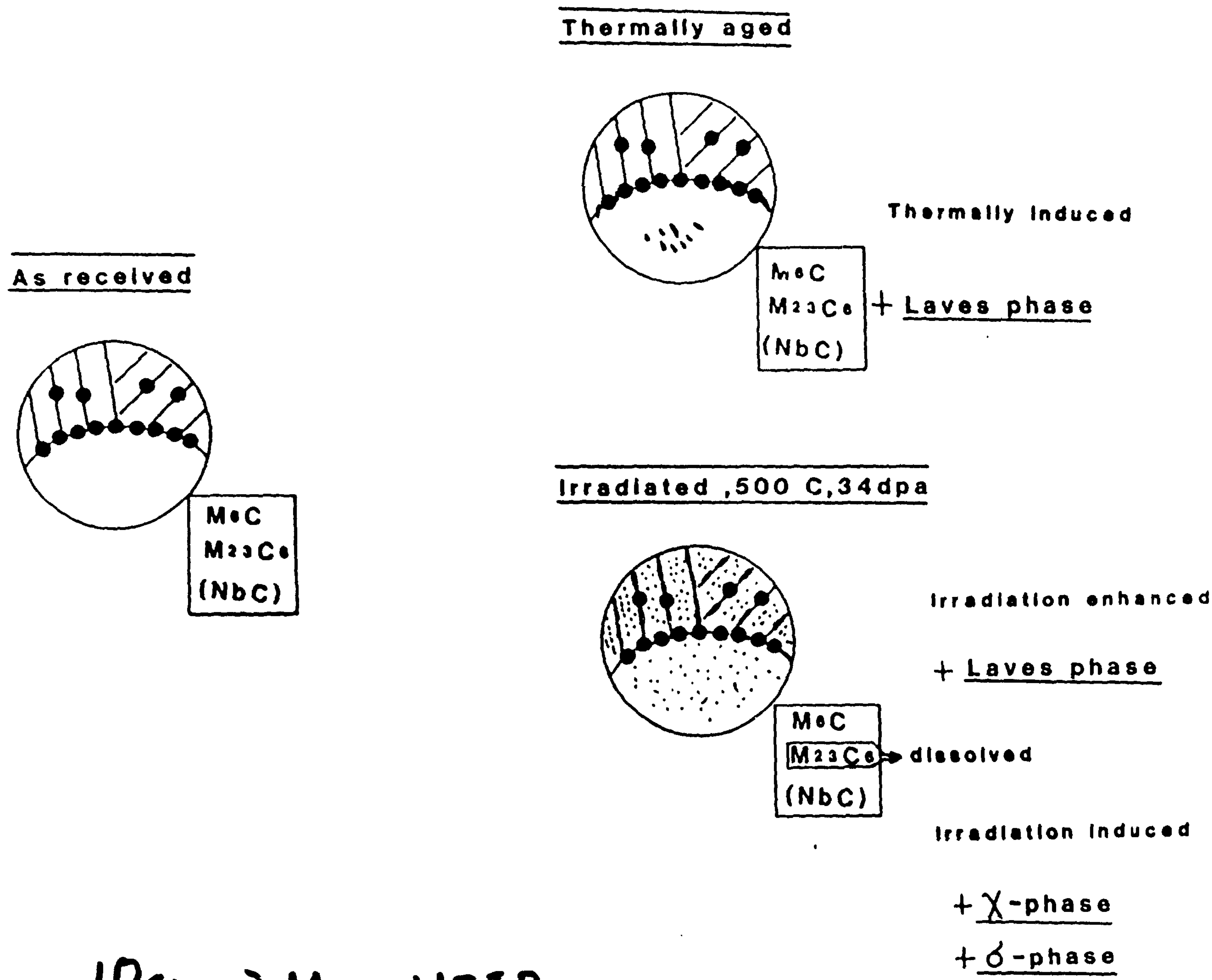

10cr-2Mo, HFIR

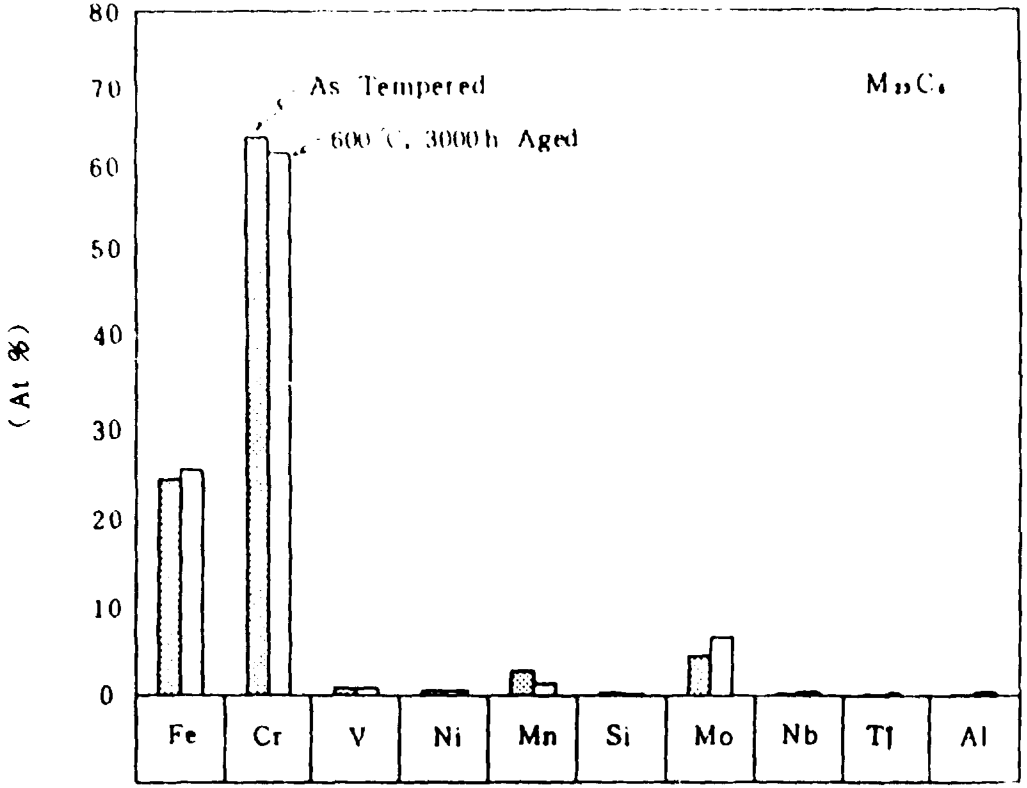
(At %)
80
70
60
50
40
30
20
10
0
As Tempered
600 ℃, 3000 h Aged
$M_{23}C_6$
Fe
Cr
V
Ni
Mn
Si
Mo
Nb
Ti
Al

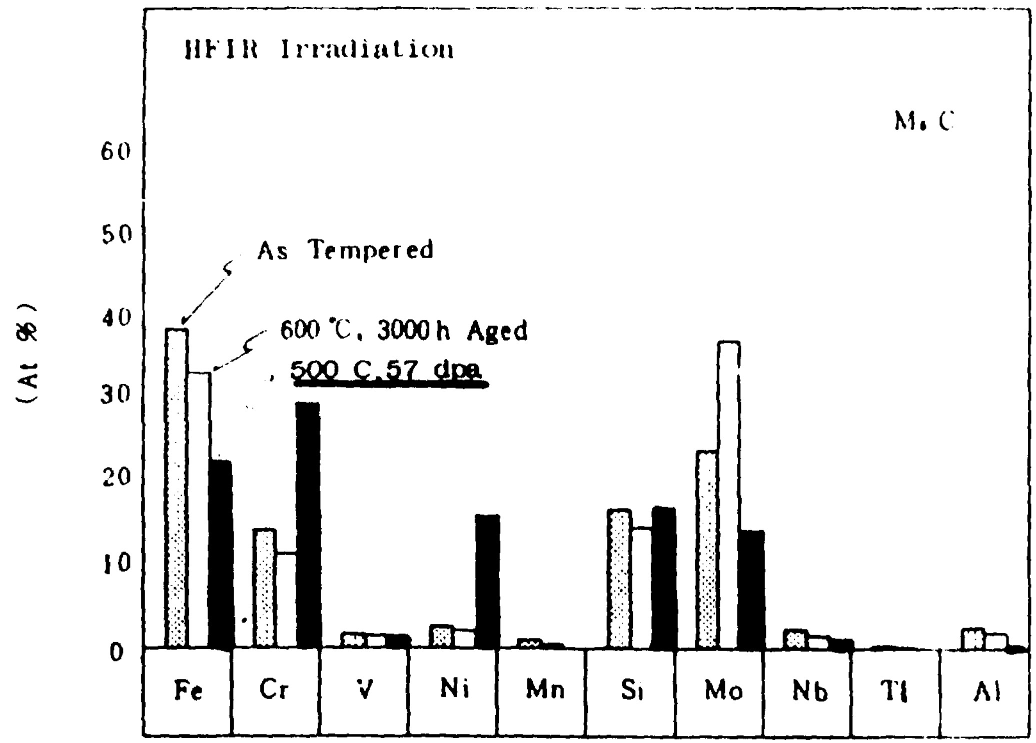
HFIR Irradiation
M₆C
As Tempered
600 °C, 3000 h Aged
500 C,57 dpa
(At %)
0
10
20
30
40
50
60
Fe
Cr
V
Ni
Mn
Si
Mo
Nb
Ti
Al

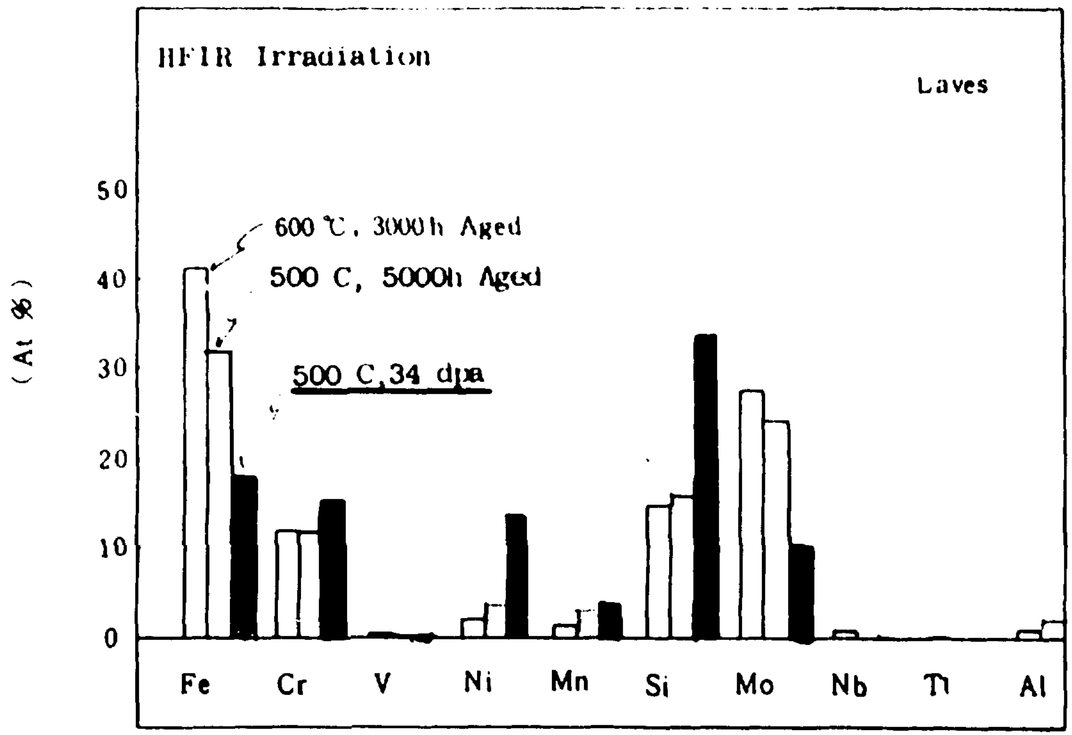

HFIR Irradiation
Laves
600 ℃, 3000 h Aged
500 C, 5000h Aged
500 C,34 dpa
(At %)
50
40
30
20
10
0
Fe
Cr
V
Ni
Mn
Si
Mo
Nb
Ti
Al

ORNL-Photo 6579-88

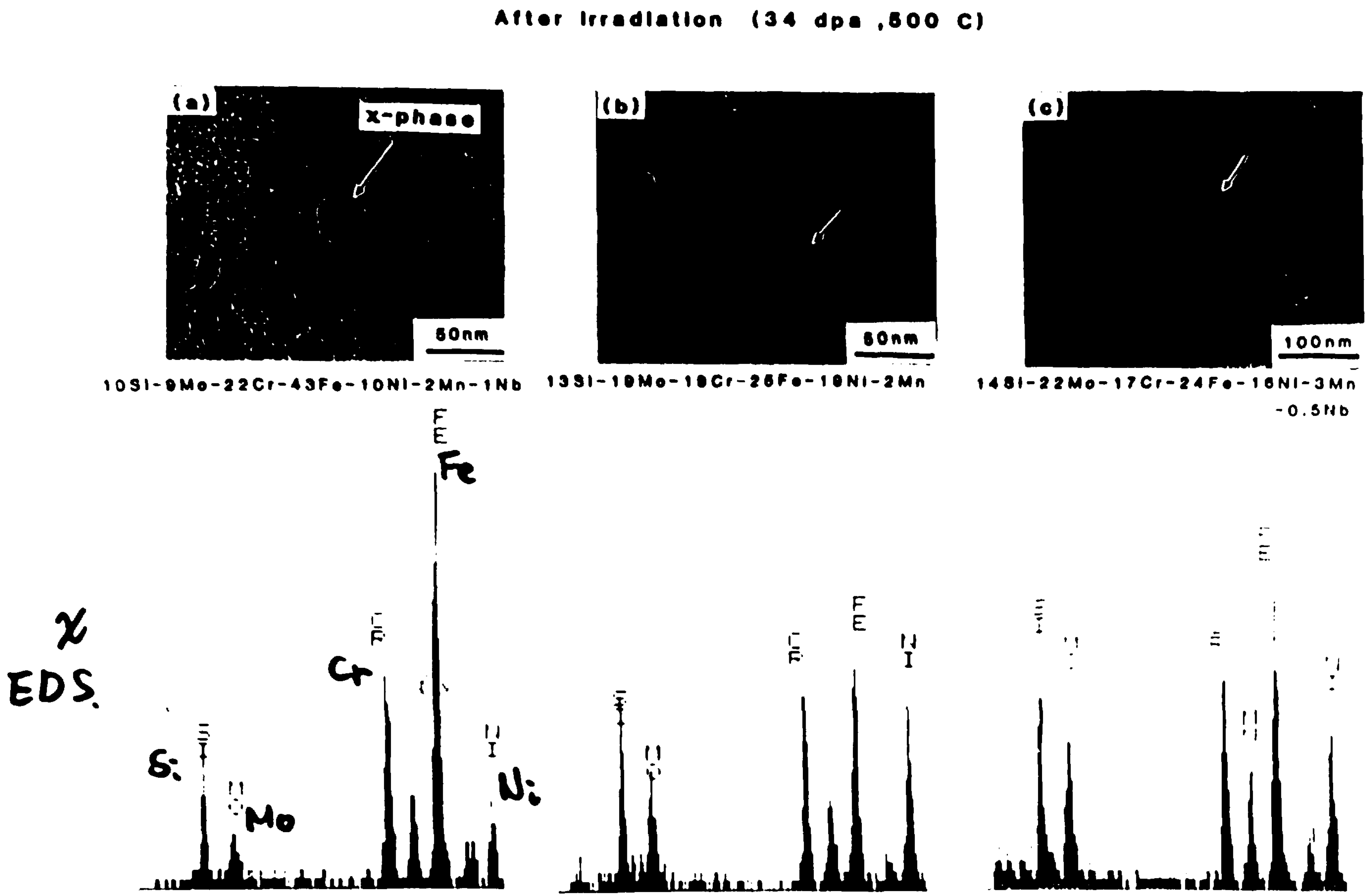

helium bubble
formation at dislocations
, boundary
, etc.

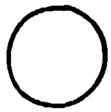

Ni, Si segregation
by Inverse Kirkendall effect
or other

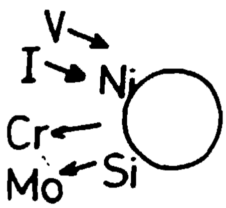

First stage

Second stage

PPT nucleation

Cr also began to segregate

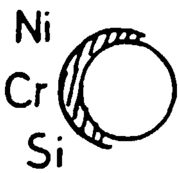

caused by sink strength change
or chemical effect

PPT development

Competitive precipitation development
between thermal and RIS precipitates

ORNL-Photo 6378-88

Carbon Extracted Replica

500 C ,34dpa

500 C ,57dpa

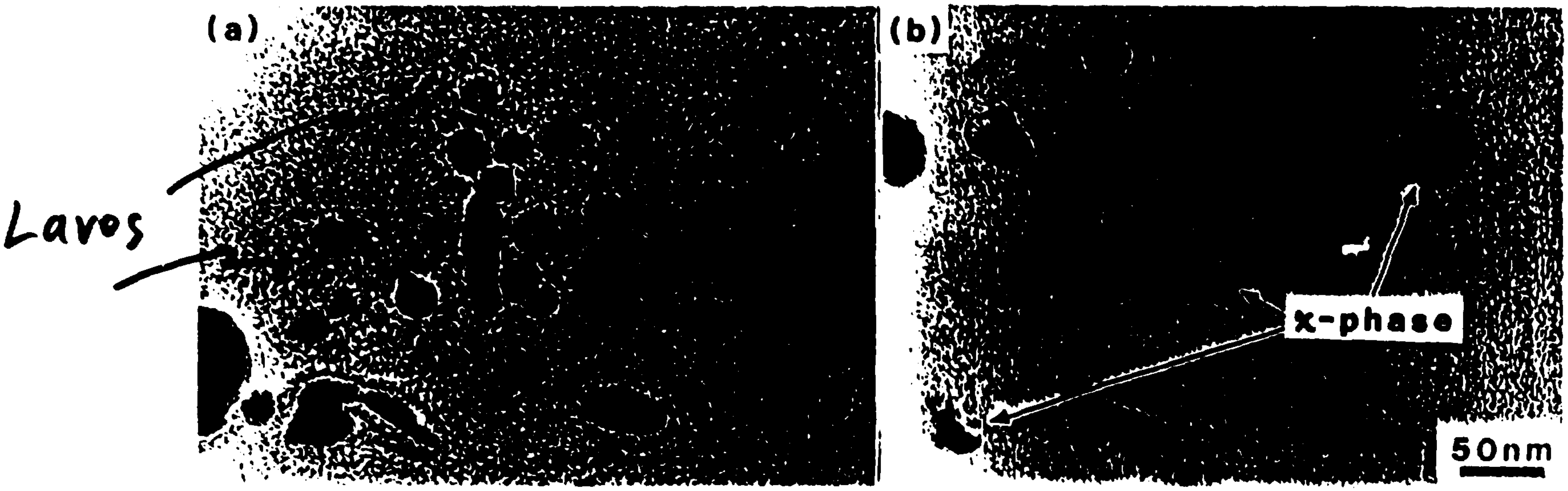

EFFECT OF HELIUM GENERATION ON SWELLING BEHAVIOR OF FERRITIC STEEL -FROM THE OBSEVATION OF 10CR-2MO STEEL IRRADIATED IN HFIR-

(1) Observation of fluence dependency of cavity development suggests that the swelling was enhanced by the conversion of helium bubbles into voids.

(2) Peak swelling temperature was observed at ~500℃, while most of the data without helium generation show ~400℃ as a peak swellinng temperature.

(3) The swelling rate was, however, still low compared with austenitic stainless steel; ~0.03%/dpa

(4) Helium bubbles also affected the precipitation behavior greatly probably through RIS.

(5) Correct He/dpa ratio is required to higher dose experiment, as helium affects both swelling and precipitation behavior.

CORRELATION OF TEM AND DENSITY DATA

Tomotsugu Sawai

ABSTRACT

Part I

In our collaborative research, the swelling values of irradiated material are determined by precision densitometry and microstructural observation with TEM. In many cases, however, the values of densitometry and TEM do not coincide very well. The accuracy of the data obtained by TEM is examined. The effect of polished out voids on the surface of the TEM specimen and the overestimation of foil thickness are the possible reasons of the underestimated value of swelling obtained with TEM. A method to obtain more reliable values for foil thickness is proposed. After taking appropriate care, the TEM swelling value of examined specimens was successfully corrected, although in some specimens the discrepancy between the data by precision densitometry and TEM is too large to be corrected only by the TEM value.

Part II

Contamination Spot Separation (CSS) method has been employed to determine the foil thickness of irradiated specimens in our collaborative research, especially by the Japanese side. This method includes appreciable error (overestimates) in measurement. A new imaging model is proposed to explain this error and some other features of this method. This model has several advantages over the currently accepted model.

Void swelling has been determined by two methods;

① Densitometory

The density is determined from the Archimedean method of comparing wet and dry weights of the TEM disks.

Void swelling is determined from the two values of density measured for irradiated and unirradiated disks.

② TEM

Voids are observed by TEM and size and number data are used to calculate void swelling.

Quantitative analysis always requires the data of foil thickness where the micrograph was taken.

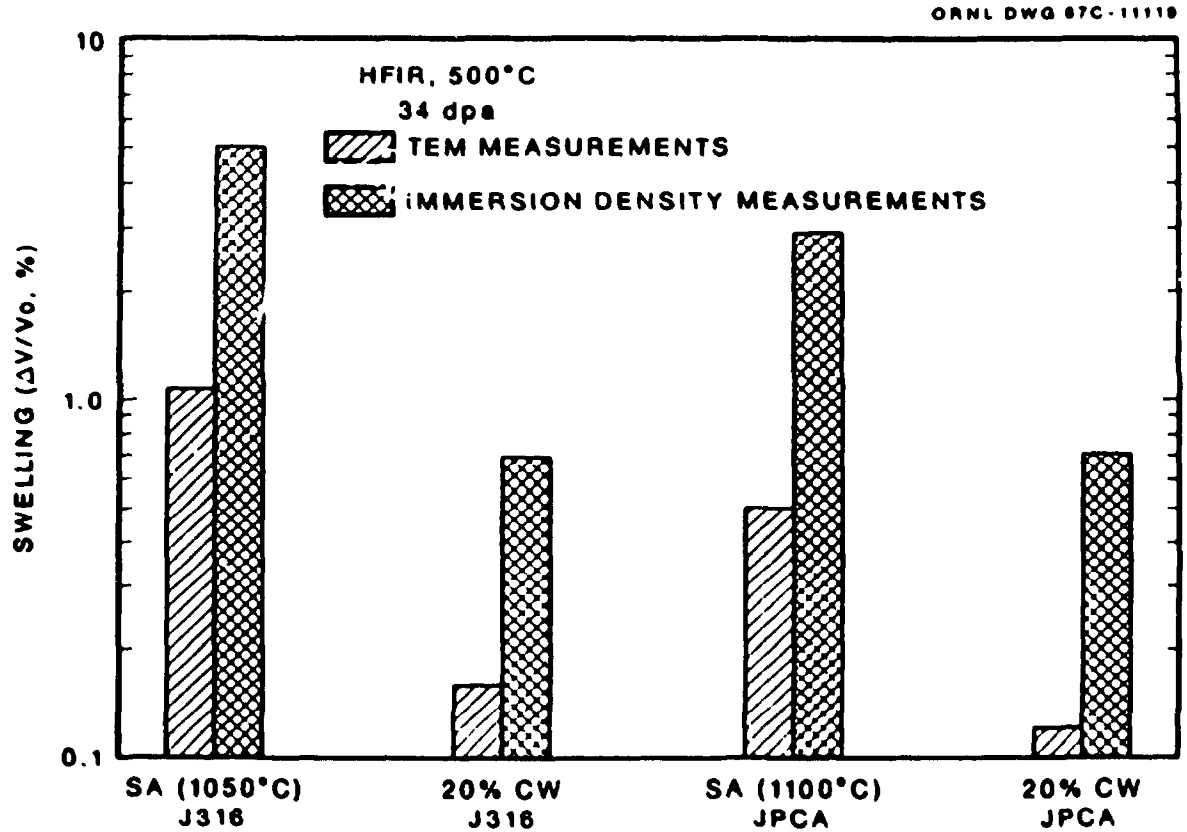

Fig. 4. A comparison of swelling measured by TEM and by immersion density change for SA and 20% CW J316 and JPCA irradiated at 500°C to 34 dpa in HFIR.

from P. J. Maziasz et al.

"Fusion Reactor Material Semiannual Progress Report for Period Ending March 31, 1987"

PART I

I Possible reasons for underestimated values of swelling in microscopy.

a. Polished-out voids
b. Overestimated foil thickness

PART II

2 A new image interpretation of tilted contamination spots.

-proposed model to understand the overestimated foil thickness

a. Polished-out voids

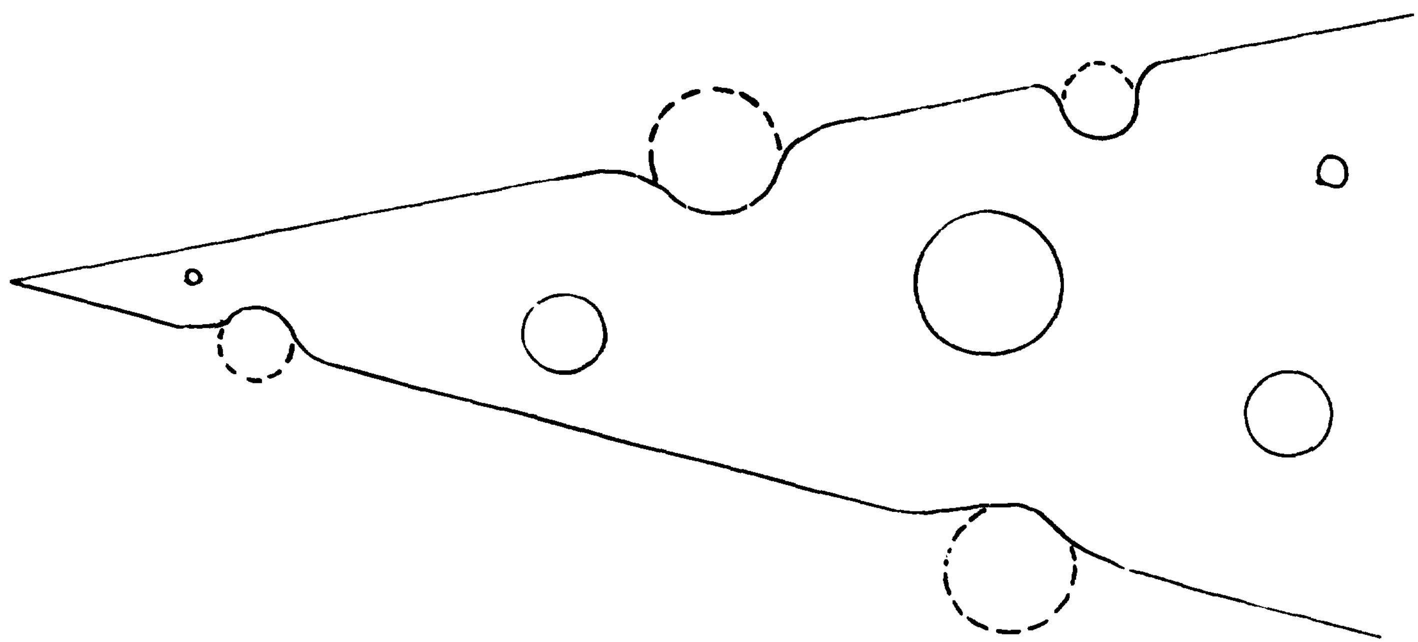

a. Polished-out voids

- This effect alone cannot explain the discrepancy at low swelling case, where voids are enough small.

- It depends on somewhat personal decision to include a void or not.

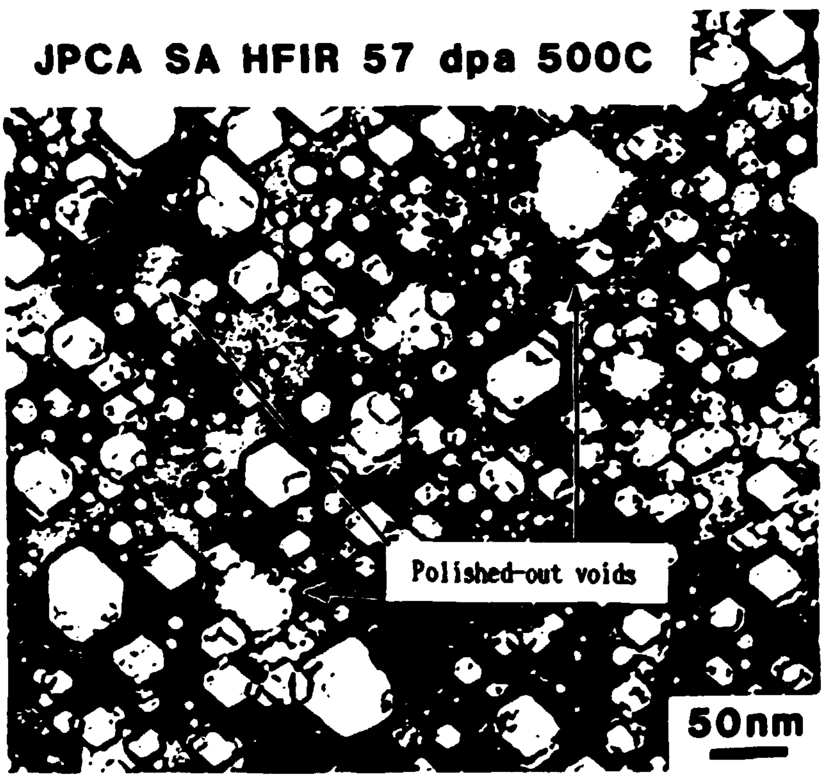

b. overestimated foil thickness

The method usually employed to determine the foil thickness is

"Contamination-Spot-Separation method" (CSS method)

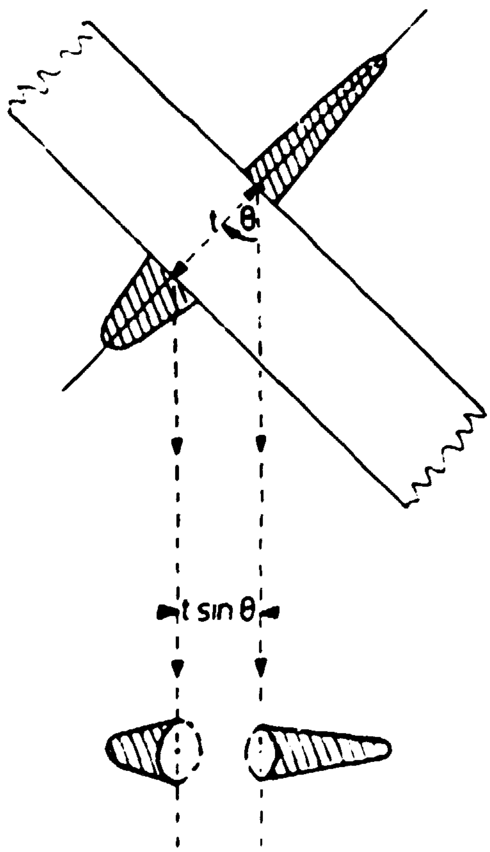

7 Expected carbon profile and plan view of spots resulting from cones of contamination produced at normal incidence to foil

Stereo Method (Conventional)

To take two micrographs at the tilting angles of specimen $\pm\theta$.

θ: 5~10°

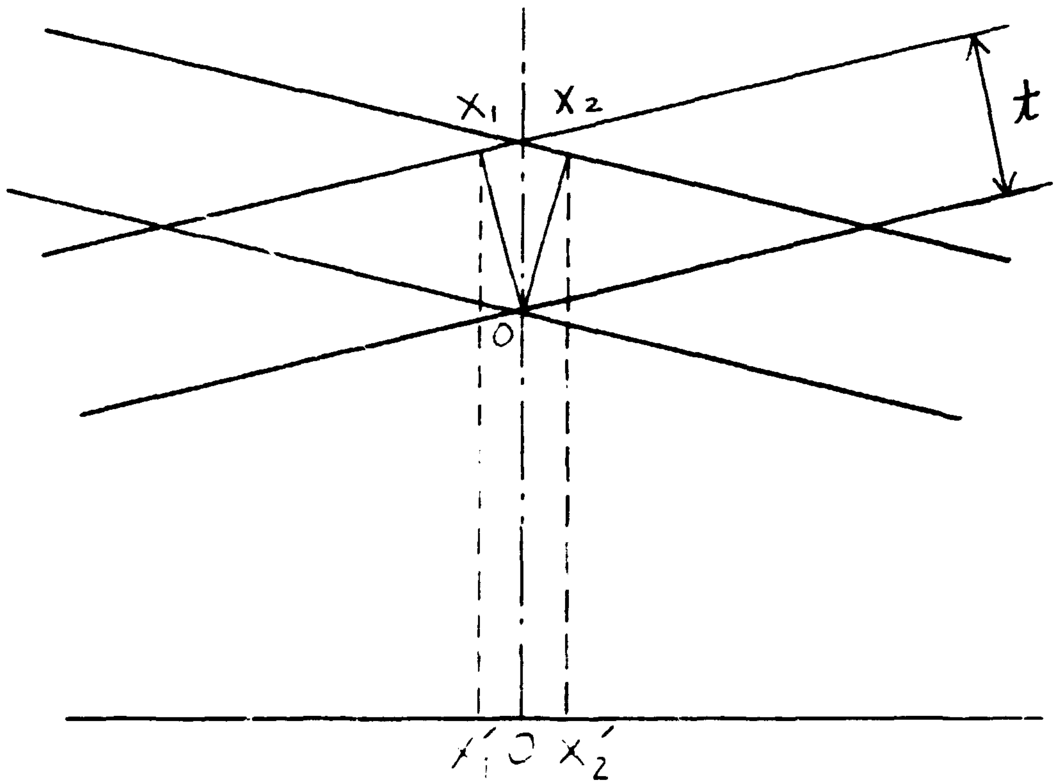

$$P = \overline{X_1' X_2'}$$

$$= 2t \sin\theta$$

Stereo Method (Modified)

To take many micrographs at the tilting angles of specimen within the limit of specimen holder.

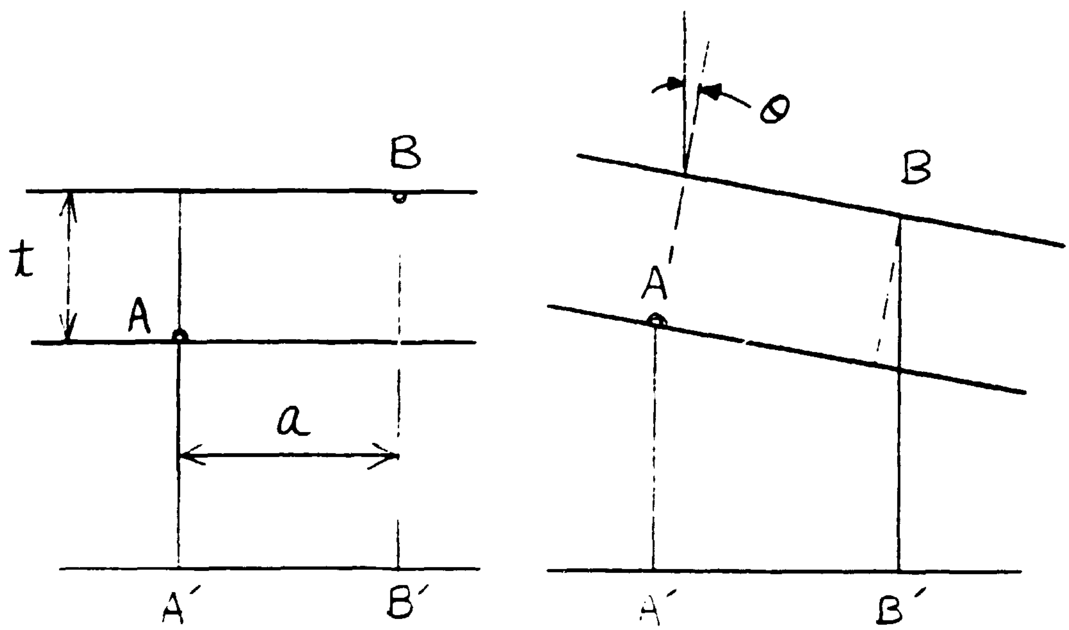

$$A'B' = a \cdot \cos\theta - t \cdot \sin\theta$$

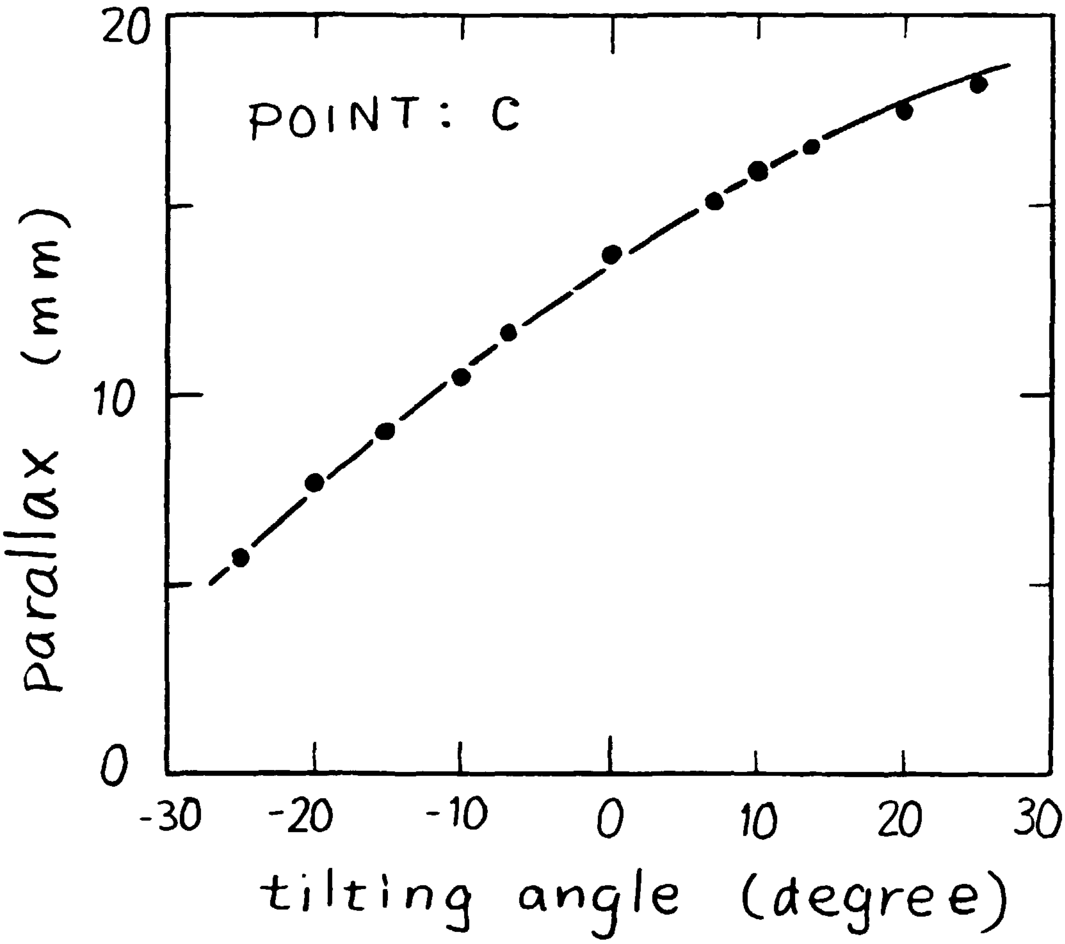

fitting curve

$a = 13.5$ mm

$t = 15.0$ mm

$$P = a \cdot \cos\theta - t \cdot \sin\theta$$

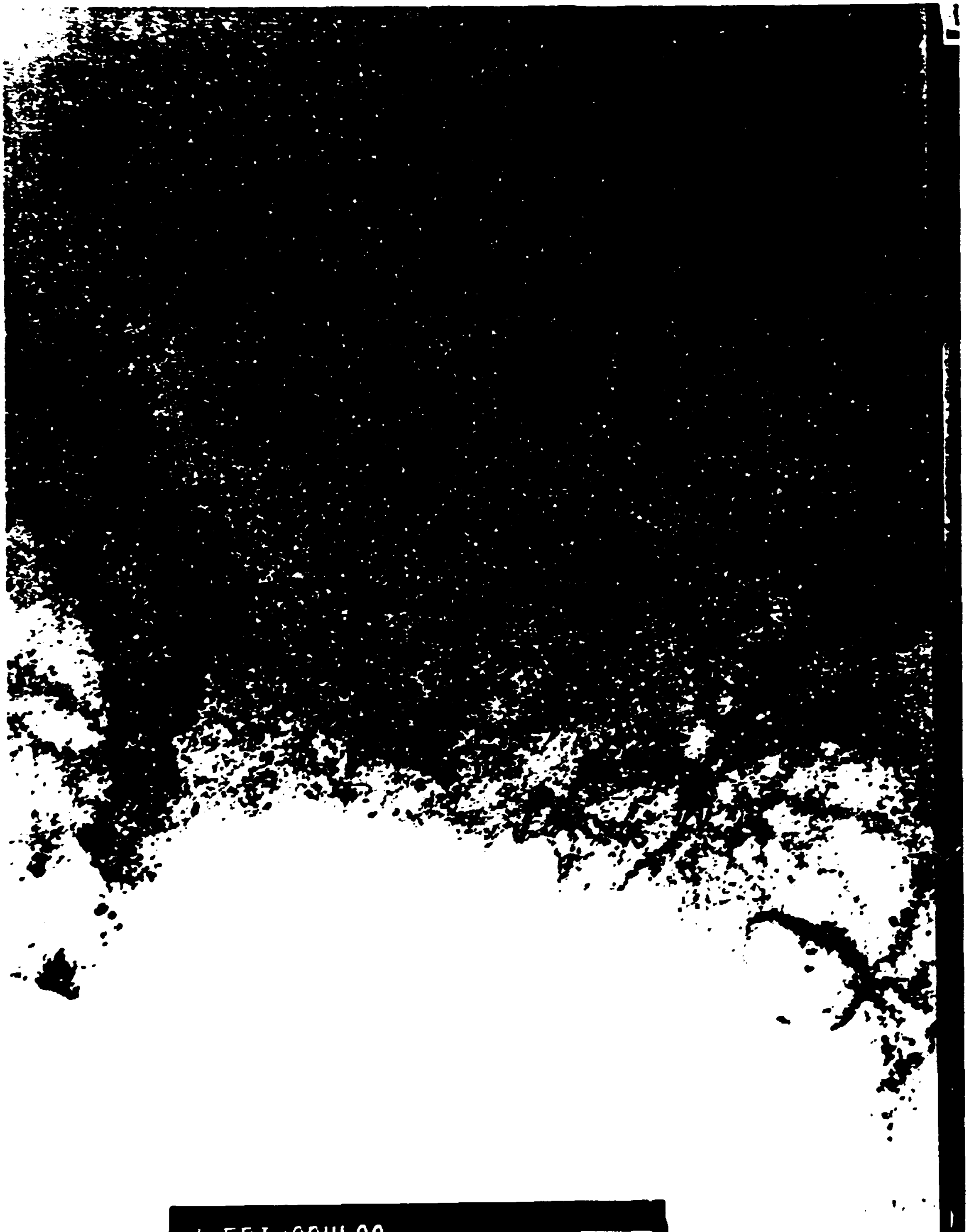
JAERI/ORNL88
014431 200.0KV X5000 1μm

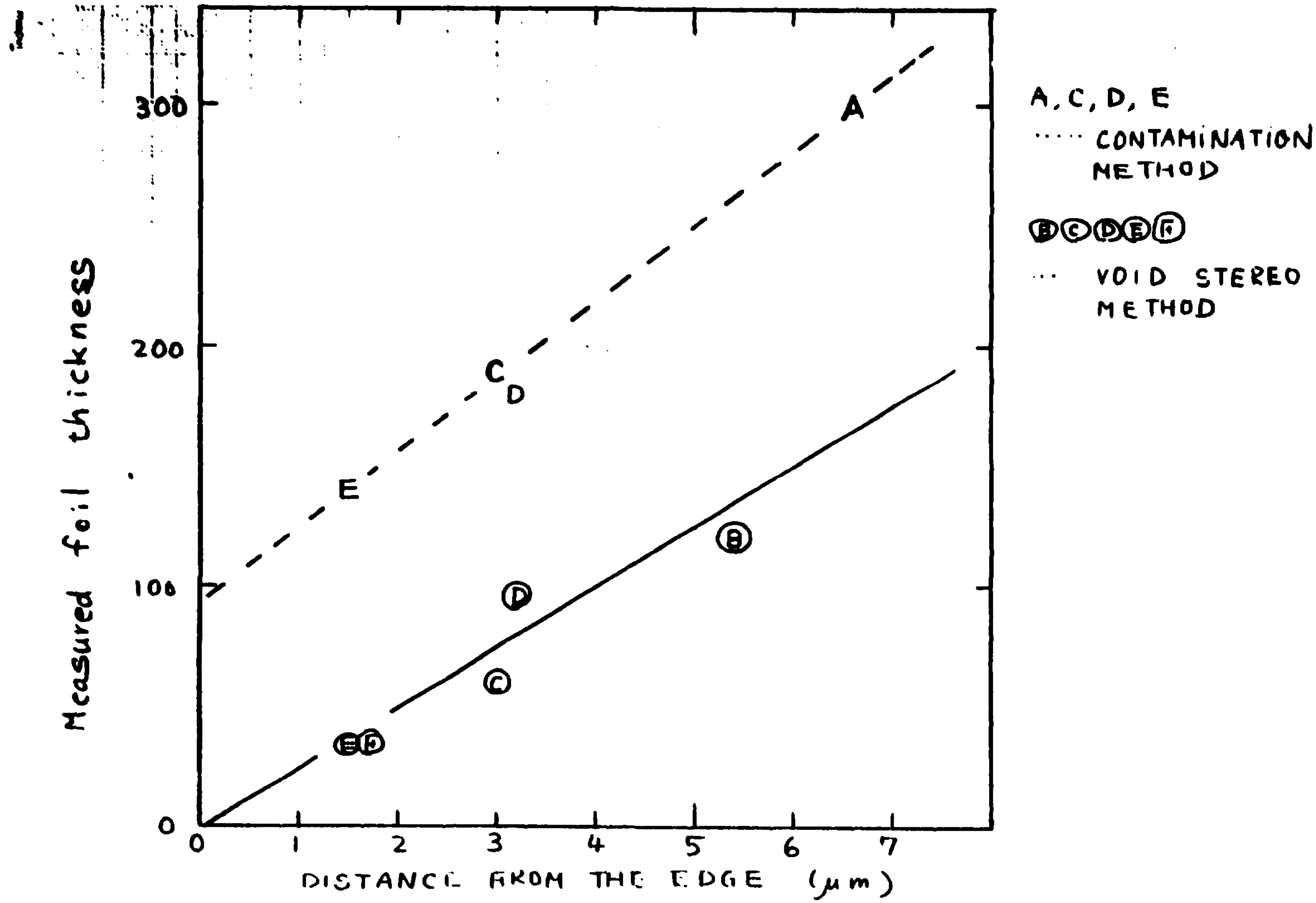

A, C, D, E
····· CONTAMINATION METHOD
BCDEF
··· VOID STEREO METHOD
A
C
D
E
B
D
C
E F
Measured foil thickness
300
200
100
0
0
1
2
3
4
5
6
7
DISTANCE FROM THE EDGE (μm)

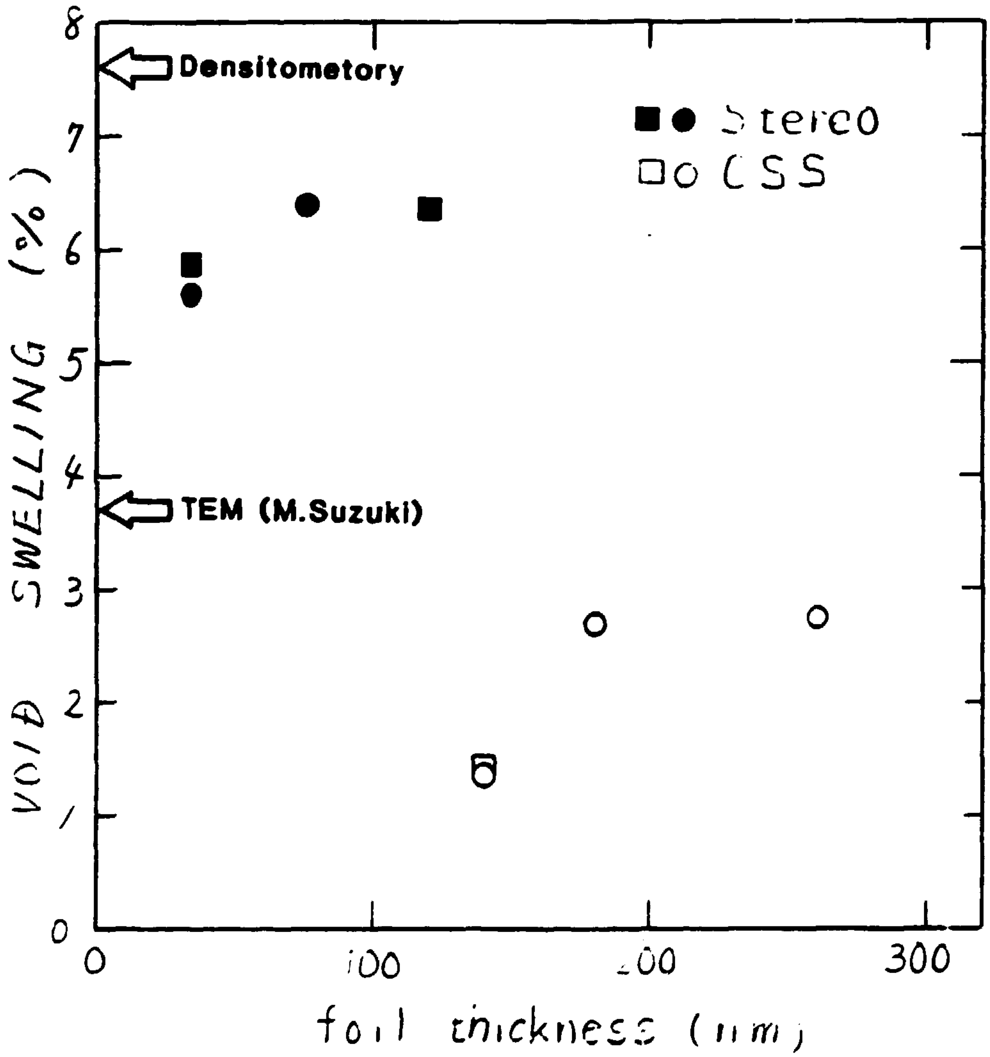
Densitometory
TEM (M.Suzuki)
Stereo
CSS
VOID SWELLING (%)
foil thickness (nm)
0
1
2
3
4
5
6
7
8
100
200
300

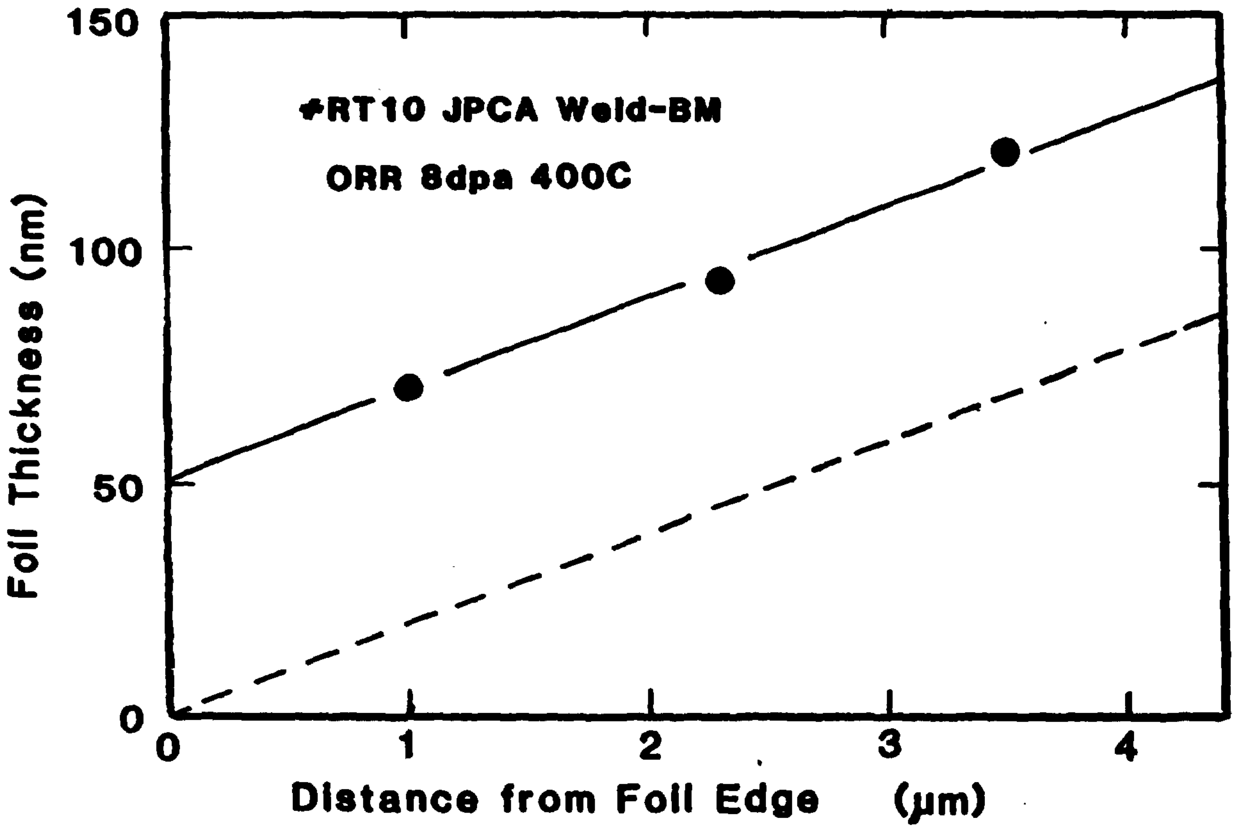

150
100
50
0
0
1
2
3
4
#RT10 JPCA Weld-BM
ORR 8dpa 400C
Foil Thickness (nm)
Distance from Foil Edge (μm)

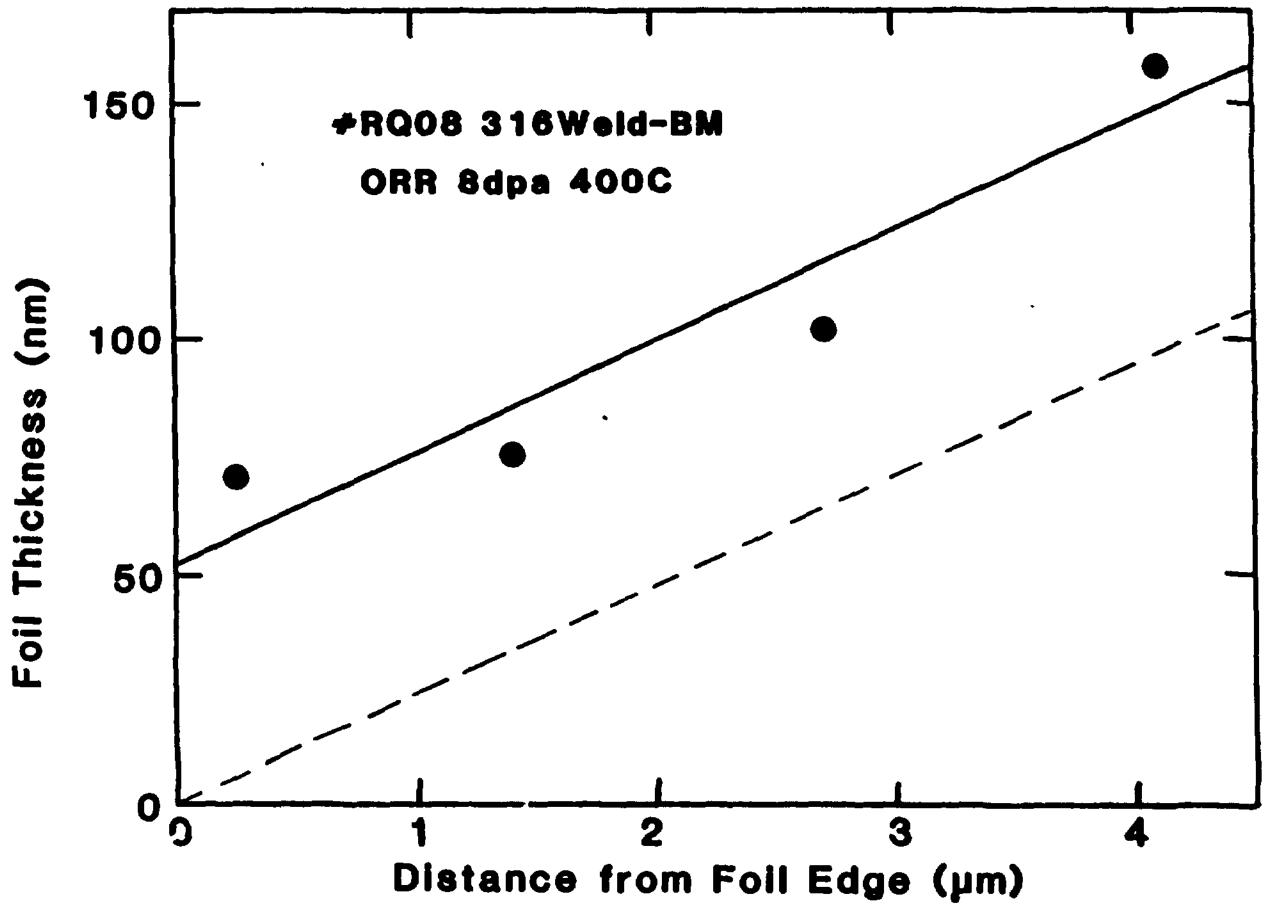
#RQ08 316Weld-BM
ORR 8dpa 400C
150
100
50
0
0
1
2
3
4
Foil Thickness (nm)
Distance from Foil Edge (μm)

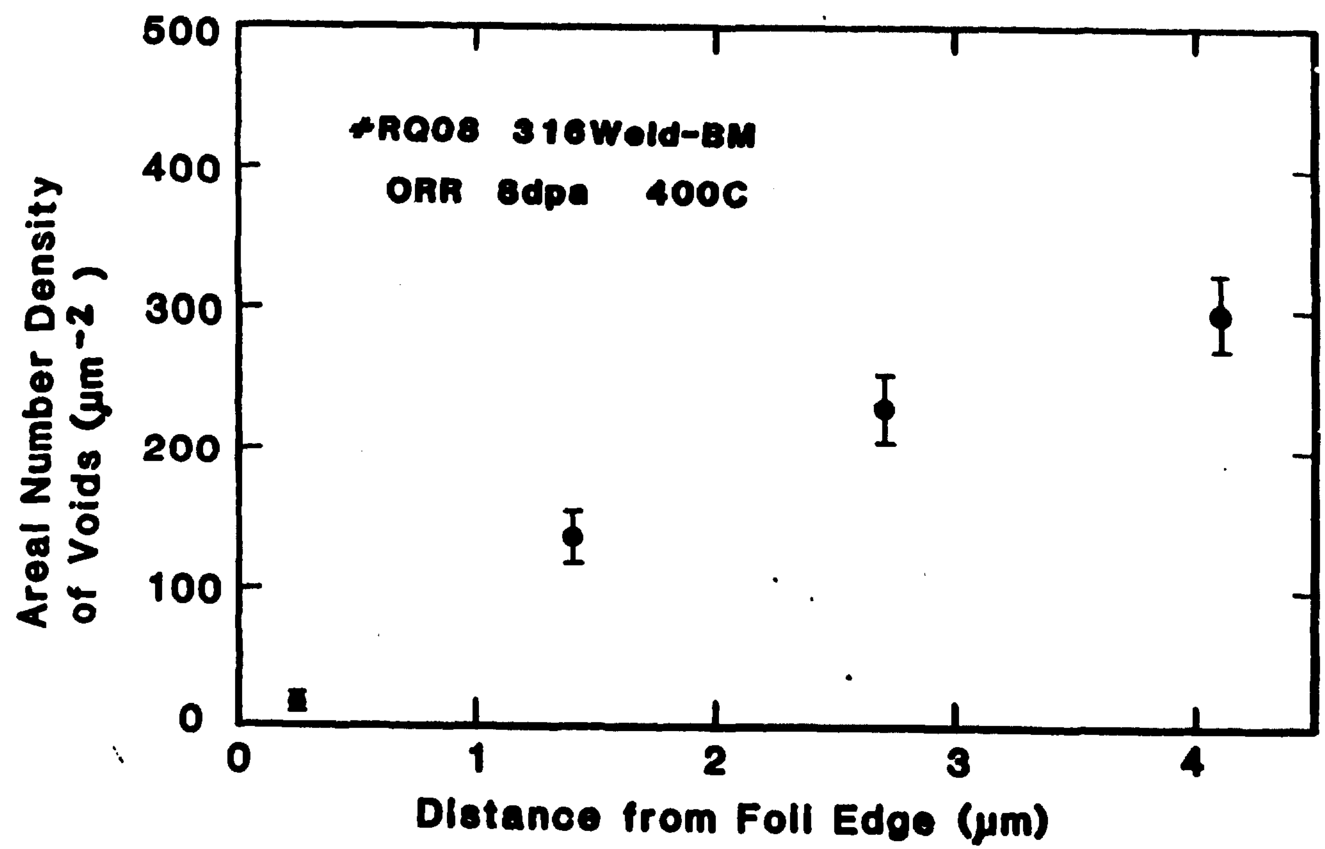

#RQ08 316Weld-BM
ORR 8dpa 400C
Areal Number Density of Voids (μm⁻²)
0
100
200
300
400
500
0
1
2
3
4
Distance from Foil Edge (μm)

SUMMARY OF PART 1

1. Microstructural data, including void swelling data, obtained our Phase-I HFIR irradiation program may suffer from some error caused by the overestimated foil thickness determined by CSS method.

2. Void swelling of JPCA SA irradiated in HFIR up to 57dpa at 500 C was re-calculated from the micrograph with the thickness determined by stereo method. The obtained value was closer to the value by densitometory than prior microstructural data, although complete coincidence was not achieved.

3. A method was proposed to obtain more reliable thickness data from irradiated TEM disk. This method includes the correction of CSS data by assuming wedge shape of specimen foil.

PART II

--A new image interpretation of tilted contamination spots.

Simple Questions:

① Why overestimate?

② Why base-oval appears only outer side?

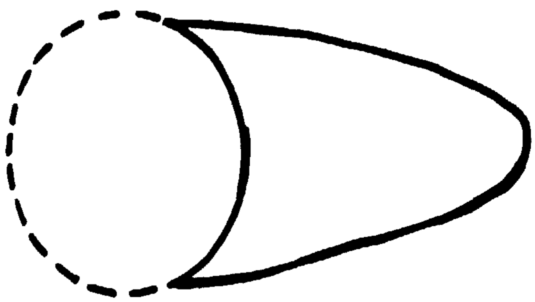

Overestimated foil thickness is a common matter with CSS method.

A model has been proposed to explain this overestimate:

"witch's hat model"

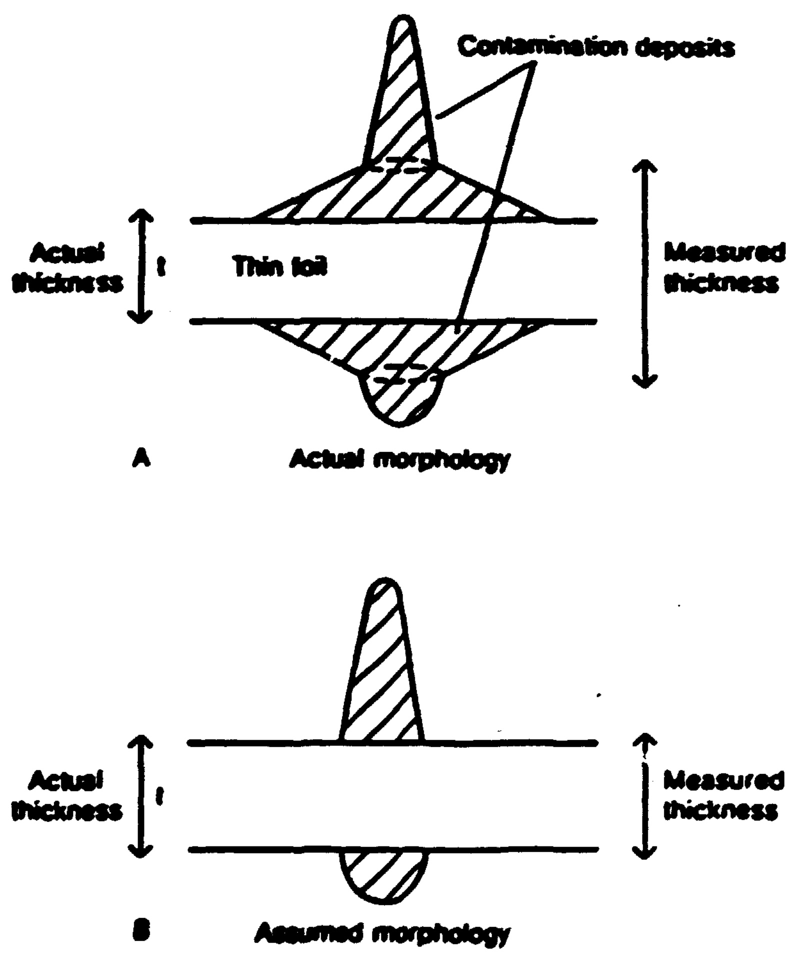

Figure 4.28. Schematic diagrams of a) contamination deposits observed by Rae et al. (1981) and b) deposits usually observed (see Figure 4.27) and used to measure thickness. The reason why this method overestimates thickness is apparent.

drawing taken from: "Practical Analytical Electron Microscopy in Materials Science" by D. B. Williams

New model:

"Tangent imaging model from Gaussian profiled contamination"

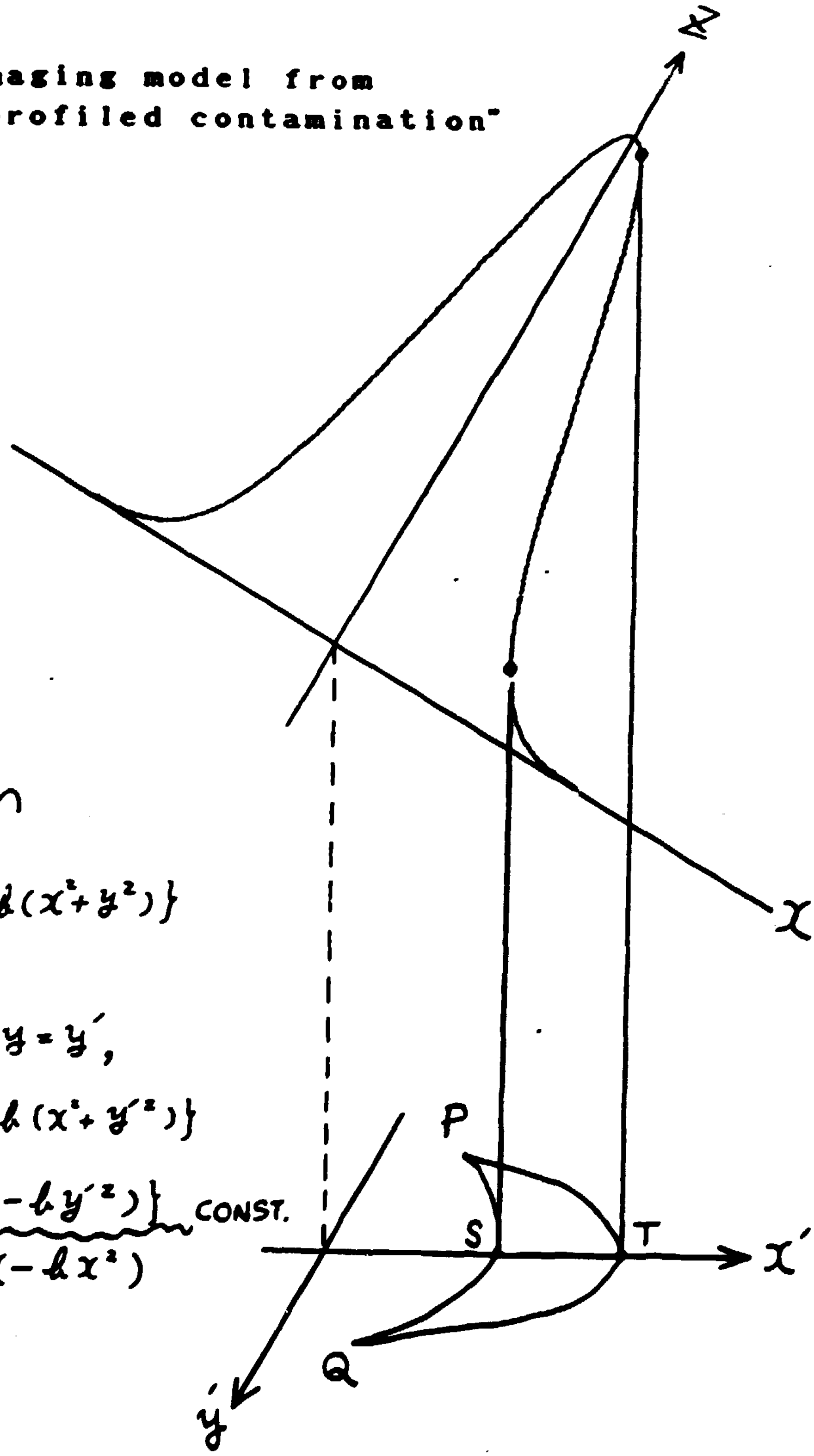

rotated Gaussian

$$z = a\cdot \exp\{-b(x^2+y^2)\}$$

on a plane $y = y'$,

$$z = a\cdot \exp\{-b(x^2+y'^2)\}$$

$$= \underbrace{\{a\cdot \exp(-by'^2)\}}_{\text{CONST.}} \times \exp(-bx^2)$$

$$Z = a \cdot \exp\{-b(x^2 + y^2)\}$$

on the plane $y = y_0$,

$$Z = a \cdot \exp(-b y_0^2) \cdot \exp(-b x^2)$$

$$\therefore \; Z' = a \cdot \exp(-b y_0^2) \cdot \; x \cdot \exp(-b x^2)$$

tilt $= Z' = \cot\theta$ (θ is measured

from Z axe!), then

$$\boxed{x \cdot \exp(-b x^2) = \frac{-\cot\theta}{2a \cdot b \cdot \exp(-b y_0^2)}}$$

$\Downarrow$

numeric solution (Newton-Raphson method)

$\Downarrow$

(x, y, Z) on contamination surface

$\Downarrow$ projection

(x', y') on film plane

at points P and Q,

condition

$$\begin{cases} z' = \cot\theta \\ z'' = 0 \end{cases}$$

solution

$$\begin{cases} x = \pm \dfrac{1}{\sqrt{2b}} \\ y = \pm\sqrt{\dfrac{1}{b}\left\{\ln\left(\dfrac{a\sqrt{2b}}{\cot\theta}\right) - \dfrac{1}{2}\right.} \\ z = \cdots\cdots \end{cases}$$

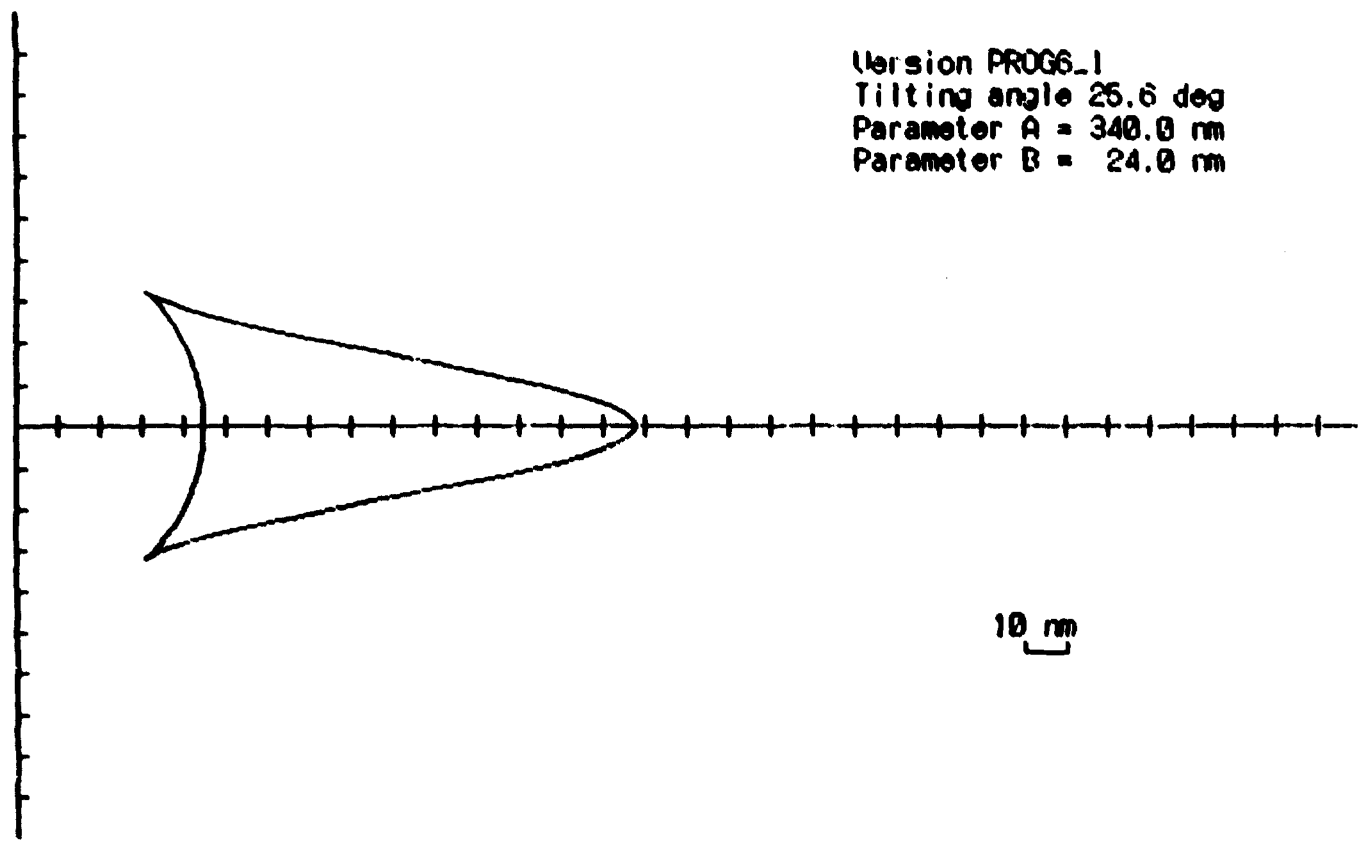

Version PROG6_1
Tilting angle 25.6 deg
Parameter A = 340.0 nm
Parameter B = 24.0 nm
10 nm

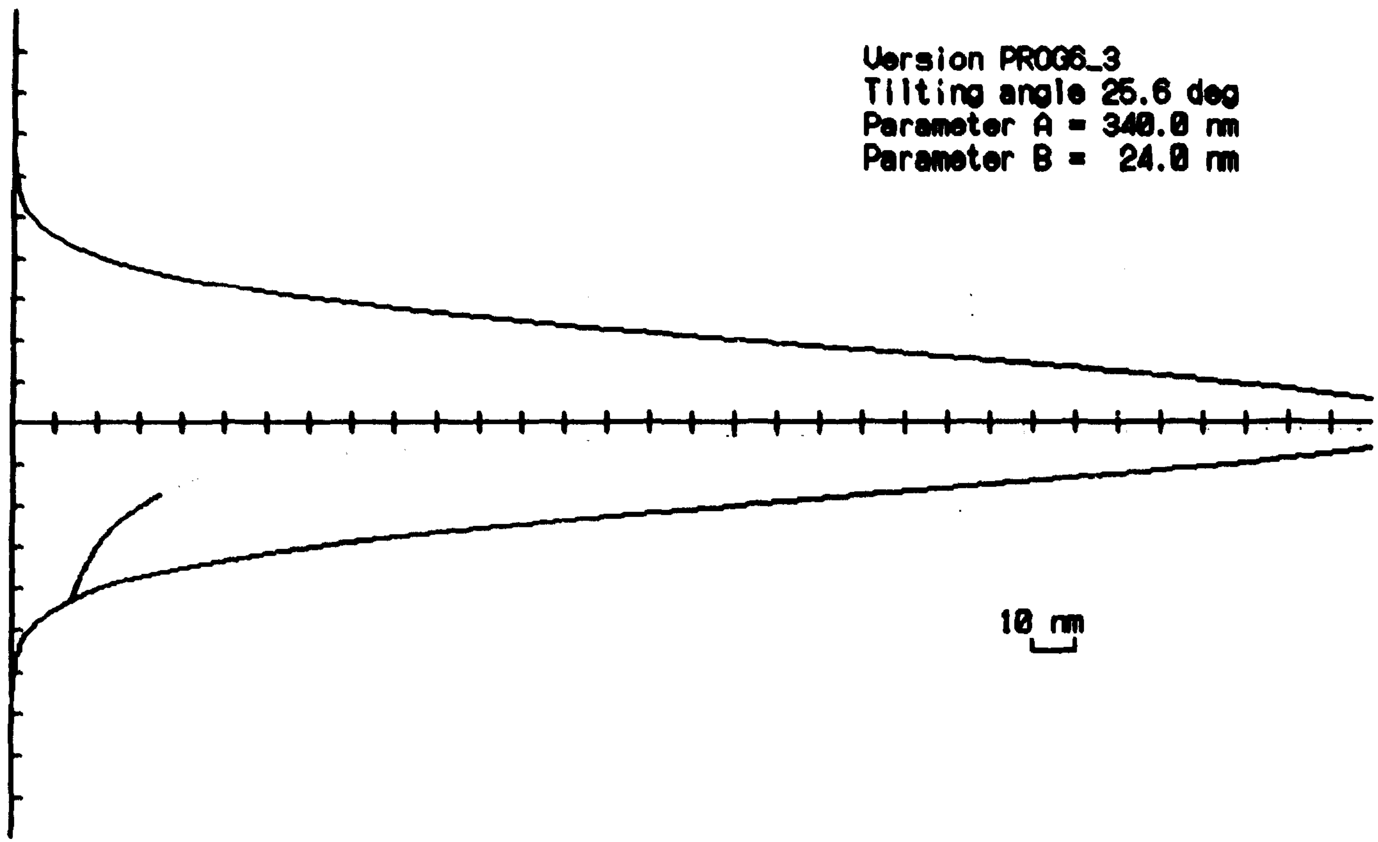
Version PROG6_3
Tilting angle 25.6 deg
Parameter A = 340.0 nm
Parameter B = 24.0 nm
10 nm

Characteristics and Advantages
of new model
----SUMMARY---

1. The base oval (strictly, not a true obal) appears only outer side.

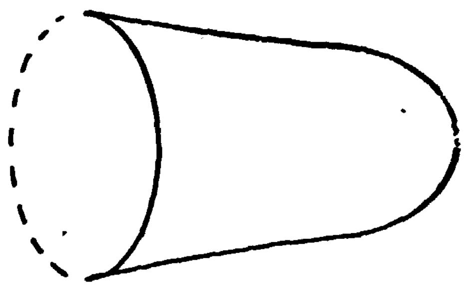

2. Points P and Q appear well off the ideal center line, which leads to the overestimation of parallax, then overestimation of foil thickness if measured, for example, PP'.

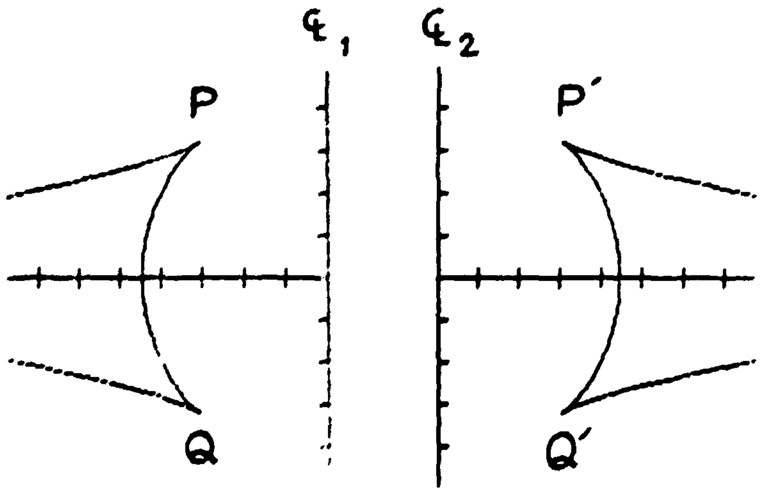

3. New model assumes smooth profile of contamination rather than somewhat artificial two step profile.

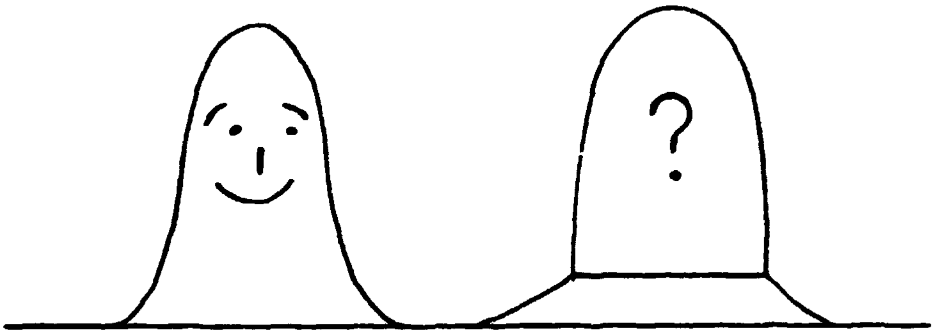

4. Using the tailing profile of contamination, the obtained image still looks like the contamination cone. stands steeply from specimen with slight tail, which is often the case with actual micrograph.
This steep appearance may have led microscopists to the base-plane-edge imaging model.

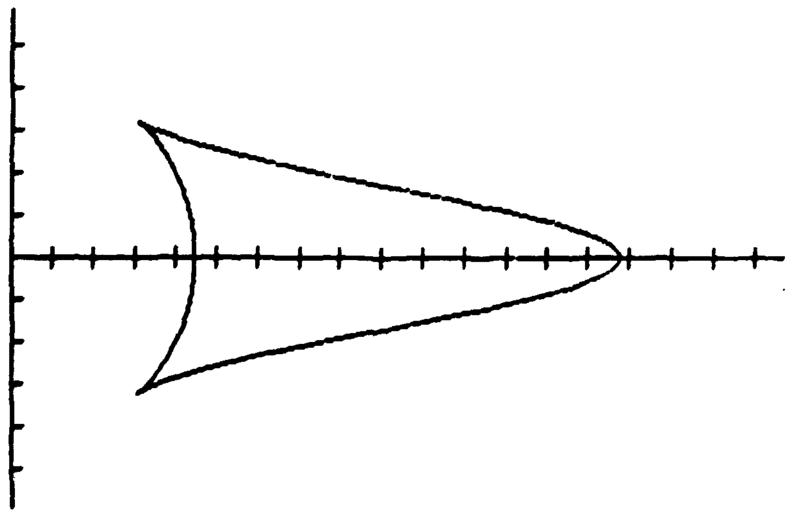

5. Fitting oval to the inner line can cross the extension of outer line.

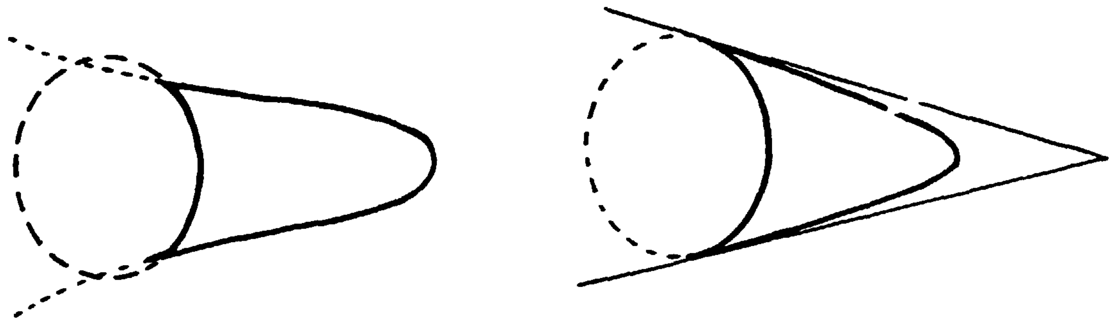

6. Calculated image coincides with the actual micrograph at the point that the ratio RS/PR is much smaller than $\cos\theta$. Base-plane-edge imaging model requires that this rate should be $\cos\theta$, and this has been neglected by many microscopists.

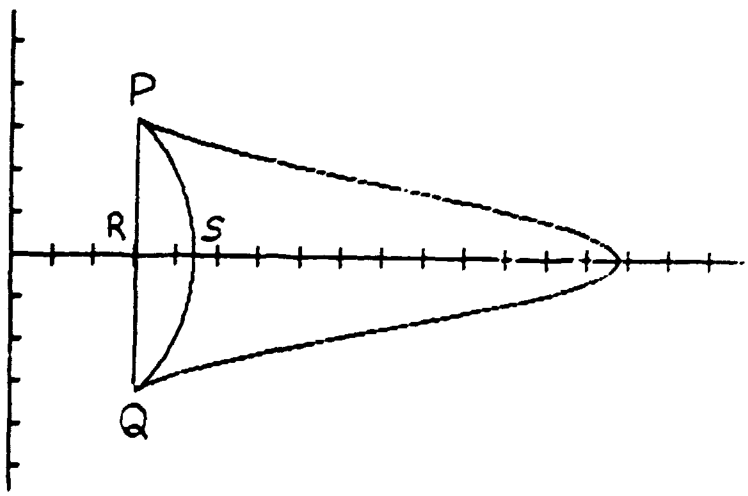

STATUS OF HFIR RB* SPECTRALLY TAILORED EXPERIMENTS

A. W. Longest

ABSTRACT

Irradiation capsule assembly and facility preparations for testing magnetic fusion energy (MFE) first-wall materials in two of the eight new removable beryllium (RB*) positions in the High Flux Isotope Reactor (HFIR) are proceeding satisfactorily. As planned, Japanese and U.S. MFE miniature mechanical property specimens are being re-encapsulated in four HFIR RB* capsules following irradiation to 7.5 displacements per atom (dpa) at temperatures of 60, 200, 330, and 400°C in Oak Ridge Reactor (ORR) experiments ORR-MFE-6J and -7J. Beginning with return of the HFIR to full power, the HFIR-MFE RB* capsules will be irradiated in pairs (first the 60 and 330°C capsules, then the 200 and 400°C capsules) to a damage level of 16 dpa. After these four irradiations, the test specimens will be removed, examined, and approximately one-half re-encapsulated for irradiation to 24 dpa.

The HFIR-MFE RB* capsule designs are of two basic types: an uninstrumented capsule with the test specimens in contact with reactor coolant water for the 60°C capsule and an instrumented and singly contained capsule for the elevated-temperature capsules (200, 330, and 400°C) where the specimen temperatures will be monitored by 21 thermocouples and controlled by varying the thermal conductance of a small gap region between the specimen holder and the containment tube. Hafnium liners surrounding each capsule will be used to tailor the neutron spectrum.

Design of the remaining two (200 and 400°C capsules) of the first four HFIR-MFE-RB* capsules has been completed and issue of construction drawings is near. In addition to accommodating the planned test specimen loadings, a packet of transmission electron microscopy (TEM) specimens in the 200°C capsule and an hourglass fatigue specimen in the 400°C capsule will be simulated and instrumented with three thermocouples to obtain temperature rise data for these respective specimen-specimen holder configurations.

Disassembly of the 200°C section of the ORR-MFE-6J capsule was recently completed and all specimens and dosimeters were recovered in good condition. This completes removal of specimens from the ORR-MFE-6J and -7J capsules.

Assembly of the HFIR-MFE-330J-1 (330°C) capsule was successfully completed in June 1988, and the capsule was transported to the HFIR pool to await startup along with the previously completed 60°C capsule. With the aid of a special loading device and good support fixtures, re-encapsulation of the several hundred radioactive specimens into this capsule was carried out efficiently and demonstrated the overall feasibility of the specimen re-encapsulation plan set forth at the beginning of the project.

Facility preparations completed or under way at this time include installation of a storage rack for HFIR RB* capsules at the west end of the HFIR pool, issue of instrument application and wiring diagrams for Materials Irradiation Facility No. 3 (MIF-3) and MIF-4 which will be used for the HFIR-MFE RB* capsules, checkout of the MIF-3 and -4 facilities, assembly of the in-pool flexible hose sections for connection of the instrumented capsules to MIF-3 and -4, and preparation of detailed installation and operating procedures. In addition, a 69-p experiment information and safety analysis document for the 60 and 330°C capsules was prepared and submitted with the request to operate these capsules in the HFIR.

PROJECT OBJECTIVES

- PROVIDE HFIR RB* FACILITIES FOR TESTING MFE FIRST WALL MATERIALS
- DESIGN AND CONSTRUCT FOUR HFIR-MFE RB* SPECTRALLY TAILORED CAPSULES FOR IRRADIATION TO 16 DPA OF JAPANESE AND U.S. MFE SPECIMENS PREIRRADIATED TO 7.5 DPA AT TEMPERATURES OF 60, 200, 330, AND 400°C IN THE ORR-MFE-6J AND -7J CAPSULES
- IRRADIATE FIRST FOUR HFIR-MFE RB* CAPSULES IN PAIRS (FIRST THE 60 AND 330°C CAPSULES, THEN THE 200 AND 400°C CAPSULES) TO 16 DPA
- FOLLOWING THESE IRRADIATIONS, REMOVE AND EXAMINE MFE SPECIMEN, AND RE-ENCAPSULATE 1/2 OF THEM FOR IRRADIATION TO 24 DPA

ORNL-DWG 85-10488R2

NEW EXPERIMENTAL FACILITIES IN HFIR

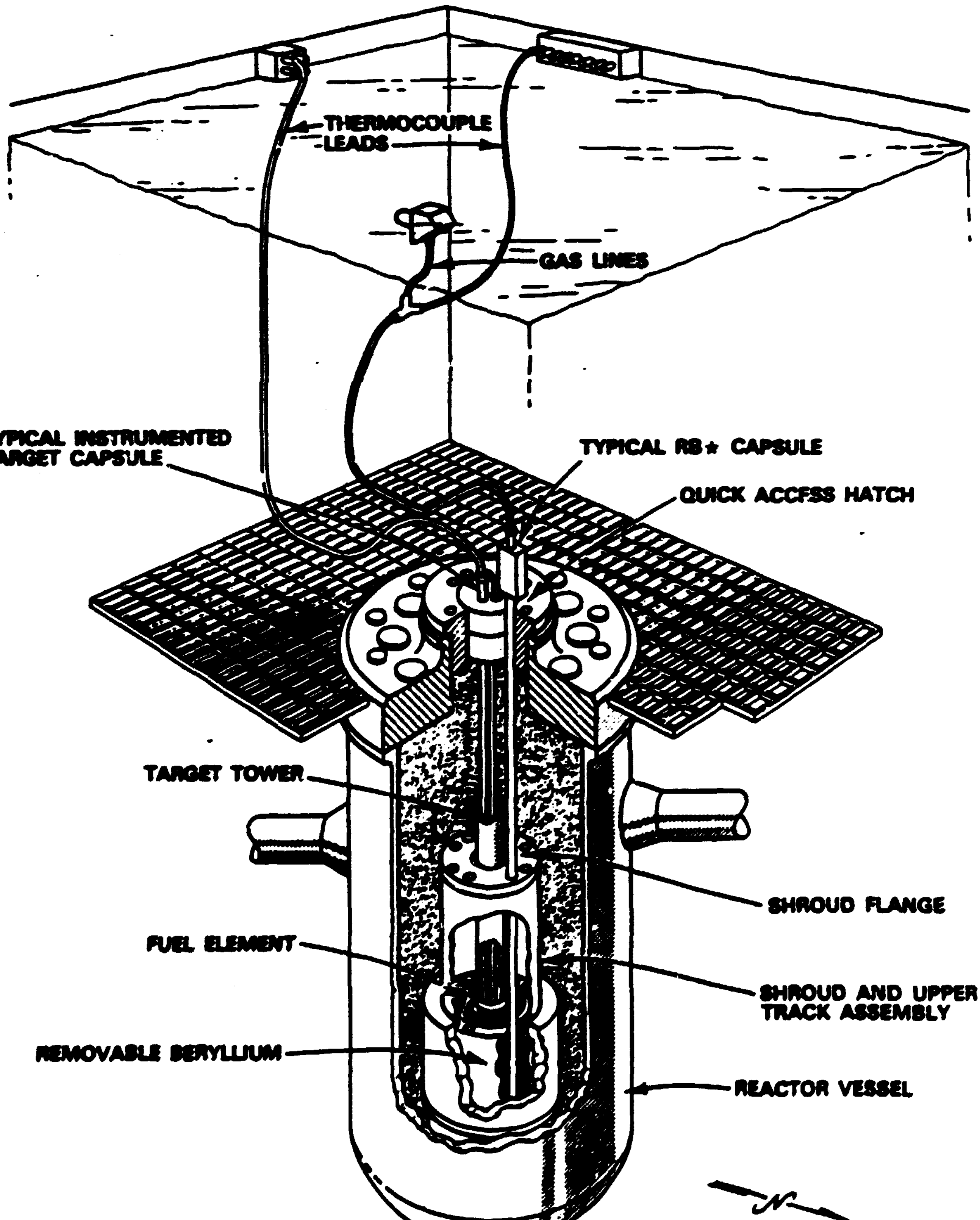

SPECIAL FEATURES OF THE RB* IRRADIATION FACILITY

- STRAIGHT ACCESS INTO ANY OF EIGHT LARGE DIAMETER POSITIONS (46 mm)

- 180° CAPSULE ROTATION TO PROVIDE NEAR UNIFORM EXPOSURE TO ALL SPECIMENS AT A GIVEN ELEVATION

- PEAK UNPERTURBED THERMAL AND FAST NEUTRON FLUX LEVELS OF APPROXIMATELY 1.3E15 AND 4.3E14 (>0.1 MeV) Neutrons/cm^2·s, RESPECTIVELY, AT 85 MW HFIR POWER LEVEL

- PEAK UNPERTURBED GAMMA HEATING RATE OF APPROXIMATELY 15 W/g AT 85 MW HFIR POWER LEVEL

- PROVISION FOR SPECTRAL TAILORING THE NEUTRON FLUX TO CLOSELY MATCH THE He PRODUCTION-TO-ATOM DISPLACEMENT RATIO (14 appm He/dpa) EXPECTED IN A FUSION REACTOR FIRST WALL

- STANDARD CAPSULE LEAD TUBE DESIGN

- CONTAINMENT TUBE DESIGN PARAMETERS OF 6.9 MPa EXTERNAL PRESSURE DIFFERENTIAL AT 93 °C

MINIATURE MECHANICAL PROPERTY SPECIMENS ARE EMPLOYED TO OBTAIN A LARGE AMOUNT OF IRRADIATION DATA IN A SINGLE CAPSULE EXPERIMENT

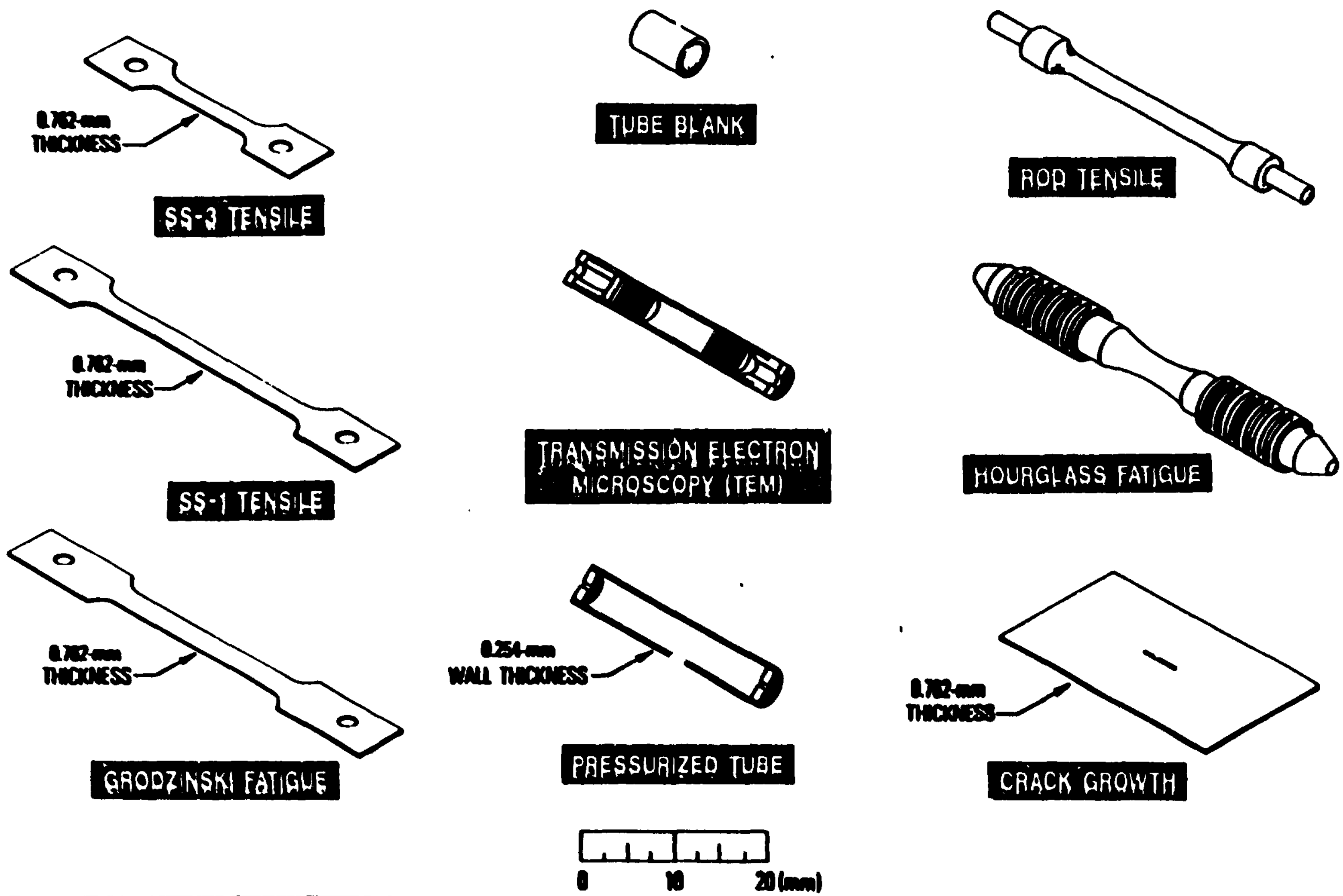

ABOUT 1000 MFE SPECIMENS FROM THE SPECTRALLY TAILORED ORR-MEF-6J AND -7J CAPSULES WILL BE RELOADED INTO FOUR RB★ CAPSULES

Specimen Type	Number of Specimens 60°C Capsule	200°C Capsule	330°C Capsule	400°C Capsule
Pressurized Tube	38	26	45	39
Tube Blank	9	9	9	9
Transmission Electron Microscopy Tube				
Length (mm)				
16.5	2	2	0	0
19.1	0	0	4	4
25.4	5	7	6	6
SS-1 Tensile	90	83	76	64
SS-3 Tensile	54	54	15	15
Grodzinski Fatigue	56	24	56	40
Crack Growth	30	30	10	10
Rod Tensile	0	0	4	0
Hourglass Fatigue	0	0	0	5

HFIR-MFE RB* CAPSULE DESIGNS ARE OF TWO BASIC TYPES

- UNINSTRUMENTED CAPSULE WITH MFE SPECIMENS IN CONTACT WITH REACTOR COOLANT WATER (60°C CAPSULE)
- INSTRUMENTED, SINGLY CONTAINED CAPSULE WITH A CONVENTIONAL TEMPERATURE CONTROL GAS GAP (200, 330, AND 400°C CAPSULES)

DESIGN OF THE 330°C CAPSULE IS TYPICAL OF THE THREE ELEVATED TEMPERATURE CAPSULES

- Containment tube of 6061-T6 aluminum in in-core region and 304L stainless steel in upper region with a special aluminum-to-stainless steel transition tube connecting the two

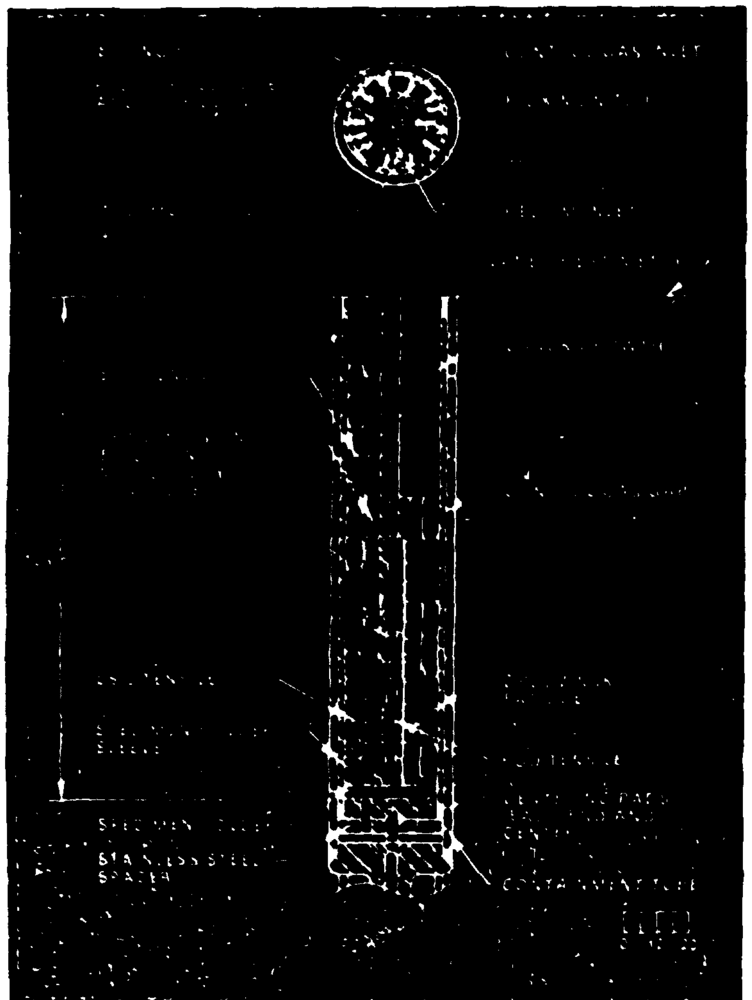

- Specimen holder of oxide dispersion strengthened aluminum alloy (Al-7WT% AL_2O_3) to provide adequate strength and good dimensional stability under irradiation at temperatures up to 500°C. Meets requirements of high thermal conductivity (close to that of AL) and reasonably low density (2.74 G/CM^3)
- Temperature monitored by 21 type K thermocouples and controlled by varying the thermal conductance of a small gap between specimen holder and containment tube
- Axial fast neutron exposure variation of only 30% (mean value ± 15%) over the 0.31-m length of specimen holder
- 180° capsule rotation to provide near uniform circumferential exposure
- Cooled with 49°C reactor coolant water — flow rate of 1.5 L/s with water temperature rise of approximately 8°C

DESIGN OF THE 60°C CAPSULE

- **Uninstrumented with test specimens in contact with reactor coolant water**
- **Specimen temperatures within 10°C of 60°C**
- **Cooled with 49°C reactor coolant water — flow rates of 0.63 L/s over capsule surface, 0.57 L/s between capsule tube and specimen holder, and 0.063 L/s through each of the five interior specimen holes**

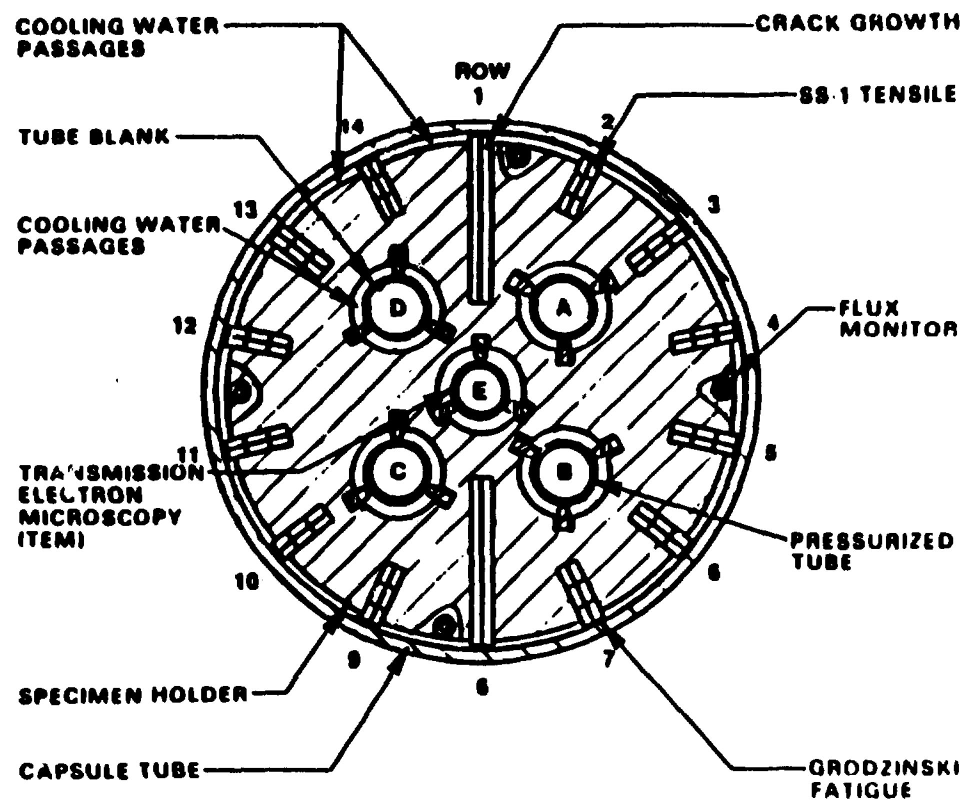

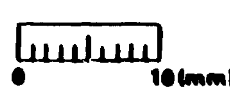

ORNL-DWG 88-18086R

CALCULATED RADIAL TEMPERATURE PROFILE FOR THE HFIR-MFE-330J-1 CAPSULE SHOWS THAT CAPSULE DESIGN MAXIMIZES TEMPERATURE CONTROL RANGE.

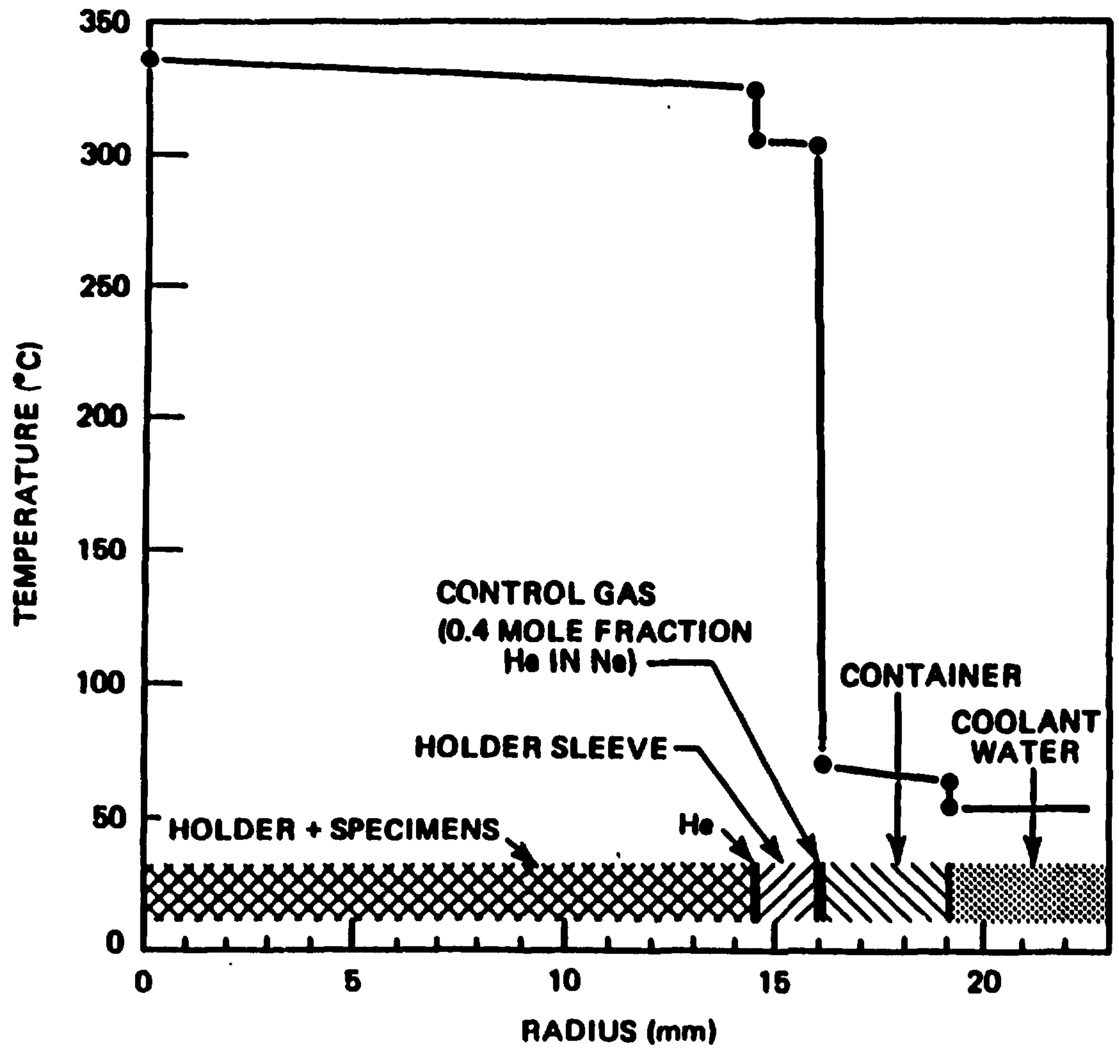

ORNL-DWG-89-7850

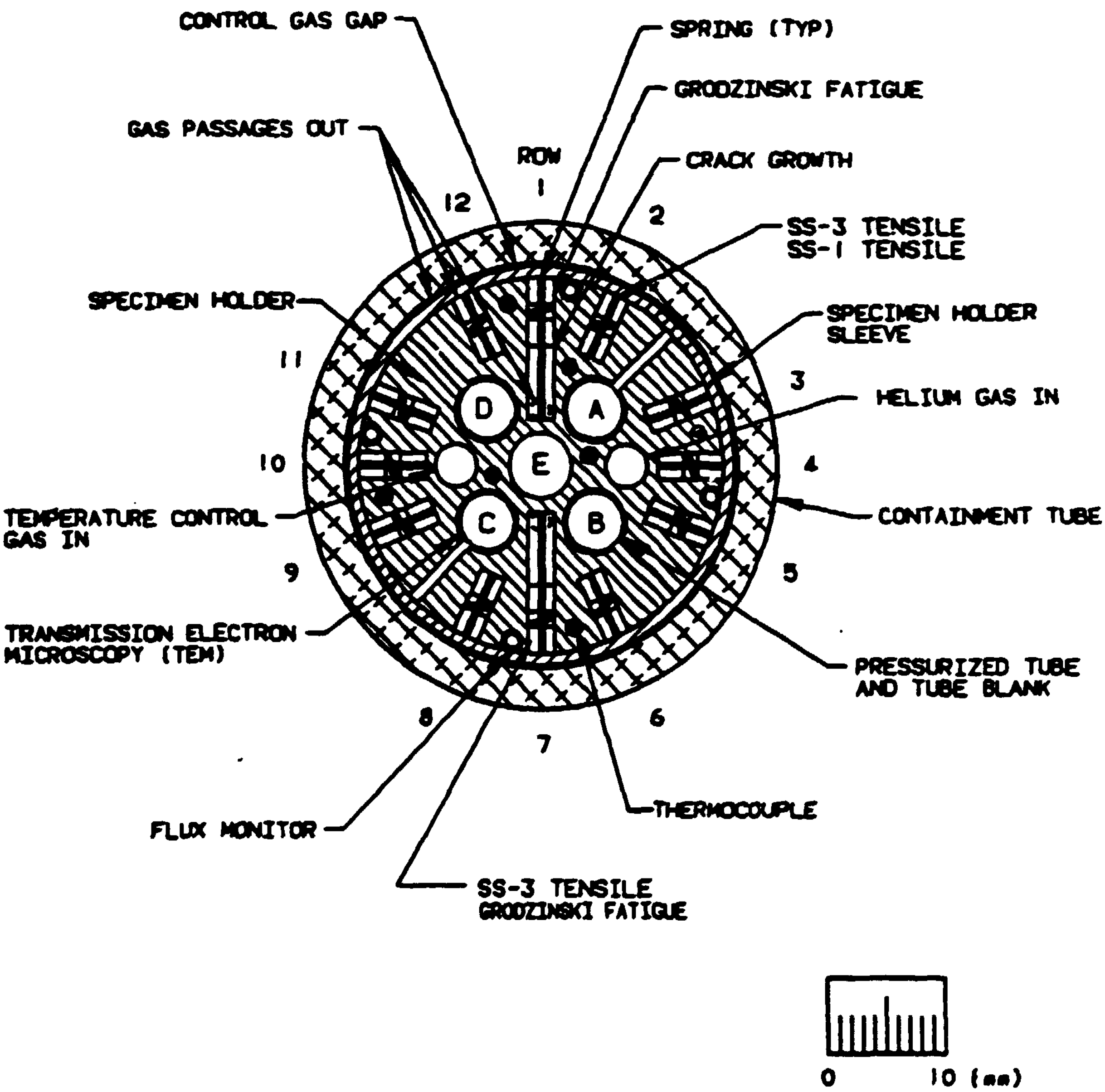

HORIZONTAL SECTION THROUGH THE
HFIR-MFE-200J-1 CAPSULE

ORNL-DWG-89-7861

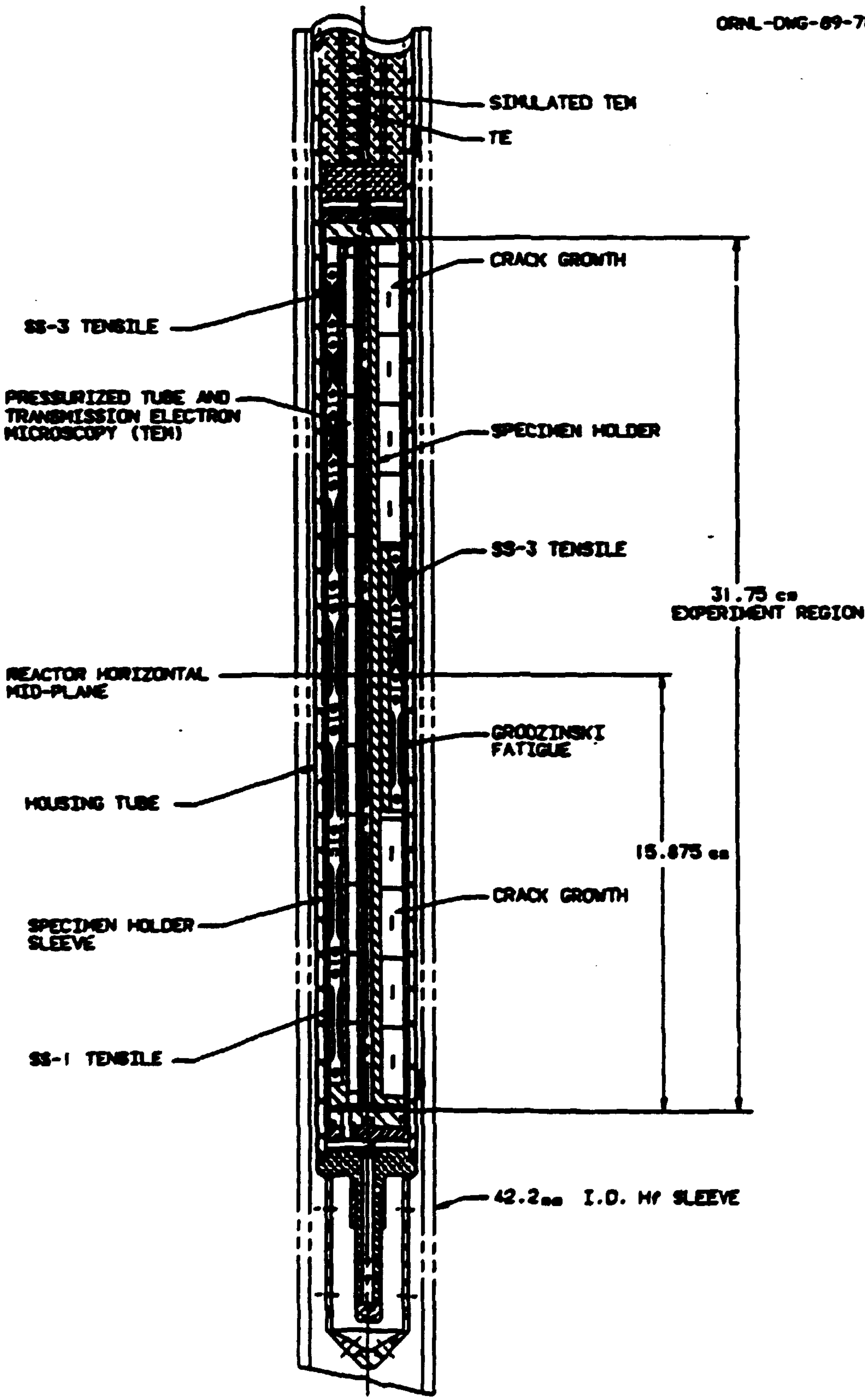

VERTICAL SECTION THROUGH HFIR-MFE 200J-1 CAPSULE

ORNL-DWG-89-7852

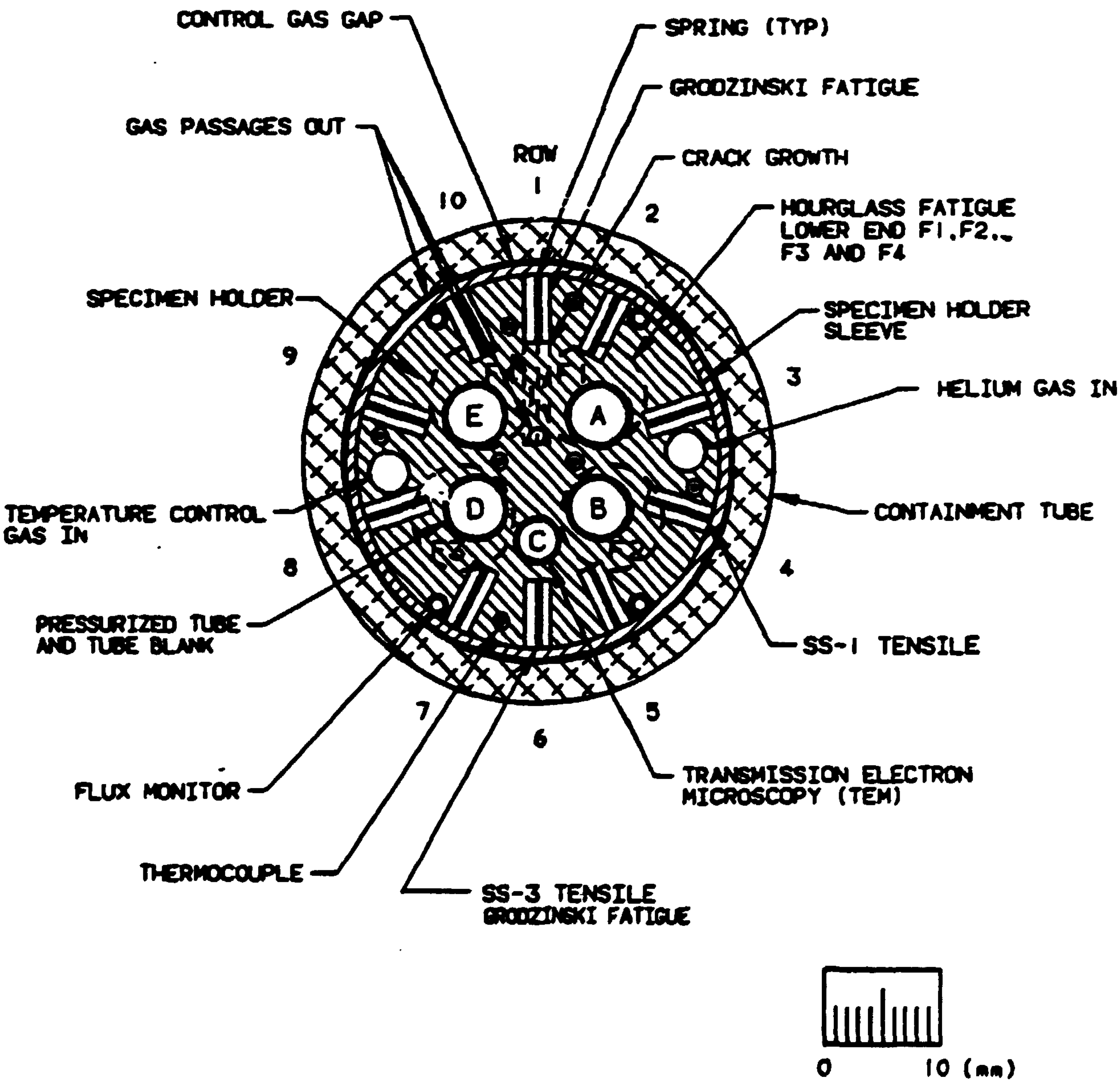

HORIZONTAL SECTION THROUGH THE
HFTR-MFE-400J-1 CAPSULE

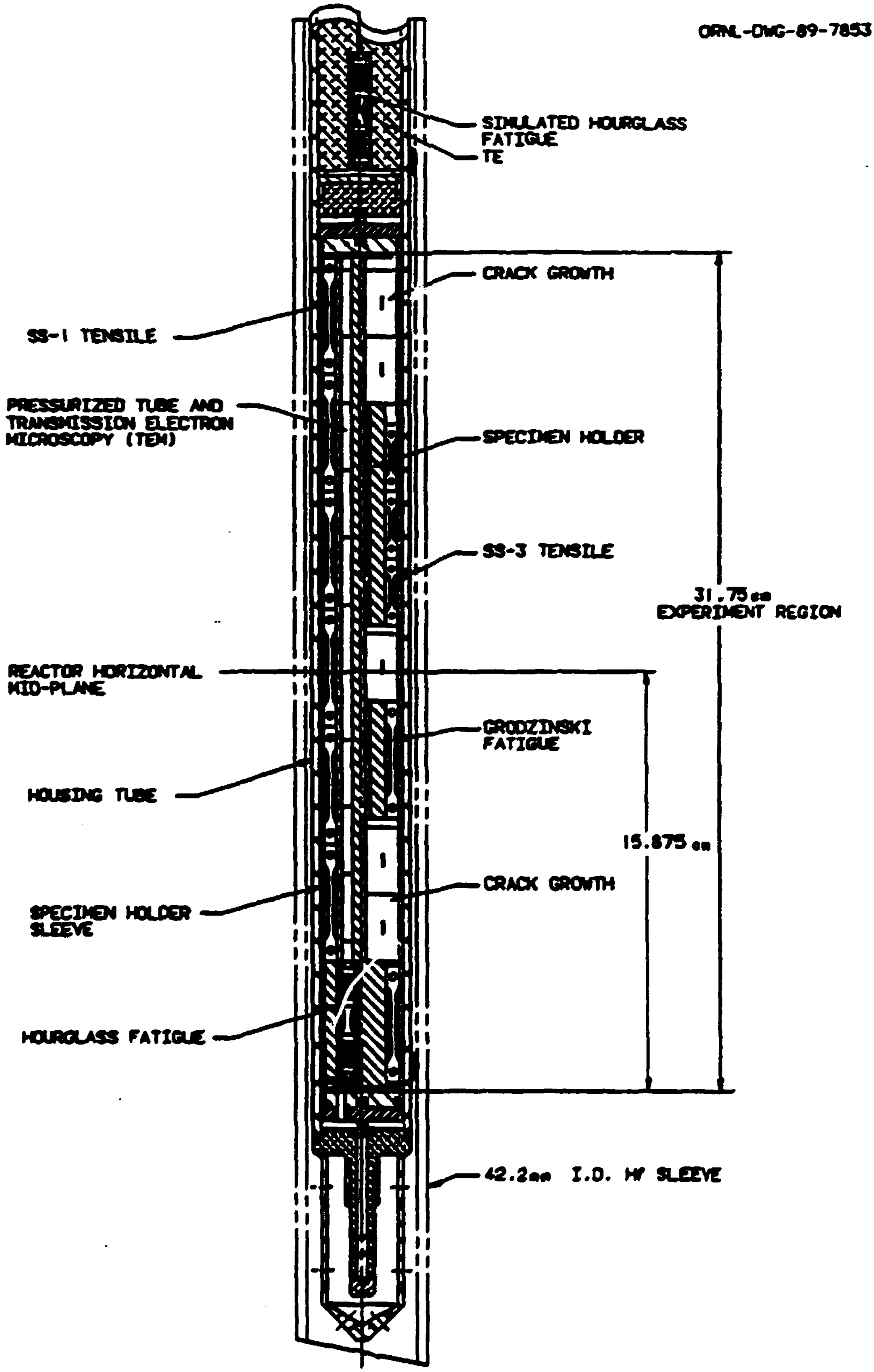

VERTICAL SECTION THROUGH HFIR-MFE 400J-1 CAPSULE

ORNL-PHOTO 1369-89

INCONEL X-750 SPRINGS HOLD THE SHEET TENSILE, FATIGUE, AND CRACK GROWTH SPECIMENS IN CONTACT WITH HOLDER IN THE 200, 330, AND 400°C CAPSULES.

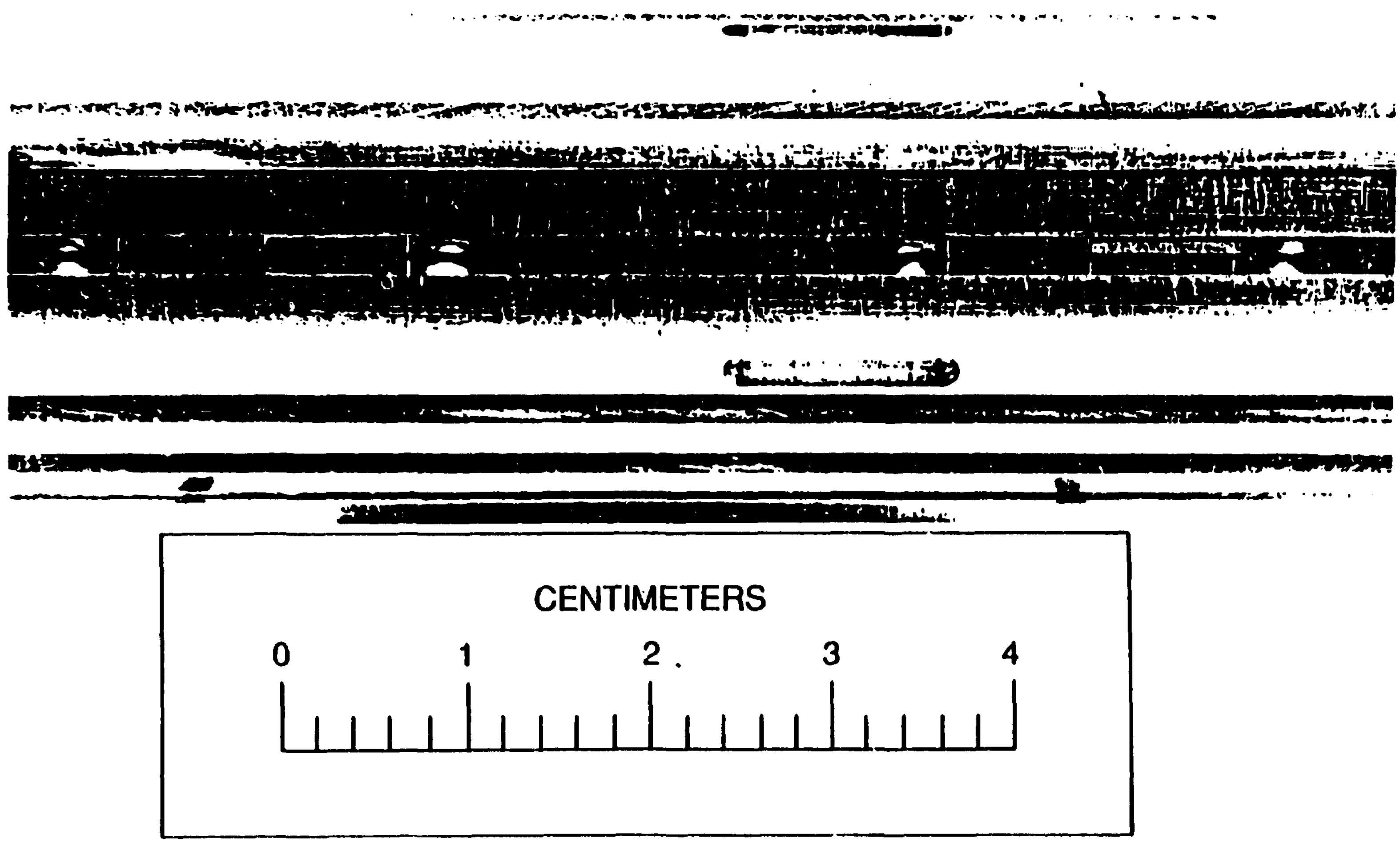

DISASSEMBLY OF ORR-MFE-6J AND -7J CAPSULES ARE SUCCESSFULLY COMPLETED

- RECOVERY OF MFE SPECIMENS FROM ALL BUT 200°C SECTION OF ORR-MFE-6J COMPLETED PREVIOUSLY
- RECENT DISASSEMBLY OF 200°C SECTION WENT EXTREMELY WELL AND ALL SPECIMENS AND DOSIMETERS WERE RECOVERED IN GOOD CONDITION

ORNL-DWG 84-6518R3

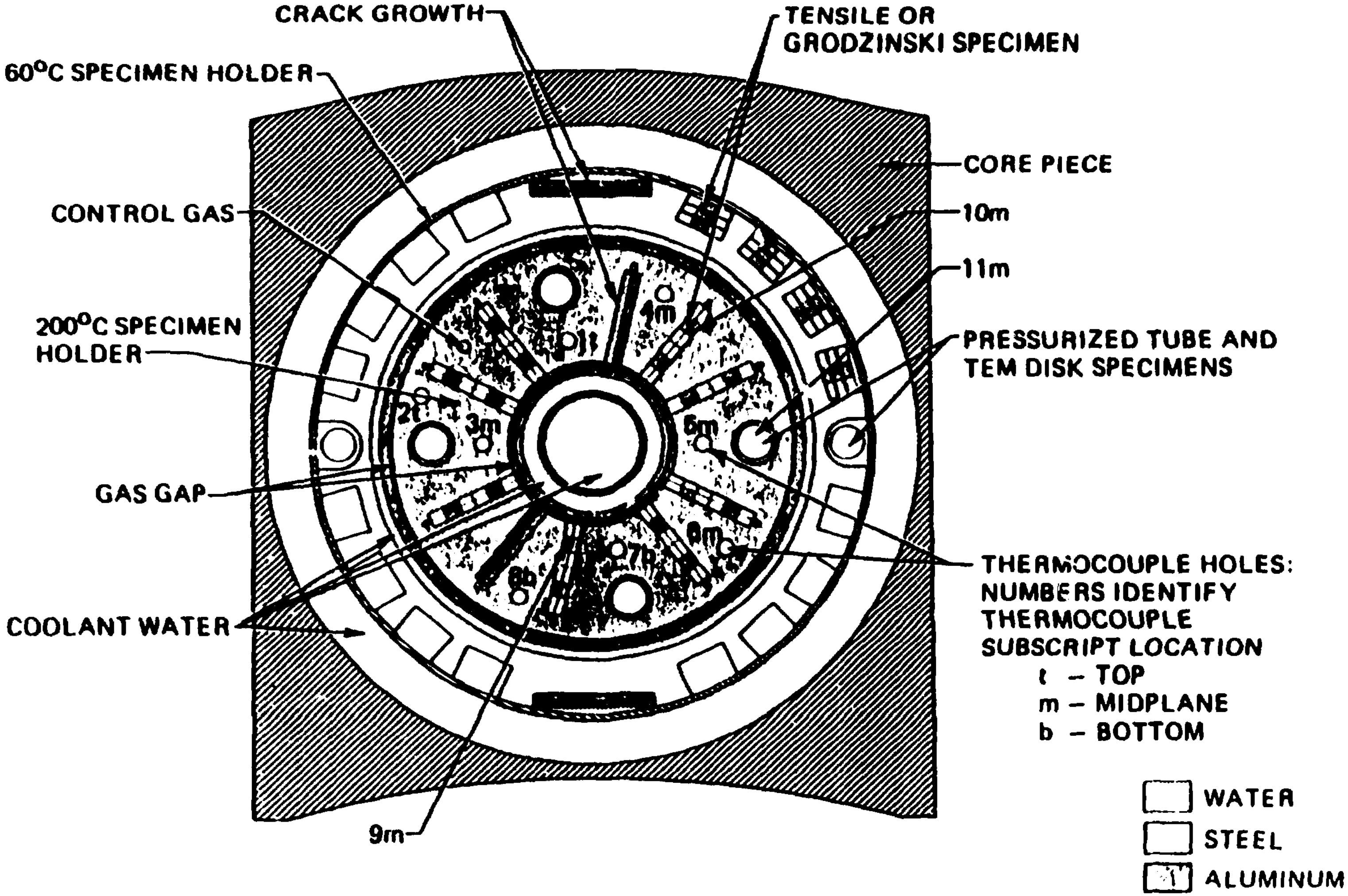

HORIZONTAL CROSS SECTION THROUGH SPECIMEN REGION OF IRRADIATION CAPSULE ORR-MFE-6J

ORNL-DWG 84 6603R4

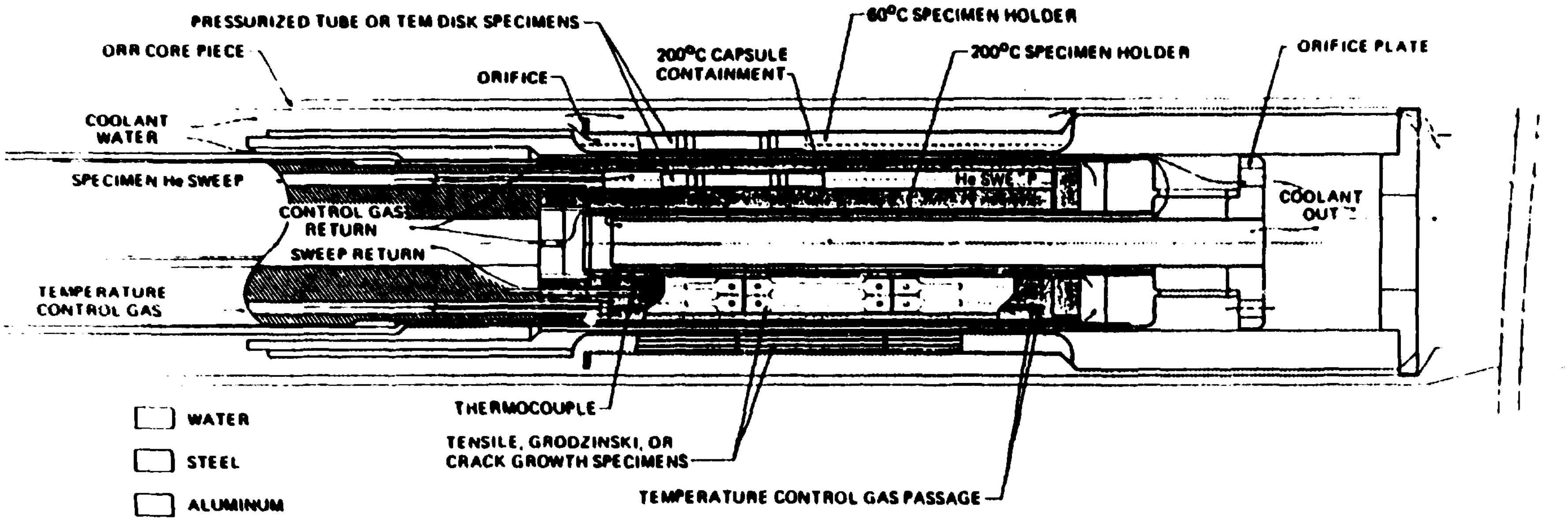

VERTICAL CROSS SECTION THROUGH IN-CORE REGION OF IRRADIATION CAPSULE ORR-MFE-6J

ASSEMBLY OF FIRST FOUR HFIR-MFE RB* CAPSULES IS AT MIDPOINT

- 60°C CAPSULE ASSEMBLY AND TEST SPECIMEN LOADING DATA REPORTED AT LAST MEETING
- 330°C CAPSULE ASSEMBLY COMPLETED IN JUNE, 1988, AND TEST SPECIMEN LOADING DATA REPORTED HEREINBELOW
- PARTS FABRICATION AND SUBASSEMBLY OF 200 AND 400°C CAPSULES SCHEDULED FOR COMPLETION EARLY NEXT YEAR

ORNL-PHOTO 1367-69

RADIOACTIVE TEST SPECIMENS WERE SUCCESSFULLY LOADED INTO THE 330°C CAPSULE USING A SPECIAL LOADING DEVICE AND GOOD SUPPORT FIXTURES.

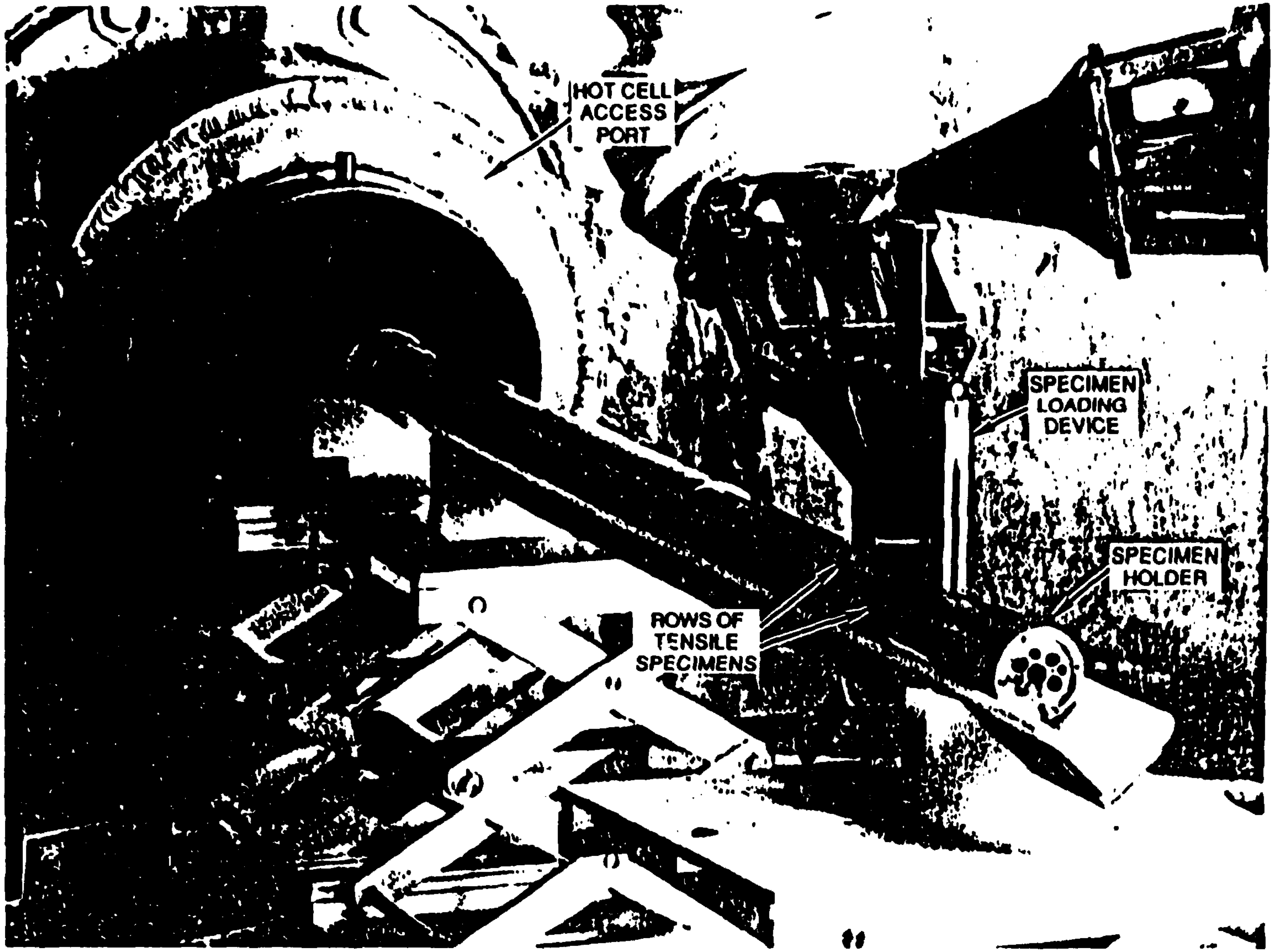

ORNL-PHOTO 1368-89

330°C CAPSULE COMPONENTS NEAR READY FOR LOADING OF TEST SPECIMENS IN HOT CELL

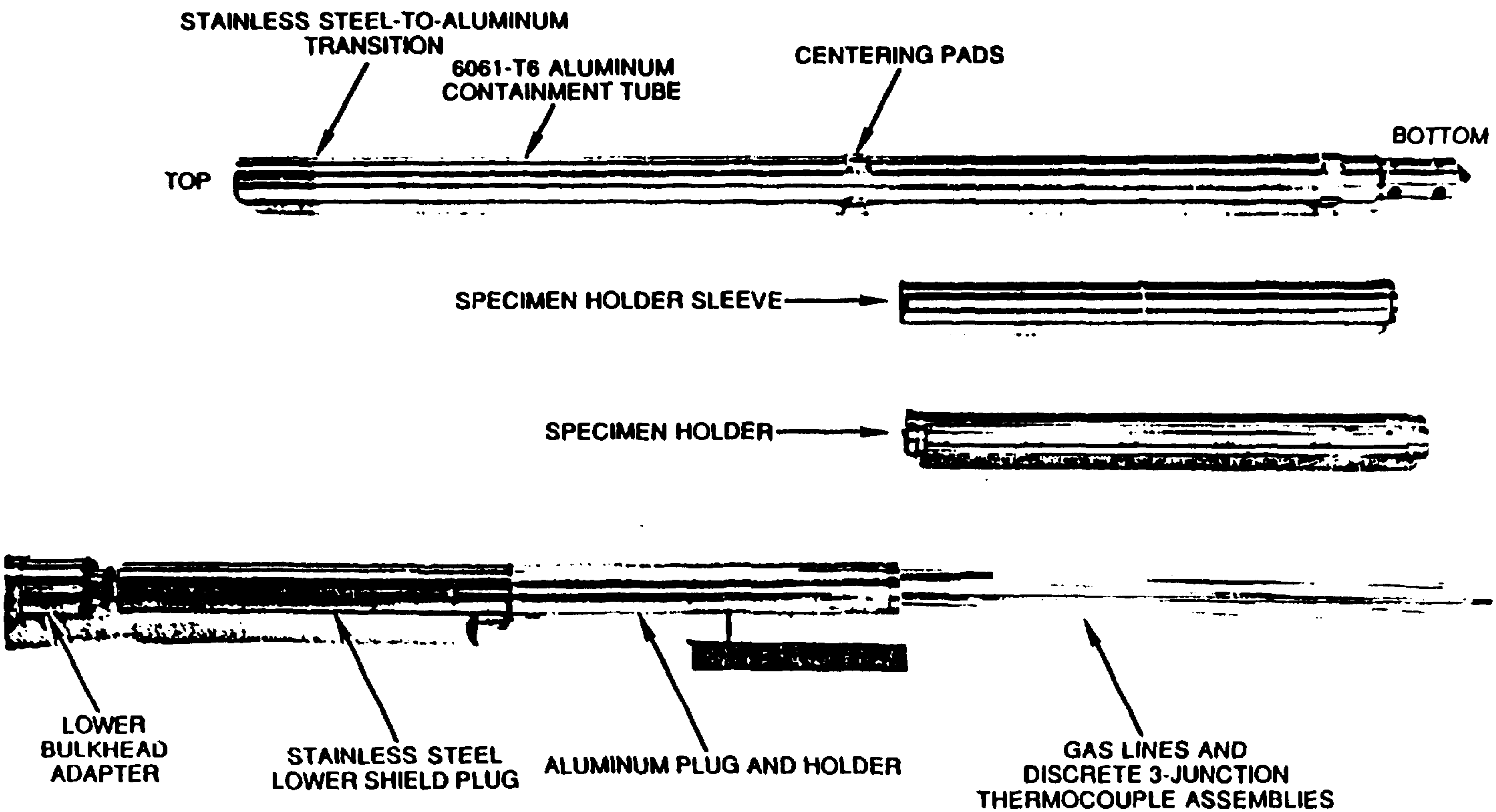

ORNL-PHOTO 1366-89

RADIOACTIVE TEST SPECIMENS ARE PLACED INTO LOADING DEVICE IN PAIRS WITH A SPRING BETWEEN EACH PAIR.

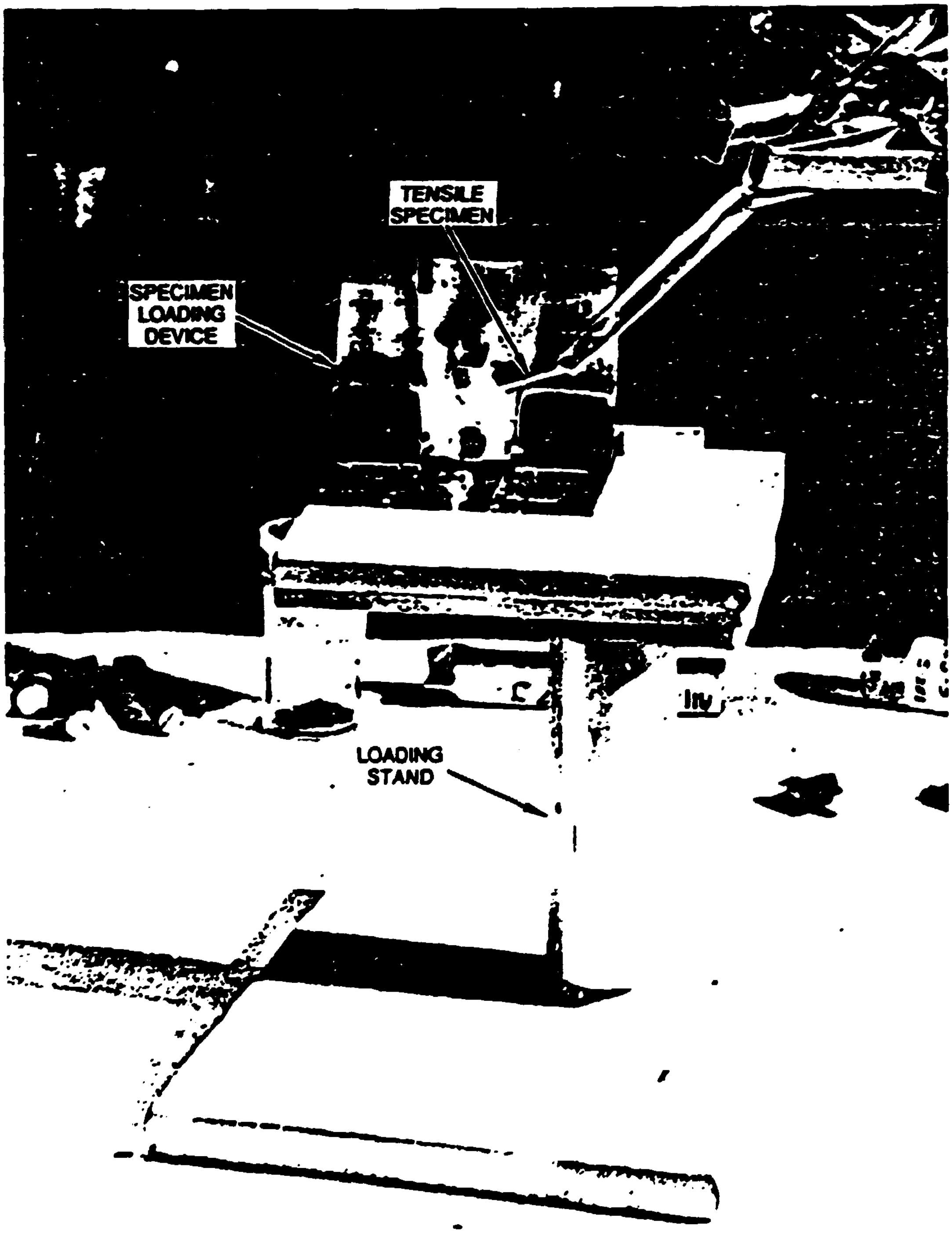

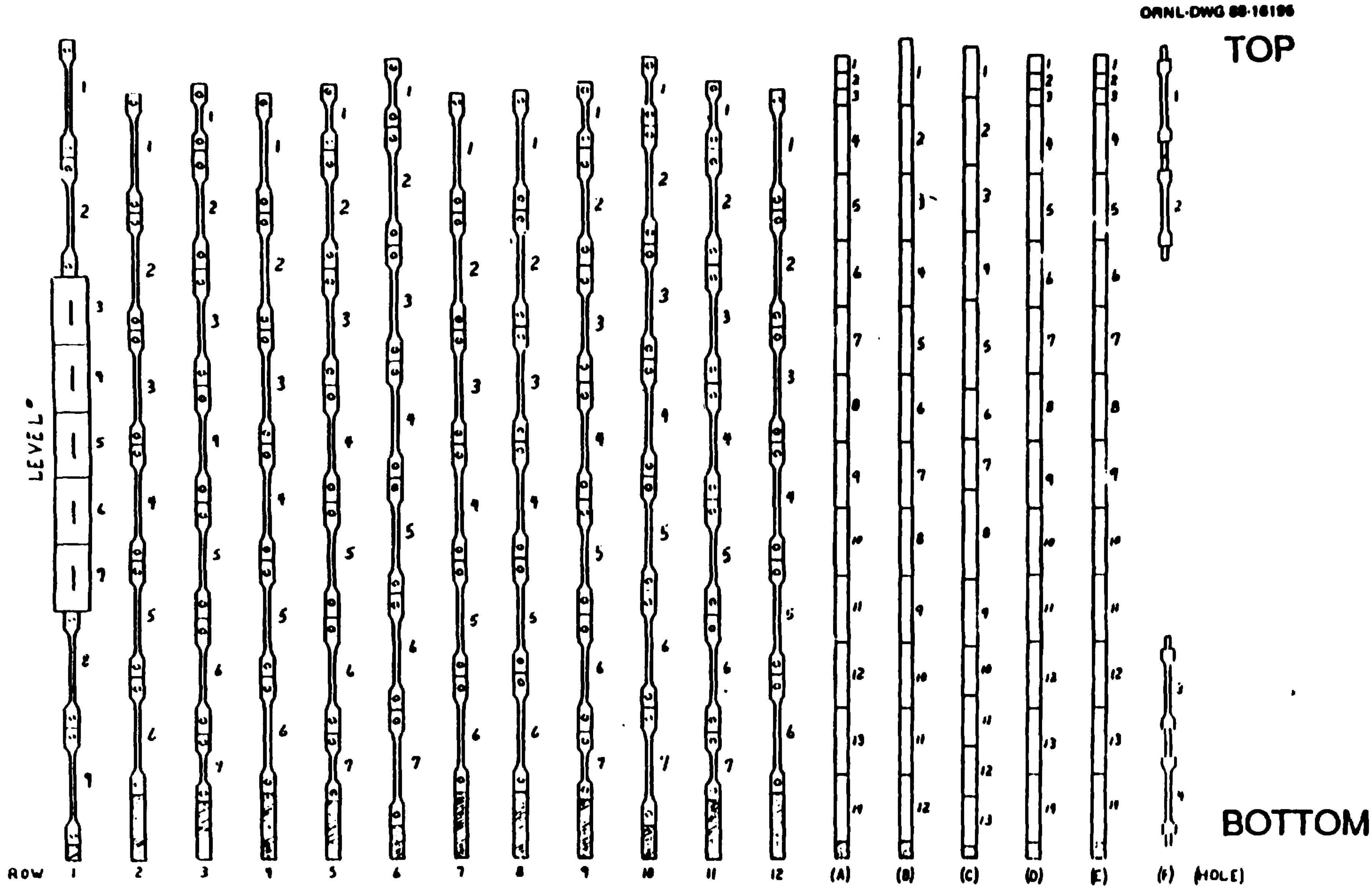

TEST SPECIMEN LOADING ARRANGEMENT IN HFIR-MFE-330J-1 CAPSULE

ORNL-DWG-86-17330 (REV. 1)

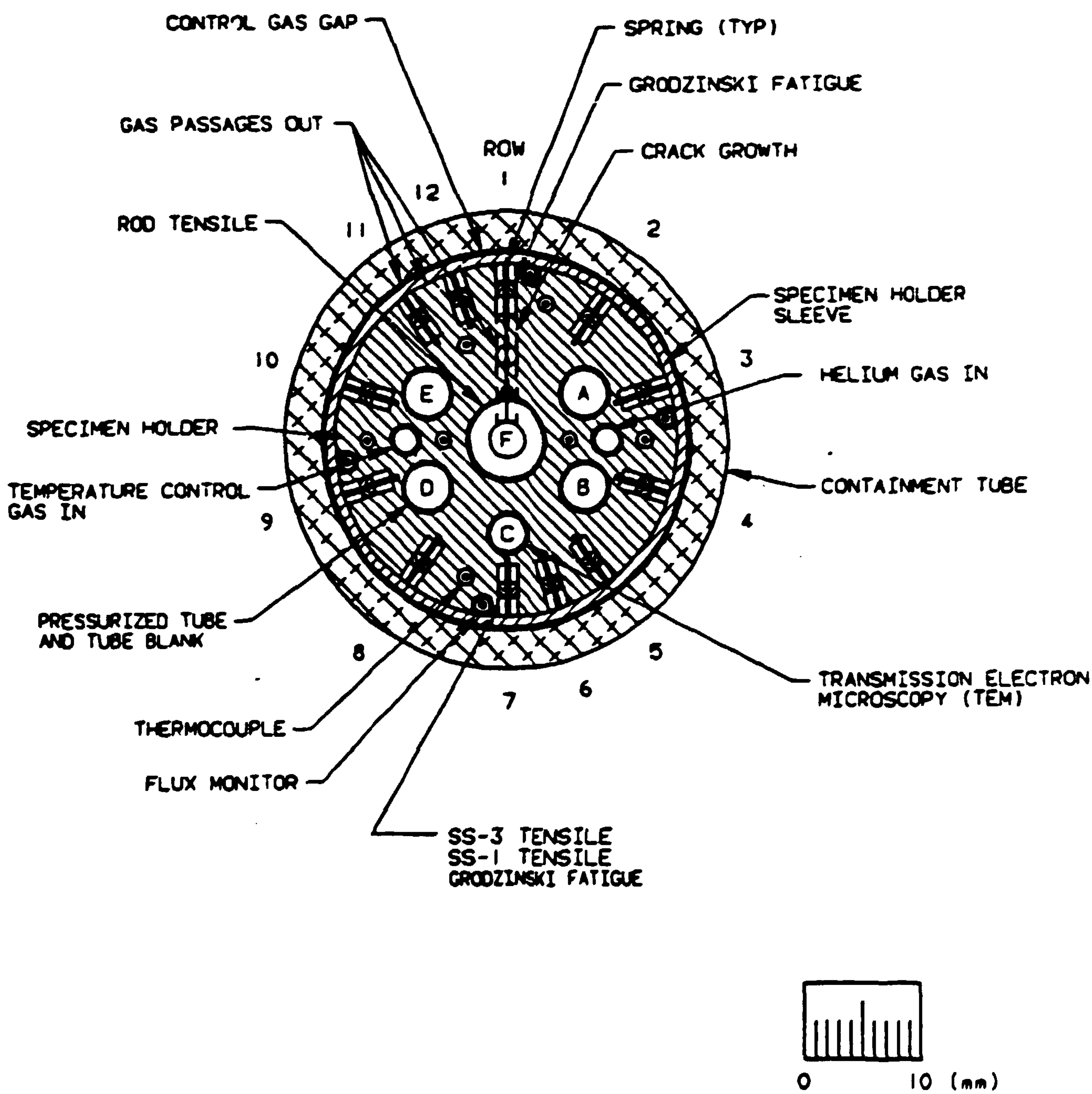

HORIZONTAL SECTION THROUGH THE HFIR-MFE-330J-1 CAPSULE

ORNL- DWG 88-18184

	Row 1	Row 2	Row 3	Row 4	Row 5	Row 6	Row 7	Row 8	Row 9	Row 10	Row 11	Row 12	Hole A	Hole B	Hole C	Hole D	Hole E	Hole F
Level 1	EL-13 CLU5	A01 A04	TU-12 TZ-14	FL-18 KL-2	TR-14 TT-13	8X-10 4X-08	FL-16 CL-13	F01 F02	TR-13 TU-14	TL-12 TF-13	TN-12 2L-08	EL-11 IL-1	SA1	C4B9	C	CA1	SXAX-1	TB-30
Level 2	GL-4 FL-23	B01 B03	GFB-11 GFA-10	CL-11 ML-2	GFD-13 GFC-5	HT-16 MU-17	DL-15 KL-1	104 105	GFB-5 GFA-6	FL-17 CL-18	GFD-6 GFC-11	FL-22 DLA-4	CC1	FA34	J-4	3S11-1	3S10-1	TB-31
Level 3	CGE-2 CGA-2	MX-02 MX-14	GFA-14 GFC-6	BL-3 ML-2	GFA-11 GFD-5	107 F03	ML-1 CLU-6	D01 D04	GFB-6 GFD-11	CL-10 CL-16	GFB-9 GFC-12	DL-18 EL-9	CD1	SA09	J-6	PS11-1	FA-1	TE-29
Level 4	CGE-3 CGE-1	A03 A05	GFA-12 GFC-13	BL-1 ML-1	GFB-10 GFB-12	B02 A02	DLA-1 CL-12	C02 C03	GFB-14 GFD-10	DL-17 EL-4	GFA-8 GFD-8	DL-11 EL-8	3C03	C1C5	J-2	C4A6	C1A9	TE-32
Level 5	CG-A1 CG-F1	A06 A07	GFA-7 GFC-10	DL-10 EL-5	GFA-5 GFC-7	102 103	FL-19 DLA-3	B05 B06	GFA-9 GFA-13	BL-7 EL-6	GFD-14 GFC-9	DL-16 CL-15	C1C2	SA16	Spacer	S1A6	C5B3	
Level 6	CGB-2 CGB-1	T01 T06	GFC-8 GFC-14	B02 B03	GFB-7 GFB-9	C01 C04	DL-13 DL-14	B04 B07	GFB-8 GFD-7	DL-12 CL-14	GFB-13 GFD-12	CL-17 IL-2	3B06	C2C9	B	C4B5	SA38	
Level 7	CG-A3 CGF-2		TE-12 TZ-13		TP-12 TF-14	MJ-11 MJ-20			TU-13 TT-14	FL-20 FL-24	DL-13 4L-08		3B03	S1A2	JP-15	3C06	C5B1	
Level 8	EL-7 EL-12												FA19	FA08	Spacer	SA56	PS03	
Level 9	FL-21 DLA-2												FA33	FA28	J-5	C3C7	C3C3	
Level 10													C3B9	C4A1	JP-13	FA27	C3B3	
Level 11													S2A4	C4C9	JP-14	SA05	S1A7	
Level 12													C5B5	SA33	LF	C4A3	C3C8	
Level 13													S3A0		LE	SA01	S2A3	
Level 14													PS10			C1A0	C3A1	

TEST SPECIMEN IDENTIFICATION IN
HFIR-MFE-330J-1 CAPSULE

INFORMATION AND SAFETY ANALYSIS FORM ADDRESSES THE FOLLOWING TOPICS

1. GENERAL INFORMATION
2. EXPERIMENT FACILITY INFORMATION
3. EXPERIMENT ASSEMBLY INFORMATION
4. INSTRUMENTATION AND CONTROLS
5. MATERIALS
6. RADIOACTIVITY
7. SHIELDING
8. THERMODYNAMICS
9. ESTIMATED OR MEASURED REACTIVITY EFFECTS
10. PROCEDURES
11. HAZARDS
12. QUALITY ASSURANCE

HFIR-MFE RB* FACILITIES (MIF-3 AND MIF-4) BEING READIED FOR CAPSULE OPERATION

- IN-POOL STORAGE RACK FOR HFIR RB* CAPSULES BEING INSTALLED
- INSTRUMENT APPLICATION AND WIRING DIAGRAMS FOR MATERIALS IRRADIATION FACILITIES MIF-3 AND MIF-4 ISSUED
- ASSEMBLY OF IN-POOL FLEXIBLE HOSE SECTIONS COMPLETED
- MIF-3 AND MIF-4 FACILITY CHECKOUT IN PROGRESS
- INSTALLATION AND OPERATING PROCEDURES PREPARED
- EXPERIMENT INFORMATION AND SAFETY ANALYSIS FORM PREPARED AND SUBMITTED TO RRD ALONG WITH REQUEST FOR APPROVAL TO OPERATE 60 AND 330°C CAPSULES

SUMMARY REMARKS

- MUCH PROGRESS MADE IN THE LAST YEAR
  - DESIGN OF HFIR-MFE 200 AND 400°C CAPSULES COMPLETED
  - REPORT DESCRIBING SELECTION OF HFIR-MFE RB• CAPSULE STRUCTURAL MATERIALS PREPARED
  - RECOVERY OF REMAINING MFE SPECIMENS (200°C) FROM ORR-MFE CAPSULES SUCCESSFULLY COMPLETED
  - ASSEMBLY OF HFIR-MFE 330°C CAPSULE SUCCESSFULLY COMPLETED
  - VARIOUS FACILITY PREPARATIONS COMPLETED OR IN PROGRESS
- OVERALL FEASIBILITY OF MFE SPECIMEN REMOVAL, EXAMINATION, AND RE-ENCAPSULATION AT INTERMEDIATE EXPOSURE LEVELS DEMONSTRATED
- SPECTRALLY TAILORING OF NEUTRON FLUX IN TWO HFIR-MFE RB• POSITIONS, 180 DEGREES APART, FEASIBLE BUT EXPENSIVE

TENSILE DATA FROM THE ORR SPECTRAL TAILORING EXPERIMENT ORR-MFE-6J AND -7J

M. L. Grossbeck and T. Sawai

ABSTRACT

The ORR Spectral Tailoring Experiment of Phase I of the U.S./Japan Collaboration is particularly valuable for two reasons: it attained the fusion-relevant level of helium, and it addressed the temperature and fluence ranges of importance to the ITER project.

The tensile results, like the HFIR experiments, showed little difference in strength between alloys. However, even more evident at 8 dpa than at higher damage levels, there was a significant difference between annealed and cold-worked alloys. Also evident was that strength increased with temperature from 60 to 300°C. This can be explained in terms of increasing loop diameter in this range since hardening is proportional to the product of loop size and loop number to the 2/3 power. Rather striking was the low uniform elongation observed below 400°C. In annealed material, this value increased considerably as temperature decreased to 60°C, but in cold-worked material, uniform elongation remained very low. An increase in ductility was achieved by aging the cold-worked material.

Both tungsten inert gas (TIG) and electron beam (EB) welded specimens were irradiated. The strength of the welded cold-worked specimens was similar to that of annealed specimens, but otherwise followed the same trends as unwelded material. As might be expected, the welding produced higher ductility at 60°C similarly to annealing. Nonetheless, uniform elongation remained low in the region of 300°C as in the unwelded specimens.

Future work will consist of testing unirradiated specimens as well as testing the specimens irradiated at 200°C.

EXPERIMENTAL CONDITIONS

1. 60,200,330,400 C

2. 8 dpa

3. 60 C WATER ENVIRONMENT

   200 C HE ENVIRONMENT
   330 C NaK ENVIRONMENT
   400 C NaK ENVIRONMENT

Tensile Properties from ORR-MFE-6J and -7J

Specimen	Alloy	Temperature, °C		Stress, MPa		ϵ_u (%)	ϵ_T (%)
		Irrad.	Test	Yield	Ultimate Tensile		
FL31	J316 20 CW	60	RT	834	869	0.64	8.5
FL32	J316 20 CW	60	RT	855	883	0.63	7.5
FL13	J316 20 CW	330	330	862	876	0.44	2.3
FL14	J316 20 CW	330	330	993	1007	0.34	2.0
FL15	J316 20 CW	330	330	972	993	0.41	2.4
FL1	J316 20 CW	400	400	415	457	1.	2.8
FL3	316 20 CW	400	400	800	848	1.6	3.4
EL33	316 SA	60	RT	703	752	24.5	29.9
EL34	316 SA	60	RT	690	745	27.6	32.5
EL1	316 SA	330	330	848	855	0.29	3.1
EL2	316 SA	330	330	869	869	0.31	2.9
EL14	316 SA	400	400	595	677	4.6	7.0
EL15	316 SA	400	400	650	717	4.3	6.8
DL36	PCA 15 CW	60	RT	876	889	0.38	8.1
DL37	PCA 15 CW	60	RT	862	869	0.44	7.3
DL7	JPCA 15 CW	330	330	876	889	0.38	2.3
DL8	JPCA 15 CW	330	330	938	945	0.38	2.2
DL19	JPCA 15 CW	400	400	855	896	0.59	2.9
DL20	JPCA 15 CW	400	400	827	841	0.38	1.9
TE31	JPCA 15 CW Rod	330	330	931	945	0.42	5.3
TE30	JPCA 15 CW Rod	330	330	958	958	0.31	5.4
GL6	JPCA 25 CW	60	RT	910	924	0.44	4.5
GL7	JPCA 25 CW	60	RT	917	931	0.44	4.5
DLA6	JPCA Aged	60	RT	910	917	0.44	5.6
DLA7	JPCA Aged	60	RT	896	903	0.40	5.5
CL7	JPCA SA	330	330	821	821	0.23	2.5
CL8	JPCA SA	330	330	800	807	0.38	3.2
CL9	JPCA SA	330	330	876	883	0.25	2.7
CL19	JPCA SA	400	400	505	652	10.5	12.9
CL20	JPCA SA	400	400	549	667	2.5	10.5
AE05	316 20 CW (SS3)	60	400	647	717	3.3	11.0
AE02	316 20 CW (SS3)	60	RT	903	903	0.4	19.0
AE01	316 20 CW (SS3)	60	RT	903	917	0.5	20.1
EK20	PCA 25 CW (SS3)	60	RT	862	869	0.5	15.7
EK18	PCA 25 CW (SS3)	60	RT	848	848	0.5	13.5
EK19	PCA 25 CW (SS3)	60	RT	848	855	0.4	14.1

Specimen	Alloy	Temperature, °C		Stress, MPa		ϵ_u (%)	ϵ_T (%)
		Irrad.	Test	Yield	Ultimate Tensile		
D58	J316 CW TIG WM	60	RT	635	675	7.2	9.4
D57	J316 CW TIG WM	60	RT	631	683	11.1	14.2
D50	J316 CW TIG WM	330	330	652[a]	655	0.03	2.2
D49	J316 CW TIG WM	330	330	687[a]	690	0.06	1.9
D53	J316 CW TIG WM	400	400	598	603	0.5	2.4
D54	J316 CW TIG WM	400	400	614	627	1.2	3.1
FLW6	J316 CW TIG WJ	60	RT	710	710	5.6	8.4
FLW1	J316 CW TIG WJ	60	RT	682	731	6.4	8.6
D29	J316 SA TIG WM	60	RT	655	675	24.2	27.1
D30	J316 SA TIG WM	60	RT	607	643	13.8	16.8
D16	J316 SA TIG WM	330	330	703	703	0.25	2.0
D17	Damaged						
D23	J316 SA TIG WM	400	400	591	611	1.3	2.8
D24	J316 SA TIG WM	400	400	587	611	1.9	4.4
ELW1	J316 SA TIG WJ	60	RT	659	687	3.9	6.8
ELW2	J316 SA TIG WJ	60	RT	678	710	3.6	5.9
JL6	J316 SA EB WJ	60	RT	637	676	2.8	5.6
JL7	J316 SA EB WJ	60	RT	660	696	2.7	6.5
JL1	J316 SA EB WJ	330	330	731	738	0.7	2.8
JL2	J316 SA EB WJ	330	330	724	731	0.7	2.7
JL3	J316 SA EB WJ	400	400	637	656	0.6	2.6
JL4	J316 SA EB WJ	400	400	610	625	0.8	3.1

WM = weld metal

WJ = weld joint

[a]Not 0.2% YS

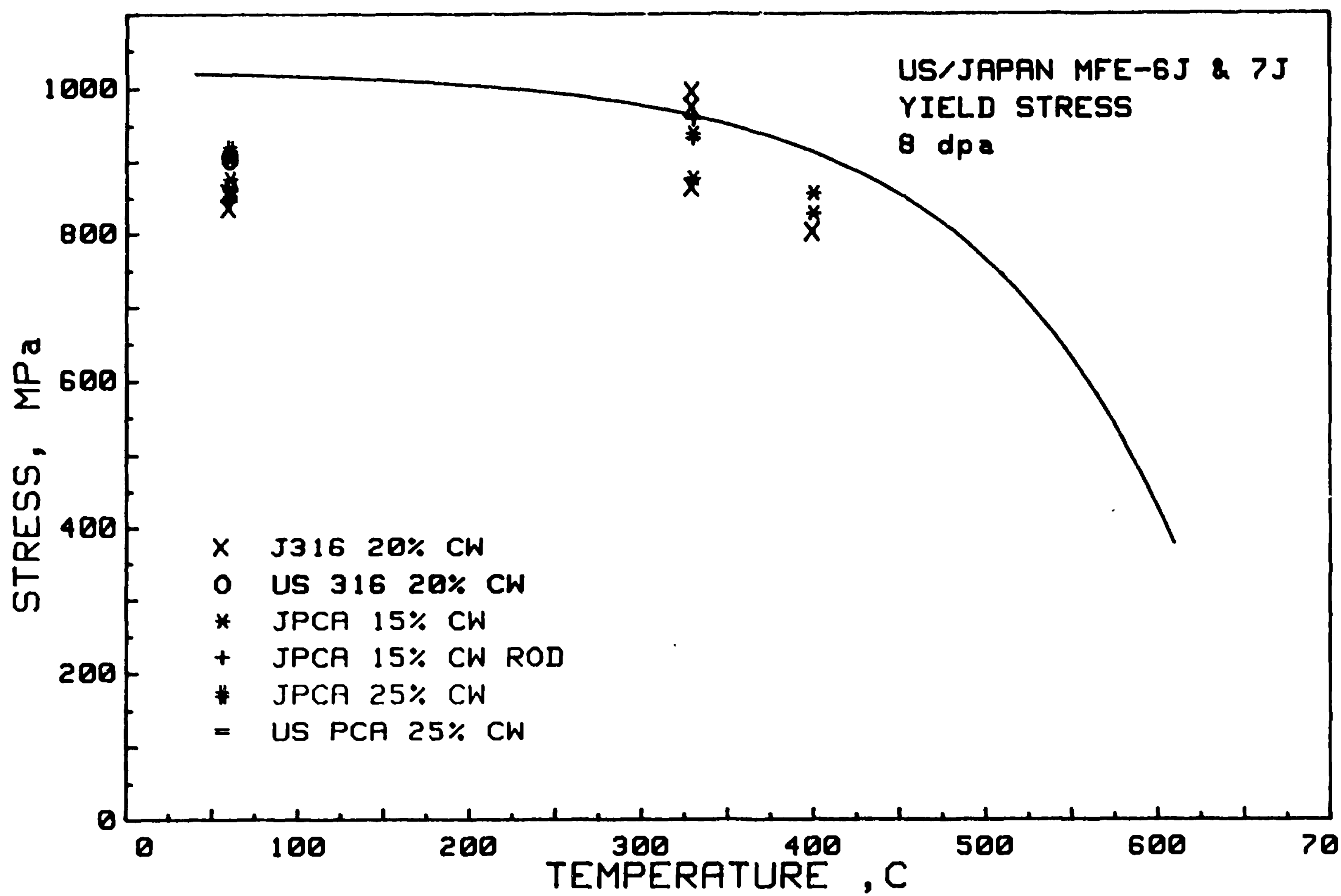
US/JAPAN MFE-6J & 7J
YIELD STRESS
8 dpa
STRESS, MPa
1000
800
600
400
200
0
X J316 20% CW
O US 316 20% CW
* JPCA 15% CW
+ JPCA 15% CW ROD
# JPCA 25% CW
= US PCA 25% CW
0
100
200
300
400
500
600
70
TEMPERATURE ,C

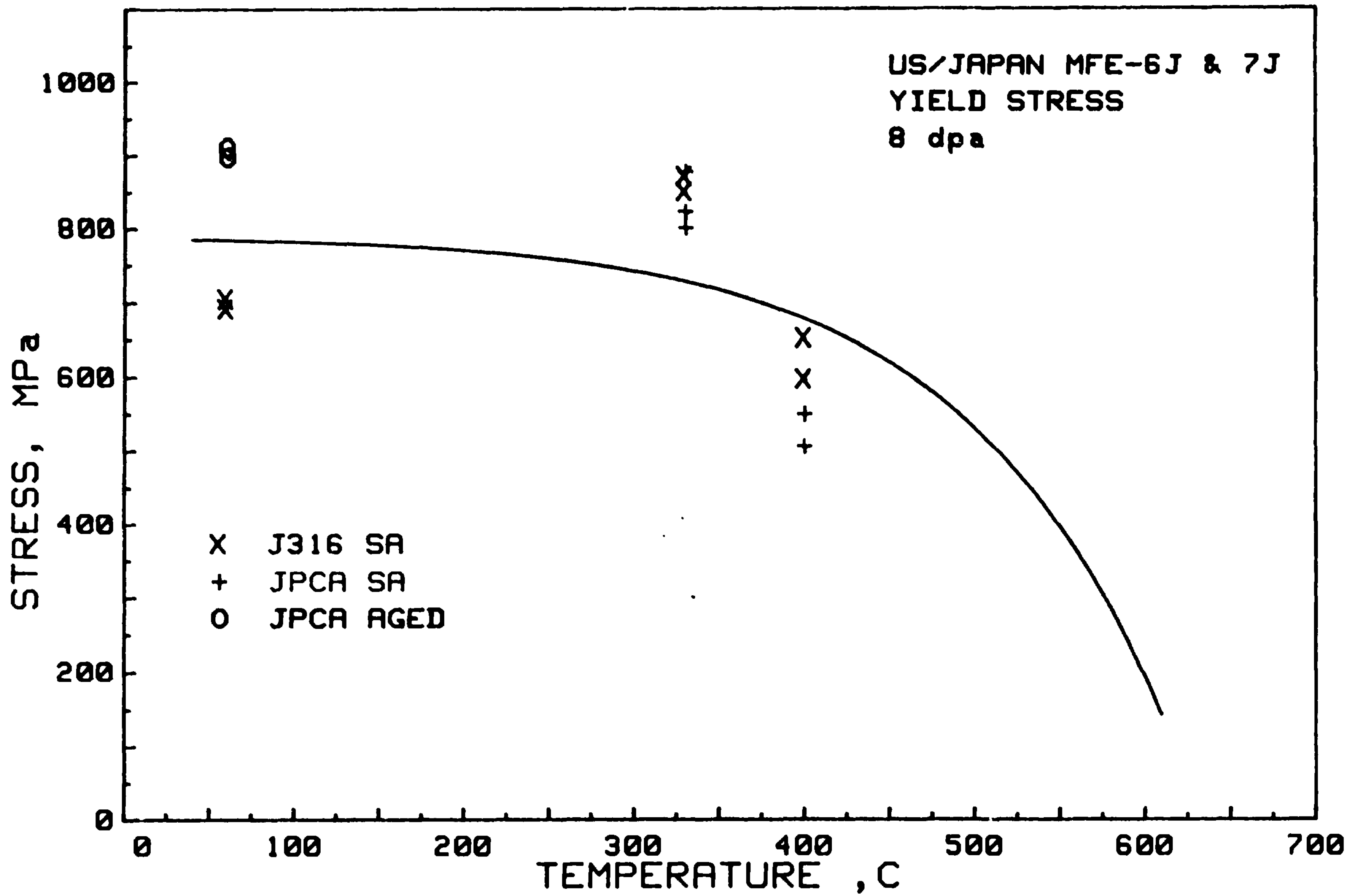

US/JAPAN MFE-6J & 7J
YIELD STRESS
8 dpa
X J316 SA
+ JPCA SA
O JPCA AGED
STRESS, MPa
TEMPERATURE ,C
0
200
400
600
800
1000
0
100
200
300
400
500
600
700

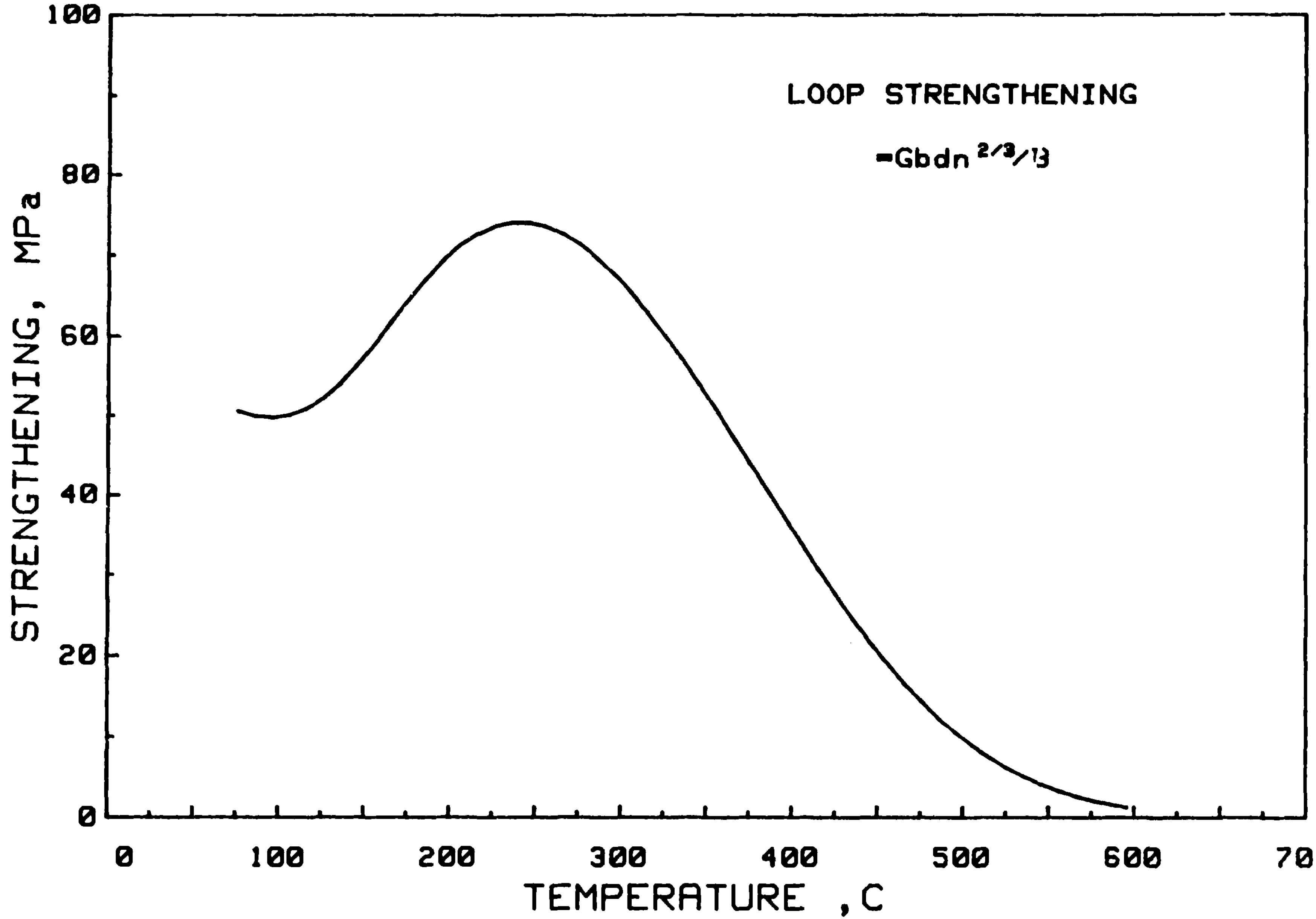

LOOP STRENGTHENING
=Gbdn 2/3/13
STRENGTHENING, MPa
TEMPERATURE ,C
100
80
60
40
20
0
0
100
200
300
400
500
600
70

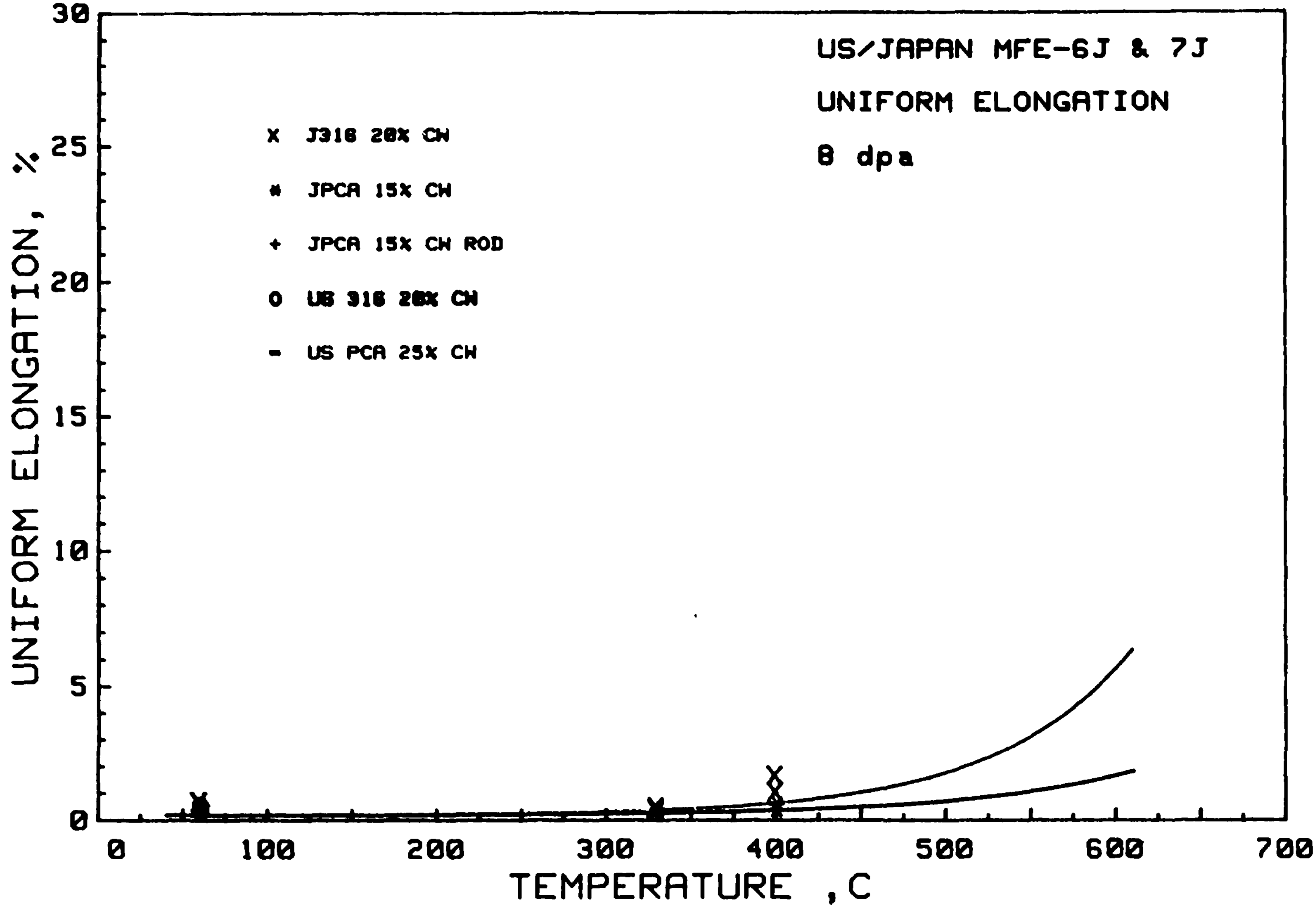
US/JAPAN MFE-6J & 7J
UNIFORM ELONGATION
8 dpa
x J316 20% CW
* JPCA 15% CW
+ JPCA 15% CW ROD
O US 316 20% CW
- US PCA 25% CW
UNIFORM ELONGATION, %
0
5
10
15
20
25
30
0
100
200
300
400
500
600
700
TEMPERATURE ,C

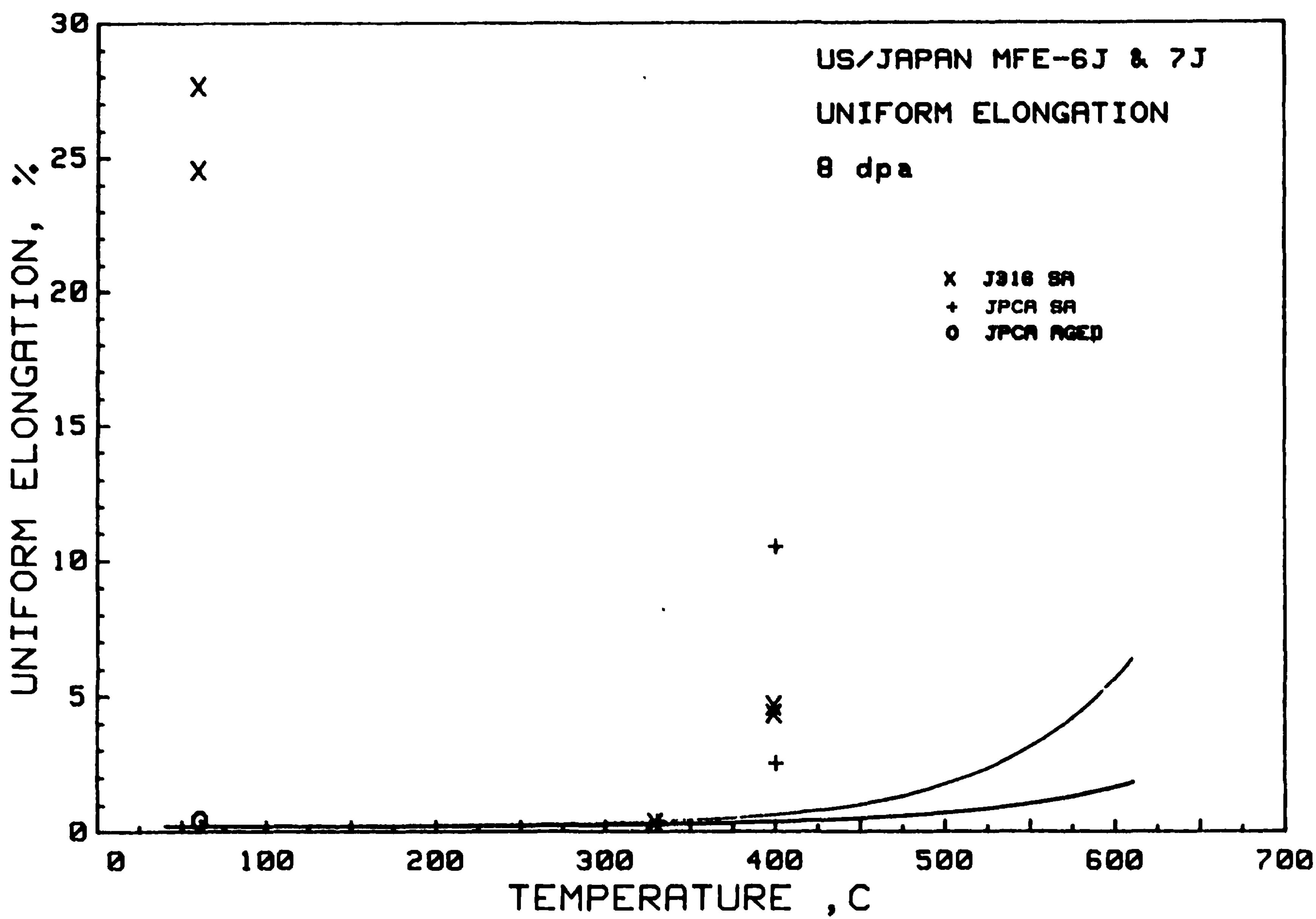
US/JAPAN MFE-6J & 7J
UNIFORM ELONGATION
8 dpa
X J316 SA
+ JPCA SA
O JPCA AGED
UNIFORM ELONGATION, %
TEMPERATURE ,C
0
5
10
15
20
25
30
0
100
200
300
400
500
600
700

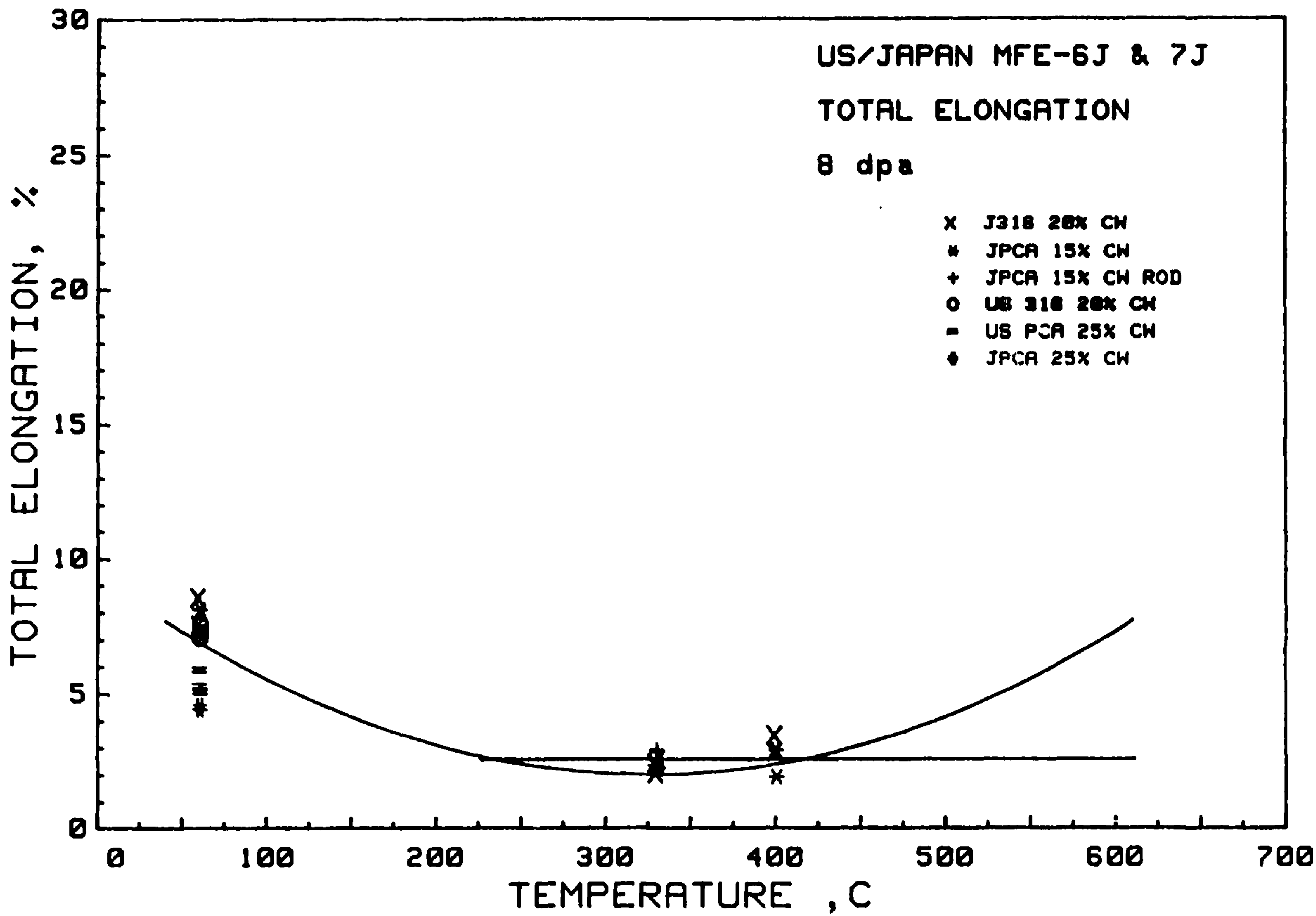
US/JAPAN MFE-6J & 7J
TOTAL ELONGATION
8 dpa
X J316 20% CW
* JPCA 15% CW
+ JPCA 15% CW ROD
O US 316 20% CW
- US PCA 25% CW
JPCA 25% CW
TOTAL ELONGATION, %
TEMPERATURE ,C
0
5
10
15
20
25
30
0
100
200
300
400
500
600
700

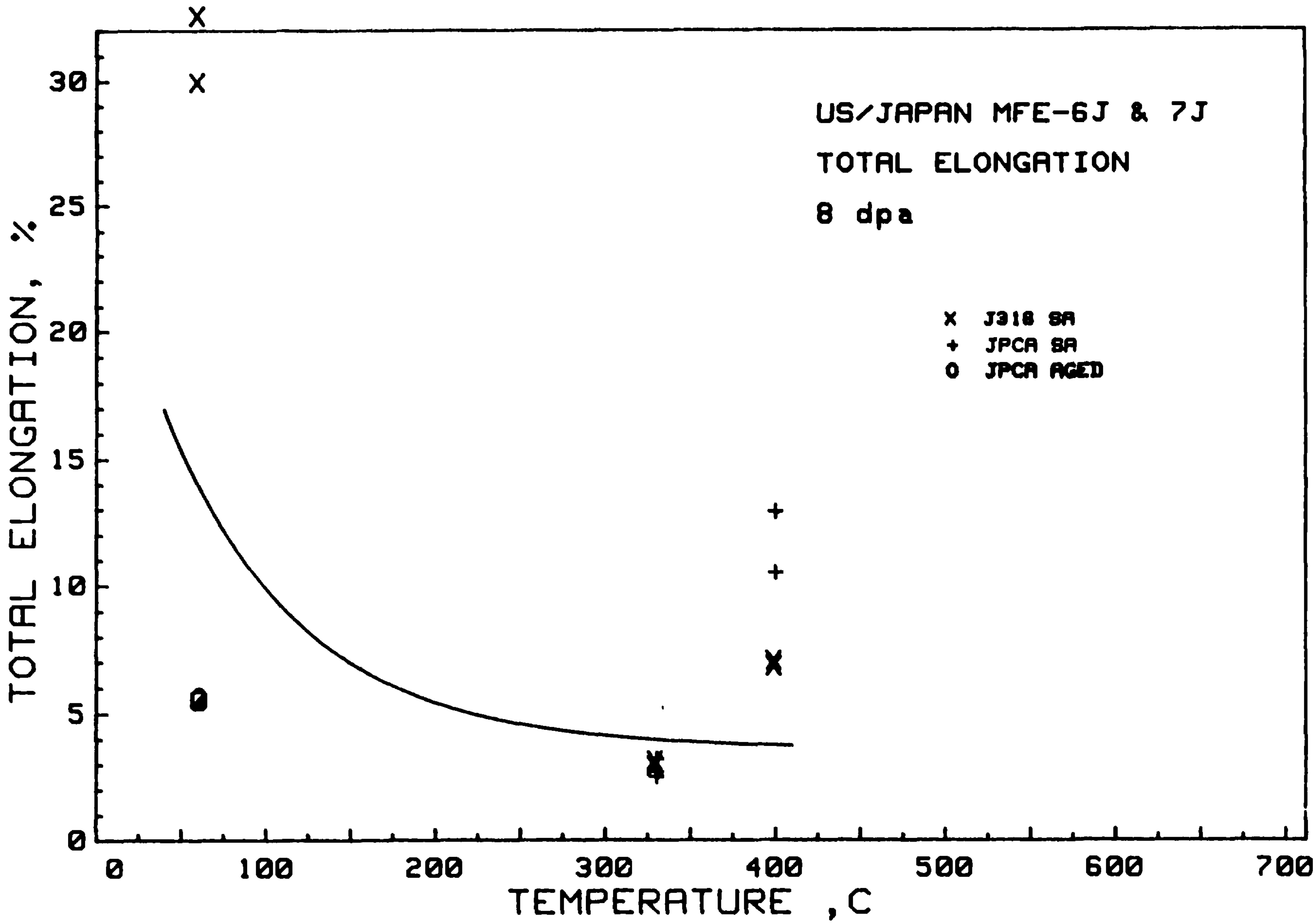
US/JAPAN MFE-6J & 7J
TOTAL ELONGATION
8 dpa
x J316 SA
+ JPCA SA
0 JPCA AGED
TOTAL ELONGATION, %
TEMPERATURE ,C
0
5
10
15
20
25
30
0
100
200
300
400
500
600
700

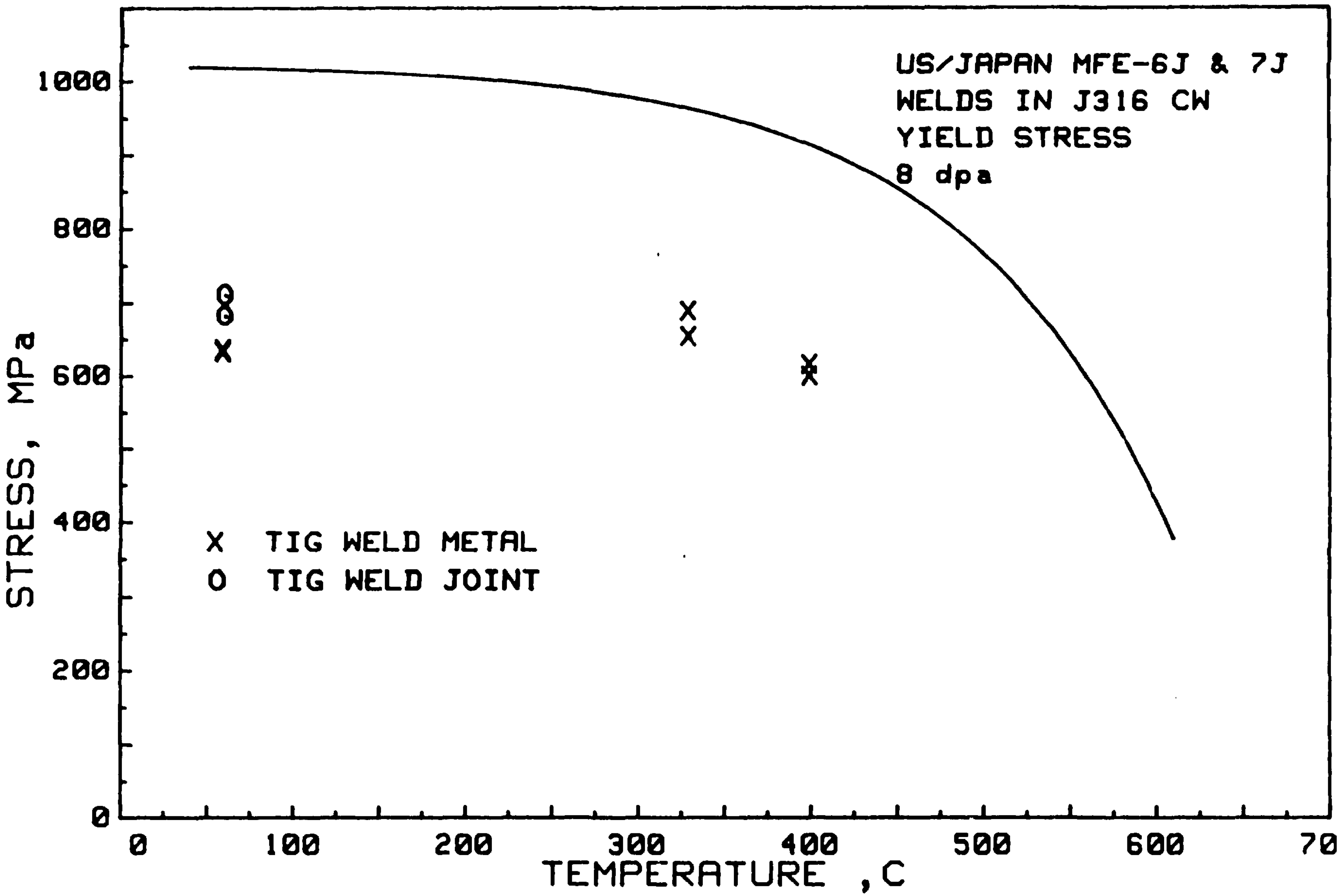

US/JAPAN MFE-6J & 7J
WELDS IN J316 CW
YIELD STRESS
8 dpa
X TIG WELD METAL
O TIG WELD JOINT
STRESS, MPa
TEMPERATURE ,C
0
200
400
600
800
1000
0
100
200
300
400
500
600
70

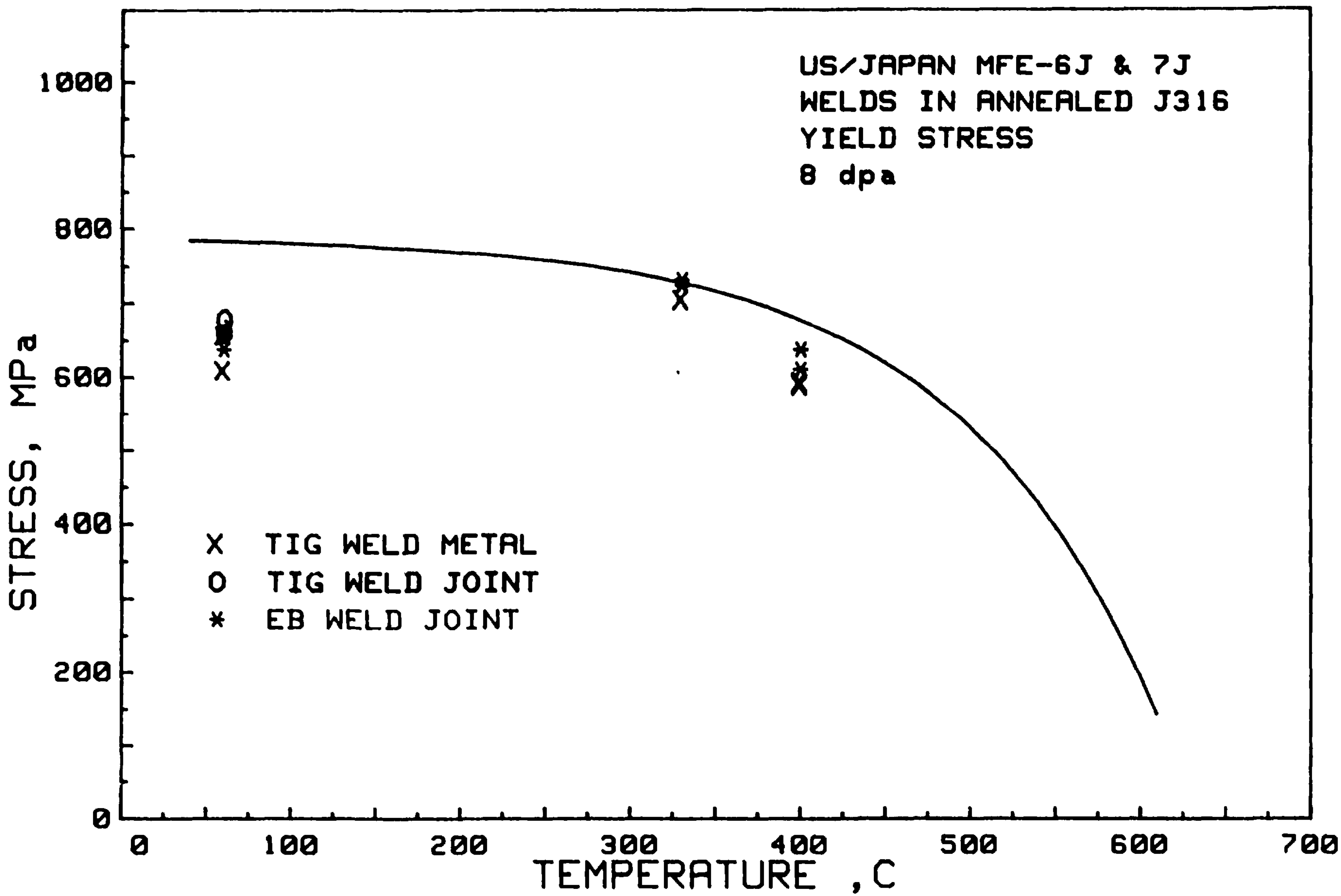

US/JAPAN MFE-6J & 7J
WELDS IN ANNEALED J316
YIELD STRESS
8 dpa
X TIG WELD METAL
O TIG WELD JOINT
* EB WELD JOINT
STRESS, MPa
TEMPERATURE ,C
0
200
400
600
800
1000
0
100
200
300
400
500
600
700

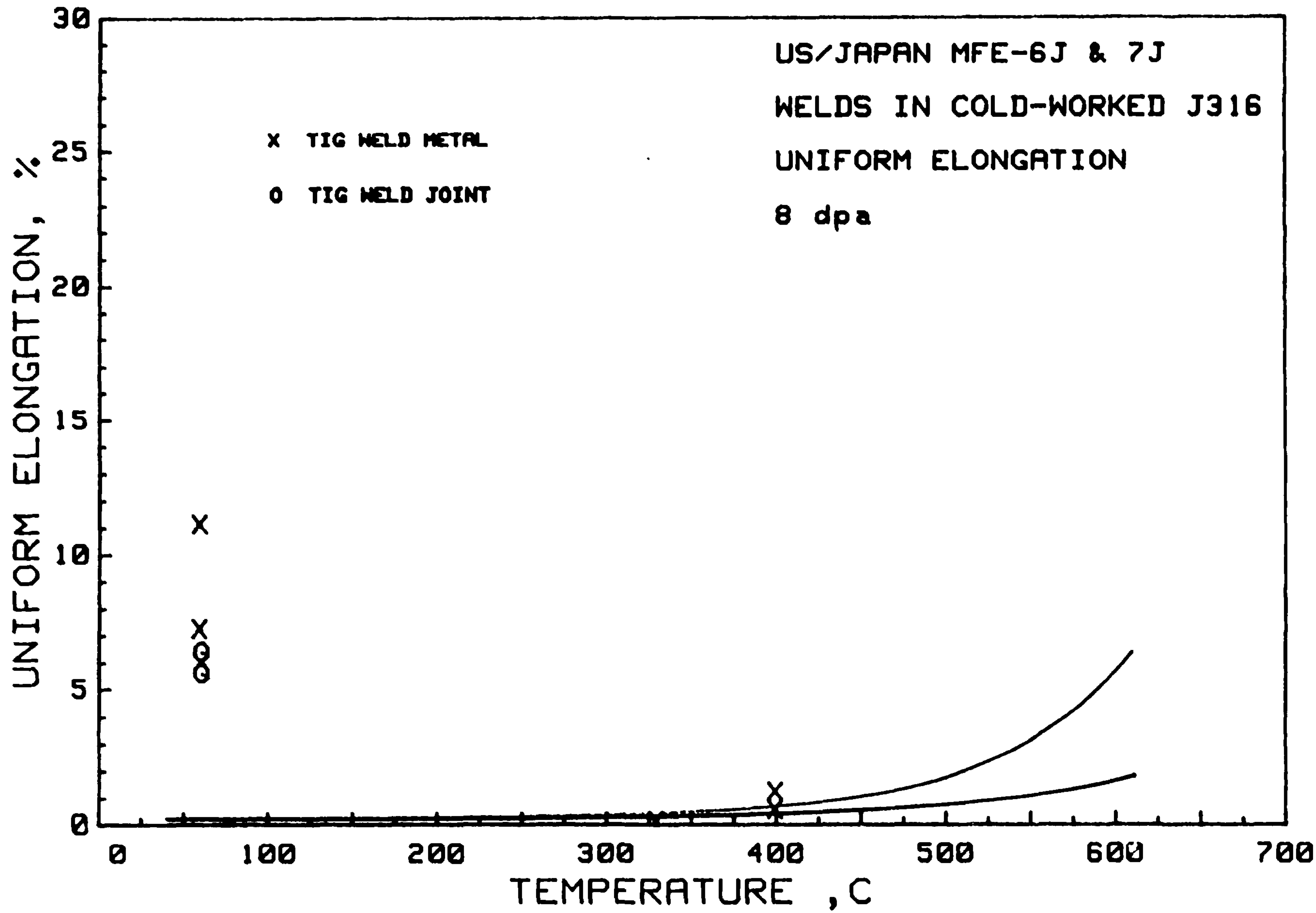

US/JAPAN MFE-6J & 7J
WELDS IN COLD-WORKED J316
UNIFORM ELONGATION
8 dpa
x TIG WELD METAL
0 TIG WELD JOINT
UNIFORM ELONGATION, %
TEMPERATURE ,C
0
5
10
15
20
25
30
0
100
200
300
400
500
600
700

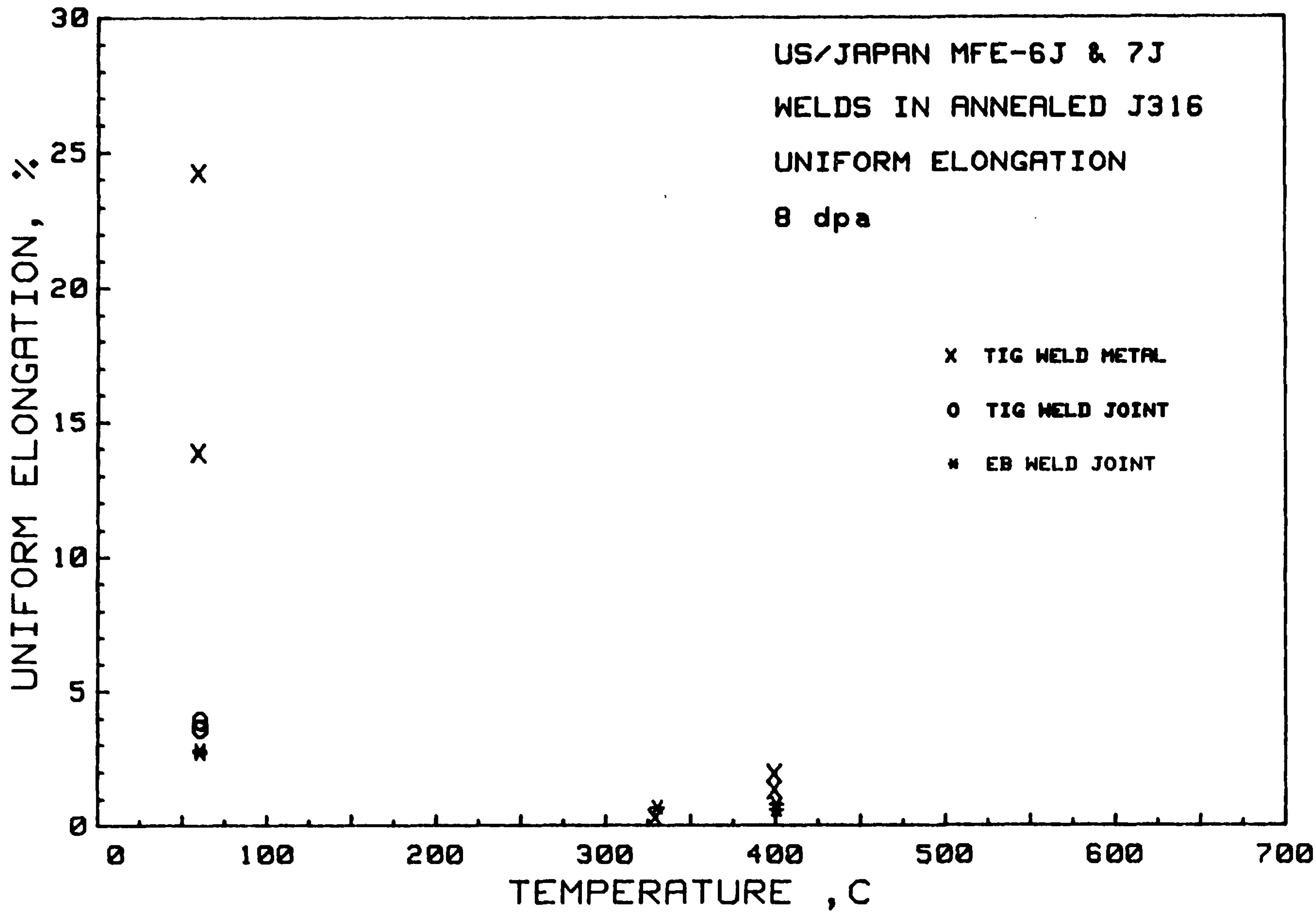
US/JAPAN MFE-6J & 7J
WELDS IN ANNEALED J316
UNIFORM ELONGATION
8 dpa
X TIG WELD METAL
O TIG WELD JOINT
* EB WELD JOINT
UNIFORM ELONGATION, %
TEMPERATURE ,C
0
5
10
15
20
25
30
0
100
200
300
400
500
600
700

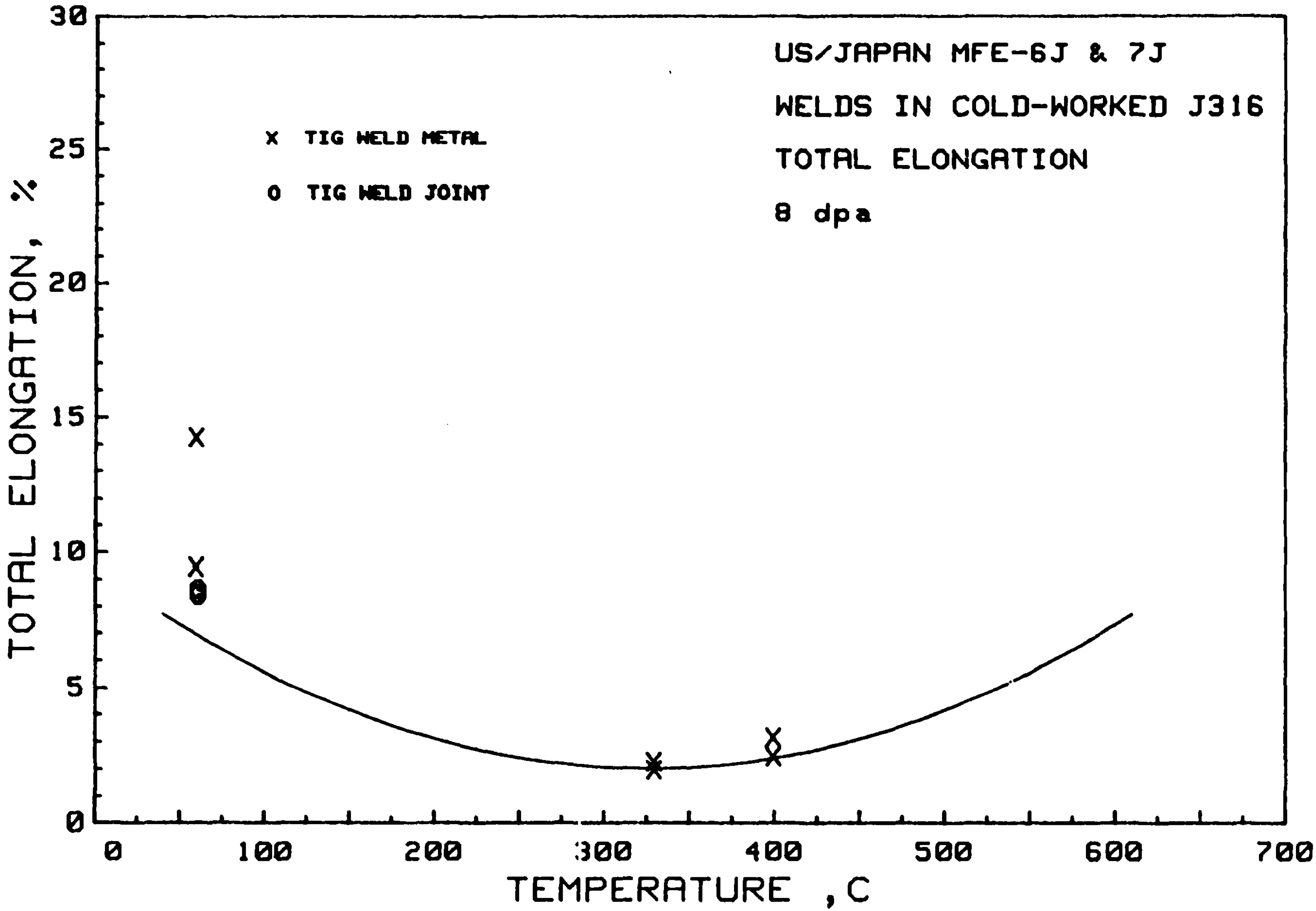

US/JAPAN MFE-6J & 7J
WELDS IN COLD-WORKED J316
TOTAL ELONGATION
8 dpa
X TIG WELD METAL
O TIG WELD JOINT
TOTAL ELONGATION, %
TEMPERATURE ,C
0
5
10
15
20
25
30
0
100
200
300
400
500
600
700

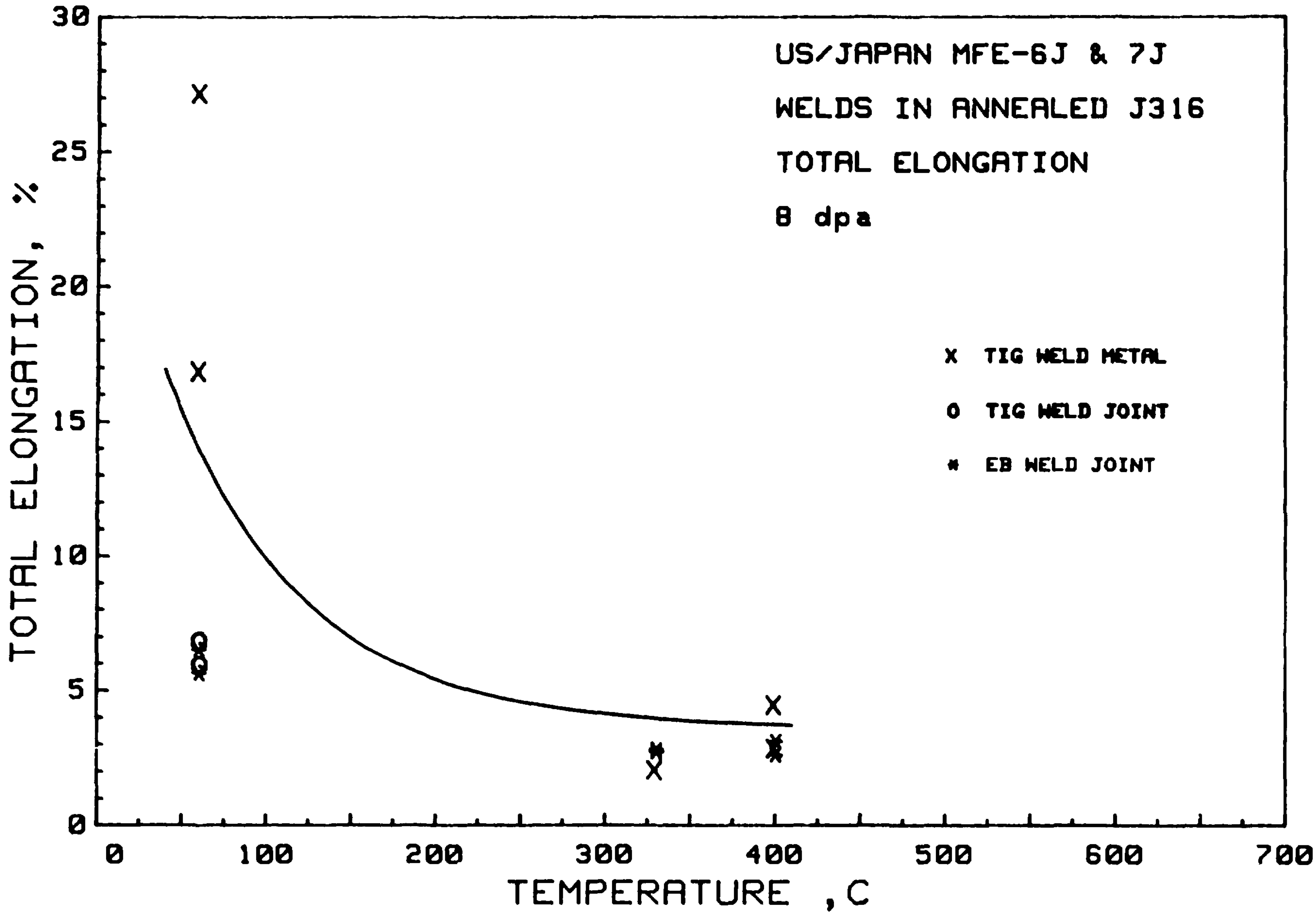
US/JAPAN MFE-6J & 7J
WELDS IN ANNEALED J316
TOTAL ELONGATION
8 dpa
X TIG WELD METAL
O TIG WELD JOINT
* EB WELD JOINT
TOTAL ELONGATION, %
TEMPERATURE ,C
0
5
10
15
20
25
30
0
100
200
300
400
500
600
700

SUMMARY

1. RESULTS CONSISTENT WITH JP 1–8
2. INCREASE IN STRENGTH BETWEEN 60 AND 300 C
3. LOW UNIFORM ELONGATION IN COLD–WORKED ALLOYS BELOW 400 C
4. STRENGTH OF WELDS COMPARABLE WITH ANNEALED MATERIAL
5. GOOD DUCTILITY IN WELDS AT 60 C
6. RESULTS OF 200 C SPECIMENS EAGERLY AWAITED

MICROSTRUCTURAL DATA FROM THE 6J/7J CAPSULES

Tomotsugu Sawai

ABSTRACT

The first four Japanese TEM disks from ORR were observed. They are specimens taken from weld joints. Specimens from base metal and weld metal were examined in both 316 and JPCA; however, the weld metal specimen of 316 was not successfully thinned for microscopy. The microstructure was observed in the other three specimens. The swelling values of 316 and JPCA base metal were 0.003% and 0.006%, respectively. Most of the cavities are smaller than 10 nm in diameter. Hoterogeneous damage microstructure was observed in JPCA weld metal. Less void swelling at the cell boundary than cell core region. This is considered to be caused by the initial heterogeneity in the microstructure before irradiation.

Table 1
Chemical compositions of material used (wt%)

	C	Si	Mn	P	S	Cr	Ni	Mo	Ti	N	sol Al	Co	Nb
316	0.055	0.75	1.5	0.020	0.004	16.4	13.9	2.3	0.08	0.0084	0.021	0.013	0.06
JPCA	0.052	0.51	1.8	0.028	0.005	14.3	15.5	2.3	0.24	0.0037	-	0.003	-

Table 2
EB-welding conditions

	316	JPCA
Plate thickness	18 mm	8 mm
Accelerating voltage	90 kV	90 kV
Beam current	90 mA	100 mA
Vacuum	10^{-2} Pa	10^{-2} Pa
Welding rate	500 mm/min	600 mm/min
Welding position	Horizontal	Horizontal
Joint type	Butt joint	Bead-on-plate (melt through)

IRRADIATION: ORR−MFE−7J

DOSE: 8dpa

TEMPERATURE: 400℃

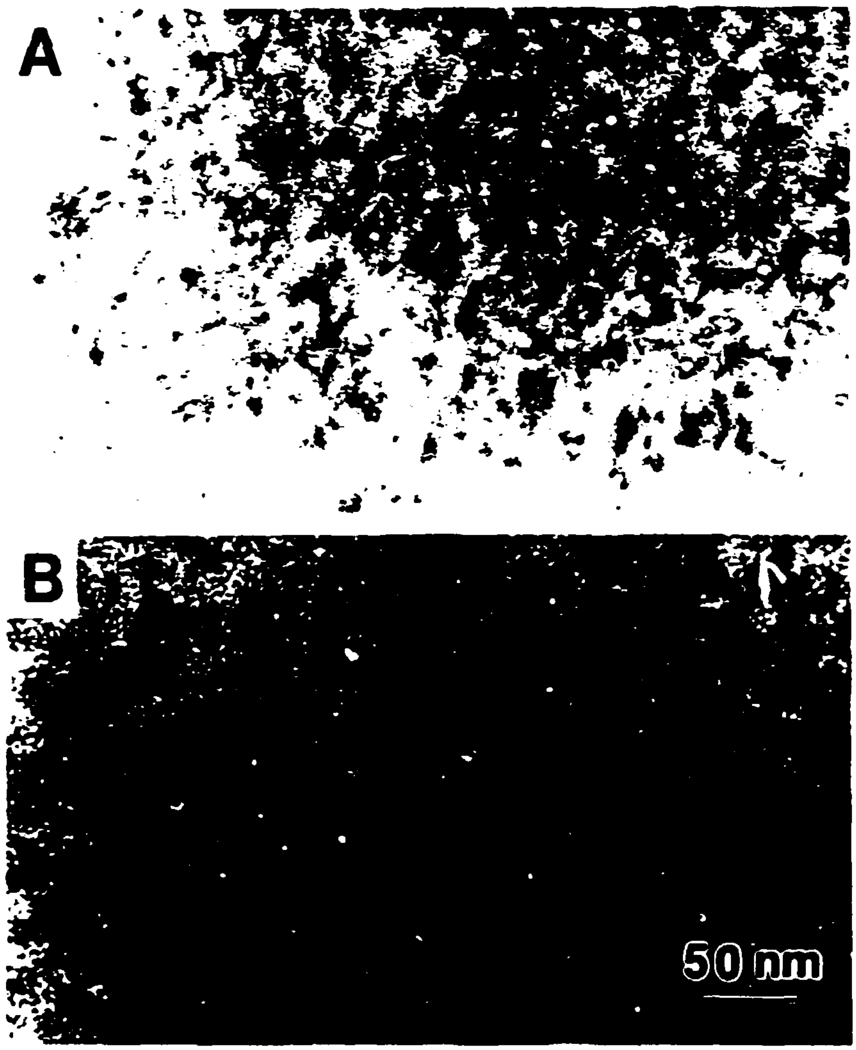

Void microstructure of 316(A) and JPCA(B). Both pictures are taken at the area of almost same thickness (35nm).

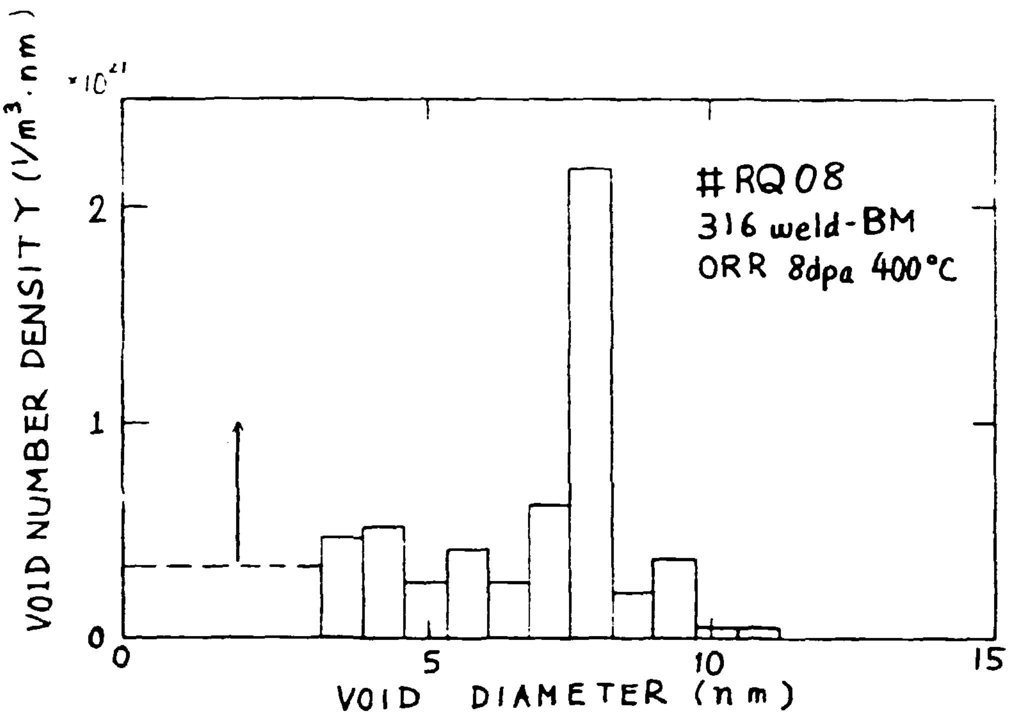

×10^21
VOID NUMBER DENSITY (1/m³·nm)
#RQ08
316 weld-BM
ORR 8dpa 400°C
0
1
2
0
5
10
15
VOID DIAMETER (nm)

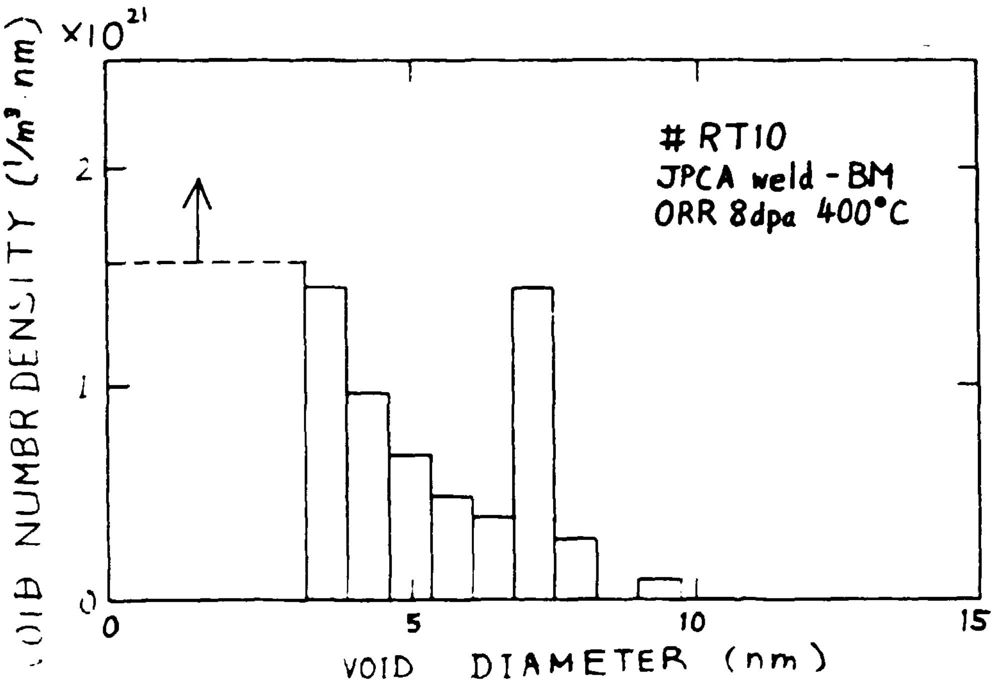

×10^21
VOID NUMBR DENSITY (1/m³·nm)
#RT10
JPCA weld-BM
ORR 8dpa 400°C
0
1
2
0
5
10
15
VOID DIAMETER (nm)

VOID DATA OF BASE METALS

316

Number density: 5.6E21 (mm^{-3})
Mean Diameter : 5.27 (nm)
Swelling : 0.060 (%)

JPCA

Number density: 9.1E21 (mm^{-3})
Mean Diameter : 3.24 (nm)
Swelling : 0.033 (%)


JAERI/ORNL89

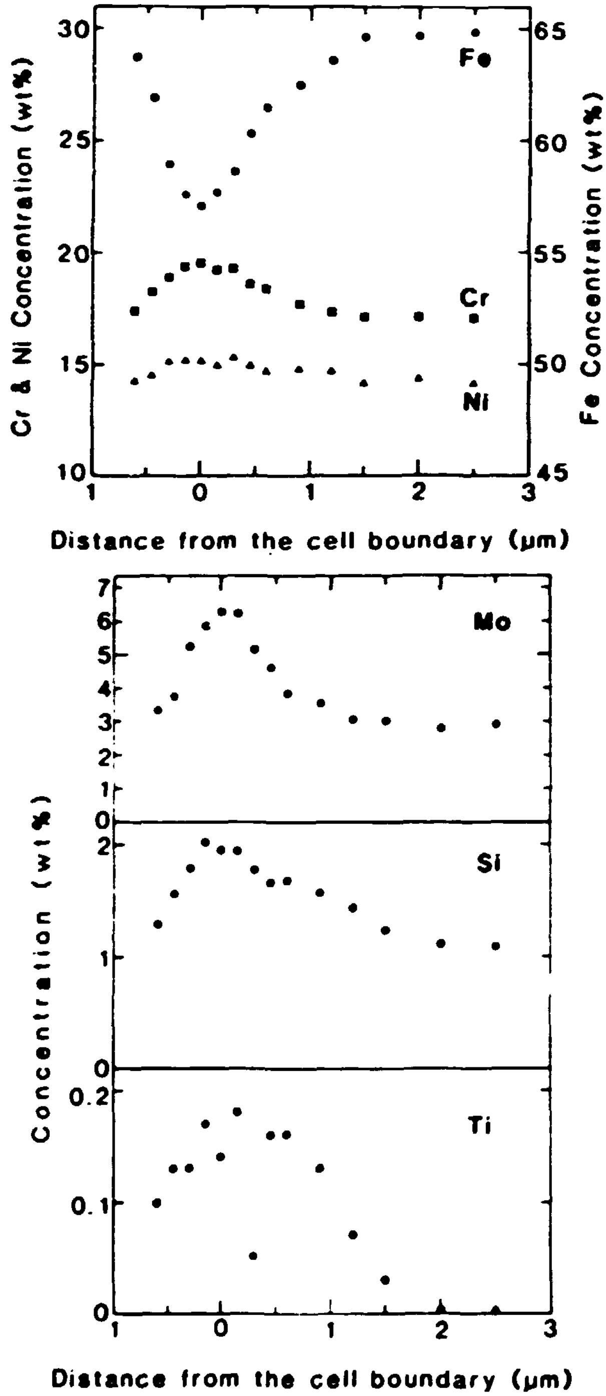

Fig. 5. Concentration profiles of major and minor element of 316 SS weld metal across in the cell boundary.

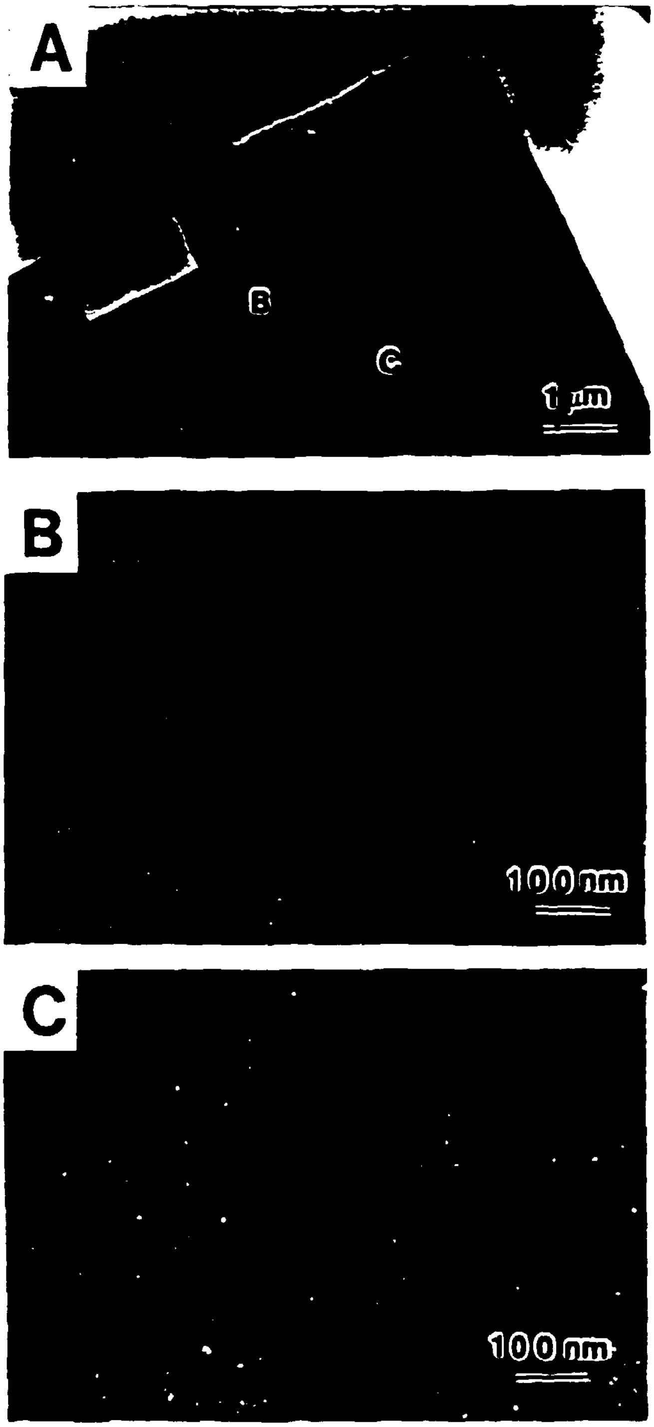
A
B
C
1 μm
B
100 nm
C
100 nm

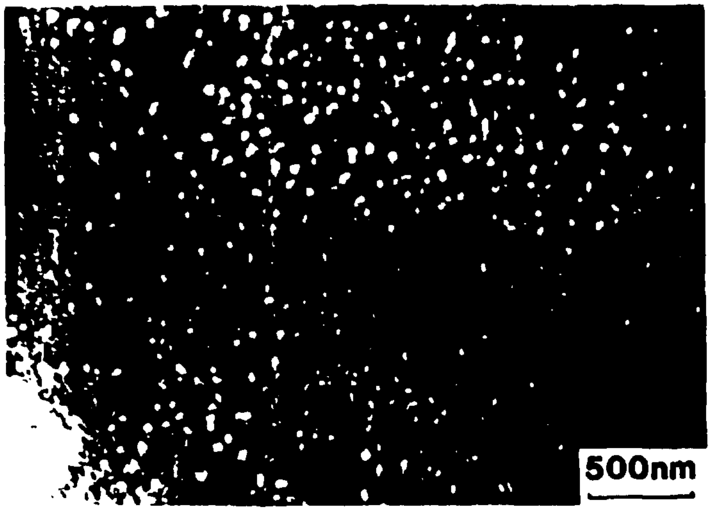

Fig. 6. Transmission electron micrograph of 316 SS weld metal irradiated around cell boundary.

the cell boundary was also revealed in fig. 5. Niobium may also be enriched at the cell boundary in 316 SS, although it was usually not detected. The depletion of inhibitor elements in the cell center results from this segregation at the cell boundary and the precipitation. For the major elements Fe, Cr and Ni segregation is detected in good agreement with the results of Brooks et al. [7], but the compositional difference between the cell center of the weld metal and the base metal is too small to affect the swelling characteristics.

The segregation of inhibitor elements is reflected in the micrograph of the 316 SS weld metal irradiated near the cell boundary to 15 dpa (fig. 6). This shows less cavity formation at the cell boundary, although the cell boundary in this thick area for HVEM irradiation is not

5. Conclusions

EB weld joints of 316 SS with 0.08 wt% Ti and 0.06 wt% Nb and JPCA were irradiated in HVEM at 773 K to 15 dpa and examined by analytical electron microscopy. The results can be summarized as follows:

(1) The void swelling of the 316 SS base metal so 0.94%, lower than that reported on typical Type 316 stainless steel without Ti and Nb.

(2) In 316 SS the void swelling is 6.1% at the cell center in the solidification structure of the weld metal and 4.6% at the heat affected zone. Both values are higher than swelling in the base metal. Irradiation near the cell boundary of 316 SS induced inhomogeneous swelling, with less cavity formation at the cell boundary.

(3) In JPCA, the void swelling is about 0.5% at the cell center in the weld metal, while no cavities formed in the base metal irradiated under the similar condition. The weld metal recovered its swelling resistance in the heat treatment at 1473 K for 1 h.

(4) Solute enrichment at the cell boundary in the weld metal of both steels was detected. The increase in void swelling of the weldment is due to the depletion of inhibitor elements from the matrix caused by the segregation of such solute atoms at the cell boundary and/or by the formation of precipitates enriched in these solute elements during the welding and the solidification.

The author are grateful to Mr. H. Yoshida (Hitachi Ltd.) for the manufacturing the EB-weld joints and to Dr. T. Kodaira (JAERI) for this stimulating suggestions in this work.

References

[1] W.F. Savage, E.F. Nippes and G.J. Bruck, Welding J. 60

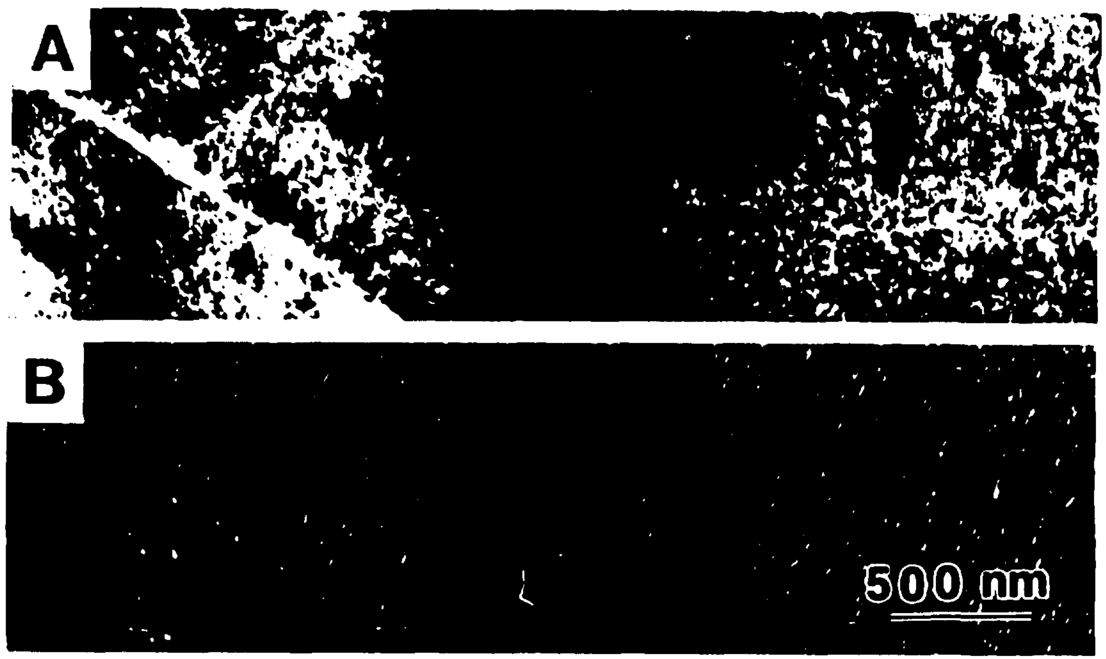
A
B
500 nm

Technical Improvement

1. Thickness measurement

2. Washing after electro-polishing

3. Condensor ajustment for dark field image of loops.

Now

electro polishing

7 : CH_3CH_2OH
1 : H_2SO_4

↓

Washing

9 : CH_3CH_2OH
1 : H_2O

Improved Washing

- increased H_2O ratio (5 : 5)
- solution heating

Manual adjustment of condensor
(JEM 2000FX)

Dark field loop image taken with the streak beam close to (200) reflection requires parallel beam

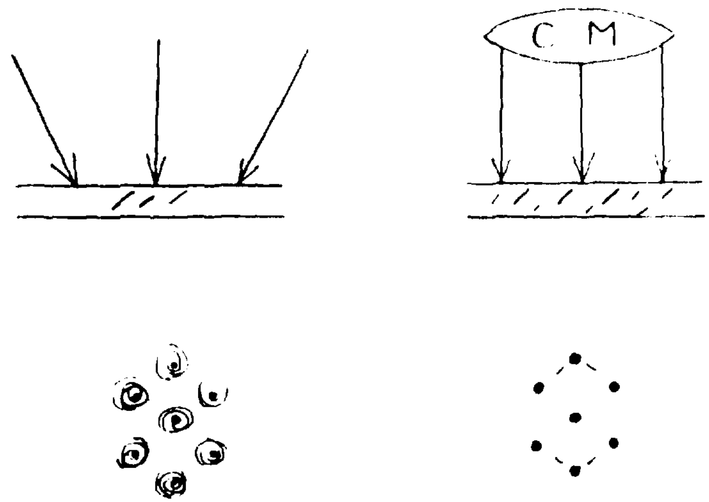

DOSIMETRY IN SUPPORT OF PHASE I IRRADIATION EXPERIMENTS

M. L. Grossbeck

ABSTRACT

Dosimeters are provided for all fusion materials irradiation experiments by Dr. L. R. Greenwood at Argonne National Laboratory (ANL). Dosimeter target materials are selected for each individual experiment but consist of elements such as Fe, Co, Ti, Cu, and Mn. Following irradiation, the dosimeters are removed and shipped to ANL for counting and analysis of the activation data. Calculations of fluxes, fluences, dpa, and helium are provided for the reactor midplane, and values at the positions of the dosimeters are provided. These results are further analyzed at Oak Ridge to obtain values of dpa and helium concentration in the actual specimens. This includes developing a least squares fit for the displacements and helium concentrations as a function of position and then calculating the helium concentrations based upon the fraction of nickel in each alloy.

This effort is in progress with the ORR-MFE-6J data in the final stage of analysis at ANL and the dosimeters from the 200°C capsule awaiting shipment to ANL.

Table I.
Measured Activities for HFIR-JP2, JP6, JP7
Values (at/at-s) at 100 MW; ±3% accuracy

Height, cm	$^{58}Fe(n,\gamma)^{59}Fe$ JP2	JP6	JP7	$^{59}Co(n,\gamma)^{60}Co$ JP2	JP6	JP7
	($\times 10^{-9}$)			($\times 10^{-8}$)		
25.4	1.23	1.15	-	3.64	3.68	-
16.5	1.79	1.70	1.84	5.36	5.71	5.80
7.1	2.20	2.15	-	6.25	6.65	-
2.1	2.36	2.23	2.36	6.33	6.50	6.51
-12.1	2.02	1.91	-	5.48	5.81	-
-21.0	1.39	1.35	-	4.39	4.48	-

Height, cm	$^{54}Fe(n,p)^{54}Mn$ JP2	JP6	JP7	$^{55}Mn(n,2n)^{54}Mn$ JP2	JP6	JP7
	($\times 10^{-9}$)			($\times 10^{-8}$)		
25.4	2.59	2.27	-	0.782	0.708	-
16.5	5.21	5.21	5.40	1.51	1.35	1.53
7.1	6.75	6.80	-	1.97	1.92	-
2.1	6.99	7.07	6.95	2.10	2.06	2.10
-12.1	5.93	5.89	-	1.72	1.81	-
-21.0	3.91	3.88	-	1.17	1.16	-

Table II.
Neutron Fluences for HFIR-JP2, JP6, JP7
Values are accurate to ±10%
Fluence $\times 10^{22}$ n/cm^2

Energy	JP2	JP6, JP7
Total	24.66	14.80
Thermal (<0.5 eV)	10.09	6.09
0.5 eV-0.11 MeV	7.97	4.77
>0.11 MeV	6.59	3.95
>1 MeV	3.35	2.02

Table III.
Damage Parameters for HFIR-JP2, 6, 7
Values at midplane; for gradients, use Eq. (1)

Element		JP2		JP6, JP7	
		He, appm	DPA	He, appm	DPA
Al		41.9	86.4	25.2	51.8
Ti		27.9	54.8	16.9	33.0
V		1.41	61.4	0.85	36.9
Cr		9.61	54.1	5.78	32.5
Mn[a]		8.48	59.6	5.10	35.8
Fe		17.07	47.9	10.28	28.8
Co[a]		8.40	60.1	5.05	36.1
Ni	Fast	226.0	51.5	137.0	31.0
	^{59}Ni	25,402.0	44.8	15,015.0	26.5
	Total	25,628.0	96.3	15,152.0	57.5
Cu	Fast	12.4	46.7	7.4	28.1
	^{65}Zn	119.2	0.2	38.3	0.1
	Total	131.6	46.9	45.7	28.2
Nb		3.12	46.3	1.88	27.8
Mo		-	34.5	-	20.7
316SS[b]		3345.0	55.2	1978.0	33.1

[a] Thermal self-shielding important for Mn, Co.
[b] 316SS: Fe (0.645), Ni (0.13), Cr (0.18), Mn (0.019), Mo (0.026).

Table IV.
Damage Gradients for HFIR-JP2, JP6, JP7
DPA includes thermal effect from ^{59}Ni.
Helium includes ^{59}Ni and fast reactions

Height, cm	JP2 He, appm	JP2 DPA	JP6, JP7 He, appm	JP6, JP7 DPA
0	3345	55.2	1978	33.1
3	3316	54.7	1957	32.8
6	3229	53.3	1897	31.9
9	3082	50.8	1796	30.4
12	2873	47.3	1653	28.3
15	2592	42.7	1464	25.5
18	2242	37.2	1234	22.2
21	1811	30.7	961	18.2
24	1293	23.1	650	13.7

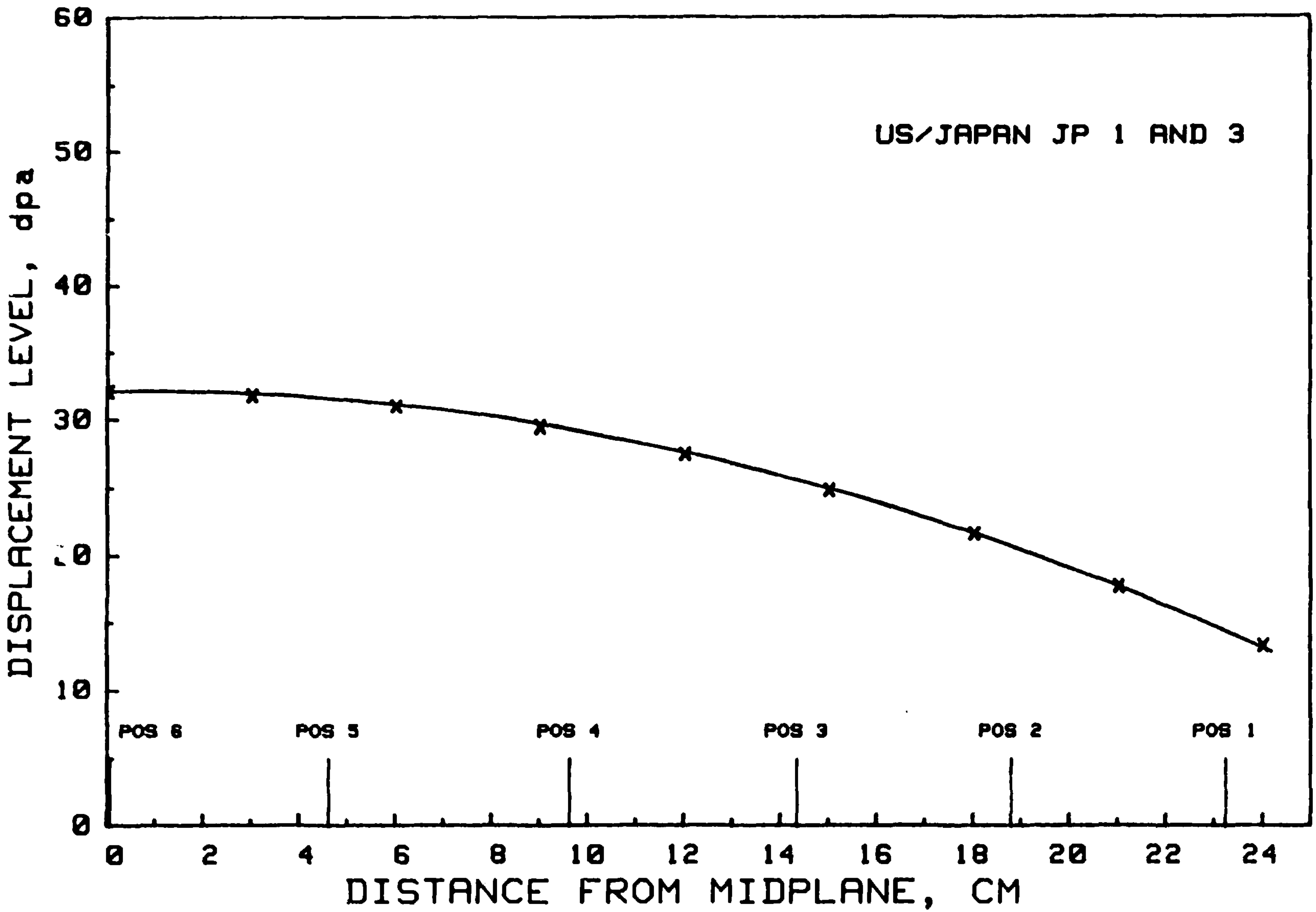
US/JAPAN JP 1 AND 3
DISPLACEMENT LEVEL, dpa
DISTANCE FROM MIDPLANE, CM
POS 6
POS 5
POS 4
POS 3
POS 2
POS 1
0
10
30
40
50
60
0
2
4
6
8
10
12
14
16
18
20
22
24

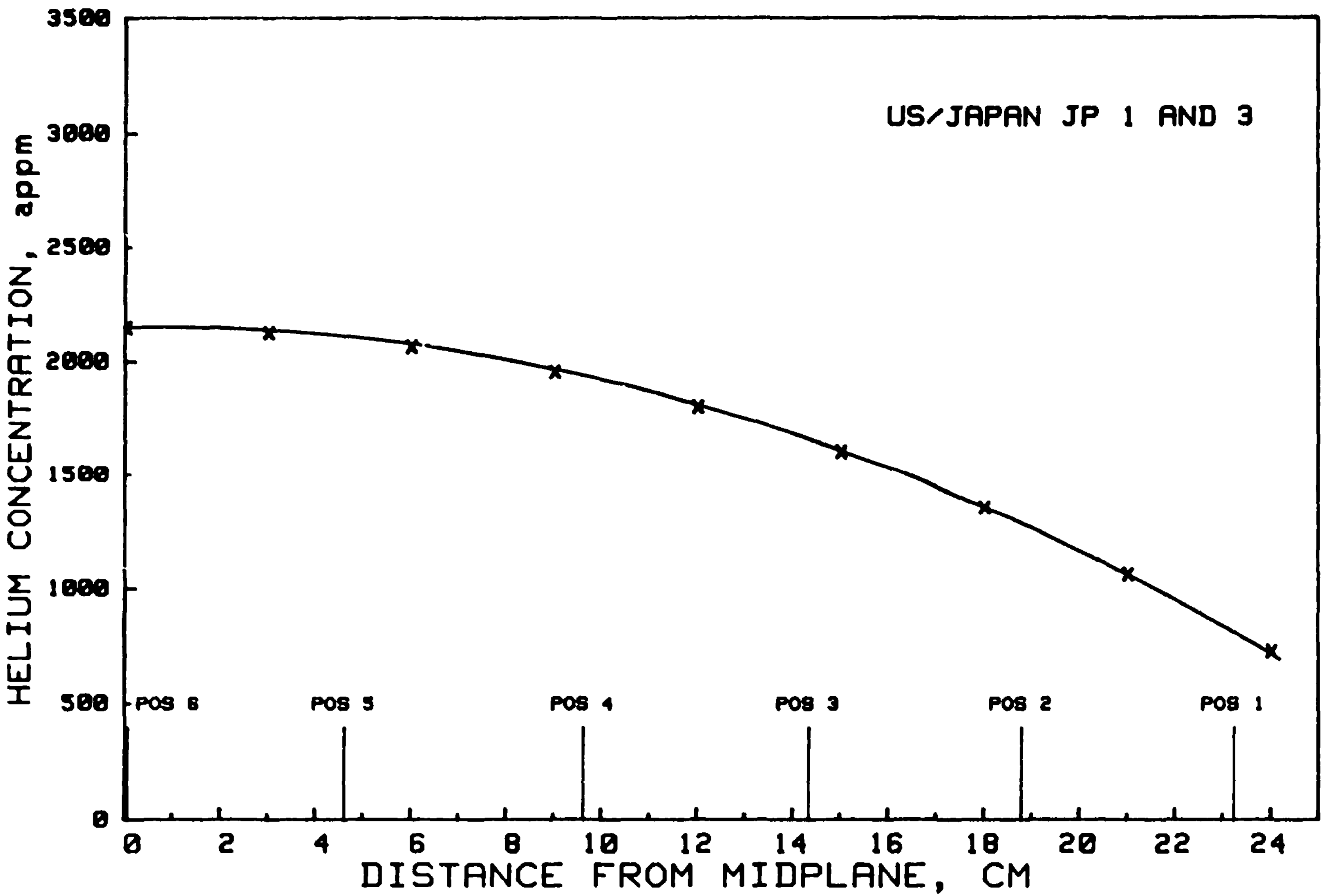

US/JAPAN JP 1 AND 3
HELIUM CONCENTRATION, appm
DISTANCE FROM MIDPLANE, CM
0
500
1000
1500
2000
2500
3000
3500
0
2
4
6
8
10
12
14
16
18
20
22
24
POS 6
POS 5
POS 4
POS 3
POS 2
POS 1

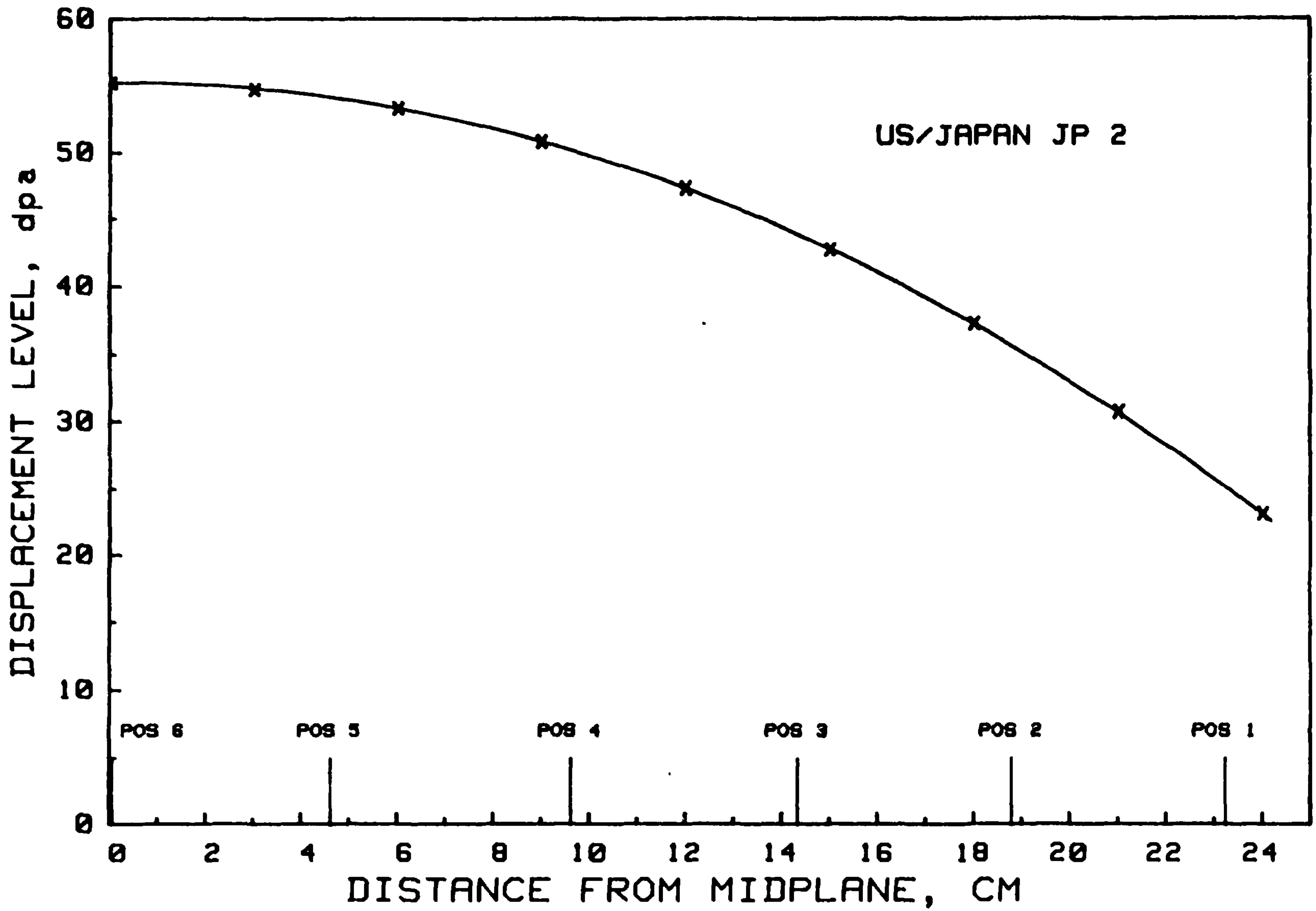
US/JAPAN JP 2
DISPLACEMENT LEVEL, dpa
DISTANCE FROM MIDPLANE, CM
POS 6
POS 5
POS 4
POS 3
POS 2
POS 1
0
10
20
30
40
50
60
0
2
4
6
8
10
12
14
16
18
20
22
24

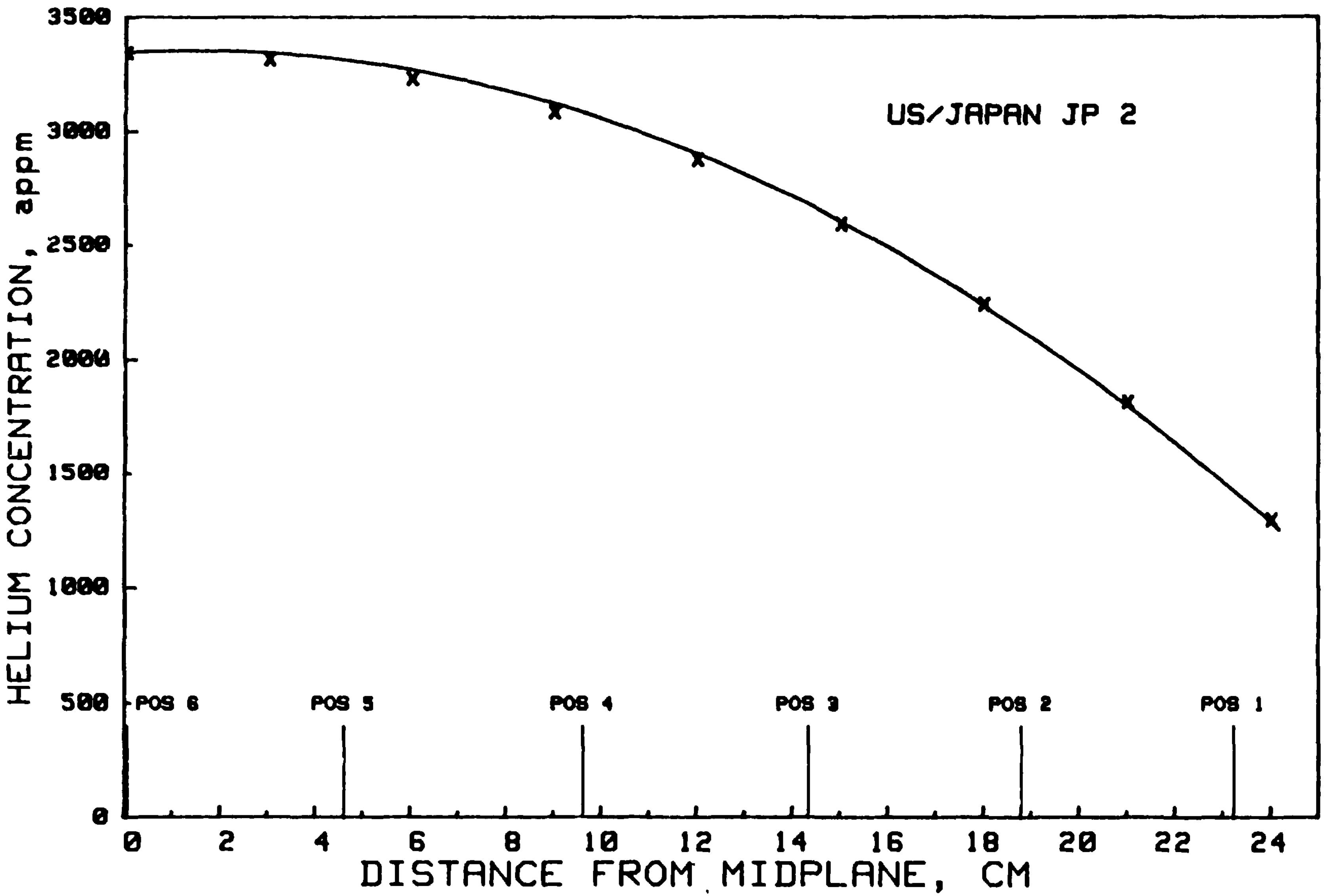
US/JAPAN JP 2
HELIUM CONCENTRATION, appm
DISTANCE FROM MIDPLANE, CM
3500
3000
2500
2000
1500
1000
500
0
POS 6
POS 5
POS 4
POS 3
POS 2
POS 1
0
2
4
6
8
10
12
14
16
18
20
22
24

Measured damage levels and helium concentrations for JP 1

Position	Distance from Reactor Midplane (cm)	Specimen	Alloy	Damage Level (dpa)	Helium Concentration (appm)
1	23.2	EL15	PCA	14	1090
2	18.8	EL21	PCA	21	1690
3	14.3	EL28	PCA	26	2170
4	9.6	AA1	316	29	1940
5	4.6	AA2	316	32	2110
6	0	TEM		32	2150
7	4.6	FE1	JPCA	32	2660
8	9.6	FE2	JPCA	29	2440
9	14.3	TB1	JPCA	26	2090
10	18.8	TB2	JPCA	21	1620
11	23.2	TE1	JPCA	14	1030

Measured damage levels and helium concentrations for JP 2

Position	Distance from Reactor Midplane (cm)	Specimen	Alloy	Damage Level (dpa)	Helium Concentration (appm)
1	23.2	EL36	PCA	25	1870
2	18.8	EL37	PCA	36	2790
3	14.3	EL39	PCA	44	3510
4	9.6	EC157	PCA	50	4040
5	4.6	AA3	316	54	3310
6	0	TEM		55	3350(316)
7	4.6	FE3	JPCA	54	4170
8	9.6	FE4	JPCA	50	3880
9	14.3	TB4	JPCA	44	3370
10	18.8	TB5	JPCA	36	2690
11	23.2	TB6	JPCA	25	1800

Measured damage levels and helium concentrations for JP 3

Position	Distance from Reactor Midplane (cm)	Specimen	Alloy	Damage Level (dpa)	Helium Concentration (appm)
1	23.2	EL30	PCA	14	1070
2	18.8	EL34	PCA	21	1690
3	14.3	EL29	PCA	26	2170
4	9.6	EC152	PCA	29	2540
5	4.6	AA8	316	32	2110
6	0	TEM		32	2150(316)
7	4.6	FE5	JPCA	32	2660
8	9.6	FE6	JPCA	29	2440
9	14.3	TB7	JPCA	26	2090
10	18.8	TB8	JPCA	21	1620
11	23.2	TB9	JPCA	14	1030

Measured damage levels and helium concentrations for JP 4

Position	Distance from Reactor Midplane (cm)	Damage Level (dpa)	Helium Concentration for 316 SS (appm)
1	22.7	26	1520
2	18.1	37	2180
3	13.6	45	2690
4	9.1	51	3040
5	4.6	54	3250
6	0	55	3310
7	4.6	54	3250
8	9.1	51	3040
9	13.6	45	2690
10	18.1	37	2180
11	22.7	26	1520

Measured damage levels and helium concentrations for JP 5

Position	Distance from Reactor Midplane (cm)	Specimen	Alloy	Damage Level (dpa)	Helium Concentration (appm)
1	23.2	EC34	PCA	25	1880
2	18.8	EC31	PCA	36	2750
3	14.3	EC32	PCA	44	3430
4	9.6	EC153	PCA	50	3940
5	4.6	AA27	316	54	3250
6	0	TEM		55	3310(316)
7	4.6	FE10	JPCA	54	4100
8	9.6	FE11	JPCA	50	3790
9	14.3	TE7	JPCA	44	3300
10	18.8	TE8	JPCA	36	2640
11	23.2	TE9	JPCA	25	1810

Measured damage levels and helium concentrations for JP 6

Position	Distance from Reactor Midplane (cm)	Specimen	Alloy	Damage Level (dpa)	Helium Concentration (appm)
1	23.2	EL24	PCA	15	960
2	18.8	TEM		21	1170(316)
3	14.3	AA42	316	26	1520
4	9.6	EC156	PCA	30	2330
5	4.6	EC161	PCA	32	2540
6	0	TEM		33	1980(316)
7	4.6	FE12	JPCA	32	2440
8	9.6	FE13	JPCA	30	2240
9	14.3	TE10	JPCA	26	1910
10	18.8	TE11	JPCA	21	1480
11	23.2	TE12	JPCA	15	920

Measured damage levels and helium concentrations for JP 7

Position	Distance from Reactor Midplane (cm)	Specimen	Alloy	Damage Level (dpa)	Helium Concentration (appm)
1	23.2	EC36	PCA	15	960
2	18.8	EL29	PCA	21	1530
3	14.3	EL31	PCA	26	1990
4	9.6	AA54	316	30	1780
5	4.6	EF5	PCA	32	2540
6	0	TEM		33	1980(316)
7	4.6	TE16	JPCA	32	2440
8	9.6	TE17	JPCA	30	2240
9	14.3	TE18	JPCA	26	1910
10	18.8	TE19	JPCA	21	1480
11	23.2	TE20	JPCA	15	920

Measured damage levels and helium concentrations for JP 8

Position	Distance from Reactor Midplane (cm)	Specimen	Alloy	Damage Level (dpa)	Helium Concentration (appm)
1	23.2	EL26	PCA	25	1880
2	18.8	EL26	PCA	36	2750
3	14.3	EL25	PCA	44	3430
4	9.6	EC163	PCA	50	3940
5	4.6	AA53	316	54	3250
6	0	TEM		55	3310(316)
7	4.6	TE21	JPCA	54	4100
8	9.6	TE22	JPCA	50	3790
9	14.3	TB12	JPCA	44	3300
10	18.8	TE23	JPCA	36	2640
11	23.2	TE24	JPCA	25	1810

Dosimetry of Phase I Capsules

Experiment	Status	Ref.
JP-1	Complete	ADIP DOE/ER-0045/17, p. 17
JP-2	Complete	FRM DOE/ER-0313/2, p. 33
JP-3	Complete	ADIP DOE/ER-0045/17, p. 17
JP-4	Complete	FRM DOE/ER-0313/3, p. 30
JP-5	Complete	FRM DOE/ER-0313/3, p. 30
JP-6	Complete	FRM DOE/ER-0313/2, p. 33
JP-7	Complete	FRM DOE/ER-0313/2, p. 33
JP-8	Complete	FRM DOE/ER-0313/3, p. 30
ORR-MFE-6J		
60°C	In progress	
200°C	Dosimeters at ORNL	
ORR-MFE-7J		
330°C	In progress	ANL-CMTI-9728, p. I-1
400°C	In progress	ANL-CMTI-9728, p. I-1

LOW-TEMPERATURE IRRADIATION CREEP DATA FROM SPECTRALLY TAILORED EXPERIMENTS

M. L. Grossbeck, L. K. Mansur, and M. P. Tanaka

ABSTRACT

The ORR-MFE-6J and -7J experiments addressed low temperature relevant to near-term fusion devices such as the ITER. The temperature range of 60 to 400°C was investigated, and a damage level of 8 dpa was achieved. Of particular interest was the irradiation creep behavior observed at 60°C. In fact, any irradiation creep at all was somewhat unexpected. In fact, higher creep deformations were observed at 60°C than at 330 and 400°C. Although other alloys were irradiated and exhibited similar behavior, data from PCA, JPCA, and two heats of AISI 316 stainless steel have been analyzed and reported.

Tubes pressurized to stress levels of 50 to 400 MPa were irradiated in the ORR with the spectrum tailored to achieve a He:dpa value of 12 appm/dpa in AISI 316 stainless steel. Irradiation creep rates of 2.2 to 14 × 10^{-6}/MPa-dpa were observed at 60°C. At 330 and 400°C, irradiation creep rates of 1.3 to 3.5 × 10^{-6} were observed, similar to those found previously in ORR-MFE-4. The low-temperature irradiation creep was interpreted in terms of a new model for irradiation creep based on transient climb-enabled glide. Transient conditions where interstitials can diffuse to dislocations but vacancies are frozen persist for about 100 years at 60°C. The result is very high rates of creep because the vacancies cannot cancel the climb produced by the interstitials.

These results are especially important in the design of experimental fusion reactors where temperatures below 100°C are being considered for the operation of high-flux components.

The 200°C irradiation vehicle has been disassembled and the pressurized tubes will be profiled in the near future. This is an important measurement since theory predicts perhaps an even higher creep rate at 200°C than at 60°C.

ORNL WSZ-9920

IRRADIATION CREEP IN AUSTENITIC ALLOYS AT 60 – 400 °C WITH A FUSION REACTOR He/dpa RATIO

M. L. GROSSBECK
M. P. TANAKA
L. K. MANSUR

US/JAPAN PROGRAM REVIEW

MARCH 1989

ORNL WSZ-6184

PURPOSE:

TO EVALUATE IRRADIATION CREEP IN CANDIDATE FUSION REACTOR MATERIALS AT LOW IRRADIATION TEMPERATURES IN A NEUTRON SPECTRUM PRODUCING A He/dpa RATIO OF ABOUT 12

ORNL-DWG 88Z-11558

EXPERIMENTAL CONDITIONS

PRESSURIZED TUBES

1 x 0.180 in.
He GAS
50 - 400 MPa

OAK RIDGE RESEARCH REACTOR

60°C

WATER ENVIRONMENT
7 dpa

330, 400°C

Nak ENVIRONMENT
8 dpa

MEASURED USING A NON-CONTACTING LASER PROFILOMETER WITH A PRECISION OF ± 250nm

ORNL-DWG 88Z-11283

THE NEUTRON SPECTRUM WAS TAILORED TO ACHIEVE THE FUSION REACTOR He/dpa RATIO

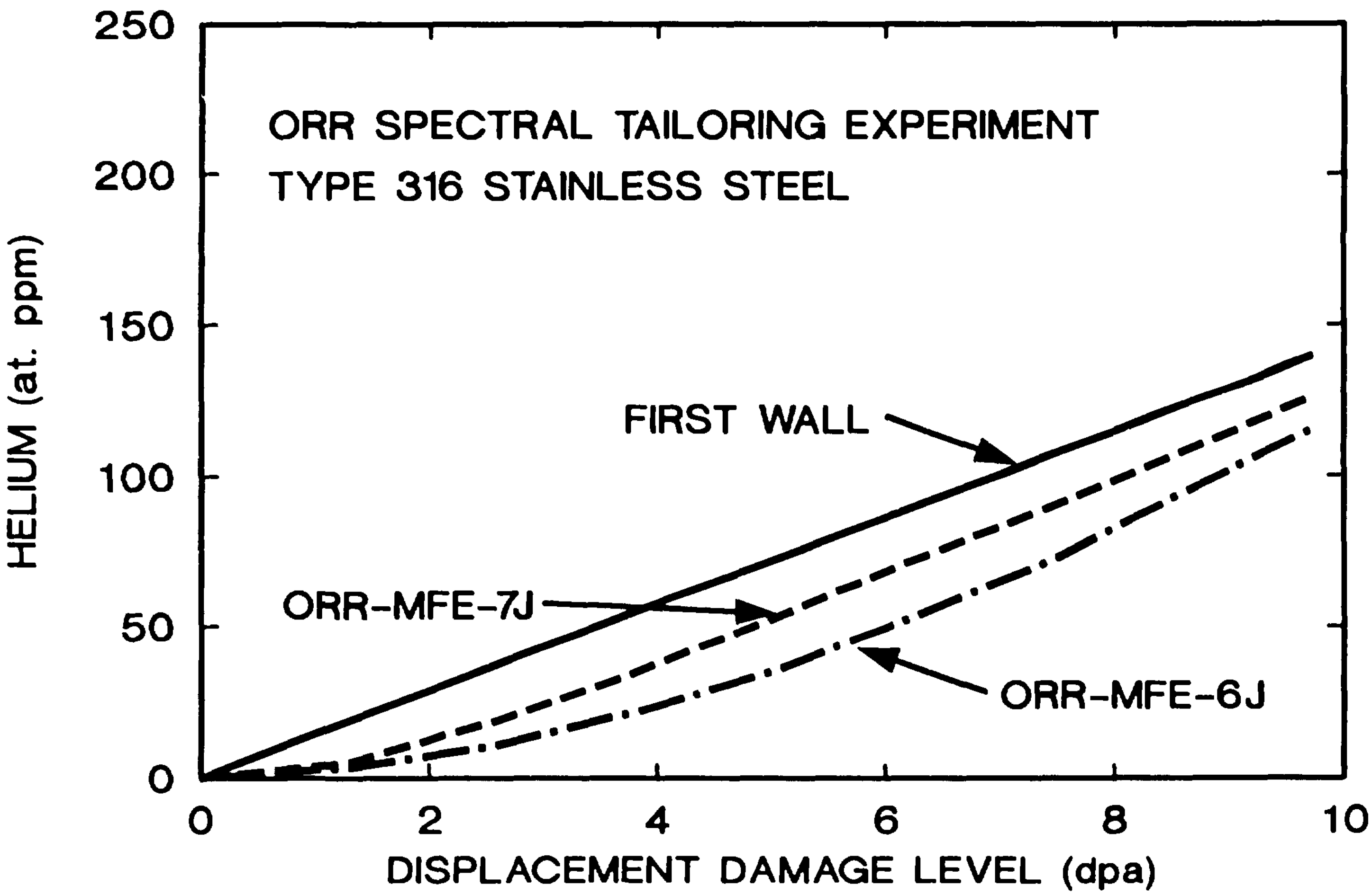

ORNL-DWG 88Z-11669

ALLOYS STUDIED

PCA 25% CW   Fe - 16Ni - 14Cr - 2Mn + 2Mo - .25Ti

JPCA ANNEALED

316 20 % CW

316 ANNEALED

ONRL-DWG 88Z-11284

AT 60° C, IRRADIATION CREEP WAS FOUND TO BE EQUAL TO OR GREATER THAN THAT AT 300–400 °C

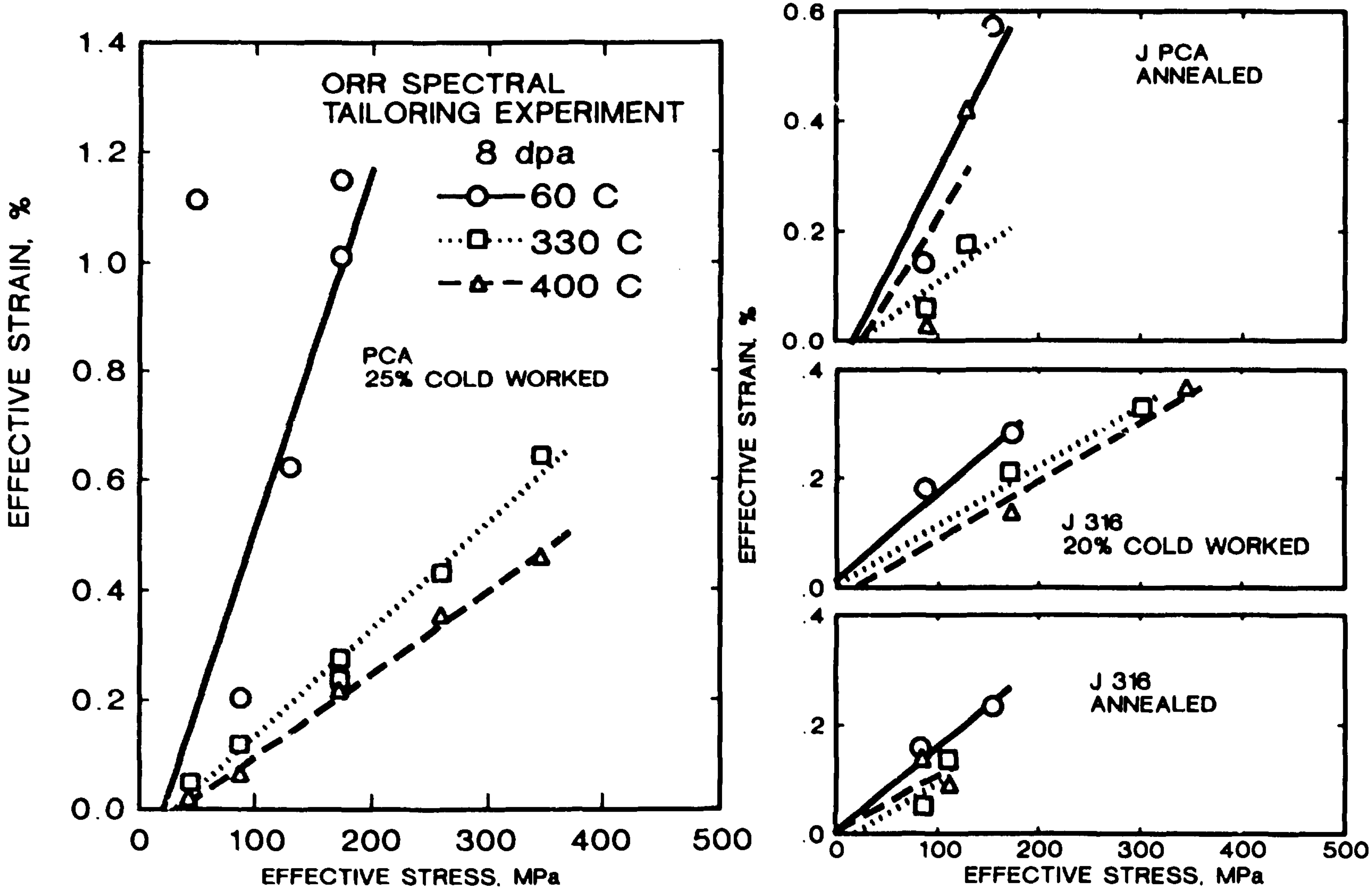

ORNL-DWG 88Z-11560

LOOK TO THE RATE EQUATIONS FOR POINT DEFECTS TO EXPLAIN TEMPERATURE DEPENDENCE

$$\frac{\partial C_i}{\partial t} = G - RC_iC_v - K_iC_i$$

$$\frac{\partial C_v}{\partial t} = G - RC_iC_v - K_vC_v$$

ASSUME STEADY STATE AND ONE TYPE OF SINK

$$O = G - RC_iC_v - K_iC_i$$

$$O = G - RC_iC_v - K_vC_v$$

$$Z_vC_vD_v = Z_iC_iD_i$$

CAN SOLVE FOR C_i AND C_v

ORNL-DWG 88Z-11281

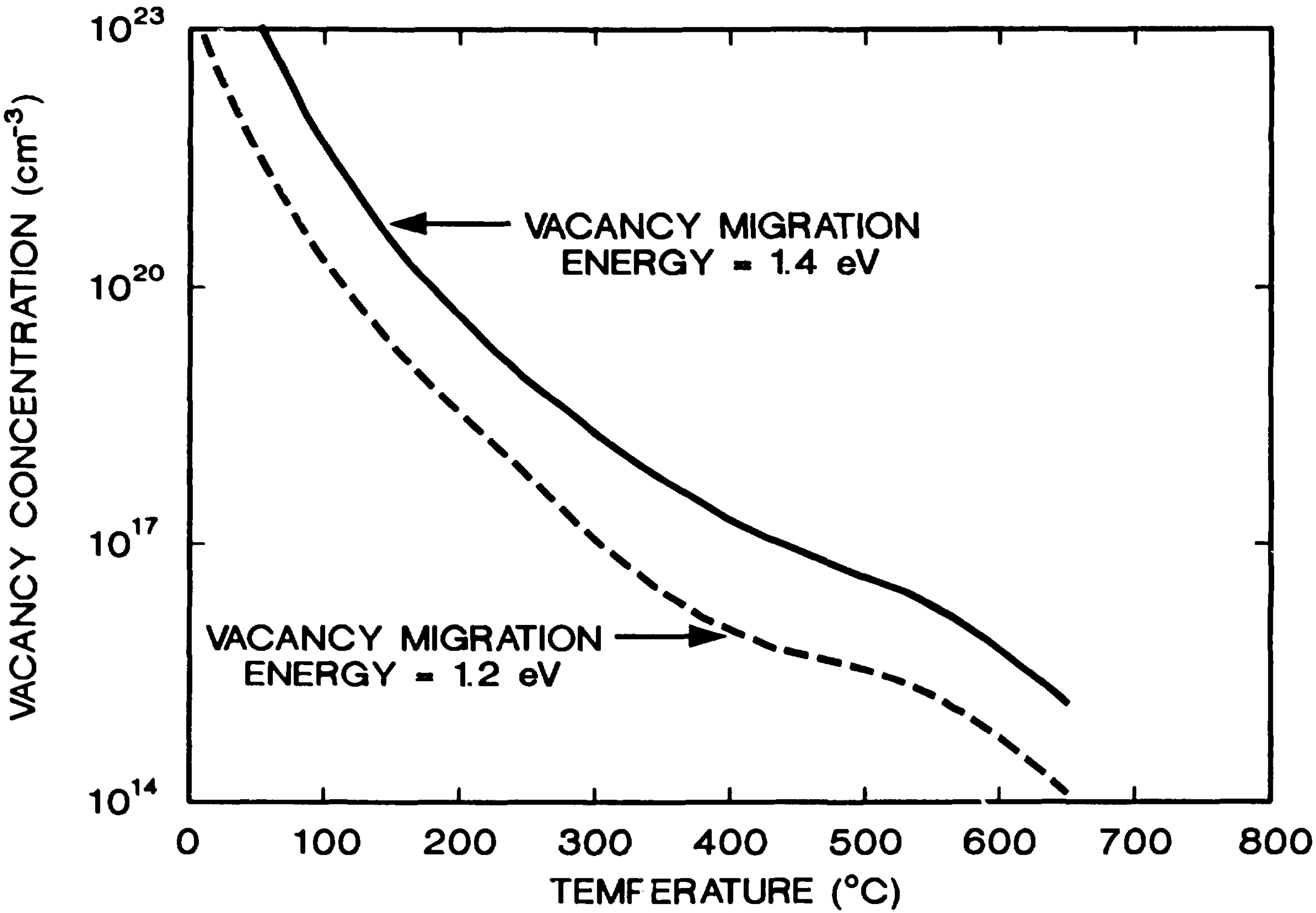

ORNL-DWG 88Z-11280

THE TEMPERATURE DEPENDENCE OF INTERSTITIAL CONCENTRATION DOES NOT PREDICT LOW TEMPERATURE IRRADIATION CREEP

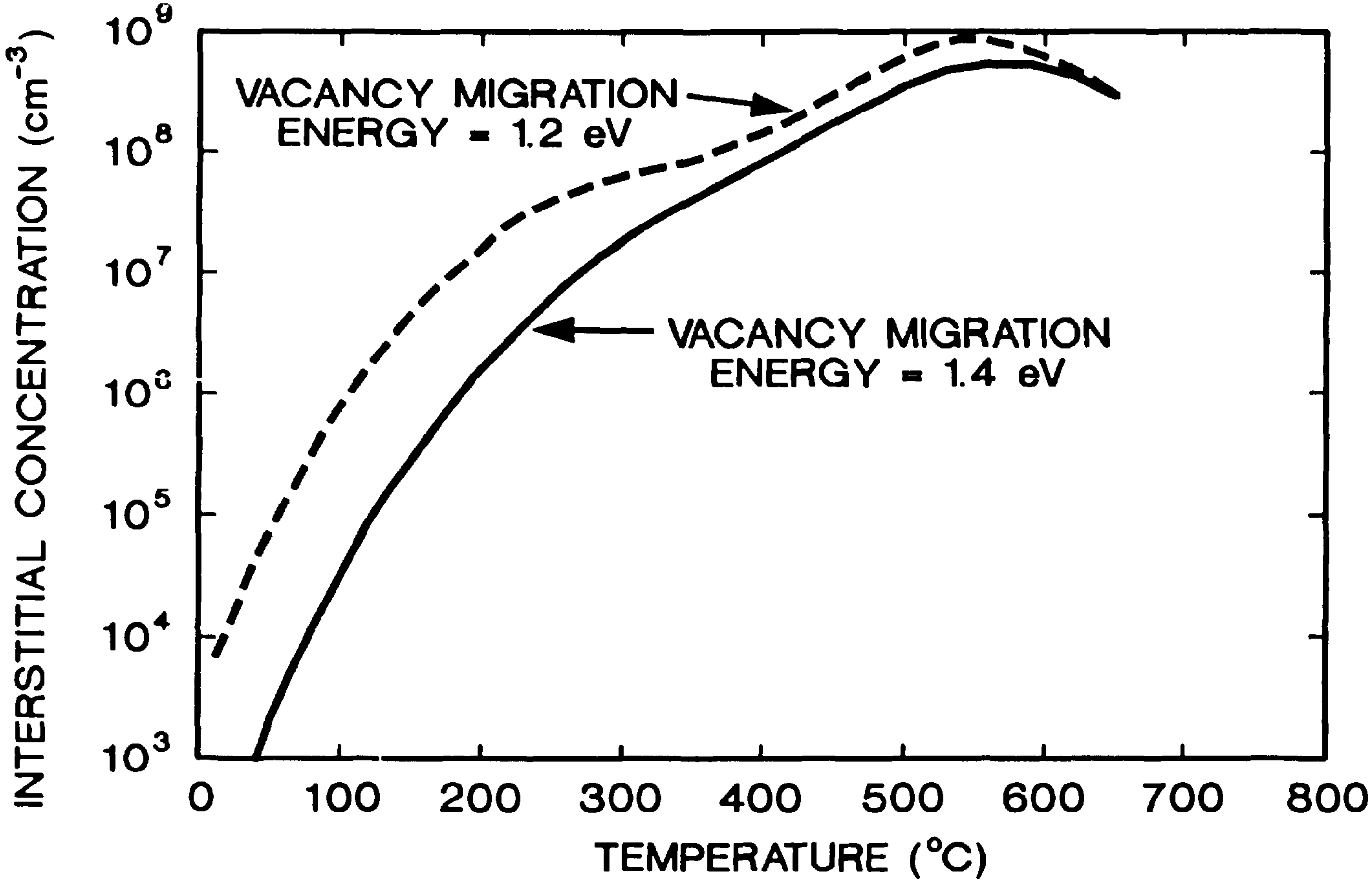

ORNL-DWG 88Z-11661

$$\dot{E} = \frac{2}{9}\,\Omega\, L\, D_i C_i \Delta Z_i$$ SIPA

$$\dot{E} = \frac{4}{9}\,\frac{\in}{b}\,(\pi L)^{1/2}\,\Omega\, D_i C_i \Delta Z_i$$ CLIMB-ENABLED GLIDE

EXPRESSIONS FOR MICROSTRUCTURAL PARAMETERS WERE DEVELOPED FROM EXPERIMENTAL DATA IN LITERATURE

MAZIASZ
BRAGER & STRAALSUND
STOLLER

ORNL-DWG 88Z-11282

THE SIPA MECHANISM PREDICTS THE TEMPERATURE INDEPENDENCE OBSERVED FROM 300 TO 600 °C

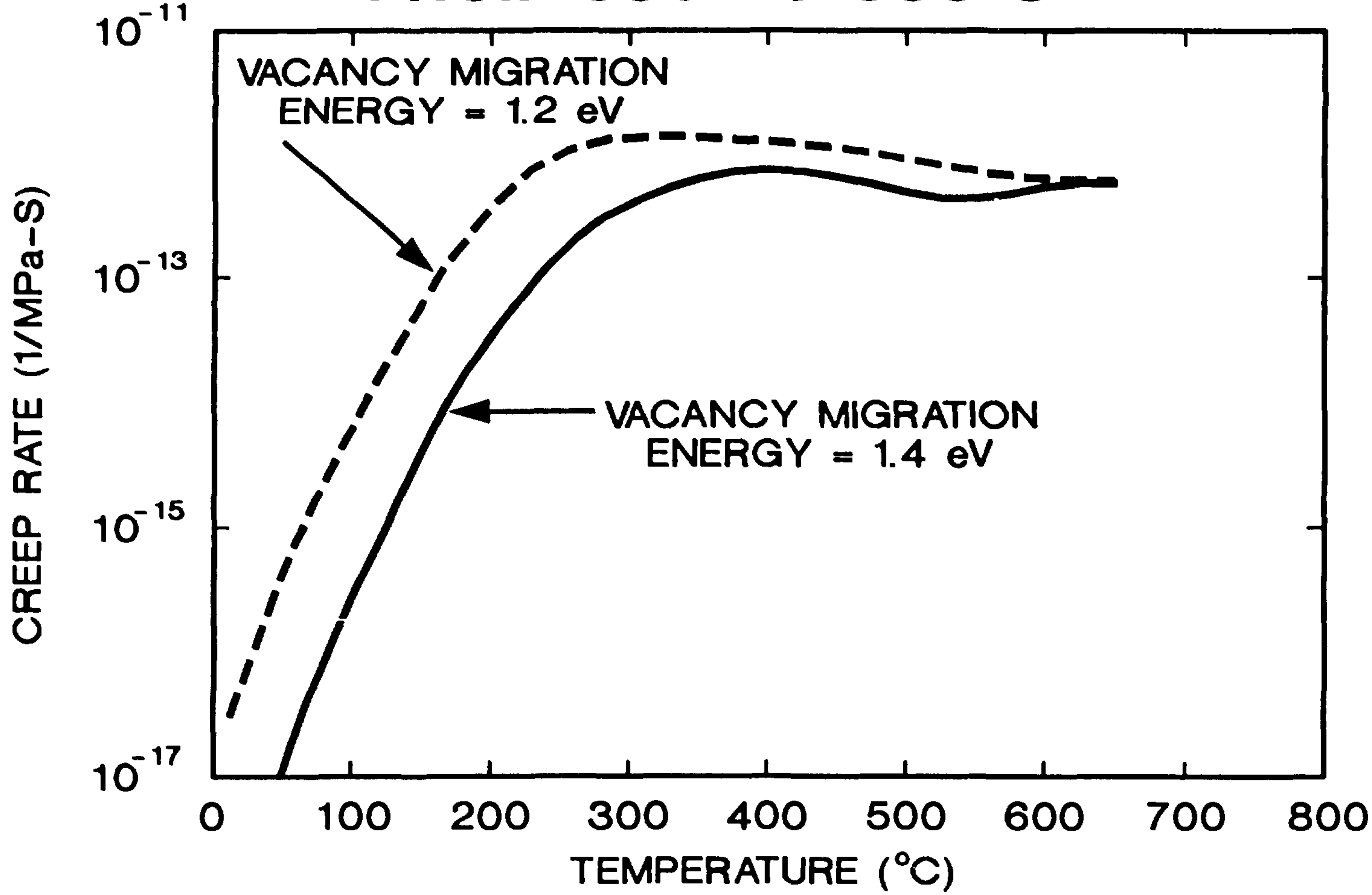

ORNL-DWG 88Z-11564

SINCE THE VACANCIES ARE NOT MOBILE, THEY DO NOT CANCEL CLIMB BY INTERSTITIALS AT LOW TEMPERATURES SO DISLOCATIONS IN ANY DIRECTION WITH RESPECT TO THE STRESS CAN CLIMB THEN PRODUCE CREEP BY GLIDE.

$$\frac{E_{c-g}}{\sigma} = \frac{(\pi L)^{1/2}}{E} \frac{\Omega}{bL} \quad \mathrm{Ni}$$

ORNL-DWG 88Z-11563

AT LOW TEMPERATURES, HIGH INTERSTITIAL CONCENTRATIONS CAN PERSIST FOR SIGNIFICANT TIMES

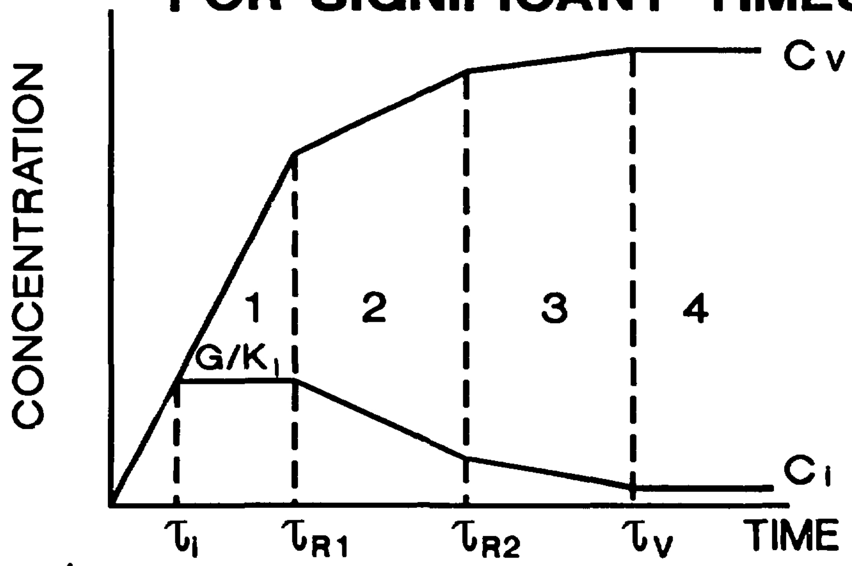

$\tau_i = \dfrac{1}{k_i}$ INTERSTITIALS ABSORBED BY SINKS

$\tau_{R1} = \dfrac{\delta_1 k_i}{RG}$ INTERSTITIALS AND VACANCIES BEGIN TO RECOMBINE

$\tau_{R2} = \dfrac{\delta_2 k_i}{RG}$ RECOMBINATION DOMINANT LOSS MECHANISM

$\tau_V = \dfrac{1}{K_v}$ VACANCIES ABSORBED BY SINKS

ORNL-DWG 88Z-11562

CALCULATE NUMBER OF INTERSTITIALS LOST TO SINKS IN EACH INTERVAL OF THE TRANSIENT

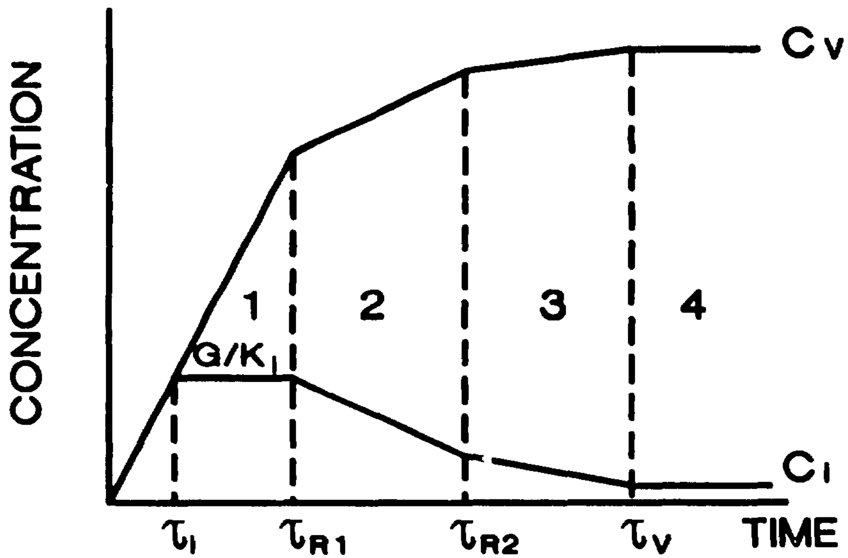

1. $N_1 = G\tau_{R1} - G/k_i$

2. $N_2 = fG(\tau_{R2} - \tau_{R1})$

3. $N_3 = C_i^{ss} D_i S_i (\tau_V - \tau_{R2})$

ORNL-DWG 89Z-6609

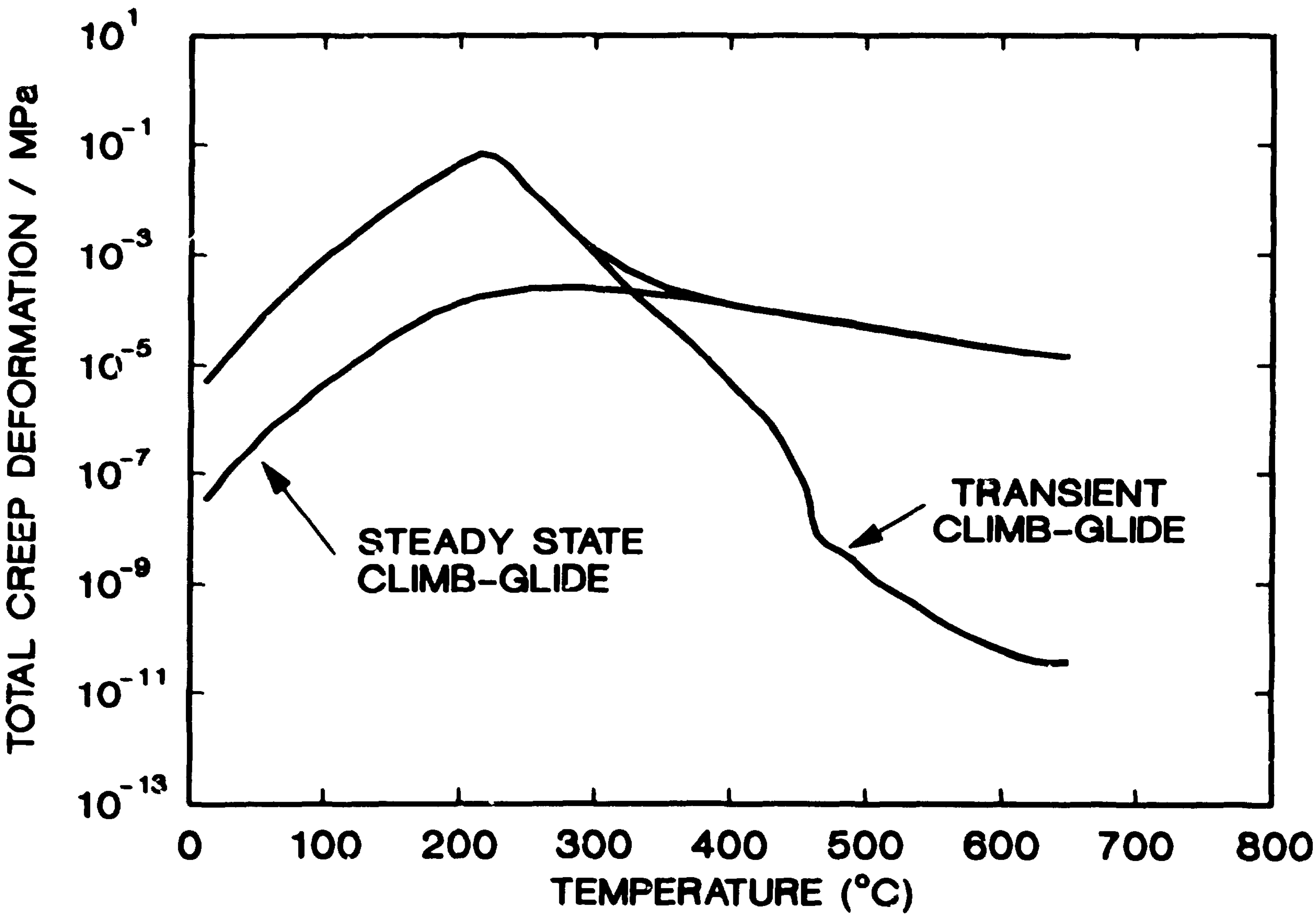

ORNL WSZ-6185

CONCLUSIONS

1. NO FIRM CONCLUSIONS CAN BE DRAWN AT 8 dpa, BUT THERE APPEARS TO BE IRRADIATION CREEP AT 60°C.

2. LOW TEMPERATURE IRRADIATION CREEP CAN BE EXPLAINED BY TRANSIENT INTERSTITIAL ABSORPTION, BUT NOT YET CALCULATED QUANTATIVELY.

3. IRRADIATION CREEP CAN ARREST CRACKS IN FUSION REACTOR COMPONENTS OR CAUSE UNDESIRABLE DEFORMATION UNDER PRIMARY LOADS. IT MUST BE ACCOUNTED FOR IN DESIGN.

STATUS OF PHASE II TARGET EXPERIMENTS

R. L. Senn

ABSTRACT

Eight U.S./Japan Phase II HFIR target capsules, JP-9 through -16, have been assembled and are ready for installation in the HFIR target region during the first full power cycle after restart.

The planned time period for completion of these capsules and estimated construction costs were extended over the course of the assembly period because of a number of design changes that were required for various reasons. These included readjustments of the matrix to accommodate more or less of certain types of specimens, misunderstandings regarding some material types, correction of an error in the thermal analysis, and confusion resulting from application of old drawings from previous work rather than those specifically made for this series. Some of these problems were probably exacerbated because we were assembling all eight capsules at one time (as opposed to one or two at a time as was done previously) and the resulting large number of specimens of various types to be handled and coordinated by the several responsible parties involved. These problems were ultimately resolved, however, and an "as-built" matrix of the final specimen arrangements that was satisfactory to all parties was published.

After completion of capsule assembly, a successful QA audit was performed by personnel from ORNL's Quality Department reviewing the materials of construction, parts, and application of the required assembly procedures.

Requests for official approval for irradiation of this series of experiments were made in June 1988. The Research Reactors Division and ORNL's Office of Operational Safety have subsequently approved installation and operation of the experiments.

US/JAPAN PHASE II
HFIR TARGET CAPSULES

STATUS
MARCH 17, 1989

- EIGHT PHASE II CAPSULES - JP-9 THROUGH JP-16 - ARE READY FOR INSTALLATION
  - FINAL ASSEMBLY COMPLETED FEBRUARY 3, 1989
  - SUCCESSFUL QA AUDIT COMPLETED FEBRUARY 10, 1989
  - APPROVAL FOR OPERATION OBTAINED FROM
    - RESEARCH REACTORS DIVISION
    - ORNL'S OFFICE OF OPERATIONAL SAFETY

ornl

US/JAPAN PHASE II
HFIR TARGET CAPSULES

PLANNED OPERATION

- INSTALL ALL EIGHT CAPSULES AT THE BEGINNING OF FIRST FULL POWER HFIR CYCLE
  - JP-10,-11,-13,-16 SCHEDULED FOR IRRADIATION TO 33 DPA
    - 1.5 CALENDAR YEARS - 18 FUEL CYCLES
  - JP-14 SCHEDULED FOR IRRADIATION TO 55 DPA
    - 2.5 CALENDAR YEARS - 30 FUEL CYCLES
  - JP-9,-12,-15 SCHEDULED FOR IRRADIATION TO 100 DPA
    - 4.5 CALENDAR YEARS - 54 FUEL CYCLES
- IRRADIATION TIME BASED ON REACTOR OPERATION AT 85 MW FOR 25 DAYS/CYCLE - 12 CYCLES/YEAR
  - 2125 MWD/CYCLE - 8.73 E-4 DPA/MWD

ornl

3-17-89

US/JAPAN PHASE II
HFIR TARGET CAPSULES

FINAL PHASE II EXPERIMENT MATRIX

- AN EXPERIMENT MATRIX AGREEABLE TO ALL PARTIES WAS DEVELOPED AND USED FOR FINAL DESIGN
  - THESE DATA WERE PRESENTED IN A SERIES OF TABLES DEFINING POSITION, TYPE AND DESIGN OPERATING TEMPERATURE FOR EACH SPECIMEN
    - TEST SPECIMENS OPERATE FROM 300 TO 600 C

      JP-9 WITH 2 TEM AND 9 TB

      JP-10,-11 EACH WITH 5 TEM, 6 T(2), 2 T(4), 2 FAT.

      JP-12 WITH 6 TEM, 4 TB

      JP-13 WITH 1 TEM, 8 T(2), 2 T(4) 4 FATIGUE

      JP-14 WITH 5 TEM, 3 T(2), 5 T(4), 2 SHEET

      JP-15 WITH 2 TEM, 8 TB

      JP-16 WITH 1 TEM, 8 T(2), 6 T(4), 2 TB

ornl

US/JAPAN PHASE II
HFIR TARGET CAPSULES

LESSONS LEARNED - DESIGN

- PROBLEMS ENCOUNTERED DURING EXPERIMENT DESIGN
  - LARGE NUMBER OF EXPERIMENTS AND CONSEQUENT VERY LARGE NUMBER OF SPECIMENS CONTRIBUTED TO COMPLEXITY
  - DESIGN REVISIONS AFTER PARTS ORDERED
    - CHANGES IN MATERIAL SPECIFICATIONS
    - PARTS MADE FROM PRELIMINARY DRAWINGS NOT COMPATIBLE WITH NEW DRAWINGS
    - MANY REVISIONS OF ORIGINAL THERMAL ANALYSIS WEF REQUIRED BY CHANGES OF SPECIMENS, MATERIALS, AND CORRECTION OF MATERIAL PROPERTIES USED

ornl

3-17-88

US/JAPAN PHASE II
HFIR TARGET CAPSULES

LESSONS LEARNED - ASSEMBLY

- PROBLEMS ENCOUNTERED DURING CAPSULE ASSEMBLY
  - DISASSEMBLY AND REASSEMBLY OF CERTAIN CAPSULES TO CHANGE REVISED PARTS
  - DISASSEMBLY AND REASSEMBLY OF CERTAIN TEM PACKETS TO ADD LATE ARRIVING SPECIMENS
  - DIFFICULTY OBTAINING SATISFACTORY WELDS

US/JAPAN PHASE II
HFIR TARGET CAPSULES

OPPORTUNITIES FOR NEXT SERIES

- DESIGN AND BUILD EXPERIMENTS IN SMALLER GROUPS
- REQUIRE MORE DESIGN REVIEW MEETINGS WITH ALL COGNIZANT PERSONNEL DURING COURSE OF EXPERIMENT DESIGN AND CONSTRUCTION
  - REVIEW SPECIMEN AND CAPSULES MATERIALS AND OBTAIN AGREED-UPON MATERIAL SPECIFICATIONS AND PROPERTIES
  - REVIEW DRAWINGS TO ENSURE SPECIMENS, MATERIALS, AND OTHER EXPERIMENT FEATURES MEET CUSTOMER'S REQUIREMENTS
- IMPROVE WELDING SITUATION
  - REPLACE 1100-6061 ALUMINUM WELDS WITH ALL 6061 MATERIAL, IF POSSIBLE
  - DEVELOP BETTER WELDING TECHNIQUES - LASER? - OTHER??

ornl

3-17-88

US/JAPAN PHASE II
HFIR TARGET CAPSULES

SUMMARY

- EIGHT US/JAPAN PHASE II HFIR TARGET CAPSULES ARE READY FOR INSTALLATION IN THE HFIR
- THESE CAPSULES CONTAIN 108 SPECIMEN HOLDERS OF VARIOUS TYPES AND DIMENSIONS DESIGNED TO OPERATE AT 300 TO 600C
  - 27 TEM PACKETS (ABOUT 120 TEM DISKS/PACKET)
  - 23 TENSILE BAR SPECIMENS
  - 31 T(2) SPEC. HOLDERS (EA. WITH 2 SS-3 SPECIMENS)
  - 17 T(4) SPEC. HOLDERS (EA. WITH 4 SS-3 SPECIMENS)
  - 8 FATIGUE SPECIMENS
  - 2 WELDED SHEET SPECIMENS
- SUCCESSFUL QA AUDIT COMPLETED
- IRRADIATION BEGINS WITH FIRST FULL POWER CYCLE AND CONTINUES FOR UP TO 4.5 YEARS

ornl

ISOTOPICALLY TAILORED ALLOYS FOR THE HFIR PHASE II TARGET EXPERIMENTS

P. J. Maziasz

ABSTRACT

The Phase II HFIR target experiments include TEM disks of several unique sets of alloys whose isotopic nickel composition has been deliberately altered and tailored to control the He:dpa ratio during irradiation. Helium is produced by the two-step reaction of thermal neutrons with nickel to produce helium and iron — $^{58}Ni(n,\gamma)^{59}Ni \rightarrow$ $^{59}Ni(n,\alpha)^{56}Fe$. This is the first time isotopic tailoring experiments on steels has been attempted. Very small melts (30 g) were made of most alloys with very high quality, and with accurate and precise compositional control.

Natural nickel with about 68 at. % ^{58}Ni and 26% ^{60}Ni was used as a baseline for the highest He:dpa ratio of 70 appm/dpa, to link these experiments with previous HFIR experiments. Alloys with the same chemical composition were then doped with ^{60}Ni, which produces no helium, to decrease the He:dpa ratios to 12, 4, and <1 appm/dpa. Special alloys were prepared by Dave Gelles at Pacific Northwest Laboratories (PNL) to obtain 12 appm/dpa using radioactive ^{59}Ni to produce helium linearly with dose at the beginning of the irradiation, for comparison with the early nonlinear transient period obtained from natural nickel. Twelve small heats of austenitic stainless steel were produced with two to four different He:dpa ratios and 20% cold-worked and/or solution-annealed pretreatments. Larger heats of martensitic HT-9, Japanese F-82H doped with ^{59}Ni + ^{60}Ni, ^{59}Ni, or natural nickel to produce He:dpa ratios of 12 or less without having to add more than 2 wt % to these alloys. Dave Gelles also produced a series of higher purity 12Cr steels with controlled alloying additions to complement the studies of HT-9. The austenitic alloys include type 316, some minor compositional variants of optimized PCA, and some Fe–15Cr–15Ni and Fe–15Cr–35Ni alloys with and without titanium additions.

These alloys will produce unambiguous, single variable experiments on the effects of He:dpa ratio on microstructure and swelling of alloys irradiated at 300 to 600°C to 90 to 100 dpa. At 300°C, they will also provide the first helium-free data on microstructural evolution.

ISOTOPICALLY TAILORED NICKEL-BEARING ALLOYS

- *HELIUM GENERATION IN NICKEL-BEARING ALLOYS*

  $^{58}Ni(n,\gamma)^{59}Ni(n,\alpha)^{56}Fe$

- *NATURAL ISOTOPIC COMPOSITION, %*

^{58}Ni	^{60}Ni	^{61}Ni	^{62}Ni	^{64}Ni
68.3	26.1	1.1	3.6	0.9

- *IRRADIATION OF 316 IN HFIR AND FFTF PRODUCES He:dpa RATIOS OF ~70 AND ~0.2*

- *ISOTOPICALLY TAILORED ALLOYS*
  - PREPARE MASTER COMPOSITIONS (450-g HEATS) WITHOUT NICKEL BUT WITH CORRECT IMPURITY LEVELS
  - RE-MELT 30-g QUANTITIES WITH VARIOUS CONCENTRATIONS OF ^{58}Ni, ^{60}Ni, AND NATURAL NICKEL
  - ^{59}Ni ADDED TO SOME ALLOYS TO INVESTIGATE TRANSIENT EFFECTS

ISOTOPICALLY TAILORED EXPERIMENTS WITH AUSTENITIC STEELS

- *ALLOYS*

  AISI 316, PCA

  Fe-15Cr-15Ni   Fe-15Cr-15Ni-Ti

  Fe-15Cr-35Ni   Fe-15Cr-35Ni-Ti

- *He:dpa RATIOS*

  <1, 4, 12, 70

- *OBJECTIVES*

  - EFFECT OF He:dpa RATIO ON CAVITY DENSITY, MICROSTRUCTURAL DEVELOPMENT, DOSE DEPENDENCE OF SWELLING

  - DEPENDENCE OF CRITICAL CAVITY SIZE ON NICKEL CONCENTRATION; DETERMINATION OF CRITICAL GAS CONCENTRATION FOR BUBBLE-VOID CONVERSION

  - DETERMINE EFFECT OF HELIUM TRANSIENT USING ^{59}Ni

ISOTOPICALLY TAILORED EXPERIMENTS WITH AUSTENITIC STEELS

- *ALLOYS*
  - AISI 316, PCA (COLD-WORKED AND ANNEALED)
  - AUSTENITICS WITH DISPERSIONS OF MIXED CARBIDES AND PHOSPHIDES
- *He:dpa RATIOS*

  <1, 4, 12, 70
- *OBJECTIVES*
  - SWELLING RESISTANCE OF AUSTENITICS AT 100 dpa; UTILIZE DATA FOR FUSION SWELLING EQUATIONS
- 316 COMPOSITIONS:

Cr	Ni^n	Ni^*	^{60}Ni	C	Si	Mo	Mn	He:dpa Ratio
17.5	0.0	0.0	13.7	0.05	0.53	2.3	1.7	<1
17.5	0.7	0.0	13.0	0.05	0.53	2.3	1.7	4
17.5	2.06	0.0	11.63	0.05	0.53	2.3	1.7	12
17.5	0.0	2.06	11.63	0.05	0.53	2.3	1.7	12
17.5	13.7	0.0	0.0	0.05	0.53	2.3	1.7	70

ISOTOPICALLY TAILORED EXPERIMENTS WITH FERRITIC ALLOY HT-9

- *OBJECTIVE*

  DETERMINE THE EFFECTS OF HELIUM GENERATION RATE ON MICROSTRUCTURAL DEVELOPMENT, SWELLING BEHAVIOR, AND MECHANICAL BEHAVIOR

- COMPOSITIONS:

	Cr	Ni^n	Ni^*	^{60}Ni	^{58}Ni	C	Si	Mo	V	W	He:dpa Ratio
1. HT-9	12.0	0.5	--	--	--	0.2	0.18	1.0	0.3	0.5	~3
2. ^{58}Ni-Doped	12.0	--	--	--	1.4	0.2	0.18	1.0	0.3	0.5	12
3. ^{60}Ni Control for (2)	12.0	--	--	1.4	--	0.2	0.18	1.0	0.3	0.5	~1
4. ^{60}Ni Control for (1)	12.0	--	--	0.5	--	0.2	0.18	1.0	0.3	0.5	<<1
5. No Transient	12.0	--	2.0	--	--	0.2	0.18	1.0	0.3	0.5	12
6. Control for (5)	12.0	2.0	--	--	--	0.2	0.18	1.0	0.3	0.5	12

ORNL-DWG 86-7521

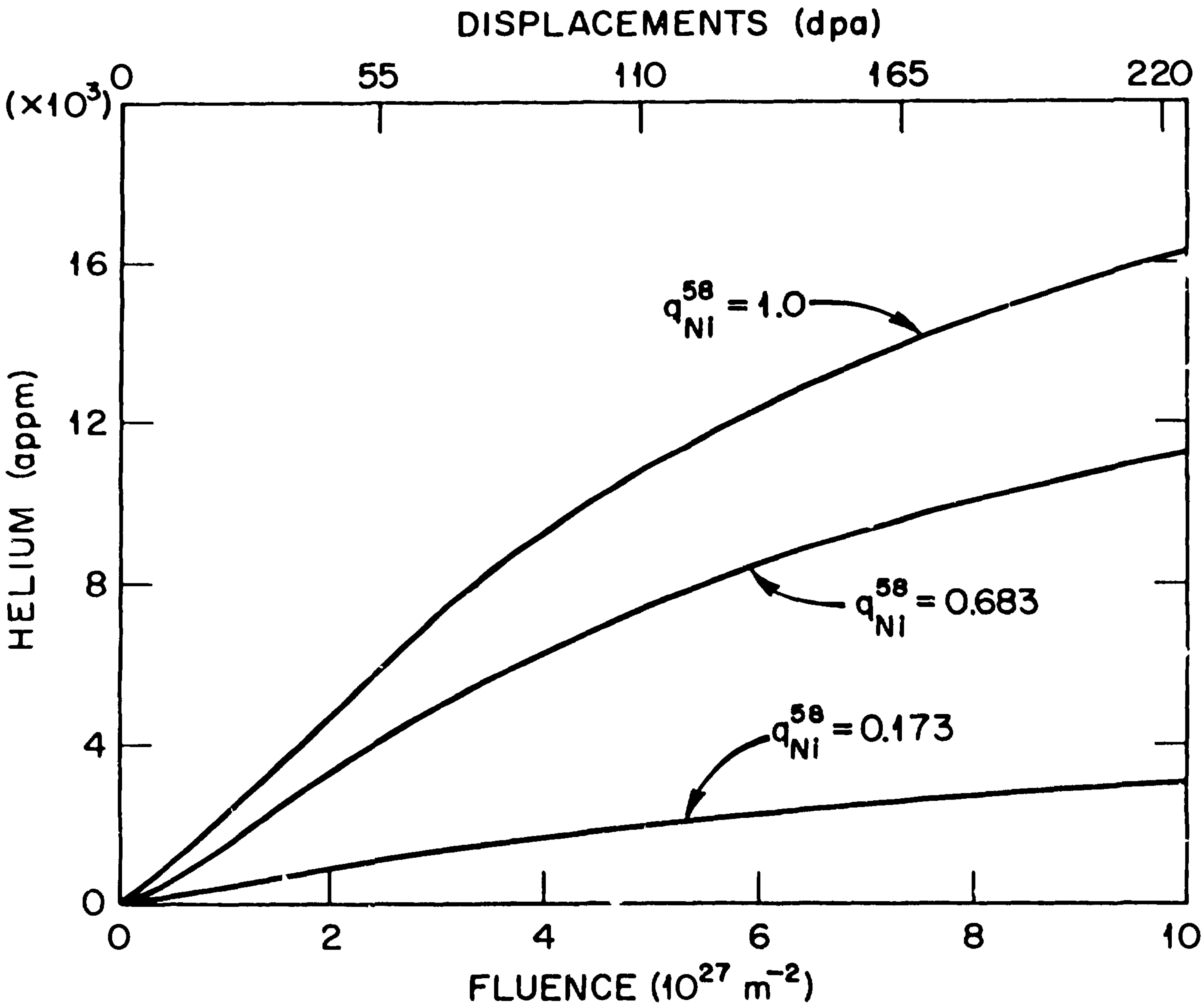
DISPLACEMENTS (dpa)
0
55
110
165
220
(×10³)
16
12
8
4
0
HELIUM (appm)
q_{Ni}^{58} = 1.0
q_{Ni}^{58} = 0.683
q_{Ni}^{58} = 0.173
0
2
4
6
8
10
FLUENCE (10^{27} m^{-2})

HIT-1 COMPOSITIONS (wt %)

Alloy Designation	Cr	Ni^N	Ni*	**Ni	**Ni	Ti	C	O	N	Si	P
B12-1	14.0			15.0		0.2	0.04		0.01	0.8	0.05
B12-12	14.0	2.10		12.9		0.2	0.04		0.01	0.8	0.05
B12-70	14.0	15.0				0.2	0.04		0.01	0.8	0.05
1535-1	15.0			35.0							
1535-4	15.0	0.35		34.65							
1535-12	15.0	1.75		33.25							
1535-130	15.0	35.0									

HIT-2 COMPOSITIONS (wt %)

Alloy Designation	Cr	Ni^N	Ni*	**Ni	**Ni	Ti	C	O	N	Si	Nb	V	W	Mo	Mn	P
316-1	17.5	0.0		13.7			0.05			0.53				2.3	1.7	
316-4	17.5	0.7		13.0			0.05			0.53				2.3	1.7	
316-12	17.5	2.06		11.63			0.05			0.53				2.3	1.7	
316-70	17.5	13.7		0.0			0.05			0.53				2.3	1.7	
316-12NS	17.5		2.06	11.63			0.05			0.53				2.2	1.7	
316-12NSC	17.5	2.06		11.63			0.05			0.53				2.2	1.7	
PCA-1	14.0	0.0		16.0		0.25	0.05		0.01	0.40				2.3	1.8	0.01
PCA-12	14.0	2.08		13.92		0.25	0.05		0.01	0.40				2.3	1.8	0.01
PCA-70	14.0	16.0		0.0		0.25	0.05		0.01	0.40				2.3	1.8	0.01

HIT-3 COMPOSITIONS (wt %)

Alloy Designation	Cr	Ni^N	Ni^*	^{60}Ni	^{58}Ni	Ti	C	O	N	Si	Nb	V	W	Mo	Mn	P	B
1416 CP1-1	14.0			16.0		0.3	0.08		0.02	0.4	0.10	0.50		2.5	2.0	0.07	0.008
1416 CP1-12	14.0	2.08		13.92		0.3	0.08		0.02	0.4	0.10	0.50		2.5	2.0	0.07	0.008
1416 CP2-1	14.0			16.0		0.3	0.08		0.02	0.2	0.10	0.50		2.5	2.0	0.07	0.008
1416 CP2-12	14.0	2.08		13.92		0.3	0.08		0.02	0.2	0.10	0.50		2.5	2.0	0.07	0.008
1416 CP3-1	14.0			16.0		0.3	0.08		0.02	0.4	0.10	0.10		2.5	2.0	0.07	0.008
1416 CP3-12	14.0	2.08		13.92		0.3	0.08		0.02	0.4	0.10	0.10		2.5	2.0	0.07	0.008
1416 CP4-1	14.0			16.0		0.3	0.10		0.02	0.4	0.10	0.50		2.5	2.0	0.07	0.008
1416 CP4-12	14.0	2.08		13.92		0.3	0.10		0.02	0.4	0.10	0.50		2.5	2.0	0.07	0.008
1416 CP5-1	14.0			16.0		0.3	0.08		0.02	0.4	0.10	0.50		2.5	2.0	0.04	0.008
1416 CP5-12	14.0	2.08		13.92		0.3	0.08		0.02	0.4	0.10	0.50		2.5	2.0	0.04	0.008
RSP1-1	13			15		0.2	0.05			0.4		0.2		1.5	1.5	0.07	
RSP1-12	13	2.1		12.9		0.2	.05			0.4		0.2		1.5	1.5	0.07	
RSP2-1	14			15		0.3	0.05			0.5				1.5	1.5	0.07	
RSP2-12	14	2.1		12.9		0.3	0.05			0.5				1.5	1.5	0.07	

HIT-4 COMPOSITIONS (wt %)

Alloy Designation	Fe	Cr	Ni^N	Ni^*	^{60}Ni	^{58}Ni	Ti	C	O	N	Si	Nb	V	W	Mo	Mn	P Max	S Max
HT-9-3		12.0	0.5					0.20	0.007	0.02	0.18	0.01	0.3	0.5	1.0	0.5	0.01	0.004
HT-9-12		12.0				1.4		0.20	0.007	0.02	0.18	0.01	0.3	0.5	1.0	0.5	0.01	0.004
HT-9-C12		12.0			1.4			0.20	0.007	0.02	0.18	0.01	0.3	0.5	1.0	0.5	0.01	0.004
HT-9-C3		12.0			0.5			0.20	0.087	0.02	0.18	0.01	0.3	0.5	1.0	0.5	0.01	0.004
HT-9-NS		12.0		2.0				0.20	0.007	0.02	0.18	0.01	0.3	0.5	1.0	0.5	0.01	0.004
HT-9 CNS		12.0	2.0					0.20	0.007	0.02	0.18	0.01	0.3	0.5	1.0	0.5	0.01	0.004

HIT-6 COMPOSITIONS (wt %)

Alloy Designation	Fe	Cr	Ni^N	Ni^*	^{60}Ni	^{58}Ni	C	Si	Mn	Mo	V	W
E62		12.0										
R168		12.0			1.5							
R169		12.0		1.5								
R170		12.0	1.5									
E95		12.0					0.1					
R171		12.0			1.5		0.1					
R172		12.0		1.5			0.1					
R173		12.0	1.5				0.1					
R174		12.0					0.1				0.3	1.0
R175		12.0			1.5		0.1				0.3	1.0
R176		12.0		1.5			0.1				0.3	1.0
R177		12.0	1.5				0.1				0.3	1.0

HIT-7 COMPOSITIONS (wt %)
(JAPAN)

Alloy Designation	Fe	Cr	Ni^n	Ni^*	^{60}Ni	^{58}Ni	Ti	C	O	N	Si	Nb	V	W	Mo	Mn	Ta
J1-12		8.0				1.4		0.1			0.2		0.2	2.0		0.5	0.04
J1-1		8.0			1.4			0.1			0.2		0.2	2.0		0.5	0.04
316 SAR-1	Use Heat 316-1																
316 SAR-12	Use Heat 316-12																

DOSE-TEMPERATURE TEM DISK MATRIX FOR ISOTOPICALLY TAILORED ALLOYS IN HFIR PHASE-II EXPERIMENTS

	TEMPERATURE, °C			
dpa	300	400	500	600
34	--	JP10 [JP16]	JP11 [JP13]	--
55	--	--	JP14	--
100	JP12	JP12	JP15	JP15

[ ] indicates high swelling variants

ALLOY CHEMISTRY – 30-g MELTS

1416 CP2

	Nominal	Measured
Cr	14	14.00
Ni	16	15.94
Mo	2.5	2.43
Mn	2.0	1.76
Ti	0.3	0.35
V	0.5	0.53
Nb	0.2	0.11
C	0.08	0.067
P	0.07	0.08
B	0.008	0.005
Si	0.2	0.19

DEVELOPMENT OF THE ITER DESIGN DATA BASE

M. L. Grossbeck

ABSTRACT

The ITER Design Data Base is a multi-national effort to provide a common source of data for the ITER designers in order that the merits of different designs may be compared. The data base effort is coordinated by Dr. J. W. Davis at McDonnell Douglas Astronautics. The data on austenitic stainless steels are being assembled by M. L. Grossbeck at ORNL. Data have been provided by scientists in participating countries on tensile properties and, thus far, tensile property equations have been submitted to the coordinator for evaluation.

Tensile data from the Oak Ridge Matrix (Fusion Implementing Agreement Annex II), the U.S./Japan collaboration, and from the available literature were reviewed. Type 316 stainless steel, in both cold-worked and annealed conditions, and PCA (both U.S. and Japanese heats) were included. Equations were developed for yield strength, uniform elongation, and total elongation. In many cases, one expression could be used for alloys and conditions; in others, separate equations had to be used. In all cases an attempt was made to provide a conservative expression rather than to have the best fit to the data. Especially in the case of strength, the value was rather insensitive to alloy composition.

The U.S./Japan program provided a major part of the data for this effort. The HFIR-irradiated materials provide what is believed to be a lower limit in ductility because of the high levels of helium. As data become available from the spectral tailoring experiments, they will be incorporated into the data base and the equations changed as necessary. These data will be of especially high value because of the correct He:dpa value and because of the low temperatures investigated in these experiments.

ORGANIZATION

STEERING COMMITTEE

S. IWATA, JAPAN
S. NAKAJIMA, JAPAN
J. NIHOUL, EC
D. SMITH, US

HANDBOOK/DATA BASE COORDINATOR

J.W. DAVIS

TASK GROUPS

STRUCTURAL MATERIALS -- M.L. GROSSBECK
BLANKET MATERIALS -- H. WATANABE
PFC MATERIALS -- K. KOIZLIK

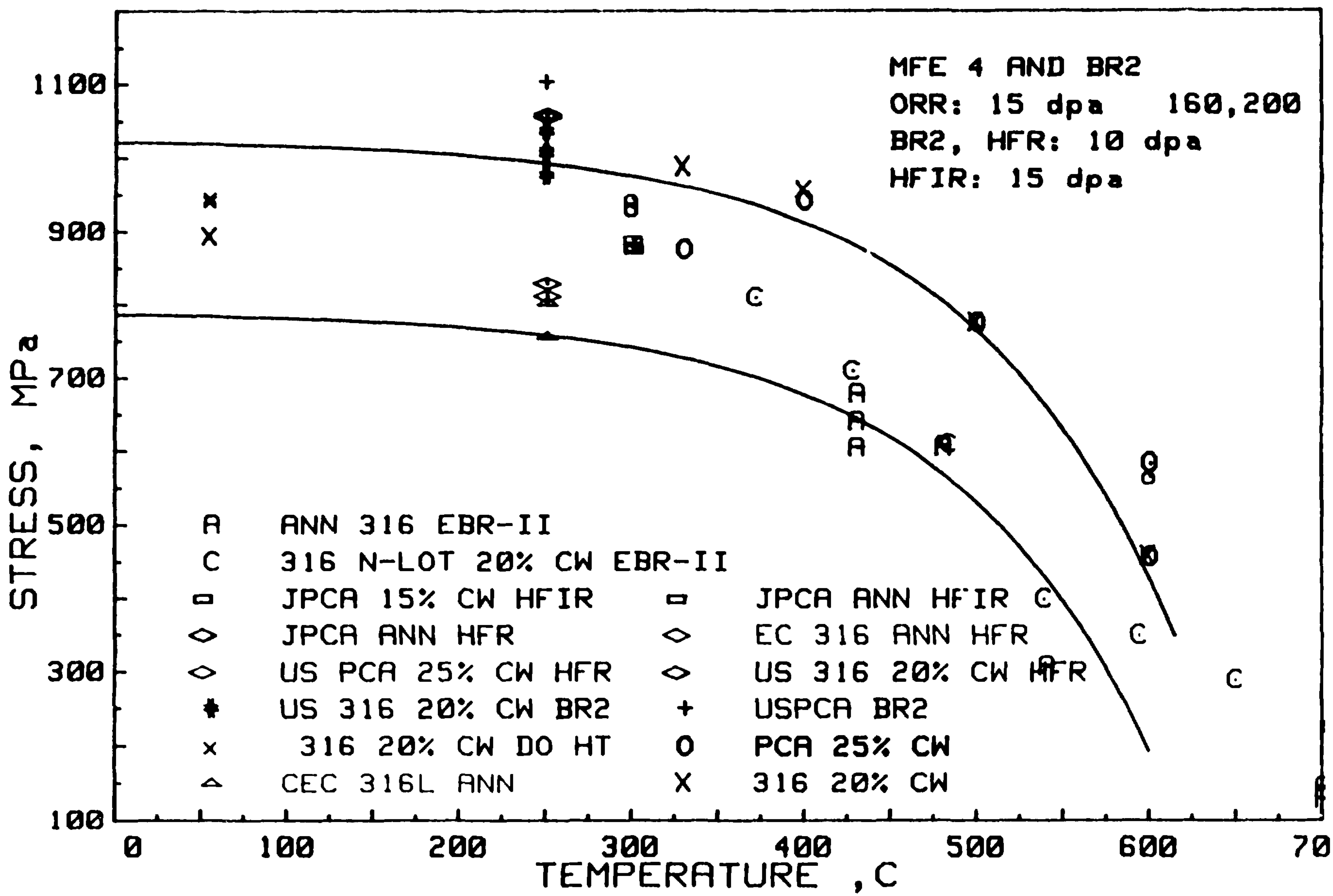

MFE 4 AND BR2
ORR: 15 dpa 160,200
BR2, HFR: 10 dpa
HFIR: 15 dpa
STRESS, MPa
TEMPERATURE ,C
1100
900
700
500
300
100
0
100
200
300
400
500
600
70
A ANN 316 EBR-II
C 316 N-LOT 20% CW EBR-II
JPCA 15% CW HFIR
JPCA ANN HFIR
JPCA ANN HFR
EC 316 ANN HFR
US PCA 25% CW HFR
US 316 20% CW HFR
US 316 20% CW BR2
+ USPCA BR2
x 316 20% CW DO HT
O PCA 25% CW
CEC 316L ANN
X 316 20% CW

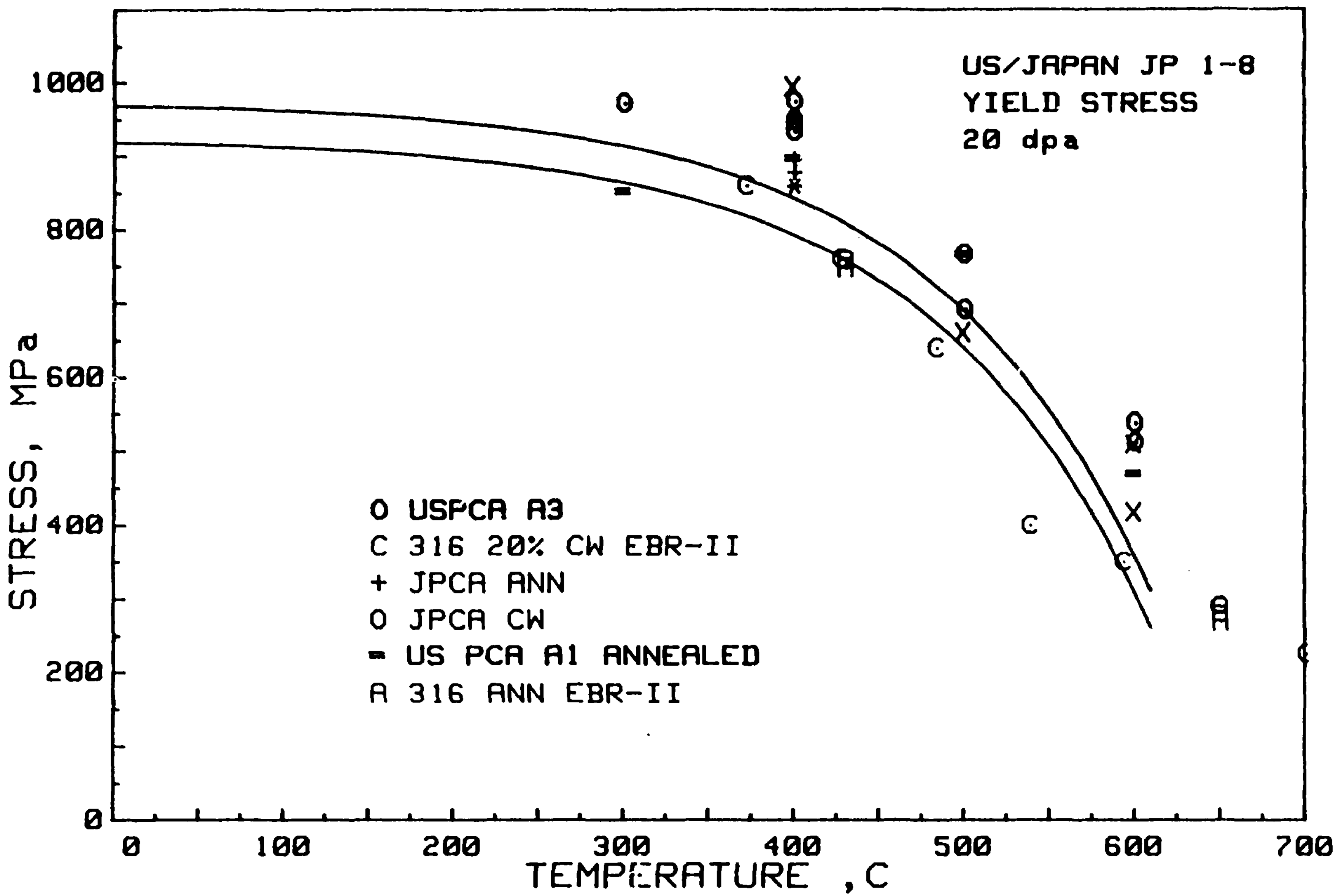

US/JAPAN JP 1-8
YIELD STRESS
20 dpa
STRESS, MPa
TEMPERATURE ,C
0
200
400
600
800
1000
0
100
200
300
400
500
600
700
O USPCA A3
C 316 20% CW EBR-II
+ JPCA ANN
O JPCA CW
- US PCA A1 ANNEALED
A 316 ANN EBR-II

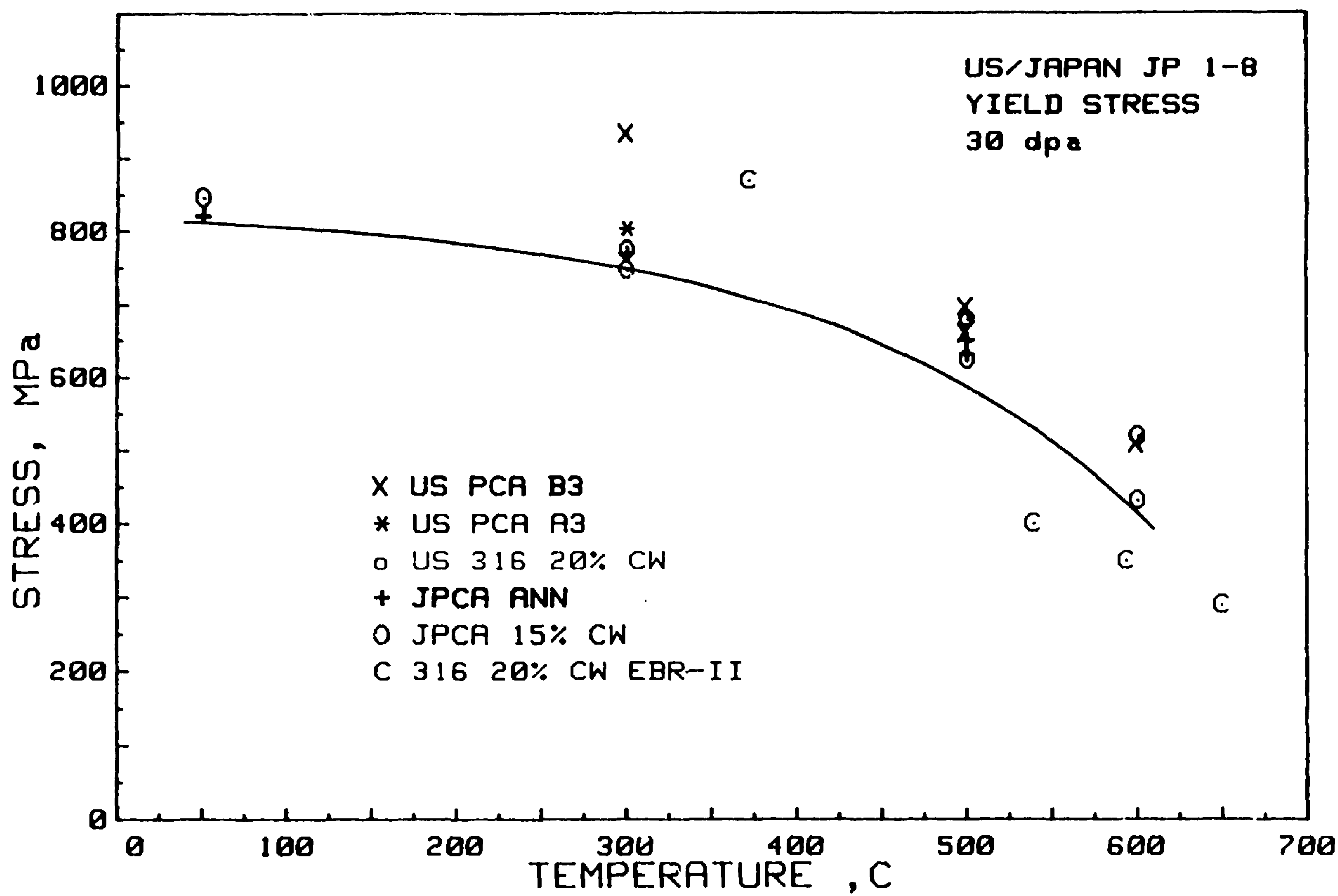
US/JAPAN JP 1-8
YIELD STRESS
30 dpa
X US PCA B3
* US PCA A3
o US 316 20% CW
+ JPCA ANN
O JPCA 15% CW
C 316 20% CW EBR-II
STRESS, MPa
TEMPERATURE ,C
0
200
400
600
800
1000
100
300
500
700

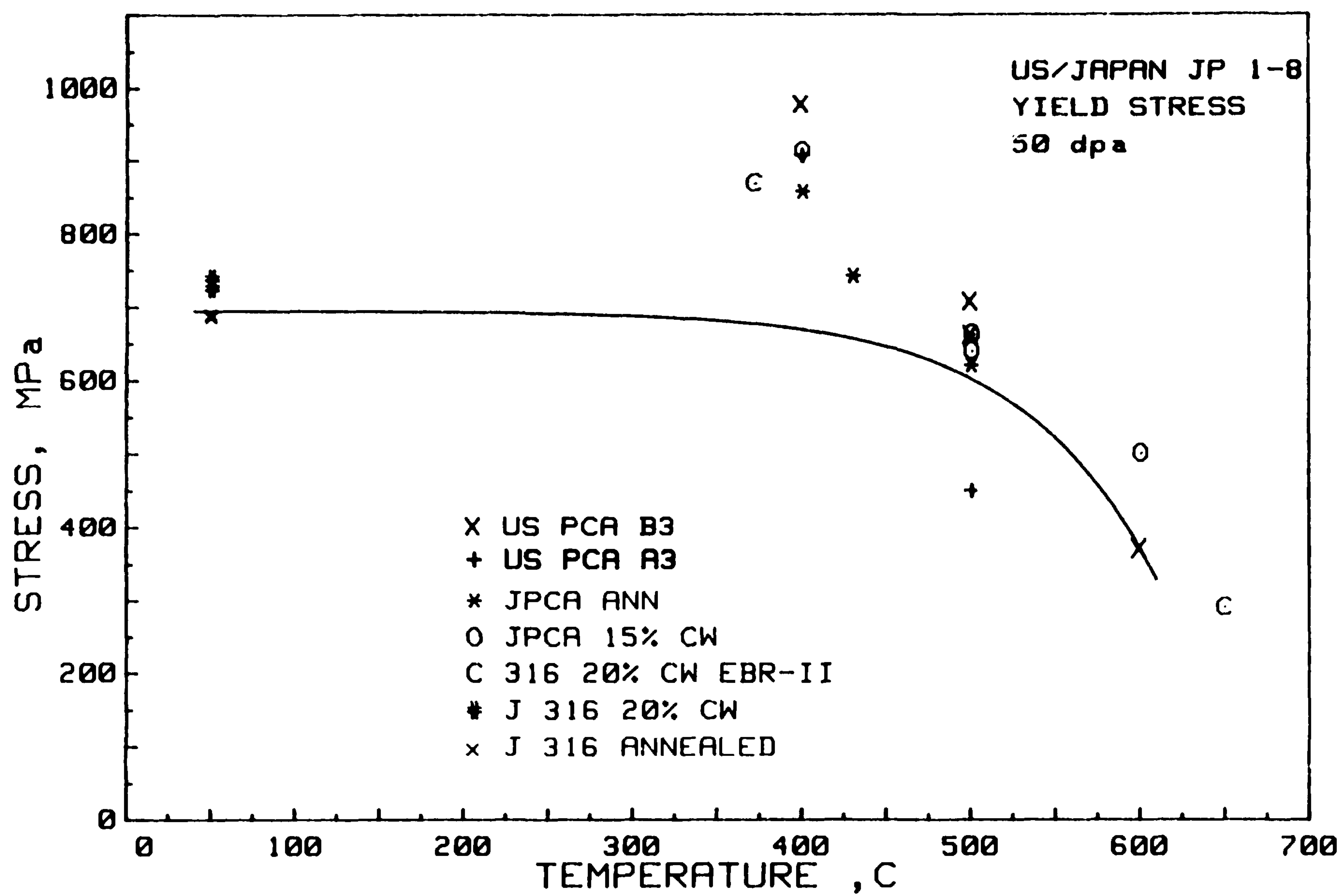

US/JAPAN JP 1-8
YIELD STRESS
50 dpa
X US PCA B3
+ US PCA A3
* JPCA ANN
O JPCA 15% CW
C 316 20% CW EBR-II
J 316 20% CW
x J 316 ANNEALED
STRESS, MPa
TEMPERATURE ,C
0
200
400
600
800
1000
0
100
200
300
400
500
600
700

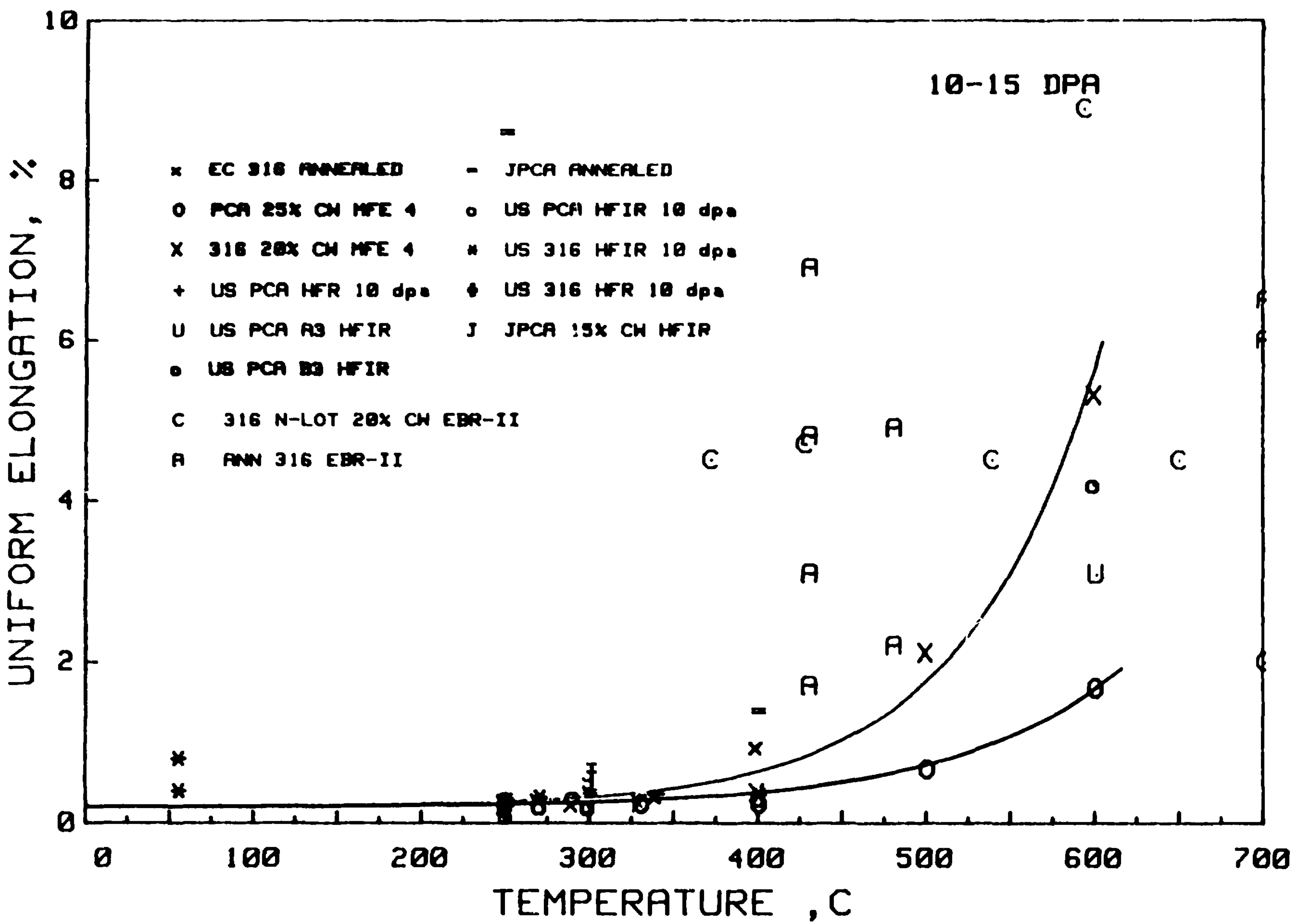

10-15 DPA
EC 316 ANNEALED
PCA 25% CW MFE 4
316 20% CW MFE 4
US PCA HFR 10 dpa
US PCA A3 HFIR
US PCA B3 HFIR
316 N-LOT 20% CW EBR-II
ANN 316 EBR-II
JPCA ANNEALED
US PCA HFIR 10 dpa
US 316 HFIR 10 dpa
US 316 HFR 10 dpa
JPCA 15% CW HFIR
UNIFORM ELONGATION, %
TEMPERATURE ,C
0
100
200
300
400
500
600
700
2
4
6
8
10

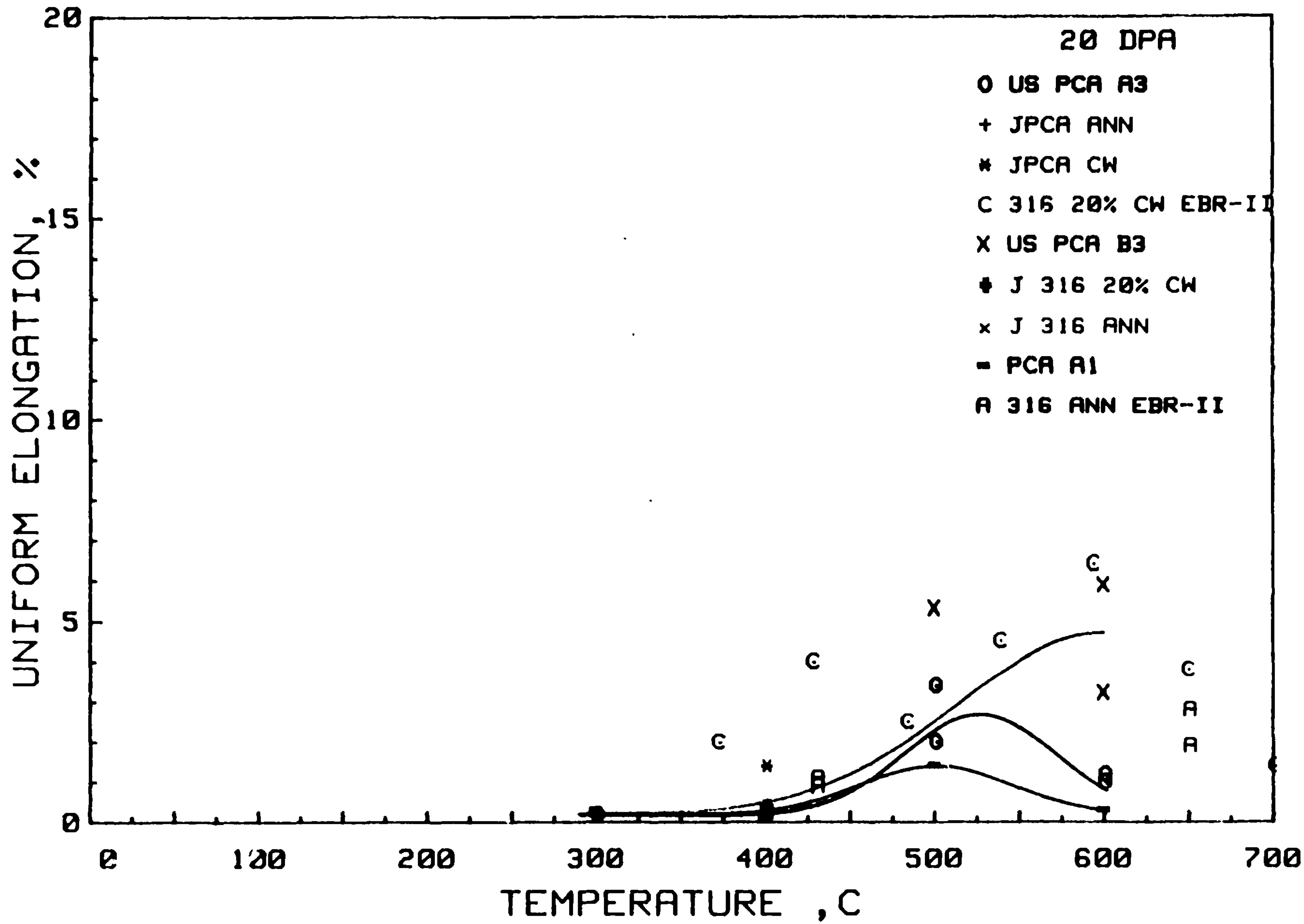
20 DPA
O US PCA A3
+ JPCA ANN
* JPCA CW
C 316 20% CW EBR-II
X US PCA B3
J 316 20% CW
x J 316 ANN
PCA A1
A 316 ANN EBR-II
UNIFORM ELONGATION, %
TEMPERATURE ,C
20
15
10
5
0
0
100
200
300
400
500
600
700

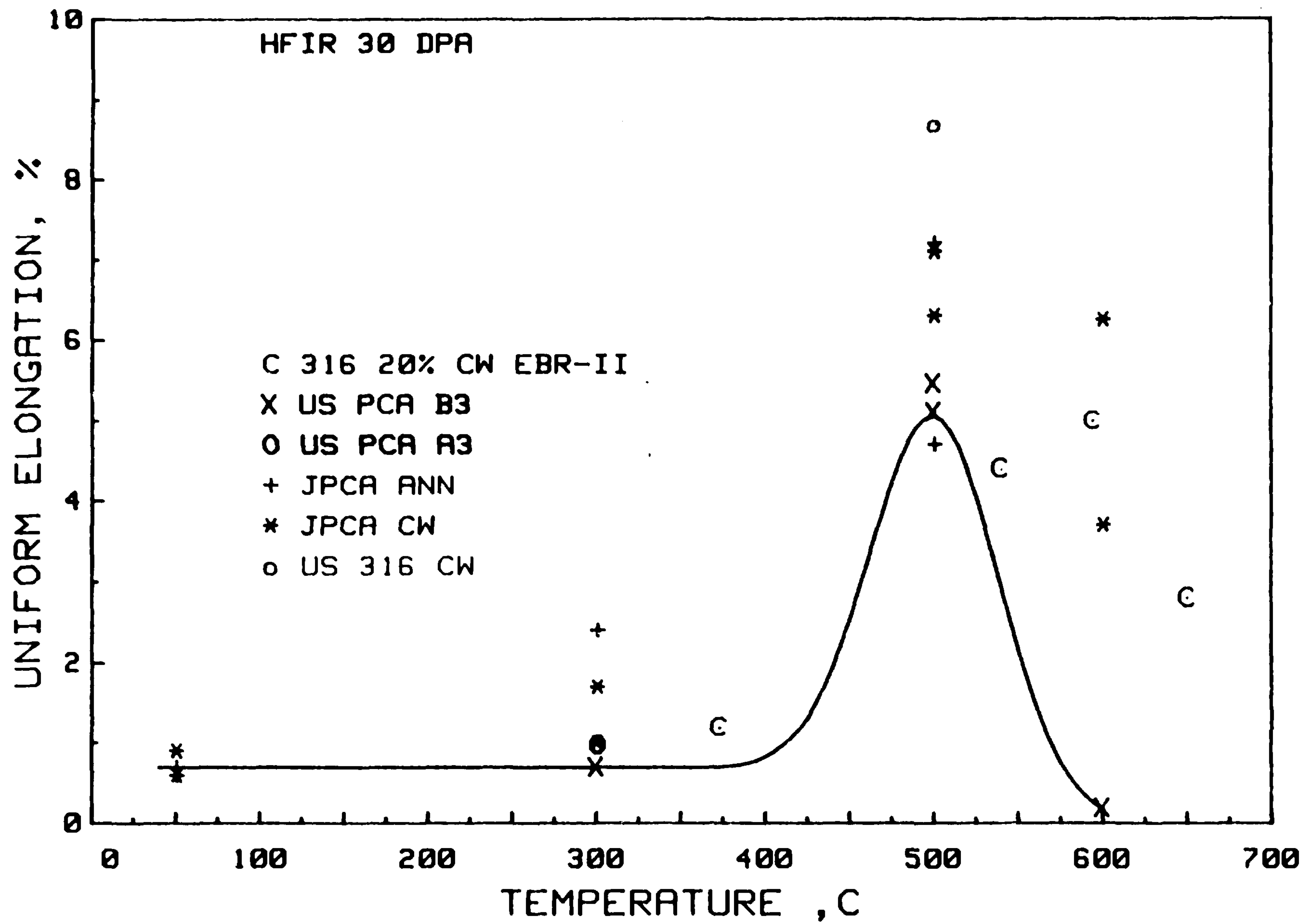
HFIR 30 DPA
C 316 20% CW EBR-II
X US PCA B3
O US PCA A3
+ JPCA ANN
* JPCA CW
o US 316 CW
UNIFORM ELONGATION, %
TEMPERATURE ,C
0
2
4
6
8
10
0
100
200
300
400
500
600
700

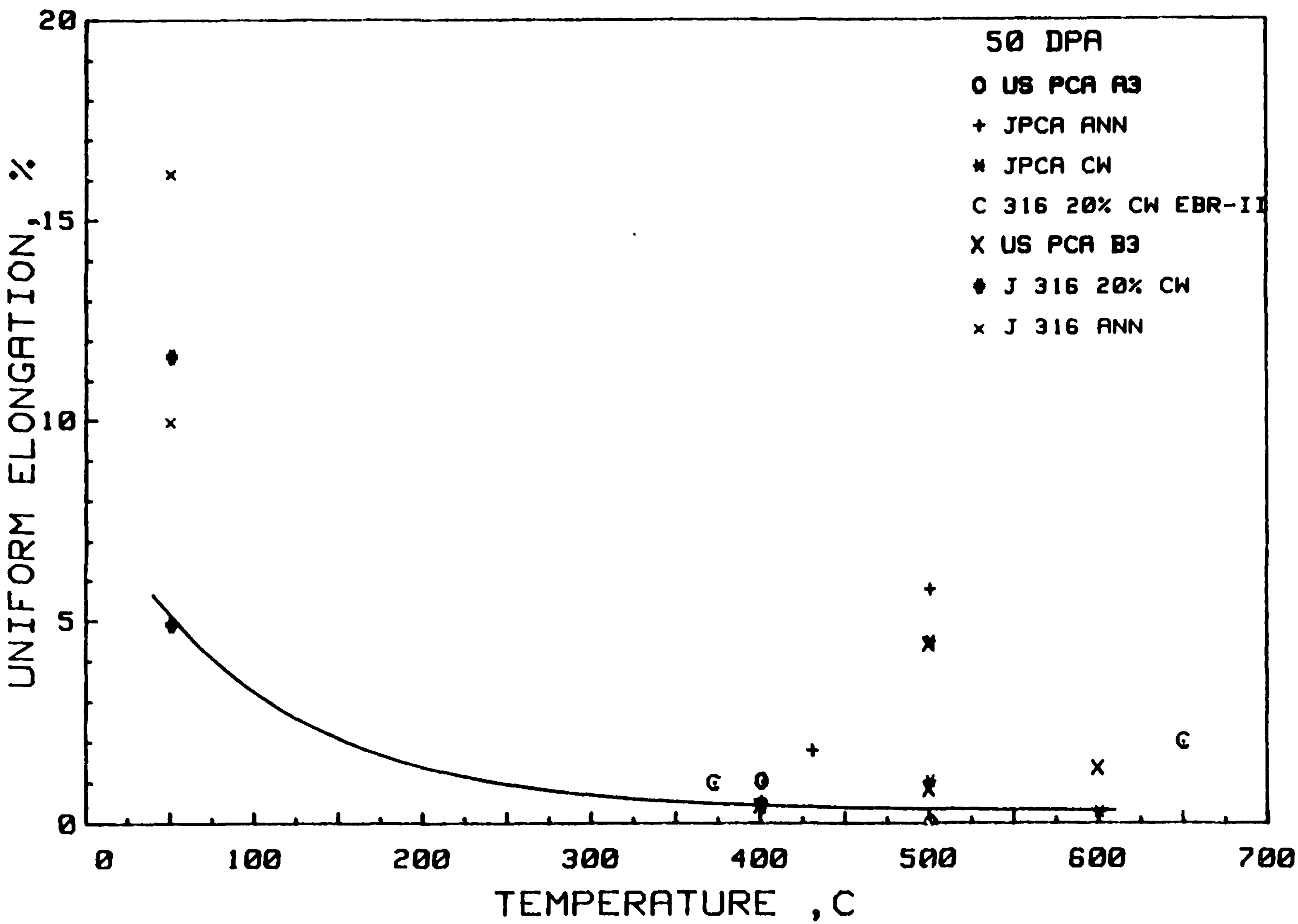

50 DPA
O US PCA A3
+ JPCA ANN
* JPCA CW
C 316 20% CW EBR-II
X US PCA B3
J 316 20% CW
x J 316 ANN
UNIFORM ELONGATION, %
TEMPERATURE ,C
0
5
10
15
20
0
100
200
300
400
500
600
700

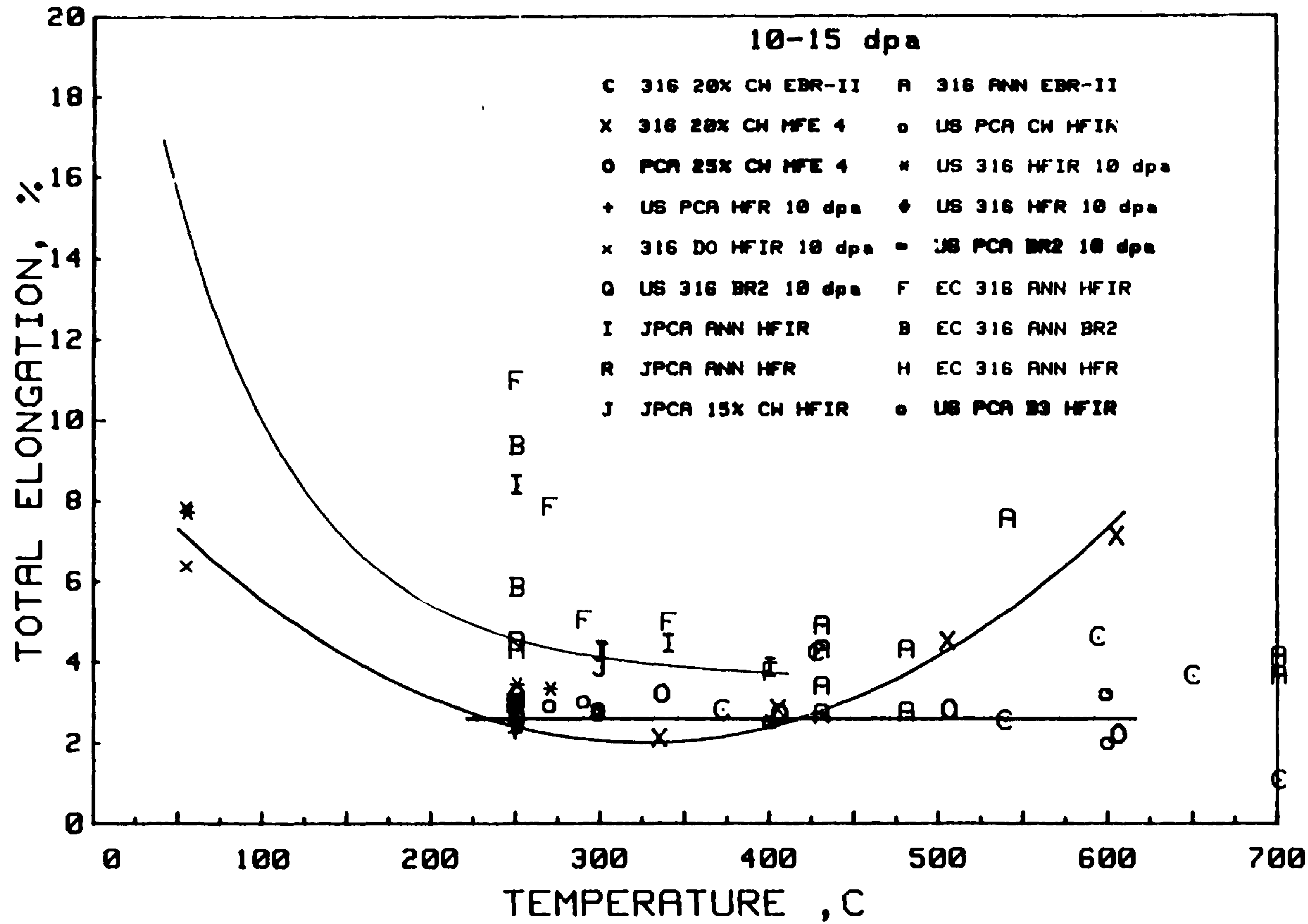
10-15 dpa
C 316 20% CW EBR-II
A 316 ANN EBR-II
X 316 20% CW MFE 4
o US PCA CW HFIR
O PCA 25% CW MFE 4
* US 316 HFIR 10 dpa
+ US PCA HFR 10 dpa
US 316 HFR 10 dpa
x 316 DO HFIR 10 dpa
US PCA BR2 10 dpa
Q US 316 BR2 10 dpa
F EC 316 ANN HFIR
I JPCA ANN HFIR
B EC 316 ANN BR2
R JPCA ANN HFR
H EC 316 ANN HFR
J JPCA 15% CW HFIR
US PCA HFIR
TOTAL ELONGATION, %
TEMPERATURE ,C
0
2
4
6
8
10
12
14
16
18
20
0
100
200
300
400
500
600
700

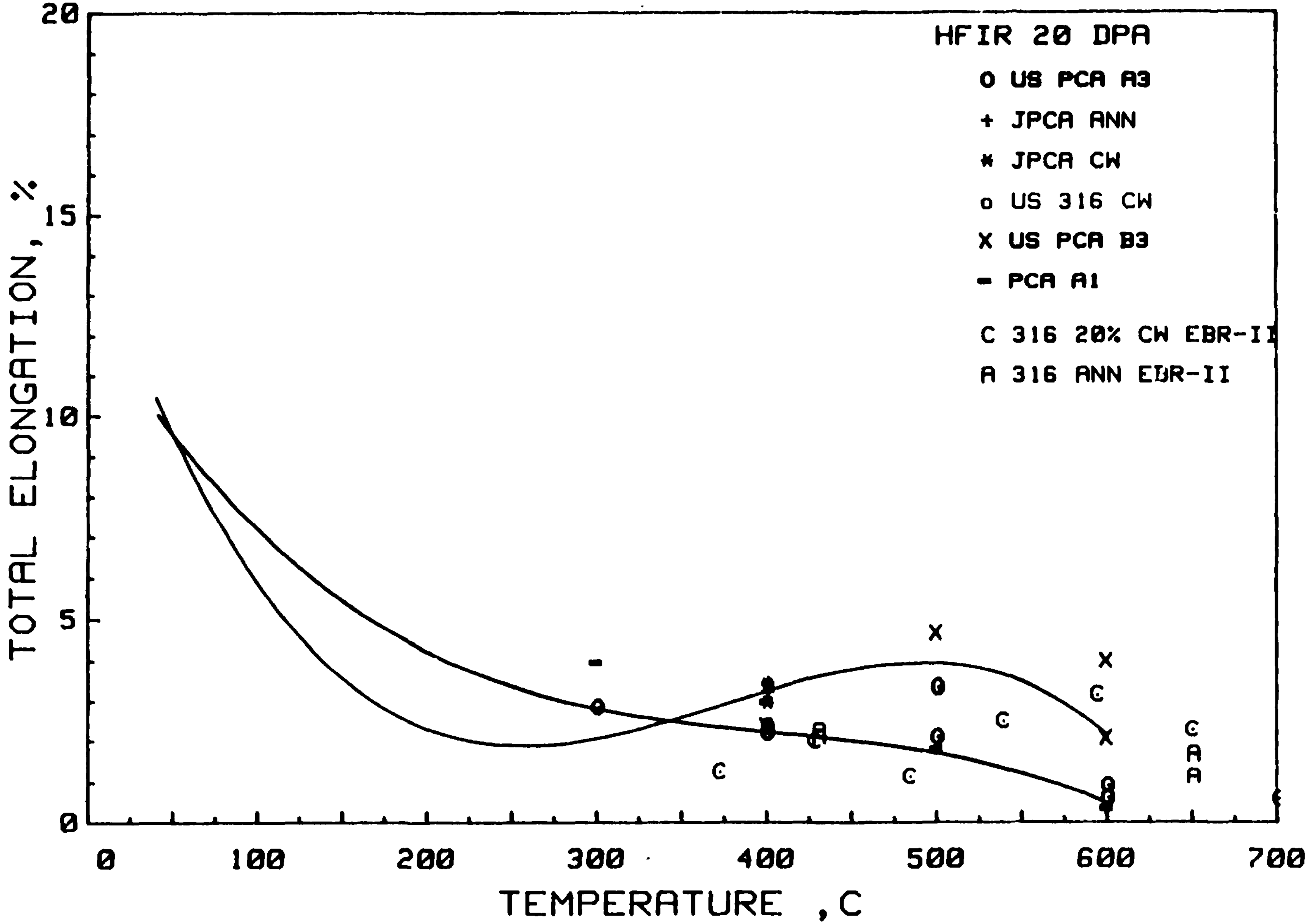
HFIR 20 DPA
O US PCA A3
+ JPCA ANN
* JPCA CW
o US 316 CW
X US PCA B3
- PCA A1
C 316 20% CW EBR-II
A 316 ANN EBR-II
TOTAL ELONGATION, %
TEMPERATURE ,C
0
5
10
15
20
0
100
200
300
400
500
600
700

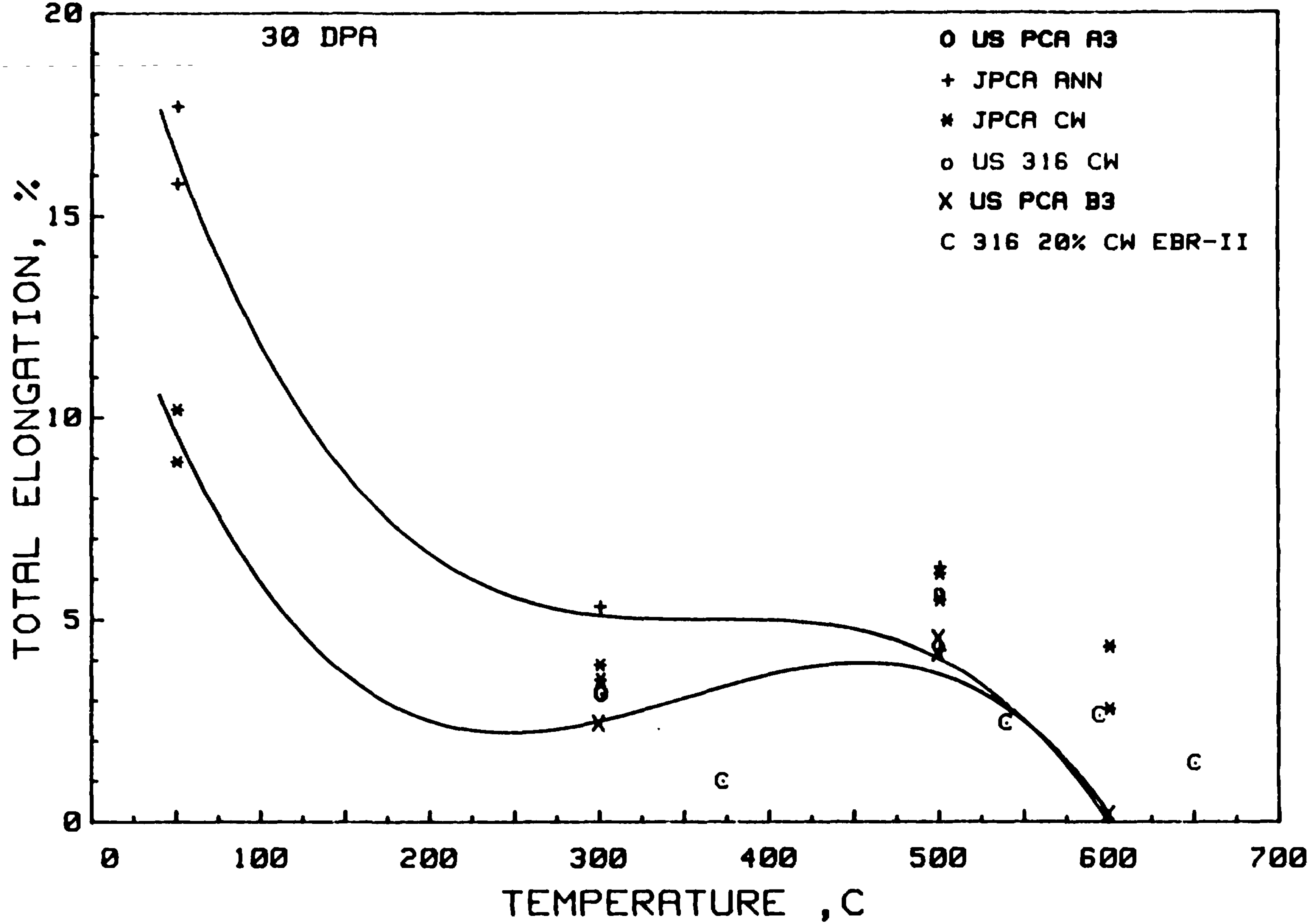
30 DPA
O US PCA A3
+ JPCA ANN
* JPCA CW
o US 316 CW
X US PCA B3
C 316 20% CW EBR-II
TOTAL ELONGATION, %
TEMPERATURE ,C
0
5
10
15
20
0
100
200
300
400
500
600
700

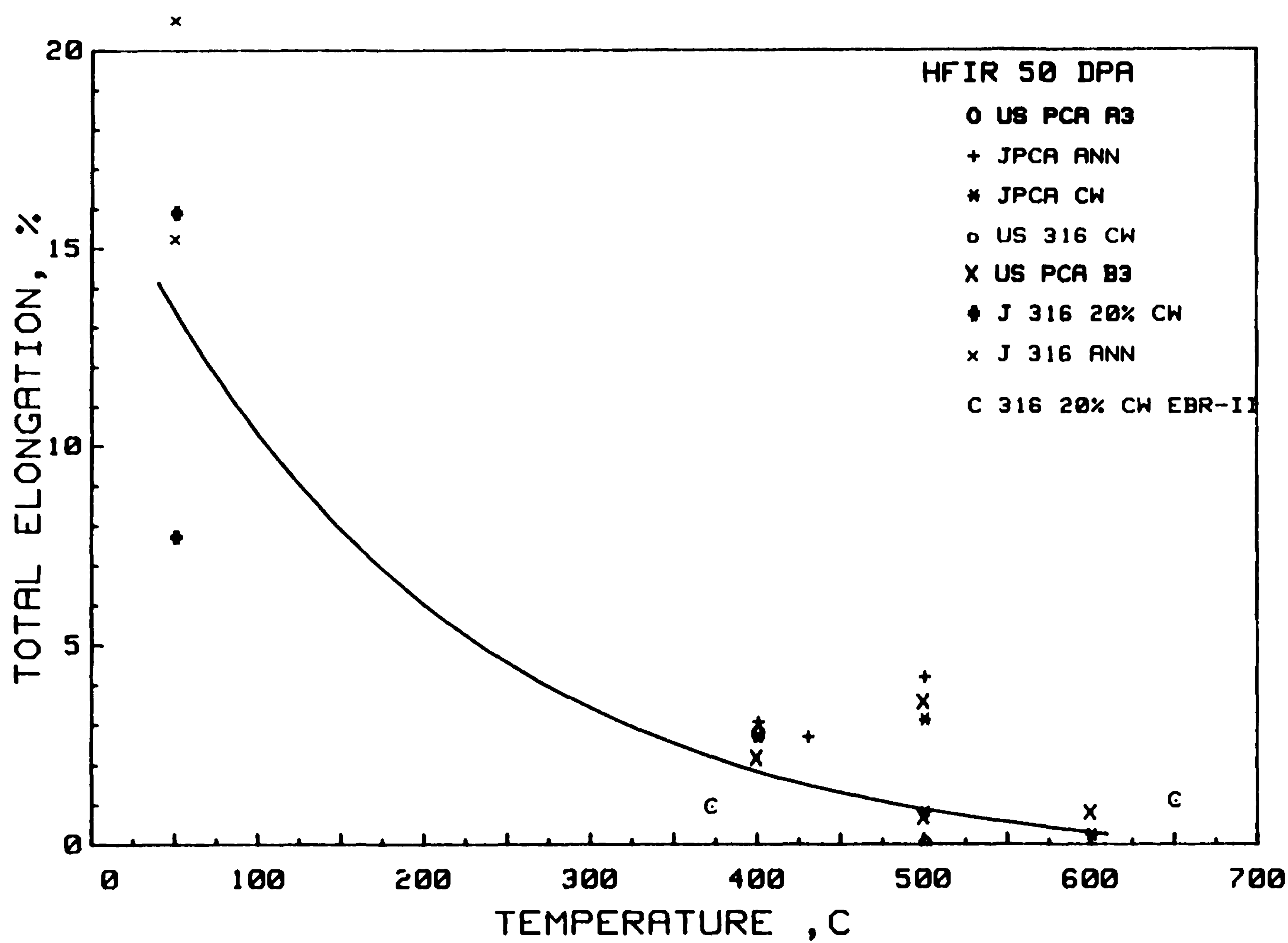
HFIR 50 DPA
O US PCA A3
+ JPCA ANN
JPCA CW
US 316 CW
X US PCA B3
J 316 20% CW
x J 316 ANN
C 316 20% CW EBR-II
TOTAL ELONGATION, %
TEMPERATURE ,C
0
5
10
15
20
0
100
200
300
400
500
600
700

Tensile Property Equations (T = °C), 10 dpa

Alloy	Yield Strength, MPa	Elongation, % Uniform	Total
Austenitic Stainless Steel			
CW	Y.S. = 1025 [1 – exp[–(665) – T)/120]		
Annealed	= 1025[1 – exp[–(665 – T)/120] – 235		
316 CW and Annealed		$UE = 3.0 \times 10^{-3}\ e^{T/80} + 0.2$	
PCA CW and Annealed		$UE = 3.7 \times 10^{-3}\ e^{T/100} + 0.2$	
PCA CW			TE = 2.6
316 CW			$= 7 \times 10^{-5}\ (T - 325)^2 + 2$
Austenitic SS Annealed			$= 22\ e^{-T/80} + 3.6$

Tensile Property Equations (T = °C), 20 dpa

Alloy	Yield Strength, MPa	Elongation, % Uniform	Elongation, % Total
All-Austenitic Stainless steel			
CW	$Y.S. = 975\ [1 - \exp[-(660) - T)/130]$		
Annealed	$= 975[1 - \exp[-(660 - T)/130] - 50$		
316 CW, PCA B3		$UE = 4.5\ e^{-(T-600)^2/15,000} + 0.2$	
PCA-A1, 316 Annealed		$= 1.2\ e^{-(T-500)^2/4000} + 0.2$	
PCA-A3		$= 2.5\ e^{-(T-525)^2/4000} + 0.2$	
PCA-B3			$TE = 14.8 - 0.122T$
			$+ 3.62 \times 10^{-4}\ T^2$
			$- 3.23 \times 10^{-7}\ T^3$
PCA-A1, A3			$= 12.5 - 6.7 \times 10^{-2}\ T$
316 Annealed			$- 1.56 \times 10^{-4}\ T^2$
			$- 1.28 \times 10^{-7}\ T^3$

Tensile Property Equations (T = °C), 30 dpa

Alloy	Yield Strength, MPa	Elongation, % Uniform	Total
Austenitic Stainless steel CW Annealed	$Y.S. = 975 [1 - \exp[-(760 - T)/190] - 140$		
Austenitic Stainless steel CW and Annealed		$UE = 0.7 \{1 + \exp [(T - 450)/20]\}^{-1} + 5 \exp [-(T - 500)^2/3000]$	
Austenitic Stainless steel CW			$TE = -3.8 \times 10^{-7} \{[T - 300](T - 200)(T - 550)] + 2.5$
Annealed			$= 22.9 - 0.148\ T + 4.08 \times 10^{-4}\ T - 3.75 \times 10^{-7}\ T^3$

Tensile Property Equations (T = °C), 50 dpa

Alloy	Yield Strength, MPa	Elongation, %	
		Uniform	Total
Austenitic Stain'ess steel CW Annealed	$Y.S. = 775 [1 - \exp[-(670 - T)/80] - 80$		
Austenitic Stainless steel CW and Annealed		$UE = 8 e^{-0.01 T} + 0.3$	
Austenitic Stainless steel CW Annealed			$TE = 18 e^{-T/200} - 0.6$

SUMMARY

1. TENSILE PROPERTIES SUBMITTED TO DATA BASE COORDINATOR

2. JP 1–8 DATA MADE A MAJOR CONTRIBUTION TO THE EQUATIONS

3. CHANGES WILL BE MADE IN LOW TEMPERATURE BEHAVIOR USING ORR–MFE–6J RESULTS

STRESS CORROSION CRACKING SENSITIVITY OF IRRADIATED STAINLESS STEELS FOR FUSION REACTOR

—DETERMINATION OF DEGREE OF SENSITIZATION BY EPR* METHOD— (*ELECTROCHEMICAL POTENTIOKINETIC REACTIVATION)

Toru Inazumi

ABSTRACT

A stress corrosion cracking study program for fusion reactor materials has started under the collaboration between ORNL and JAERI. The test equipment for the corrosion test was sent from JAERI to ORNL, and assembly was completed in Room 242, Bldg. 4508. Specimens for the test were selected from USPCA and US316 disks irradiated in FFTF/MOTA at 420°C up to 10 dpa. A thermal aging program was initiated to obtain control data for the irradiated specimens. Sensitization in thermally aged disk specimens was successfully detected by EPR (electrochemical potentiokinetic reactivation) method. The possibility of using electropolishing as the specimen surface preparation prior to EPR test was demonstrated. Determination of an optimum polishing condition and development of an electropolishing equipment for handling radioactive specimens are in progress. EPR test program with heavy-ion irradiated specimens was also proposed and is in progress.

OBJECTIVES

1. DEVELOPMENT OF CORROSION TESTING SYSTEM FOR NEUTRON IRRADIATED DISK TYPE SPECIMENS.

2. EVALUATION OF SCC RESISTANCE OF CANDIDATE STAINLESS STEELS FOR FUSION REACTOR.

3. BASIC RESEARCH ON RADIATION INDUCED SENSITIZATION MECHANISM.

1. SCOPE

This test program was initiated to examine the effect of neutron radiation on resistance of candidate stainless steels for fusion reactor to stress corrosion cracking in high tempereture water environment. Degree of sensitization in the steels caused by radiation induced segregation and/or precipitation will be detected by EPR test method with 3mm disk specimens. Microstructure observation will also be conducted to identify the cause for sensitization. The possibility to use heavy iron irradiated specimens for corrosion study will be discussed.

2. EPR (Electrochemical Potentiokinetic Reactivation) Method

Passivation	0.5M H_2SO_4 + 0.01M KSCN +200 mV SCE for 2 min
Reactivation	6 V/h
Calculation	Charge Q (Integrated Current below Polarization Curve) Peak Current Density Ia Flade Potential E_F

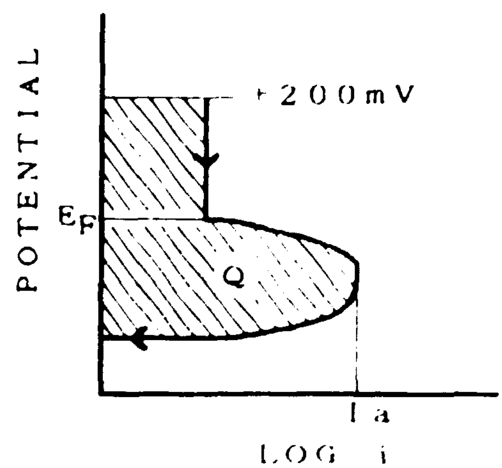

Fig.1 Schematic of reactivation curve

3. CORROSION TEST PROGRAM [STAGE I]

3-1. Materials for Corrosion Test by EPR Method

3-1-1. Neutron Irradiated Specimen
[FFTF/MOTA] - Low Radioactivity

Alloy	Designation	Condition
USPCA	PCA/A1	Annealed
	PCA/A3	25% CW
US316	DO-heat	20% CW
	N-lot	Annealed

Irradiating Condition
420℃ , 10 dpa

3-1-2. Thermally Aged Specimen

Alloy	Designation	Condition	Shape
USPCA	K-280	Annealed	Disk, Rod
		25% CW	Disk, Rod
US316	DO-heat	Annealed	Disk
		20% CW	Disk
	N-lot	Annealed	Disk
	X-15893	Annealed	Disk
316L for ITER			Rod

Temperature, ℃	Time, hr
420	300
	1000
	3000
550	300
	1000
650	2

3-1-3. Heavy Ion Irradiated Specimen

Alloy Composition (at%)

Fe	Cr	Ni	Si	Mn	Mo	Ti	C
63.85	17.41	12.88	2.07	2.06	0.99	0.17	0.37

Irradiating Condition
4 MeV Ni ion, 675℃, 1 dpa

3-2. Test Procedure

SURFACE PREPARATION *

EPR TEST *

SURFACE OBSEVATION — Optical Microscope

MICROSTRUCTURE OBSERVATION — TEM

3-2-1. Development of Equipment for EPR Test

1) Testing System

【Points in Designing】

Safety and Less Exposure to Radiation in handling Radioactive Specimens and Contaminated Waste

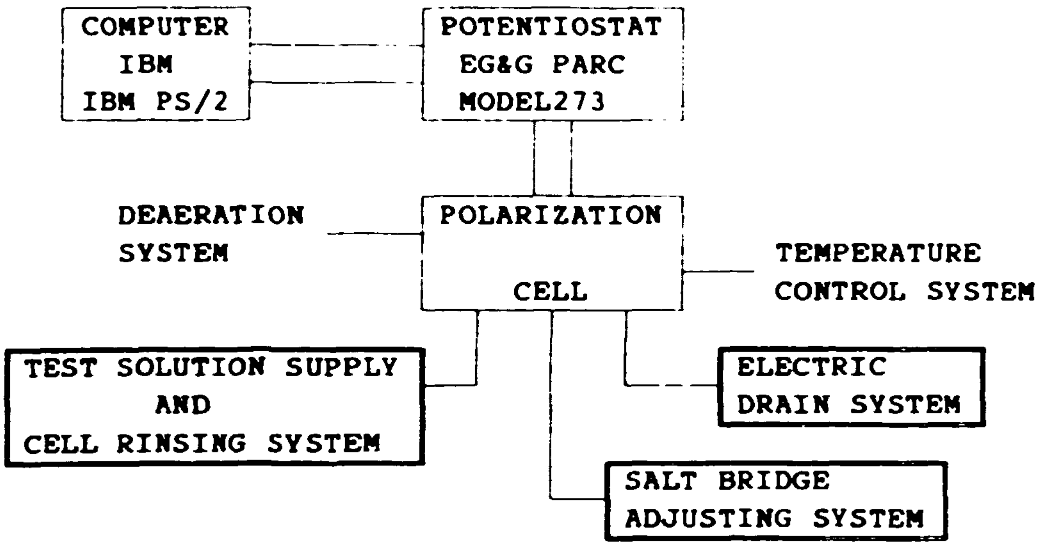

Fig.2 Corrosion testing system.

2) Specimen Holder

[Points in Designing]
Easy to set DISK SPECIMENS with
Good electrical contact and Sealing

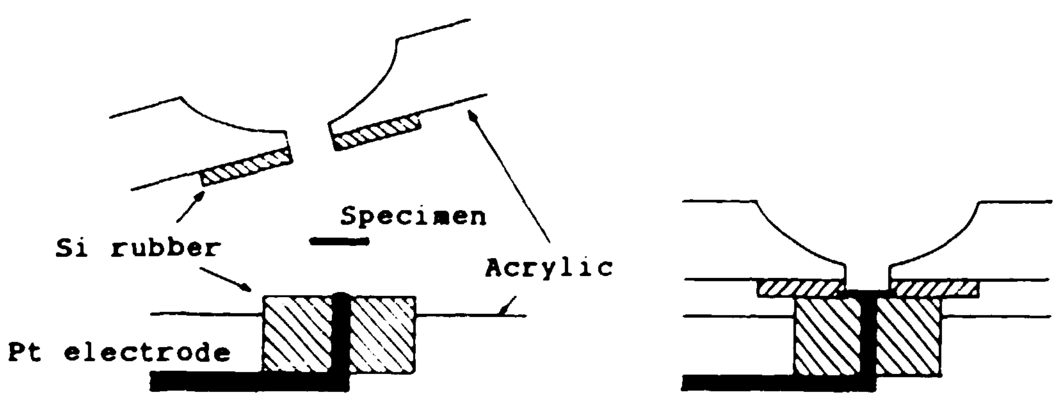

Fig.3 Specimen holder

3-2-2. Development of Surface Preparation Technique

1) Polishing Method

[Electropolishing] - <u>LESS EXPOSURE and CONTAMINATION</u>
than Mechanical Polishing

2) Polishing Standard

·No Scraches
·No Grain Boundary Etching
·No passivation

3) Polishing System

[Points in Designing]
<u>Safety and Less Exposure to Radiation</u> in handling Radioactive Specimens and Contaminated Waste

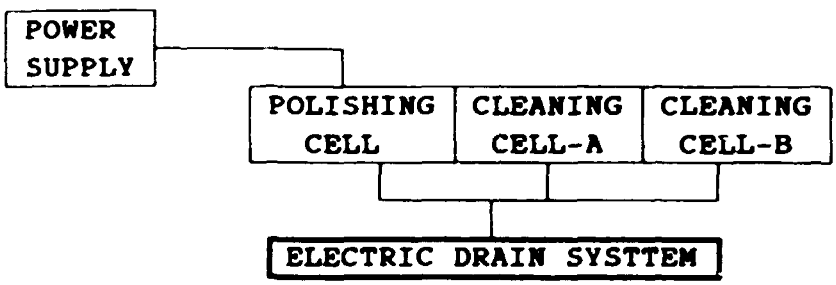

<u>*Same Type Specimen Holder as EPR Test will be used.</u>

Fig.4 Electropolishing system.

4. CORROSION TEST PROGRAM [STAGE Ⅱ]

4-1. Aged Specimens
JPCA, 316F, (USPCA, US316)

4-2. ORR Specimens
JPCA, 316F, (USPCA, US316)

SCHEDULE FOR CORROSION TEST

	1988	1989			
	4/4	1/4	2/4	3/4	4/4
TEST EQUIPMENT PREPARATION					
Shipping					
Assembling in Hood					
Trial Test					
SURFACE PREPARATION TECHNIQUE					
Electropolish Standard					
Equipment for Handling Hot Disks and Waste					
CORROSION TEST					
[STAGE I]					
Aged Specimen					
Sample Preparation					
Rod Type					
Disk Type					
HII Specimen *					
FFTF/MOTA Specimen					
[STAGE II]					
Aged Specimen					
Sample Preparation					
Disk Type					
ORR Specimens					
SPECIMEN OBSERVATION					
Optical					
TEM					

*HII: Heavy Ion Irradiated

5. SUMMARY

1) The EPR test equipment was sent from JAERI to ORNL and assembly was completed in the Room 242, Building 4508.
2) Specimens for the EPR test were selected from USPCA and US316 disks irradiated in FFTF/MOTA at 420℃ up to 10 dpa and thermal aging program was initiated to obtain standard data for the irradiated specimens. Disk and/or rod shape of USPCA and US316 have been aged at 420 ~ 650℃ for 2 ~ 3000 hr.
3) Sensitizaton in thermally aged disk type specimens was successfully detected by the newly developed test equipment.
4) Possibility of electropolishing to be used as specimen surface preparation was demonstrated. Determination of an optimum polishing condition and the development of the electropolishing equipment for handling radioactive specimens are in progress.
5) EPR test program with Heavy Ion Irradiated specimens was also proposed and is in progress.

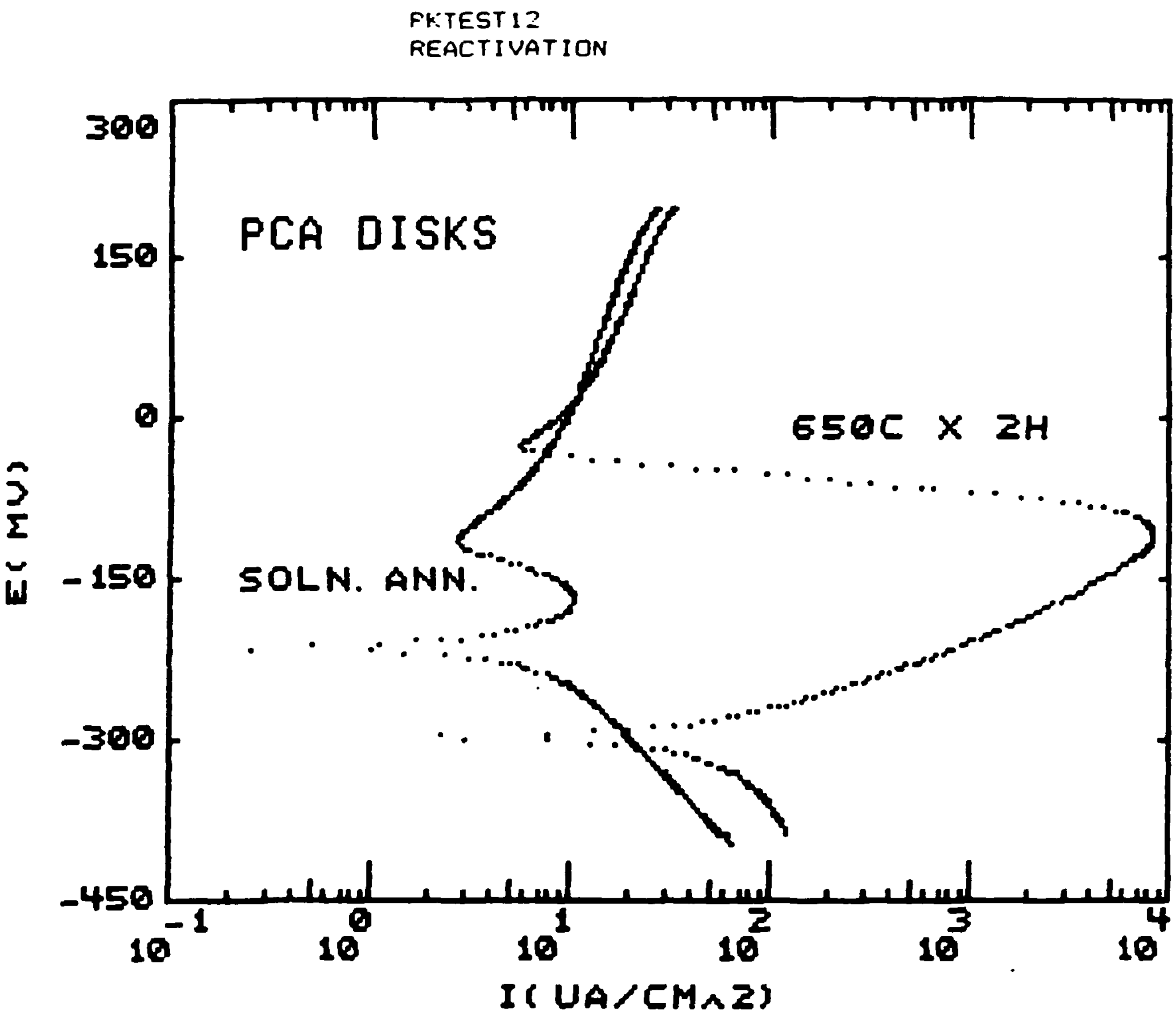

Appendix 1 EPR test results of UAPCA disk specimens.

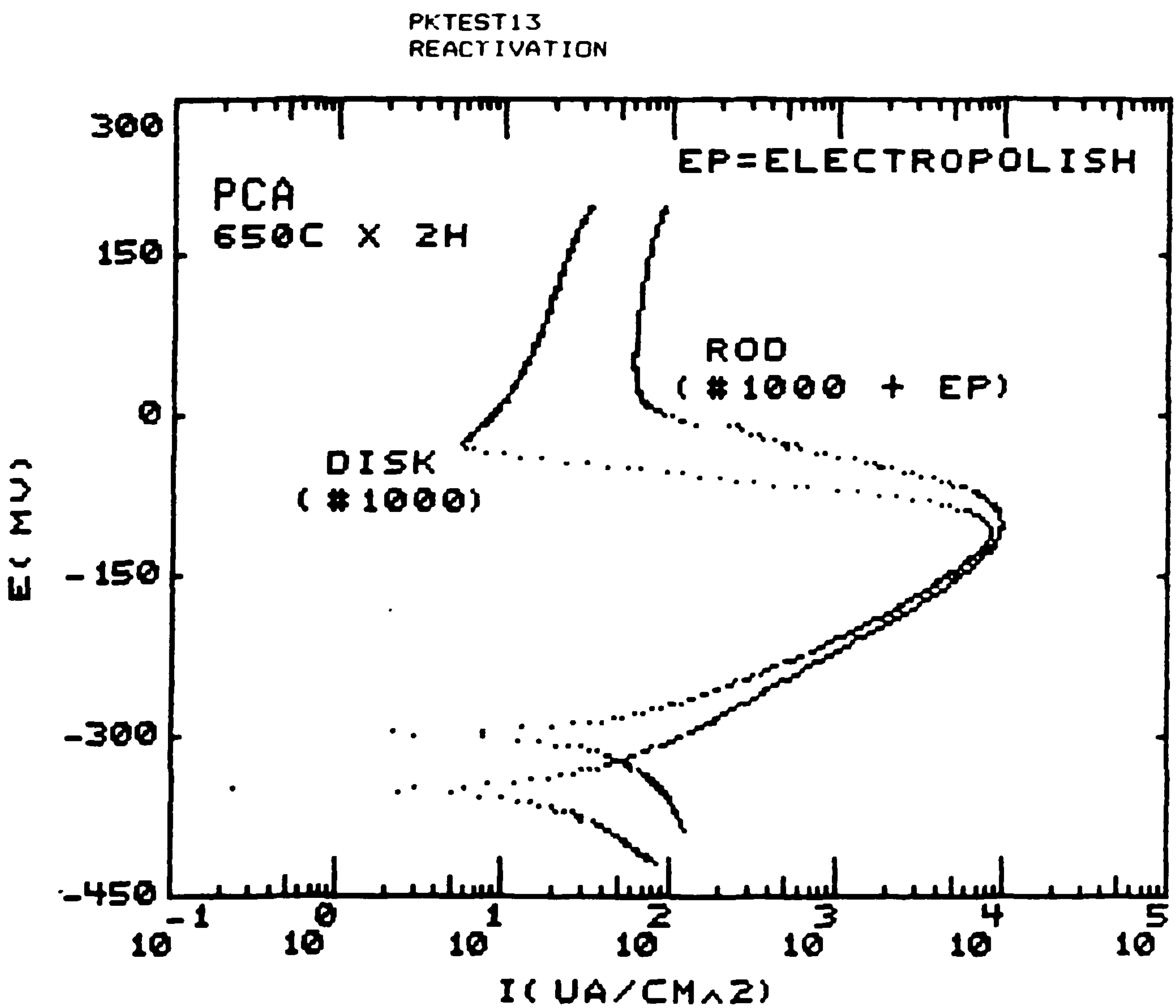

Appendix 2 Comparison of EPR test results between disk specimen and rod specimen.

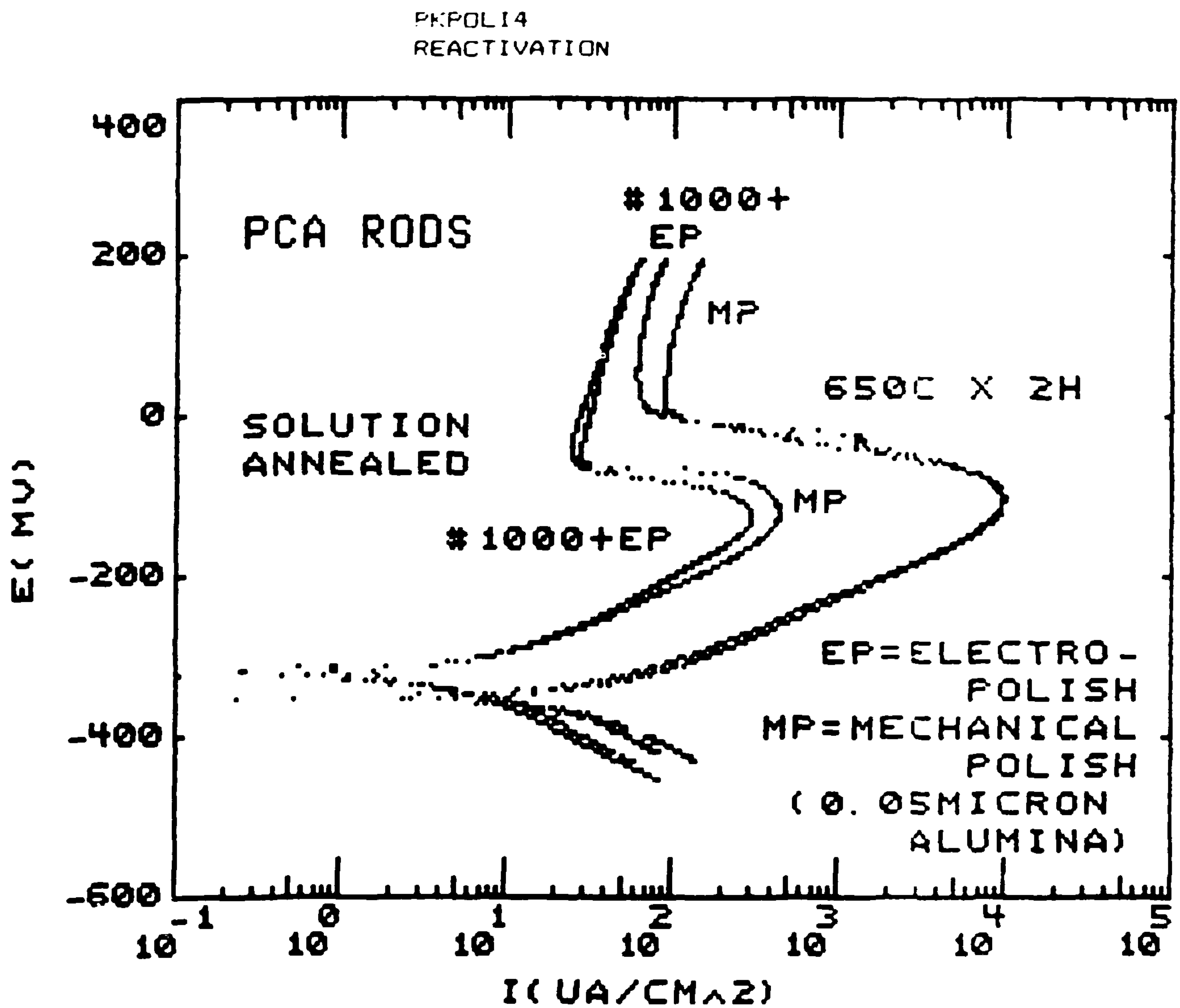

Appendix 3 Comparison of EPR test results between electropolished specimen and Alumina polished specimen (rod).

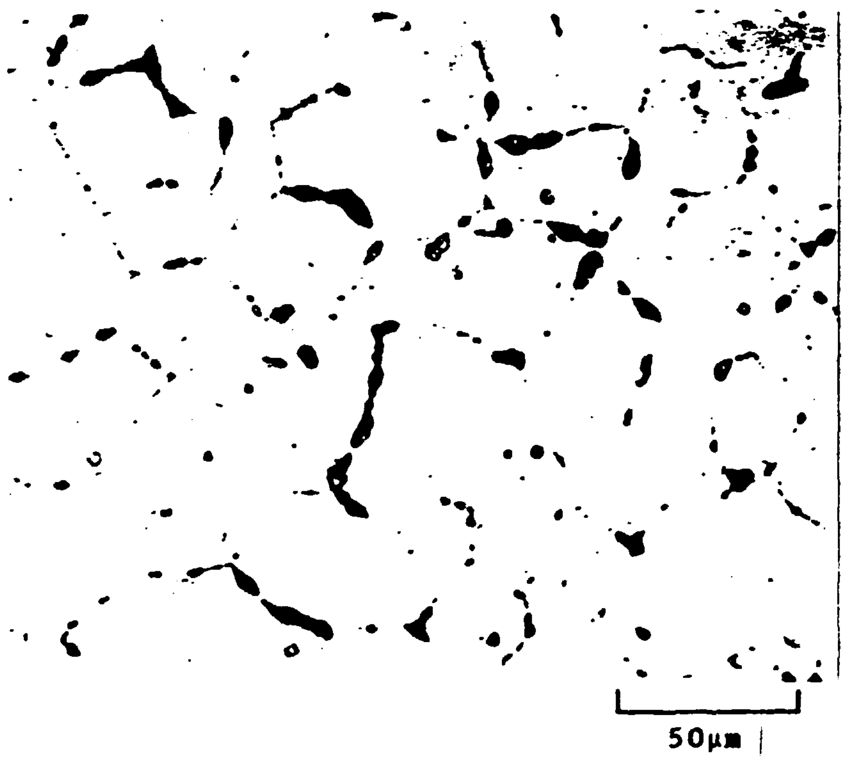

Appendix 4 Example of surface observation after EPR test.
(USPCA, cold work + 650℃ x 2hr)